UNIVERSIDADE ESTADUAL DE CAMPINAS
FACULDADE DE ENGENHARIA QUÍMICA
ÁREA DE CONCENTRAÇÃO
DESENVOLVIMENTO DE PROCESSOS QUÍMICOS

Desenvolvimento de Processos para a Aplicação do Alginato na Biofabricação

AUTOR: MSc. RODRIGO ALVARENGA REZENDE
ORIENTADOR: PROF. DR. RUBENS MACIEL FILHO
CO-ORIENTADOR: PROF. DR. PAULO JORGE DA S. BÁRTOLO

Tese de Doutorado apresentada à Faculdade de Engenharia Química da Universidade Estadual de Campinas como parte dos requisitos exigidos para a obtenção do título de Doutor em Engenharia Química.

Campinas - São Paulo

07 de Dezembro de 2010

FICHA CATALOGRÁFICA ELABORADA PELA
BIBLIOTECA DA ÁREA DE ENGENHARIA E ARQUITETURA - BAE - UNICAMP

R339d

Rezende, Rodrigo Alvarenga
Desenvolvimento de processos para a aplicação do alginato na biofabricação / Rodrigo Alvarenga Rezende. --Campinas, SP: [s.n.], 2010.

Orientadores: Rubens Maciel Filho, Paulo Jorge da Silva Bártolo.
Tese de Doutorado - Universidade Estadual de Campinas, Faculdade de Engenharia Química.

1. Engenharia tecidual. 2. Alginatos. 3. Biomaterial. 4. Prototipagem rápida. 5. Algoritmos genéticos. I. Maciel Filho, Rubens. II. Bártolo, Paulo Jorge da Silva. III. Universidade Estadual de Campinas. Faculdade de Engenharia Química. IV. Título.

Título em Inglês: Development of processes for the alginate application on to the biofabrication
Palavras-chave em Inglês: Tissue engineering, Alginates, Biomaterial, Rapid prototyping, Genetic algorithms
Área de concentração: Desenvolvimento de Processos Químicos
Titulação: Doutor em Engenharia Química
Banca examinadora: Silvio Eduardo Duailibi, Jorge Vicente Lopes da Silva, Cecília Amélia de Carvalho Zavaglia, André Luiz Jardini Munhoz
Data da defesa: 07/12/2010
Programa de Pós Graduação: Engenharia Química

Tese de Doutorado defendida por Rodrigo Alvarenga Rezende e aprovada em 07 de Dezembro de 2010 pela banca examinadora constituída pelos doutores:

Prof. Dr. Rubens Maciel Filho (Orientador)

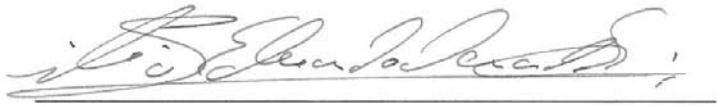

Prof. Dr. Silvio Eduardo Duailibi (Titular)

Prof. Dr. Jorge Vicente Lopes da Silva (Titular)

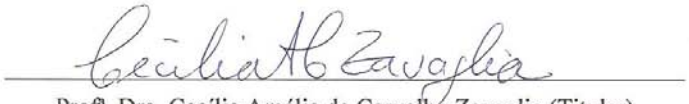

Profª. Dra. Cecília Amélia de Carvalho Zavaglia (Titular)

Prof. Dr. André Luiz Jardini Munhoz (Titular)

Este exemplar corresponde à versão final da Tese de Doutorado em Engenharia Química.

Prof. Dr. Rubens Maciel Filho (Orientador)

Às queridas mulheres da minha vida,
Mylene e Andressa, por sermos uma família.

E aos meus pais e irmãos,
sogros e cunhados pelo apoio.

Agradecimentos

Primeiramente, agradeço a Deus por estar comigo e com minha família em todos os momentos.

Faço uma menção especial à minha família (pais, irmãos, cunhados, sogros) que nos recebeu de braços abertos em seus lares quando precisamos.

Agradeço a grande amizade do Prof. Rubens Maciel Filho, desde a primeira vez que conversamos e as discussões e orientações em torno da tese. Agradeço, também, por ter prontamente nos providenciado a bolsa de fomento no nosso retorno. Agradeço, oportunamente, à Profª. Maria Regina, pela amizade e apoio sempre.

Ao Prof. Paulo Bártolo pelo tempo que passei no Departamento de Engenharia Mecânica do Instituto Politécnico de Leiria, Portugal, e pelos trabalhos realizados.

À Profª Ausenda, grande amiga e parceira de trabalho em Leiria e de viagens ao Minho para a realização de ensaios. Vou sempre lembrar o nosso "ausenato".

Ao Professor Marco Scarparo, com quem pude contar sempre em momentos bons e difíceis, e por quem tenho muita admiração.

Aos membros da banca por aceitarem participar da defesa e enriquecerem as discussões finais do trabalho.

À Sofia, nossa grande amiga portuguesa, e sua família. Por toda a sua amizade dedicada, pela companhia, pelas "boléias", pelos inúmeros favores prestados, e por todas as orientações sobre o país, que nos passou durante nossa estada em Portugal.

A todos os amigos portugueses da ESTG que estiveram conosco durante e após nosso tempo em Portugal. Aos colegas de gabinete e aos laboratoristas que colaboraram para a

realização dos experimentos. Incluo, também, as zelosas senhoras da Pousadinha José Saramago, nosso lar em Leiria. Ao Rui Adriano pela ajuda nos modelos reológicos.

Aos amigos Jorge Vicente, Izaque, Marcelo e Pedro pela abertura e disponibilidade no CTI.

A todos os amigos brasileiros ou já quase brasileiros do Lopca, principalmente, Delba, Viktor, Cibelem, Melina e Sérgio Andrés.

À Mariana Altenhofen por gentilmente ter compartilhado seus conhecimentos.

E, por fim, mas não por último, da forma mais especial possível, gostaria de expressar toda a minha gratidão, meu orgulho e meu amor pela minha esposa, parceira incansável, e também colega de trabalho, Mylene, com quem tenho a felicidade de estar junto e casado há quase uma década, tendo realizado diversos trabalhos juntos, e que me deu o maior de todos os presentes, o nosso maior tesouro, Andressa.

"A vida só pode ser compreendida olhando-se para trás;
mas só pode ser vivida olhando-se para a frente."

Soren Kierkegaard

"O impossível é o possível que nunca foi tentado.
Chega quem caminha!"

Charles Chaplin

Resumo

REZENDE, Rodrigo Alvarenga, Desenvolvimento de Processos para a Aplicação do Alginato na Biofabricação: Tese (doutorado) – Faculdade de Engenharia Química, Universidade Estadual de Campinas-SP, 2010.

A busca por soluções que resgatem a saúde e a dignidade de vítimas de acidentes ou com problemas de saúde, como perda ou danos de órgãos, tem motivado uma evolução acelerada da biofabricação. Novos materiais e técnicas de fabricação vêm sendo desenvolvidos rapidamente com o apoio dos recursos computacionais, que se torna parte imprescindível deste processo. O objeto de estudo desta tese vem ao encontro do desenvolvimento de ferramentas computacionais e procedimentos para a biofabricação, o que requer a utilização de um material biocompatível. O material em questão é o alginato, um hidrogel proveniente de algas pardas marinhas e que tem sido amplamente utilizado em diversos setores por mais de cinquenta anos. Uma caracterização mecânica do alginato é realizada, com auxílio de um reômetro de pratos e de um analisador dinâmico mecânico (DMA), bem como uma caracterização do comportamento químico, tal como o seu poder de inchamento (swelling) e o seu processo de reticulação (gelação), a fim de servirem como dados de alimentação para as aplicações das ferramentas computacionais, nomeadamente, o Ansys e a técnica de otimização dos algoritmos genéticos. O Ansys é utilizado na simulação do comportamento de escoamento do alginato puro. Já os algoritmos genéticos, como ferramentas de otimização de propriedades físicas de estruturas em alginato.

Palavras-Chave: Biofabricação, Engenharia Tecidual, Prototipagem Rápida, Biomateriais, Alginato, *Scaffolds*, Otimização, Algoritmos Genéticos.

Abstract

REZENDE, Rodrigo Alvarenga, Development of Processes for the Alginate Application onto the Biofabrication: Tese (doutorado) – Faculdade de Engenharia Química, Universidade Estadual de Campinas-SP, 2010.

The seeking for solutions which can rescue the welfare and dignity of accidents victims and diseased people, as lost or damaged organs, has been motivated the fast evolution of Biofabrication. New materials and fabrication techniques have been developed rapidly with computer aiding, which is indispensable part of this process. The study subject of this thesis embraces the development of computational tools and procedures to the Biofabrication, which requires the use of a raw-material. This material is the alginate, a hydrogel came from brown seeweed algae and that has been widely used in many areas for more than fifty years. A mechanical characterization is performed with aiding of a plate rheometer and of a dynamic mechanical analyzer (DMA), as so as a characterization of the chemical behavior, as its swelling capacity and its gelation process, in order to be used as feed source to the applications of computational tools, namely, the Ansys and the optimization technique by genetic algorithms. Ansys is used in the simulation of the pure alginate flow. The Genetic Algorithms help to optimize physical properties of alginate structures.

Key-Words: Biofabrication, Tissue Engineering, Rapid Prototyping, Biomaterials, Alginate, *Scaffolds*, Optimization, Genetic Algorithms.

Sumário

Lista de Figuras

Lista de Tabelas

Lista de Abreviaturas e Termos Estrangeiros

ANSI	Instituto Nacional de Padrões Americanos (*American National Standards Institute*).
ANSYS	Software baseado no método dos elementos finitos que possibilita análises numéricas em diversos campos da engenharia.
ASTM	Sociedade Americana para Ensaios e Materiais (*American Society for Testing and Materials*).
BIOPRINTING	Bioimpressão, técnica de impressão (deposição) camada a camada de materiais biológicos para a fabricação direta de órgãos e tecidos.
CAD	Desenho (projeto) assistido por computador (*Computer Aided Design*).
DMA	Analisador Dinâmico Mecânico.
DSC	Calorimetria Diferencial de Varredura (*Differential Scanning Calorimetry*).
EA	Algoritmos Evolutivos (*Evolutive Algorithms*).
FOAMING	Processo de fabricação de esponjas (em alginato)
FREEZING	Congelamento (com nitrogênio).
GAs	Algoritmos Genéticos (em inglês), uma técnica de otimização.
GELATION	Processo de reticulação (gelação) do alginato após a reação entre o alginato de sódio (puro) e uma solução de cloreto de cálcio.
IBGE	Instituto Brasileiro de Geografia e Estatística.
MEV	Microscopia Eletrônica de Varredura

PR	Prototipagem rápida ou Manufatura Aditiva (ME) de acordo com definições da ASTM.
SCAFFOLD	Estruturas de suporte para a Engenharia de Tecidos, arcabouços, andaimes.
SCB TEST	Ensaio de flexão (*Single Cantilever Bending Test*) simples realizado no DMA.
SQP	Técnica baseada em algoritmos para Otimização contínua não-linear (*Successive Quadratic Programming*).
SWELLING	Capacidade de absorção de fluidos de um material.
TENSION TEST	Ensaio de tensão realizado no DMA.
UNOS	Rede para Compartilhamento de Órgãos dos Estados Unidos (*United Network for Organ Sharing*).

Capítulo 1 – Introdução

A busca por melhor qualidade de vida e pelo prolongamento da expectativa de vida, o envelhecimento da população em diversos países, os atuais cuidados com a saúde (antes não praticados ou não acessíveis), a possibilidade de se proporcionar nova vida com novas perspectivas a vítimas de acidentes ou doenças são alguns das relevantes razões que têm impulsionado a engenharia tecidual, um campo multidisciplinar oriundo da interação direta e complementar entre diversas áreas da medicina aliadas às ciências da vida e engenharia, a um desenvolvimento consistente e promissor por soluções inéditas, beneficiando a humanidade.

Segundo a Rede para Compartilhamento de Órgãos dos Estados Unidos (UNOS, 2010), no início dos nos 90, cerca de 25% dos pacientes na fila por transplantes morriam enquanto esperavam por um doador compatível. A população mundial vem crescendo e as taxas de acidentes e de problemas de saúde não diminuem. As atuais demandas por transplantes de órgãos e tecidos estão muito além da oferta, e por duas décadas, esta carência continua a aumentar. Certamente, a biofabricação tem colaborado no sentido de diminuir estas estatísticas.

Numerosas terapias são disponíveis para combater problemas de saúde, inclusive com transplantes de órgãos e tecidos e, também, o uso de aparelhos pró-estéticos. No entanto, existem limitações de forma que nem todas as soluções tipicamente aplicadas e adaptadas possam suprir todas as funções naturais exercidas pelos tecidos e órgãos perdidos. Em razão disto, estudos têm sido motivados cada vez mais com o propósito principal de se desenvolver novas habilidades de recuperação.

Em pleno século XXI, já não há qualquer hipótese em não se contar com o auxílio da computação, qualquer que seja a área em que se estiver atuando. Há várias e fortes razões para este fato, mas alguns importantes são a rapidez de processamento de cálculos e análises matemáticas, a previsibilidade de fenômenos anteriormente detectados apenas por meio de tentativa-e-erro, a precisão e a consequente minimização

dos erros acumulados, a possibilidade de se variar e repetir condições de análises, dentre outras. Na biofabricação não é diferente. Dada a dimensão em que se trabalha e a precisão exigida, torna-se indispensável o auxílio do computador.

Neste sentido, existe uma forte interação da biofabricação, com a engenharia tecidual e os *scaffolds*. A biofabricação, por sua vez, consiste na aplicação de técnicas de engenharia para viabilizar a obtenção de substitutos biológicos para tecidos vivos ou órgãos humanos. Essas técnicas devem possibilitar a mimetização de estruturas vivas, tanto em forma quanto em função, tornando possível substituir tecidos defeituosos ou faltantes.

1.1 Objetivos

Partindo-se da prerrogativa de que, a biofabricação é hoje um ramo da ciência de relevância global, o aperfeiçoamento das técnicas desenvolvidas, ou ainda em desenvolvimento, nesta área, seja para a fabricação de artefatos propriamente dita para a reparação de órgãos e/ou tecidos danificados, seja para a melhoria das técnicas virtuais de design de novas estruturas, o caráter preditivo na elaboração e concepção destas novas estruturas, virtual ou realisticamente, torna-se irrevogável.

À predição de processos e de otimização é garantido um posto de destaque na biofabricação e, mais do que isso, de necessidade no sentido de se antever de que forma a fabricação se dará da melhor maneira, ou seja, quais são as configurações ótimas para se atender a melhor qualidade e se obter o artefato mais adequado para a aplicação a ser atendida.

O presente trabalho tem como objetivo desenvolver e aplicar ferramentas computacionais à biofabricação, tomando-se como material compatível o alginato, um biomaterial natural. Faz-se necessária a realização de etapas precedentes que funcionam como base para obtenção dos resultados esperados. Estas etapas são descritas a seguir:

a) A análise do comportamento reológico (viscoelástico) do alginato puro (de sódio);

b) A análise do comportamento mecânico do alginato de cálcio (reticulado), em especial a sua deformação, sob diferentes condições de composição de alginato e de cloreto de cálcio, tensão, temperatura e frequência;

c) A verificação do processo de reticulação (gelação) entre o alginato de sódio e o cloreto de cálcio;

d) A análise da capacidade de inchamento do alginato, por perda de massa, sob diferentes condições físicas;

Após o cumprimento destas etapas, os objetivos principais, os quais são mencionados a seguir, tornam-se exequíveis:

1. O ajuste de um modelo reológico aproximado e representativo do comportamento viscoelástico do alginato de cálcio;

2. A fabricação de esponjas em alginato, incluindo o método de fabricação e a morfologia das mesmas;

3. Uma análise incipiente do escoamento do alginato de sódio em superfície lisa através do método dos elementos finitos por meio do software Ansys;

4. A otimização de propriedade mecânica de estruturas em alginato, quando da sua degradação, por meio de algoritmos genéticos.

1.2 Organização da Tese

A Tese está distribuída em oito capítulos que são compostos por artigos publicados ou submetidos para periódicos internacionais e congressos.

O Capítulo 1 apresenta os objetivos do trabalho, bem como, a relação entre os assuntos tratados em cada capítulo por meio de um diagrama.

O Capítulo 2 apresenta uma breve revisão bibliográfica com conteúdo relacionado a assuntos como a prototipagem rápida, a engenharia tecidual, a biofabricação, biomateriais, dentre outros.

O Capítulo 3 descreve os trabalhos desenvolvidos com o alginato de sódio, isto é, antes da sua reticulação com cloreto de cálcio. Ensaios mecânicos foram conduzidos com um reômetro de pratos.

O Capítulo 4 avança para a caracterização do alginato pós-reticulação, ou seja, o alginato de cálcio. Experimentos mecânicos também foram realizados, porém, com um analisador dinâmico mecânico (DMA).

O Capítulo 5 descreve os ensaios voltados para os efeitos determinados a partir da composição das soluções de alginato de sódio e cloreto de cálcio sobre o inchamento (swelling), reticulação e preparação de esponjas.

O Capítulo 6 apresenta uma simulação no software Ansys em que, a partir de dados obtidos experimentalmente no Capítulo 1, é verificado o comportamento de escoamento do alginato de sódio em uma superfície lisa.

O Capítulo 7 mostra uma aplicação dos algoritmos genéticos na biofabricação em que se buscam composições iniciais ótimas de material para a obtenção de artefatos com as melhores propriedades possíveis ao longo de sua deterioração.

O Capítulo 8 apresenta as conclusões verificadas deste trabalho, além de relacionar possíveis progressos através de sugestões para futuros desenvolvimentos na continuidade desta linha de pesquisa.

O diagrama ilustrado na Figura 1.1 exibe a relação existente entre os capítulos da tese.

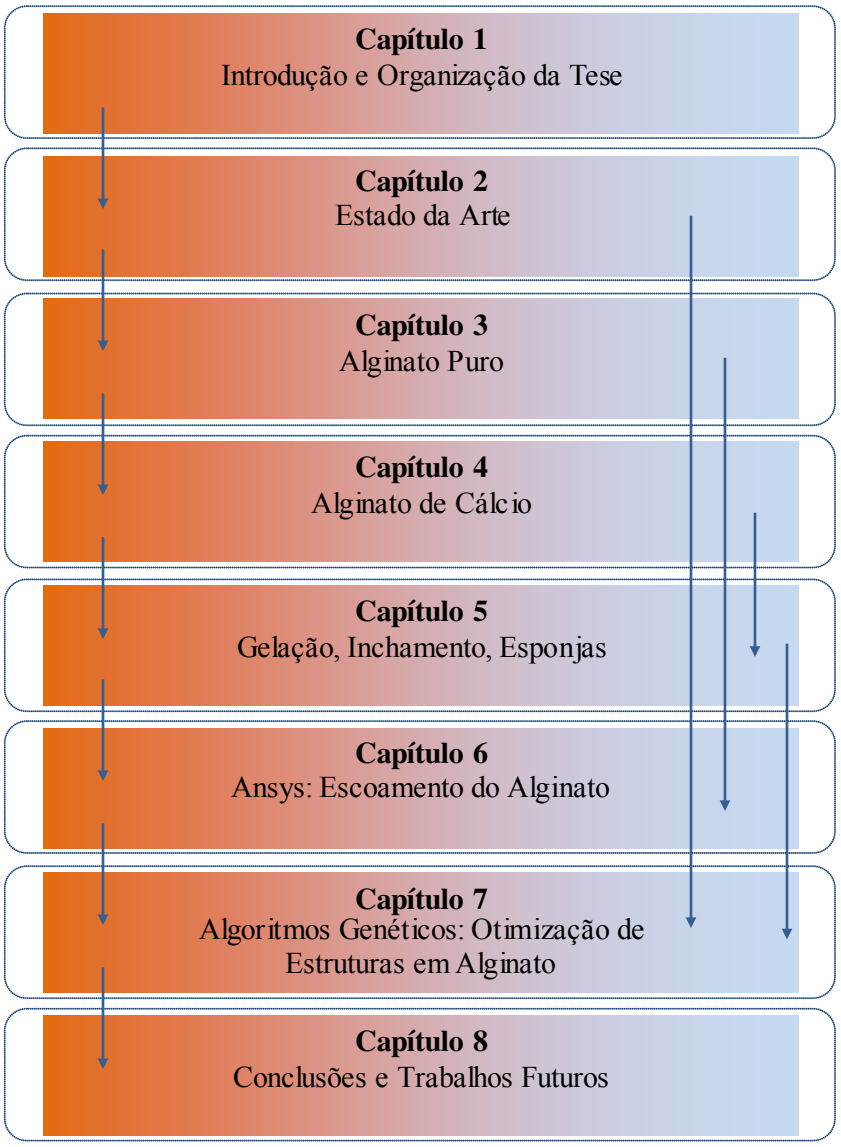

Figura 1. 1 Diagrama ilustrativo da relação entre os capítulos da tese.

1.3 Contribuições da Tese

Dentre as contribuições desta tese, destacam-se:

- A caracterização física de um biomaterial para o desenvolvimento de ferramentas computacionais e futura aplicação como matéria-prima compatível de um novo sistema de prototipagem rápida por extrusão;

- A possibilidade do uso de ferramentas computacionais, como o Ansys, para a análise de fenômenos físicos e do comportamento do biomaterial para o emprego na biofabricação.

- Desenvolvimento de um método para a otimização de estruturas em alginato por algoritmos genéticos.

1.4 Realização do Trabalho

O trabalho foi realizado em forma de Doutorado-Sanduíche no âmbito da parceria entre a Faculdade de Engenharia Química da Universidade Estadual de Campinas (UNICAMP) e o Departamento de Engenharia Mecânica do Instituto Politécnico de Leiria (IPL), em Leiria, Portugal, com os auxílios da Fundação para a Ciência e a Tecnologia (FCT) de Portugal e do Conselho Nacional de Desenvolvimento Científico e Tecnológico (CNPq) do Brasil.

Capítulo 2 – Estado-da-Arte e Conceitos Fundamentais

2.1 Introdução

O mau funcionamento ou a perda de funções totais ou parciais de um órgão ou tecido, resultante de doenças ou ferimentos é atualmente um dos mais importantes e preocupantes problemas de saúde pública atingindo um número muito significativo de pessoas mundialmente. O transplante de tecido do próprio doente ou de um doador continua a ser a técnica mais utilizada para tratar defeitos nos tecidos ou órgãos provocados por doenças ou acidentes. No entanto, esta prática apresenta sérias limitações devido à escassez de doadores, ao risco de transmissão de doenças e/ou de rejeição imunológica e ao problema da lesão dos tecidos envolventes que normalmente ocorre no local de onde é removido o tecido para o transplante.

Além disto, os custos socioeconômicos agregados e o envelhecimento vertiginoso da população, por exemplo, em países como Brasil, Espanha e Portugal, são domínios que constituem preocupação internacional, sendo objetos de significativo trabalho de pesquisa e merecedor de forte investimento público e privado.

No Brasil e na comunidade iberoamericana, nos últimos anos, sucederam-se iniciativas importantes no âmbito da biofabricação. Em 2007, foi criada a Rede Iberoamericana de Biofabricação (Rede BIOFAB), integrando 7 países (Portugal, Brasil, Espanha, México, Cuba, Venezuela e Argentina). A Rede BIOFAB tem como objetivo se desenvolver e compartilhar trabalhos de pesquisa que vêm sendo realizados de forma dispersa na comunidade Iberoamericana no âmbito da biofabricação e acentuar de forma dirigida este domínio de investigação multidisciplinar, fundamental no âmbito da medicina regenerativa.

Em 2009, foi criado o Instituto Nacional de Biofabricação (INCT-BIOFABRIS), composto oficialmente por 11 instituições brasileiras. O Instituto BIOFABRIS destina-se ao desenvolvimento de uma metodologia integrada para a biofabricação de estruturas bioativas de modo a promover e melhorar o desempenho de órgãos ou tecidos a partir de uma abordagem multidisciplinar, envolvendo conhecimentos na área da engenharia, ciências da vida e ciências básicas.

Segundo dados do Banco Mundial, a população mundial com 65 anos ou mais aumenta na média de 795 mil pessoas por mês. Os países em desenvolvimento são responsáveis por 77% desse crescimento. Em números absolutos, significa que, em 2025 haverá 816 milhões de idosos. O IBGE divulgou estudo feito a partir dos censos de 1991 e de 2000, mostrando que em 1991 havia 7 milhões de brasileiros com mais de 65 anos de idade. Em 2000, esse contingente chegou a 9,9 milhões, um acréscimo de 41%. Como o aumento dos idosos, por sua vez, foi também superior ao aumento do total da população, a proporção dos que tinham mais de 65 anos no total da população cresceu de 4,8% para 5,8% nesse período. Este processo de envelhecimento populacional não é lento a exemplo de países como a França que a sua população idosa dobrou de 7% para 14% em 120 anos (1865-1980), já no Brasil isto poderá ocorrer num período de 25 anos (2011 a 2036). Assim, espera-se que em 2020, uma em cada 13 pessoas tenha 65 anos ou mais, totalizando 16,2 milhões de idosos (Miguel Junior, 2006).

Nos Estados Unidos, segundo a Rede Norte-Americana para Compartilhamento de Órgãos, a UNOS (*United Network for Organ Sharing*), do total de pacientes que aguardam algum transplante de órgão, 25% morrem esperando por um doador compatível [UNOS (2010); Vacanti and Vacanti (1997) and Yang *et al.* (2002)]. As atuais demandas por transplantes de órgãos e tecidos superam, em muito, a sua oferta [UNOS (2010); Cohen *et al.* (1993)]. Segundo algumas projeções indicam, estas demandas vão se ampliar nos próximos anos. Tais estatísticas têm sido melhoradas com os novos desenvolvimentos da engenharia tecidual.

E, como se estes processos naturais não acontecessem rapidamente o bastante, nós alcançamos uma capacidade enorme para mutilar, esmagar, quebrar, e desfigurar o

corpo humano com veículos motores, armas e ferramentas ou como resultado de nossa participação em práticas esportivas. Uma consequência destas causas naturais e antinaturais de deterioração do corpo humano é que cerca de 2 milhões a 3 milhões de partes artificiais ou protéticas são implantadas em indivíduos nos Estados Unidos a cada ano (Oréfice, 2006).

Em 2003, levando-se em conta apenas os Estados Unidos, quase 88 mil pacientes integravam a lista de espera para transplantes (Mendes *et al.*, 2003). Em junho de 2007, este número foi elevado para 96,6 mil pacientes. Em maio de 2010, da lista constavam mais de 107 mil pacientes (UNOS, 2010). A Tabela 2.1 apresenta a distinção dos órgãos aguardados para transplantes, de acordo com a UNOS.

Tabela 2. 1 Dados da fila de espera por transplante de órgãos nos Estados Unidos (UNOS, 2010) e Brasil (Ministério da Saúde, 2010).

	Ano			
Órgãos esperados	**2003**	**2007**	**2010**	**2009**
	EUA			**BRASIL**
Rim	58.125	72.015	84.814	34.640
Fígado	17.660	16.855	15.989	4.304
Pâncreas	1.434	1.686	1.450	124
Rim/Pâncreas	2.468	2.337	2.177	576
Coração	3.736	2.702	3.145	305
Pulmão	3.937	2.724	1.825	161
Coração/Pulmão	184	119	80	-
Intestino	173	231	244	-
Córneas	-	-	-	23.756
Total (com córneas)	-	-	-	63.866
Todos os órgãos (sem córneas)	**87.717**	**96.670**	**107.379**	**40.110**

2.2 A Engenharia Tecidual

O termo "engenharia tecidual", introduzida pela primeira vez em 1987 durante uma reunião organizada pela Fundação Nacional para a Ciência, dos Estados Unidos, foi definida por Skalak e Fox (1988), como "a aplicação de princípios e métodos de engenharia e das ciências da vida em prol do entendimento fundamental das relações estrutura-função em tecidos normais e patológicos de mamíferos e do desenvolvimento de substitutos biológicos para recuperar, manter ou melhorar função".

Um *scaffold* é uma estrutura de esqueleto artificial tridimensional que serve como uma réplica de uma matriz extracelular para a adesão celular, migração, proliferação, e regeneração de tecidos em três dimensões. Sua arquitetura e microestrutura definem o formato final e estrutura dos tecidos e órgãos regenerados (Shi, 2006).

De acordo com o Instituto Nacional de Padrões Americano (ANSI), por meio da norma ASTM F2150-07, os *scaffolds* podem ser potencialmente metálicos, cerâmicos, poliméricos, naturais ou materiais compósitos. *Scaffolds* são normalmente porosos em algum grau, mas podem ser sólidos. Os *scaffolds* podem variar de mecanicamente rígido para gelatinoso e podem ser ou absorvíveis/degradáveis ou não-absorvíveis/não-degradáveis. O *scaffold* pode ou não ter um tratamento de superfície.

As técnicas de prototipagem rápida, mais recentemente também denominadas por técnicas de manufatura aditiva (ASTM F.42), habilitam a engenharia tecidual a um controle refinado no que diz respeito ao projeto, à fabricação e à modelagem de *scaffolds*, proporcionando um canal de aprendizado sistemático na investigação de interações célula-matriz. A prototipagem rápida é um candidato promissor, porém com resultados já bastante consolidados, servindo como uma metódica fronteira entre os tecidos e a engenharia (Yeong *et al.*, 2004).

Posteriormente, Langer e Vacanti (1993) definiram engenharia tecidual como "um campo interdisciplinar que aplica os princípios de engenharia e das ciências da vida em

prol do desenvolvimento de substitutos biológicos para recuperar, manter ou melhorar função". Este é um campo multidisciplinar (Figura 2.1), também conhecido por medicina regenerativa, desenvolvido para direcionar o problema de carência de órgãos. Desde o estabelecimento desde campo em 1990, o número de tipos de tecidos cultivados, biomateriais aplicáveis, fatores morfogênicos e técnicas de engenharia têm aumentado rapidamente, assim como a possibilidade de aplicações *in vivo* (ainda em animais) e *in vitro*.

Segundo Tsang e Bathia (2004), a engenharia tecidual tipicamente envolve a construção de estruturas de tecidos a partir da combinação de células e biomateriais, com o objetivo final de substituir ou restaurar funções fisiológicas perdidas, em órgãos enfermos ou danificados.

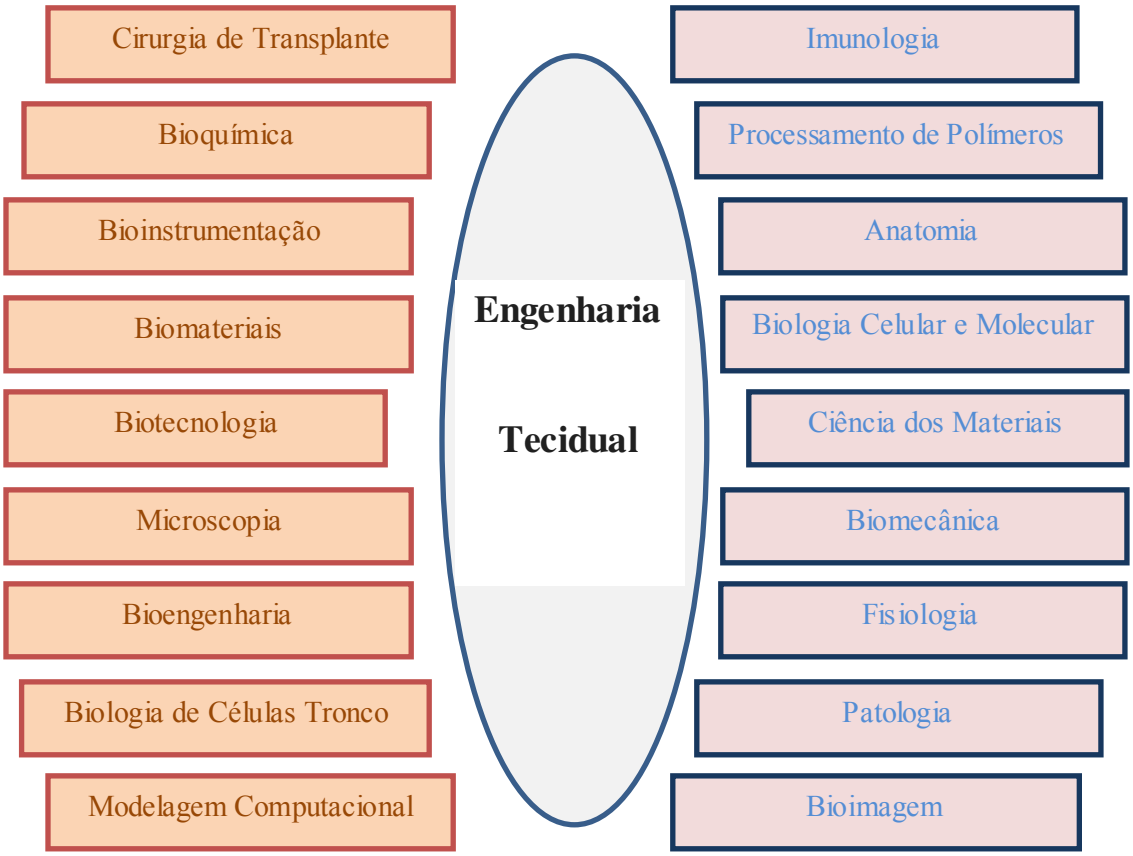

Figura 2. 1 Multidisciplinas da engenharia tecidual Langer e Vacanti (1993).

Estratégias terapêuticas em engenharia tecidual envolvem a obtenção, a seleção, o cultivo, a proliferação e a implantação celular, onde células oriundas de uma fonte endógena (autólogo (mesmo ser); homólogo (outro ser); heterólogo (outra espécie)) do paciente ou de um doador ou são injetadas no tecido danificado ou são combinadas *in vitro* com *scaffolds* biorreabsorvíveis e então implantadas, e a regeneração do tecido onde um *scaffold* implantado diretamente do tecido danificado estimula as células a promoverem o reparo local do tecido (Bártolo, 2006).

O aspecto mais complexo de *scaffolds* projetados é a apresentação de sinais ou estímulos pelo *scaffold* e externo (elétricos/mecânicos) apropriados para guiar o desenvolvimento de um tecido que preencha a função e estrutura requeridas. Uma premissa fundamental das abordagens condutiva, indutiva e de transplante é que as células que ocupam o *scaffold* têm o potencial de regenerar o tecido desejado e recuperar sua função. De todo modo, para realizar este potencial o *scaffold* deve fornecer o ambiente favorável para suportar e estimular os processos celulares envolvidos no desenvolvimento do tecido, tal como proliferação, migração, deposição de matriz e diferenciação.

A engenharia tecidual consiste em um conjunto de conhecimentos e técnicas para a reconstrução de novos órgãos e tecidos. Baseada em conhecimentos das áreas de ciência e engenharia de materiais, biológica e médica, a técnica envolve a expansão *in vitro* de células viáveis do paciente doador sobre suportes de polímeros bioreabsorvíveis. No desenvolvimento e na seleção desses materiais, o tempo de degradação é fundamental para o sucesso do implante. Os estudos e os desafios atuais são normalmente direcionados ao entendimento das relações entre composição química, cristalinidade, morfologia do suporte, e o processamento desses materiais (Barbanti et. al., 2005). Daí, a importância do estudo mecânico e químico dos biomateriais.

A abordagem da engenharia tecidual permite manipulações experimentais em três níveis: as células, os polímeros e o método de construção (Jennifer *et al.*, 1998).

2.3 Biofabricação

Embora muitos fatores responsáveis pelo envelhecimento não sejam compreendidos, as conseqüências estão bastante claras. Nossos dentes causam dor, nossas articulações tornam-se artríticas, ossos ficam frágeis e quebram, os poderes de visão e audição diminuem e podem ser perdidos, o sistema circulatório mostra sinais de bloqueio, e o coração perde controle de seu ritmo vital de bombeamento ou suas válvulas perdem a capacidade de vedação. Tumores aparecem quase aleatoriamente em ossos, seios, pele e órgãos vitais (Oréfice, 2006).

A biofabricação utiliza células ou componentes biológicos como a blocos de construção básicos em que modelos biológicos, sistemas, equipamentos e produtos são produzidos (Sun, 2009). Por esta razão, a biofabricação é, também, de uma maneira mais geral, conceituada como todo artefato construído por manufatura aditiva para a aplicação na engenharia tecidual cuja construção se faz por meio de técnicas de prototipagem rápida, usando-se como matérias-primas, biomateriais, ou seja, materiais que apresentem comportamento de compatibilidade biológica quando no organismo humano, sem provocar reações de rejeição.

A biofabricação pode ser definida como a produção de produtos biológicos complexos vivos e não-vivos a partir de matérias-primas, tais como células vivas, moléculas, matrizes extracelulares e biomateriais. Um *scaffold* é uma estrutura temporária de suporte e, de acordo com a definição, ele deve ser biodegradável (Hutmacher, 2004).

O domínio da biofabricação é um domínio emergente. A biofabricação compreende a integração de aspectos computacionais, novas técnicas de processamento e síntese e desenvolvimento de materiais através da adoção de estratégias bioinspiradas. A expressão biomimetismo emerge exatamente dessa potencialidade da biofabricação de reproduzir partes do corpo humano tanto no domínio macroscópico (anatômica) como microscópico e nas propriedades físicas, químicas e biológicas.

Os processos de biofabricação, através das técnicas de manufatura aditiva, são relativamente recentes, viabilizam a customização de um modelo a ser produzido, além de serem baseados numa construção tridimensional, camada a camada, o que garante a alta precisão na manufatura aditiva e a boa qualidade do produto final. Normalmente, são construídos protótipos para utilizações médicas, tais como implantes ou *scaffolds*. Espera-se que o contínuo aprimoramento dos processos de prototipagem rápida, com novas técnicas e materiais, possa permitir no futuro que se realize transplantes completos de órgãos, desenvolvidos por uma máquina para um ser humano – cuja técnica é conhecida por autoestruturação (Mironov, 2003) – e abre a perspectiva da eliminação das filas de transplante de órgãos e a melhoria da qualidade de vida de centenas de milhares de pessoas particularmente nos países pobres.

Uma das técnicas atualmente estudadas para este tipo de aplicação (biomimetismo) consiste no uso de tecnologia de prototipagem rápida industrial (impressão 3D) para materializar estruturas por deposição camada a camada em biomateriais, de modo a permitir a colonização por células vivas para estruturação de tecidos. Além disso, técnicas evoluídas da prototipagem rápida industrial, capazes de manipular e depositar controladamente células vivas em um processo de construção por camadas podem vir a revolucionar a biofabricação, permitindo a obtenção direta de tecidos e até mesmo órgãos completos diretamente.

A conjugação dessas técnicas e o desenvolvimento de novas, capazes de manipular diretamente células vivas e guiar seu crescimento integrado a tecidos originais do paciente, compõem os desenvolvimentos e pesquisas mais atuais na área de biofabricação.

Como tecnologia emergente de proporções globais e com possibilidade de oferecer soluções revolucionárias, a biofabricação consolida-se como uma tecnologia que está diretamente comprometida com o bem-estar e com as recuperações física e psicológica de pessoas com graves problemas de saúde, ocasionados por defeitos em tecidos ou órgãos ou por danos corpóreos causados por acidentes.

A transferência de tecnologia da prototipagem rápida para a engenharia tecidual pode ser a chave para se produzir *scaffolds* com geometrias externas e internas customizadas e predefinidas, e morfologias internas reproduzíveis, o que pode não apenas controlar o tamanho de poros, porosidade e a distribuição de poros, como também fazer estruturas para maximizar o transporte de massa de oxigênio e nutrientes em todo o *scaffold*. É apreciável que o controle computacional de complexas características internas dos *scaffolds* (tais como as acima mencionadas, além de um sistema vascular artificial), suportado pelas técnicas de prototipagem rápida, seja um grande ganho para a engenharia tecidual (Sachlos *et al.*, 2003).

Só em 2006, foram investidos mais de 600 milhões de Euros na Europa, sendo uma parte significativa destinada às áreas da prototipagem virtual em medicina e das tecnologias de produção de dispositivos para aplicações médicas.

A utilização de biomateriais como matéria-prima da prototipagem rápida criou a condição para fabricação direta (sem necessidade de moldes) de *scaffolds* que, diferentemente daqueles construídos por métodos convencionais, exibem excelente conformidade anatômica associada a uma microestrutura que contribue para o crescimento tecidual.

2.4 Biomateriais

O termo biomaterial é definido como qualquer substância ou combinação de substâncias sintéticas ou de origem natural, as quais podem ser usadas por um determinado período de tempo, como um todo ou parte de um sistema que trata, estimula o crescimento ou substitui qualquer tecido, órgão ou função do corpo (Ratner et. al, 1996).

De acordo com a *National Institutes of Health Biomaterials Consensus Conference* (NIH, 1982), "biomaterial é qualquer substância que não droga, ou combinação de substâncias de natureza sintética ou natural que pode ser usada por qualquer período de

tempo, como um todo ou parte do sistema que trata, aumenta ou substitui, qualquer tecido, órgão ou função do corpo". Posteriormente, assumiu-se como nova definição de biomaterial "todo material não vivo, usado em um dispositivo médico (ou biomédico), objetivando a interação com o sistema biológico (Williams, 1987; Callegari, 2004).

Desde a década de 1960, estruturas temporárias, confeccionados de polímeros bioreabsorvíveis, ganharam uma importância crescente na área médica, sendo utilizados em um amplo número de aplicações no corpo humano, tais como: suturas cirúrgicas, sistemas para liberação controlada de drogas, stents e dispositivos ortopédicos. Atualmente fazem parte do cotidiano dos centros cirúrgicos no mundo inteiro (Barbanti *et al.*, 2005).

Nas décadas de 1960 e 1970, a primeira geração de materiais foi desenvolvida para uso interno no corpo humano. Uma facilidade comum à maioria destes materiais foi possuir uma característica biologicamente inerte. O sucesso clínico de implantes bioinertes, bioativos e absorvíveis foi uma importante resposta às necessidades médicas de uma população com ligeiro envelhecimento. Subsequentemente, o campo dos biomateriais começou a desviar sua atenção das respostas de tecidos para a produção de componentes bioativos que pudessem evocar reações e ações controladas dentro do corpo.

Na metade dos anos 1980, materiais bioativos passaram a vigorar nas atividades clínicas em uma variedade de aplicações dentais e ortopédicas. Tais materiais incluíram composições de vidros, cerâmicos, vidro-cerâmicos e compósitos bioativos, assim como uma faixa de polímeros bioabsorvíveis. Ao passo que biomateriais de segunda geração foram projetados tanto para serem reabsorvíveis ou bioativos, muitas outras abordagens terapêuticas foram, a partir de então, sendo consideradas para combinar estas duas propriedades no desenvolvimento de implantes, os quais induzem a modalidade de cura regenerativa. Em outras palavras, ajudando o corpo humano a se recuperar por si só (Azonano, 2006).

Embora muitos dispositivos artificiais para a engenharia tecidual estejam disponíveis, poucos podem substituir completamente todas as complexas funções biológicas. Em situações clínicas mais severas somente o transplante do órgão retoma as atividades orgânicas. Assim, de uma forma idealizada, a melhor alternativa seria obter um novo órgão ou tecido, substituindo aquele que não desempenha normalmente suas funções. Nos dias de hoje, a idéia da reconstrução de órgãos e tecidos criados em laboratório é amplamente difundida e investigada no mundo todo (Barbanti *et al.*, 2005).

Nos últimos 15 anos, tem havido avanços significativos nos campos da ciência dos materiais inteligentes e estruturados, assim como, novos estudos no âmbito das propriedades nanométricas dos materiais. Um interesse significativo tem sido mostrado no uso de polímeros naturais, sintéticos ou hidrofílico biohíbridos e como transportadores para a liberação controlada de drogas. Biomateriais como polímeros, cerâmicos e metais têm sido empregados por muitos anos na medicina. A habilidade de se projetar tradicionais polímeros hidrofílicos com propriedades de materiais específicas é dificultada pela falta de controle do peso molecular, pela configuração de cadeia e pela cinética de polimerização.

Um biomaterial é usado para se construir dispositivos voltados para a substitutição de parte ou de função do corpo humano de uma maneira segura, confiável, econômica e fisiologicamente aceitável (Hench and Erthridge, 1982). Uma variedade de dispositivos e materiais frequentemente usados no tratamento de doenças ou danos incluem itens rotineiros tais como suturas, costuras, cateteres, pratos, preenchimentos dentários etc. Alguns exemplos de dispositivos que usam biomateriais relacionados a determinados órgãos podem ser conferidos na Tabela 2.2.

O desenvolvimento de novos biomateriais requer um grau de predição de controle no projeto, síntese e função da próxima geração de materiais. Desenvolvimentos recentes incluem o projeto e a síntese de novos hidrogéis e suas aplicações na engenharia tecidual, na liberação controlada de drogas e na bionanotecnologia. Em engenharia tecidual, hidrogéis podem ser usados para levar sinais para as células, para atuar como *scaffolds* para crescimento e função celular, e prover preenchimento de espaço.

Características desejadas de *scaffolds* em hidrogel incluem parâmetros físicos tais como a pequena, mas máxima, resistência mecânica e degradabilidade e a habilidade para propiciar um microambiente biologicamente relevante (Peppas *et al.*, 2006).

Tabela 2. 2 Biodispositivos em órgãos (adaptado de Park e Bronzino, 2003)

Órgão	Exemplos
Coração	Marcapasso, válvula artificial
Pulmão	Máquina de oxigênio
Olhos	Lentes de contato, lentes intraoculares
Ouvidos	Estribo artificial
Ossos	Placa, haste intramedulária
Rim	Equipamento de diálise
Bexiga	Cateter ou *stent*
Dente	Compósitos com alginato, ligas metálicas
Pele	Peles artificiais

As propriedades dos materiais podem ser divididas em dois grupos: propriedades mecânicas e físicas. As propriedades mecânicas descrevem como o material se comporta quando submetido a uma força aplicada. As propriedades mais comuns estão relacionadas com a resistência mecânica do material (o limite de resistência, o módulo de elasticidade, a dureza etc) ou a capacidade de deformação do material (ductilidade). Dependendo das condições de solicitação (p.ex., cargas de impacto, ciclos alternados de aplicação de carga) a resposta do material pode ser alterada e propriedades específicas determinadas nestas condições são definidas para melhor descrever seu comportamento mecânico. As propriedades físicas incluem propriedades elétricas, magnéticas, ópticas, térmicas e químicas (Oréfice, 2006).

Hidrogéis baseados em polímeros sintéticos ou naturais têm sido de grande interesse para o encapsulamento de células e para o campo de matrizes para a engenharia tecidual (Lee and Mooney, 2001).

As principais vantagens de biopolímeros naturais são:

- ✓ Subproduto atóxico
- ✓ Baixa toxicidade;
- ✓ Biocompatibilidade;
- ✓ Transporte de proteínas específicas ligando determinadas partes do corpo e outros sinais bioquímicos que podem ajudar na cicatrização/cura ou integração tecidual.

As limitações dos biopolímeros naturais são:

- ✓ Problemas de imunogenicidade (capacidade de induzir uma resposta imune detectável);
- ✓ Tendência a perder suas propriedades naturais ou sofrer decomposição a temperaturas abaixo de seus pontos de fusão.
- ✓ Subprodutos de degradação tóxicos;
- ✓ A relação resistência mecânica versus degradação.

Uma gama de hidrogéis biodegradáveis e biocompatíveis, como o alginato, têm sido utilizados na engenharia tecidual. O alginato é um material bastante utilizado devido ao seu relativo baixo custo, origem natural e fácil manuseio, além de vantagens relacionadas às suas propriedades físicas.

O alginato é um polissacarídeo natural relativamente abundante com potencial para a fabricação de biofilmes devido às suas propriedades colodais e para a produção de *scaffolds* para engenharia tecidual. É um copolímero linear constituído por blocos de (1-4) β-D- ácido manurônico (unidades M) eode -L ácido gulurônico (unidades G) extraído de diversas espécies de algas pardas. O alginato pode reagir com íons divalentes, por exemplo, de cálcio, formando um gel ou com íons polivalentes formando ligações cruzadas. As propriedades físicas e mecânicas dependem da proporção e dimensão dos blocos G na cadeia de alginato. A composição natural do alginato bem como o arranjo sequencial entre os blocos M e G variam de acordo com as espécies de algas exploradas, como pode ser visto na Tabela 2.3.

Tabela 2. 3 Composição típica da relação M/G para diferentes espécies de algas marrons (FMC, 2010).

Laminaria hyperborean(stem)	30	70
Laminaria hyperborean(leaf)	55	45
Laminaria japonica	65	35
Lessonia nigrescens	60	40
Durvillaea antarctica	71	29
Durvillaea potarum	77	23
Macrocystis pyrifera	60	40
Ascophyllum nodosum	65	35

Segundo Silva (2009), estudos reológicos e de dispersão de luz com alginatos sugerem que os blocos aumentam a rigidez do gel na seqüência G > MG > M. Um polímero volumoso e rígido é encontrado nas regiões de blocos G, tendo as regiões MG rigidez intermediária (Smidsrød, 1974). Segmentos da cadeia consistindo de resíduos G e M alternados não interagem com o cálcio, mas servem para formar as estruturas agregadas, produzindo uma rede tridimensional (Kester e Fennema, 1986).

Segundo Rosiak e Yoshii (1999), os biomateriais desempenham um papel fundamental na maioria das abordagens da engenharia tecidual, como substitutos para a reposição funcional, para componentes de dispositivos relacionados à terapia e à diagnose, para sistemas de liberação controlada de drogas e para *scaffolds* direcionados ao crescimento controlado de tecidos. Os materiais mais comuns utilizados na engenharia tecidual são descritos na Tabela 2.4:

Tabela 2. 4 Materiais para uso no corpo (adaptado de Park e Bronzino, 2003)

Materiais	Vantagens	Desvantagens	Exemplos
Polímeros *(naturais e sintéticos).*	*Elásticos, de fácil fabricação.*	*Não resistentes, deformam com o tempo, podem degradar.*	*Suturas, vasos sanguíneos, orelha, nariz, outros tecidos moles.*
Metais *(titânio e ligas de titânio, ligas de Co-Cr, aços inoxidáveis, prata, ouro, platina etc).*	*Resistentes, dúcteis, robustos.*	*Podem sofrer corrosão, denso.*	*Substituição de articulações, parafusos e placas para ossos, implantes de raízes dentárias, arame para suturas.*
Cerâmicos *(óxido de alumínio, fosfatos de cálcio incluindo hidroxiapatita, carbono).*	*Bastante compatíveis, inertes, resistentes na compressão.*	*Quebradiços, não-elásticos.*	*Acetábulos, revestimento de dentes e implantes ortopédicos e próteses dentárias.*
Compósitos *(carbono-carbono, cabo ou fibra reforçada para cimento ósseo).*	*Resistente, sob medida.*	*Processamento.*	*Implantes de articulações, válvulas de coração.*

2.5 Artigo produzido

A fabricação de *scaffolds* na engenharia tecidual é um tópico-chave. Desde que os pesquisadores iniciaram os desenvolvimentos na engenharia tecidual, muitos métodos de fabricação foram criados e empregados. Os métodos primordiais, chamados de Métodos Convencionais, foram indispensáveis para o desenvolvimento desta ciência e, durante muitos anos, reinaram sem técnicas concorrentes. Os métodos convencionais atualmente ainda utilizados na construção de *scaffolds* são, por exemplo, fabricação baseada em fibras trançadas e não-trançadas, fundição de solventes, separação de fases, processo de alta pressão, usinagem, moldes por injeção e prensagem fria ou quente, de acordo com YANG *et al.* (2001). Estes métodos apresentam algumas vantagens, porém muitas limitações que têm comprometido sua longa-vida. Estas limitações

compreendem a pequena capacidade, mais precisamente, do controle de tamanho, da geometria, da interconectividade e da distribuição espacial dos poros e da construção interna dos canais dentro de *scaffolds*. Tais requisitos são estritamente necessários para que o *scaffold* possa suprir as expectativas no seu uso. Além disto, métodos baseados em solventes devem garantir a remoção de todos os solventes residuais o que poderia destruir a arquitetura dos poros.

A engenharia tecidual tem sido utilizada para reparar falhas ou mal-funcionamento de órgãos como pele, fígado, pâncreas, válvulas do coração, ligamentos, cartilagem e ossos. Isto tem aumentado o interesse em aplicações com técnicas de prototipagem rápida para se construir *scaffolds* para células transplantadas para suporte e crescimento das mesmas. Estes *scaffolds* podem ser desenhados em 3D em CAD. Levando-se em conta a porosidade e a interconectividade para que a indução de tecido possa ocorrer. A função das células, assim como em regeneração de ossos e cartilagem, é dependente das relações espaciais tridimensionais. Assim sendo, a geometria desses tecidos "sólidos" é crítica em suas funções. A prototipagem rápida tem sido hábil e útil na produção de *scaffolds* de geometrias complexas.

O Capítulo 2 é complementado através do artigo intitulado "**Advanced Processes to Fabricate *Scaffolds* for Tissue Engineering**", o qual foi publicado como capítulo integrante do livro "Virtual Prototyping & Bio Manufacturing in Medical Applications" (pp.149-170, 2008).

Este artigo apresenta conceitos de engenharia tecidual, *scaffolds* e seus requisitos mecânicos e biológicos, além de uma abordagem rápida sobre as técnicas convencionais de fabricação de *scaffolds* e uma abordagem mais extensa das técnicas mais modernas, também conhecidas como prototipagem rápida.

Chapter 8
Advanced Processes to Fabricate Scaffolds for Tissue Engineering

Paulo J. Bártolo, Henrique A. Almeida, Rodrigo A. Rezende, Tahar Laoui and Bopaya Bidanda

8.1 Introduction

Tissue engineering is an interdisciplinary field that necessitates the combined effort of cell biologists, engineers, material scientists, mathematicians, geneticists, and clinicians toward the development of biological substitutes that restore, maintain, or improve tissue function (Fig. 8.1). It comprises tissue regeneration and organ substitution (Table 8.1). The first definition of tissue engineering was provided by Skalak and Fox (1988) who stated it to be "the application of principles and methods of engineering and life sciences toward the fundamental understanding of structure-function relationships in normal and phatological mammalian tissues and the development of biological substitutes to restore, maintain, or improve tissue function". An historical overview of this field can be found in a recent report published by National Science Foundation, USA (2003).

Three strategies have been explored for the creation of a new tissue (Fuchs et al. 2001; Langer, 1997; Langer and Vacanti, 1993):

- The use of isolated cells or cell substitutes. This strategy avoids potential surgical complications but has the disadvantages of possible rejection or loss of function.
- Tissue-induced substances. The success of this strategy depends on the growth factors and controlled released systems
- Cells placed on or within constructs. This is the most common strategy and involves either a closed or an open system. In a closed system, cells are isolated from the body by a permeable membrane that allows exchange of nutrients and wastes and protects cell from the immune response of the body. An open system begins with the in vitro culture of cell, which are then seeded onto a scaffold. The cells-matrix construct is then implanted into the body.

Cells used in tissue engineering may be allogenic, xenogenic, syngeneic or autologous (Fuchs et al. 2001). They should be nonimmunogenic, highly proliferate, easy to harvest and with high capacity to differentiate into a variety of cell types with specialized functions (Fuchs et al. 2001; Marler et al. 1998). Cell attachment to materials is correlated to many factors, such as the stiffness and attachment area. Skeletal muscle satellite cells, cardiomyocytes and endothelial cells have been used in many tissue engineering applications.

B. Bidanda and P. J. Bártolo (eds.), *Virtual Prototyping & Bio Manufacturing in Medical Applications.*

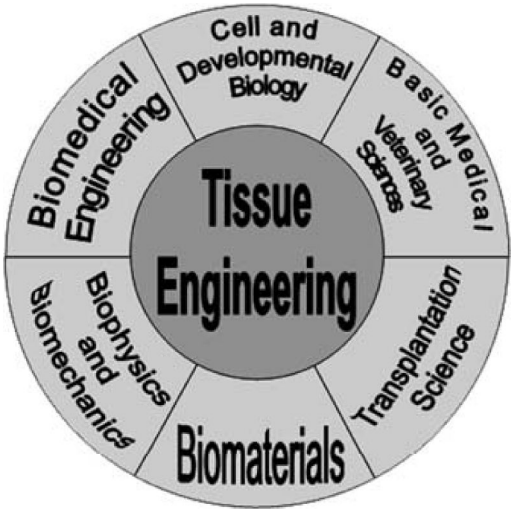

Fig. 8.1 Multidisciplinary nature of the tissue engineering field

Table 8.1 Tissue engineering main areas (Tabata, 2001)

	Purpose	Techniques/methodology
Tissue regeneration	In vitro production of tissue constructs	Cell scaffolding, bioreactor, microgravity
	In vivo natural healing process	Cell scaffolding, controlled release, physical barrier
	Ischemia therapy	Angiogenesis
Organ substitution	Immunoisolation	Biological barrier
	Nutrition and oxygen supply	Angiogenesis
	Temporary assistance for organ function	Extracorporeal system

Scaffolds provide an initial biochemical substrate for the novel tissue until cells can produce their own extra-cellular matrix (ECM). Therefore scaffolds not only define the 3D space for the formation of new tissues, but also serve to provide tissues with appropriate functions. These scaffolds are often critical, both ex vivo as well as in vivo, as they serve some of the following purposes (Gomes and Reis, 2004; Leong et al. 2002):

- Allow cell attachment, proliferation and differentiation
- Deliver and retain cells and growth factors
- Enable diffusion of cell nutrients and oxygen
- Enable an appropriate mechanical and biological environment for tissue regeneration in an organised way

To achieve these goals an ideal scaffold must satisfy some biological and mechanical requirements (Table 8.2):

a) Biological requirements:

Table 8.2 Relationship between scaffold characteristics and the corresponding biological effect (Mahajan, 2005)

Scaffold characteristics	Biological effect
Biocompatibility	Cell viability and tissue response
Biodegradability	Aids tissue remodelling
Porosity	Cell migration inside the scaffoldVascularisation
Chemical properties of the material	Aids in cell attachment and signiling in cell environment
	Allows release of bioactive substances
Mechanical properties	Affects cell growth and proliferation response
	In-vivo load bearing capacity

- Biocompatibility – the scaffold material must be non-toxic and allow cell attachment, proliferation and differentiation
- Biodegradability – the scaffold material must degrade into non-toxic products
- Controlled degradation rate – the degradation rate of the scaffold must be adjustable in order to match the rate of tissue regeneration
- Appropriate porosity macro- and microstructure of the pores and shape, highly interconnected pore structure and large surface area to allow high seeded cells and to promote neovascularisation. Large number of pores may be able to enhance vascularisation, while smaller diameter of pore is preferable to provide large surface per volume ratio. Typical desirable porosity are around 90% with pore size in the range of 20–250 μm (Freyman et al. 2001; Whang et al. 1995). Optimum pore sizes of 20 μm have been reported for fibroblast ingrowth, between 20 and 125 μm for regeneration of adult skin and 100–250 μm for the regeneration of bone. Figure 8.2 shows the effect of pore size on the percentage of cells attached onto collagen-glycosaminoglycan (CG) scaffolds.
- Should encourage the formation of ECM by promoting cellular functions
- Ability to carry biomolecular signals such as growth factors. Numerous growth factors have been identified such as fibroblast growth factor (FGF), platelet-derived growth factor, bone morphogenic protein (BMP), insulin growth

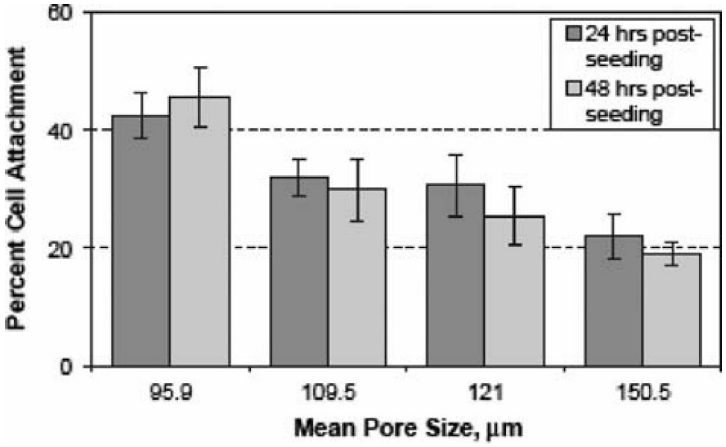

Fig. 8.2 Percentage of cells attached to the collagen-glycosaminoglycan scaffolds with different pore sizes (O'Brien et al. 2005)

Table 8.3 Biomaterials commonly used in tissue engineering

Biopolymers	
Natural polymers	**Synthetic polymers**
Alginate	Poly(glycolic acid), poly(lactic acid) and their co-polymers
Collagen	Poly(ε-caprolactone)
Chitosan	Poly(dioxanone)
Hyaluronic acid	Polyethylene oxide/polybutylene teraphthalate co-polymersPoly
Poly(hydroxybutyrate)	(propylene fumarate)
	Polyanhydride
Bioceramics	
Hydroxyapatite and other types of calcium phosphate like fluorapatite or tricalcium phosphate	
Biphasic hydroxyapatite/ tricalcium phosphate ceramics	
Bioactive glass ceramics	

factor, transforming growth factor-β, epidermal growth factor, vascular endothelial growth factor, etc. (Nathan and Sporn, 1991; Wei et al. 2007)

b) Mechanical and physical requirements

- Sufficient strength and stiffness to withstand stresses in the host tissue environment
- Adequate surface finish guaranteeing that a good biomechanical coupling is achieved between the scaffold and the tissue. New efforts to encourage cell attachment focusing on mimicking the surface chemistry of autogenous ECM has been also reported (Hynes, 1992). Surface properties such as surface charge and surface topography can influence biocompatibility
- Easily sterilised either by exposure to high temperatures or by immersing in a sterilisation agent remaining unaffected by either of these processes.

A variety of biodegradable materials have already been used for tissue scaffolds, including ceramics and polymers (Gomes and Reis, 2004). The primary use of ceramics has been in bone tissue engineering, presenting long degradation times often on the order of years. Polymeric scaffolds are used in the form of fibrous meshes, porous sponges, or hydrogels showing short degradation times, often on the order of days or months. The most common materials used for scaffolds are indicated in Table 8.3.

8.2 Conventional Fabrication Techniques

Conventional methods to fabricate scaffolds include (Gomes and Reis, 2004; Ho et al. 2004; Leong et al. 2002; Reignier and Huneault, 2006; Whang et al. 1995):

- Solvent casting/salt leaching: involves mixing solid impurities, such as sieved sodium chloride particles, into a polymer solvent solution, and casting the dispersion to produce a membrane of polymer and salt particles. The salt particles are then leached out with water to yield a porous membrane. Porosity and pore

size have been shown to be dependent on salt weight fraction and particle size. Pore diameters of 100–500 μm and porosities of 87–91% have been reported.
- Phase separation: involves dissolving a polymer in a suitable solvent, placing it in a mould, then cooling the mould rapidly until the solvent is frozen. The solvent is removed by freeze-drying, leaving behind the polymer as a foam with pore sizes of 1–20 μm in diameter.
- Foaming: is carried out by dissolving a gas, usually CO_2, at elevated pressure or by incorporating a chemical blowing agent that yields gaseous decomposition products. This process generally leads to pore structures that are not fully interconnected and produces a skin-core structure.
- Gas saturation: this technique uses high pressure carbon dioxide to produce macroporous sponges at room temperature. Polymeric sponges with large pores (~100 μm) and porosities up to 93% have been reported (Mooney et al. 1996)
- Textile meshes: these processes include all technologies successfully employed to fabricate non-woven meshes of different polymers. Major limitations are due to difficulties in obtaining high porosity and regular pore size.

Each of these techniques presents several limitations as they usually do not enable to properly control pore size, pore geometry and spatial distribution of pores, besides being almost unable to construct internal channels within the scaffold. Beyond these limitations, these techniques usually involve the use of toxic organic solvents, long fabrication times on top of being labour-intensive processes. Therefore, rapid prototyping technology (also called Solid Freeform Fabrication) is considered a viable alternative to fabricate scaffolds for tissue engineering.

8.3 Rapid Prototyping and Manufacturing Techniques for Tissue Engineering

Rapid prototyping and manufacturing (RP&M) represents a new group of non-conventional fabrication techniques recently introduced in the medical field. The main advantages of RP&M are both the capacity to rapidly produce very complex 3D models and the ability to use various raw materials. In the tissue engineering field, RP&M have been used to produce scaffolds with customised external shape and predefined internal morphology, allowing good control of pore size and pore distribution (Bártolo, 2006).

Figure 8.3 provides a general overview of the necessary steps to produce rapid prototyping scaffolds for tissue engineering. The first step is the generation of the corresponding computer solid model through one of the currently available medical imaging techniques such as computer tomography, magnetic resonance imaging, etc. These imaging methods produce continuous volumetric data (voxel-based data), which provide the input data for the digital model generation (Bártolo, 2006). The model is then tessellated as an STL file, which is currently the standard file for facetted models in RP&M. Finally, the STL model is mathematically sliced into thin layers (sliced model). RP&M technologies are similar to 2D printing and

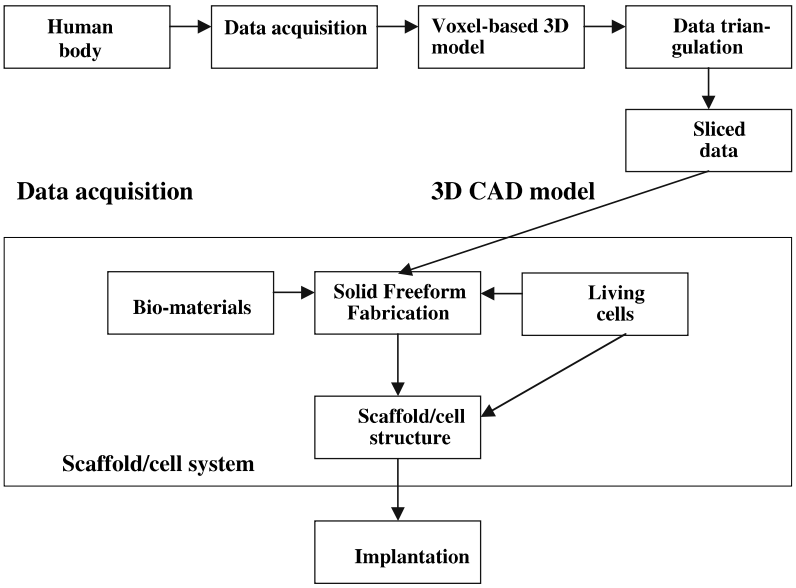

Fig. 8.3 Steps of RP&M in tissue engineering (Bártolo et al. 2004)

plotting technologies using both vector-based and raster-based imaging techniques. The various RP&M technologies for tissue engineering, described in the following sections, include stereolithographic processes, laser sintering, extrusion and three dimensional printing.

8.3.1 Stereolithographic Processes

Stereolithographic processes produce three-dimensional solid objects in a multi-layer procedure through the selective photo-initiated cure reaction of a polymer (Bártolo and Mitchell, 2003). These processes usually employ two distinct methods of irradiation. The first method is the mask-based method in which an image is transferred to a liquid polymer by irradiating through a patterned mask. The irradiated part of the liquid polymer is then solidified. In the second method, a direct writing process using a focused UV beam produces polymer structures (Fig. 8.4).

The direct or laser writing approach consists of a vat containing a photosensitive polymer, a moveable platform on which the model is built, a laser to irradiate and cure the polymer and a dynamic mirror system to direct the laser beam over the polymer surface "writing" each layer. After drawing a layer, the platform dips into the polymer vat, leaving a thin film from which the next layer will be formed.

Mask-based writing systems build models by shining a flood lamp through a mask, which lets light pass through it. These systems generally require the generation of a lot of masks with precise mask alignments. One solution for this problem is the use of a liquid crystal display (LCD) or a digital processing projection system as a flexible mask.

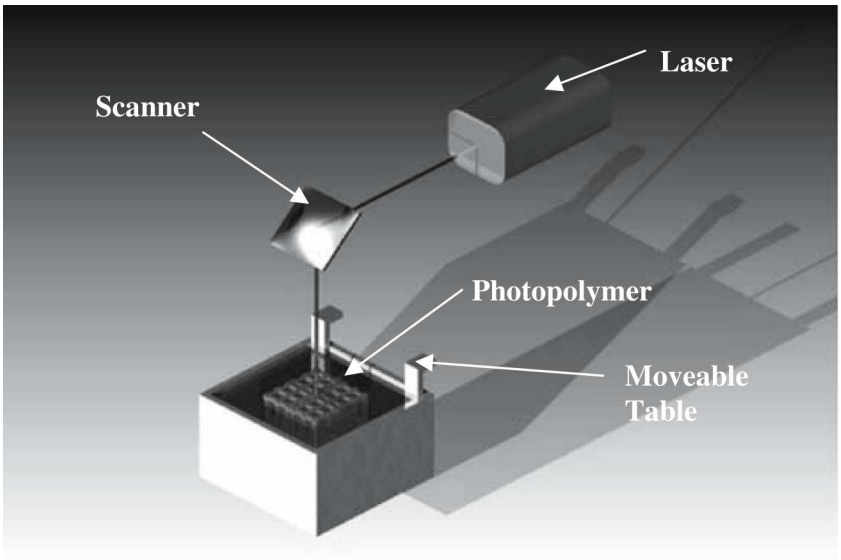

Fig. 8.4 Stereolithography system

Microstereolithography is a relatively recent development, similar to conventional stereolithography. However, to get a better resolution, the beam is focused more precisely in order to reduce the spot size to a few micrometers of diameter. Several strategies have been proposed (Bertsch et al. 2003): constrained surface techniques, free surface techniques, and integral processes. Integral microstereolithography represents the most recent advancement in this field, enabling the solidification of each layer in one irradiation step by projecting the corresponding image onto the surface of the photo-polymerisable resin through either a liquid crystal display or a digital micro mirror device. MicroTEC (Germany) is one of the few companies commercialising a microstereolithography. Their propriety technology is known as Rapid Micro Product Development (RMPD) and uses an excimer laser as a light source that works on a vector-by-vector basis.

All of the abovementioned stereolithographic approaches are based on a single-photon initiated polymerisation procedure. Two-photon-initiated polymerisation curing processes represent a useful stereolithographic alternative strategy to produce micro/nanoscale structures by using femtosecond infrared laser without photomasks (Kowata and Sun 2003; Lemercier et al. 2005; Tormen et al. 2004,). In this process, the molecule simultaneously absorbs two photons instead of one, being excited to higher singlet state. The use of two-photon-initiated polymerisation allows a submicron 3D resolution, on top of enabling both 3D fabrication at greater depth and an ultra-fast fabrication.

Many groups have used and developed stereolithographic processes for tissue engineering. Levy et al. (1997) used a direct irradiation stereolithographic process to produce hydroxyapatite (HA) ceramic scaffolds for orbital floor prosthesis. A suspension of fine HA powder into a UV-photocurable resin was formulated and used as building material. The photo-cured resin acts as a binder to hold the HA particles together. The resin is then burnt out and the HA powder assembly sintered for consolidation. A similar approach was used by Griffith and Halloran (1996) that

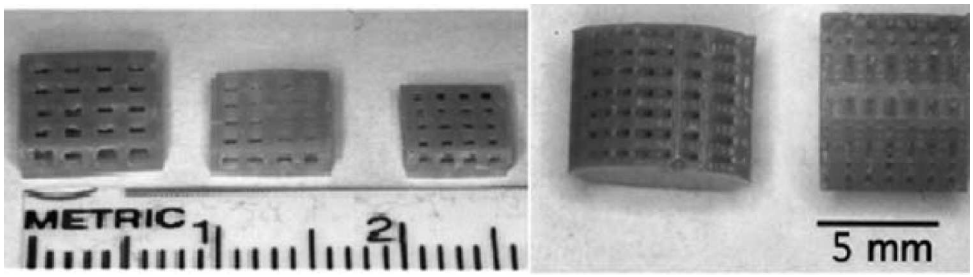

Fig. 8.5 Sintered HA scaffolds produced by a lost-mould technique (Chu et al. 2001) elective laser sintering process

produced ceramic scaffolds using suspensions of alumina, silicon nitride and silica particles with a photo-curable resin. The binder was removed by pyrolysis and the ceramic structures sintered.

Chu et al. (2001) developed a lost-mould technique to produce implants with designed channels and connection pattern (Fig. 8.5). Stereolithography was used to create epoxy moulds designed from negative image of implants. A highly loaded HA-acrylate suspension was cast into the mould. The mould and the acrylic binder were removed by pyrolysis and the HA green scaffold submitted to a sintering process. The finest channel size achieved was about 366 μm and the range of implant porosity between 26 and 52%.

In another study, Cooke et al. (2002) used a biodegradable resin mixture of diethyl fumarate, poly(propylene fumarate) and bisacylphosphine oxide as photoinitiator to produce scaffolds for bone ingrowth. Similarly, Matsuda and Mizutani (2002) developed a photopolymer containing biodegradable copolymer of trimethylene carbonate and ε-caprolactone. UV light can also be used to fabricate hydrogel polymer scaffolds. The main difficulty is the development of water-soluble components that are both functional and photolabile (Fischer et al. 2001).

8.3.2 Laser Sintering

Selective laser sintering (SLS) uses a laser emitting infrared radiation, to selectively heat powder material just beyond its melting point (Fig. 8.6). The laser traces the shape of each cross-section of the model to be built, sintering powder in a thin layer. It also supplies energy that not only fuses neighbouring powder particles, but also bonds each new layer to those previously sintered. For polymeric powders, the sintering process takes place in a sealed heated chamber at a temperature near the melting point filled with nitrogen or argon. After each layer is solidified, the piston over the model retracts to a new position and a new layer of powder is supplied using a mechanical roller. The powder that remains unaffected by the laser acts as a natural support for the model and remains in place until the model is complete.

Materials most commonly used in tissue engineering scaffolds through laser sintering are biocompatible polymers such as polycaprolactone (PCL) and poly lactic acid (PLA) and biocompatible ceramics. PCL is a bioresorbable polymer used for

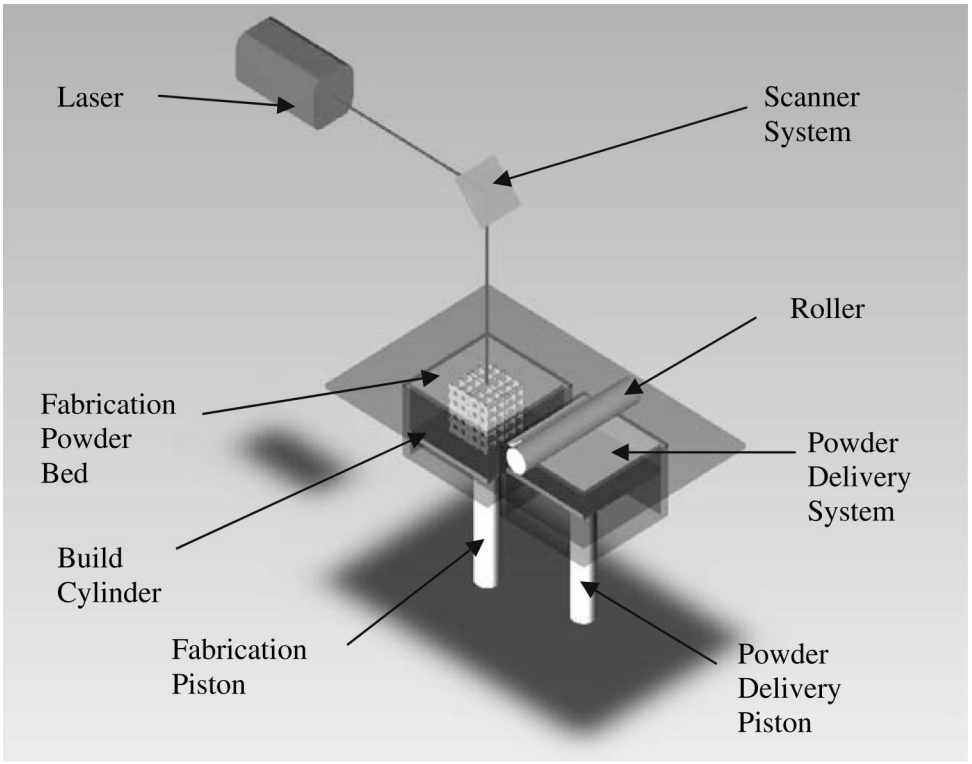

Fig. 8.6 Selective laser sintering process

bone and cartilage repair. It is more stable at ambient conditions that PCL and is also less expensive and readly available (Williams et al. 2005).

The potential of SLS to produce PCL scaffolds for replacement of skeletal tissues was shown by Williams et al. (2005). The scaffolds were seeded with bone morphogenetic protein-7 (BMP-7) transduced fibroblasts. In vivo results show that these scaffolds enhance tissue in-growth, on top of possessing mechanical properties within the lower range of trabecular bone. Compressive modulus (52 to 67 MPa) and yield strength (2.0 to 3.2 MPa) were in the lower range of properties reported for human trabecular bone.

Lee and Barlow (1996) coated calcium phosphate powder with polymer by spray drying slurry of particulate and emulsion binder. The coated powder was then sintered to fabricate calcium phosphate bone implants. Afterwards, these structures were infiltrated with calcium phosphate solution or phosphoric acid-based inorganic cement.

Popov and co-authors (2004) proposed the concept of Surface Selective Laser Sintering (SSLS) technique that enables to extend the range of polymers that can be used to extend the range of polymers that can be used for scaffold fabrication. Unlike conventional selective laser sintering, where polymer has a strong absorption at the laser wavelength, the SSLS process is based on melting the particle, which are transparent for laser radiation, due to the laser beam absorption by a small amount (<0.1 wt%) of biocompatible carbon black homogeneously distributed along the polymer surface. This process allows preventing significant overheating of the particles internal domains that can lead to properties changes and degradation.

8.3.3 Extrusion-based Processes

The extrusion-based rapid prototyping technique, commercially known as Fused Deposition Modelling (FDM), was developed by Crump (1989). By this process, thin thermoplastic filaments are melted by heating and guided by a robotic device (extruder) controlled by a computer, to form the three-dimensional object (Fig. 8.7). The material leaves the extruder in a liquid form and hardens immediately. The previously formed layer, which is the substrate for the next layer, must be maintained at a temperature just below the solidification point of the thermoplastic material to assure good interlayer adhesion.

Extrusion-based processes have been used to successfully produce scaffolds in PCL, PP-TCP, PCL-HA, PCL-TCP with resolution of 250 μm. Some of the major limitations of FDM are due to the use of filament-based materials and the high heat effect on raw material. In order to solve some limitations of the FDM process, such as the requirement of precursor filaments or high processing temperatures, some alternative processes have been proposed.

Hutmacher et al. (2001) optimised the FDM processing parameters for the production of PCL honeycomb-like scaffolds. Similar work was conducted by Zein et al. (2002) that produced PCL scaffolds with a range of channel size 160–700 μm, filament diameter 260–370 μm, porosity 48–77% and regular honeycomb pores. The compressive stiffness ranged from 4 to 77 MPa, yield strength from 0.4 to 3.6 MPa, and yield strain from 4 to 28%.

Koh et al. (2006) exploited the fact that when a warm PCL-HA/acetone solution is extruded into a reservoir containing ethanol, the extruded filament rapidly solidifies via solvent extraction producing a continuous rigid filament, to fabricate macro-channelled scaffolds. The diameter and morphology of the filament were controlled by adjusting the deposition speed and volume flow rate.

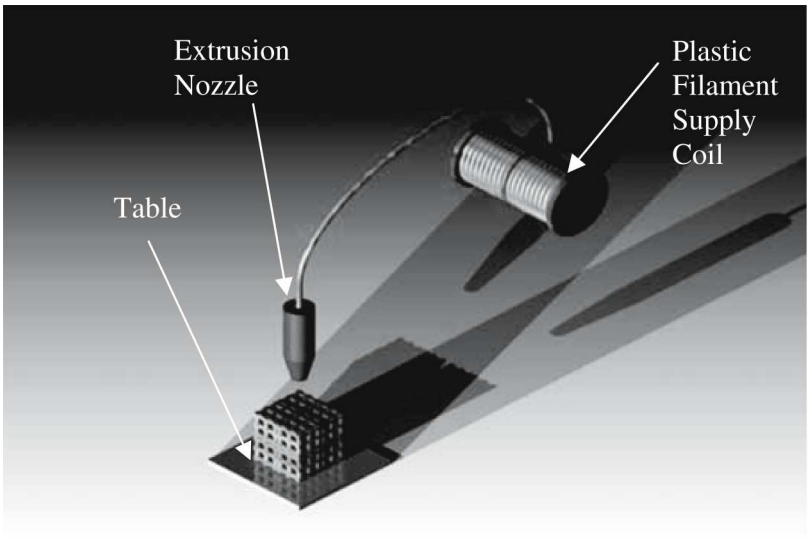

Fig. 8.7 Fused Deposition Modelling process

Woodfield et al. (2004) used a FDM-like technique, called 3D Fiber Deposition, to produce poly(ethylene glycol)-terephthalate-poly(butylenes terephthalate) (PEGT/PBT) block co-polymer scaffolds with a 100% interconnecting pore network for engineering of articular cartilage (Fig. 8.8). By varying the co-polymer composition, porosity and pore geometry, scaffolds were produced with a range of mechanical properties close to articular cartilage. The scaffolds seeded with bovine chondroccytes supported a homogeneous cell distribution and subsequent cartilage-like tissue formation.

Recently, Tellis et al. (2007) used micro CT to create biomimetic tissue engineering scaffolds. CAD models were exported to a FDM machine, producing polybutylene terephthalate (PBT) trabecular scaffolds. The scaffolds were compression tested at two different load rates (49 and 294N/s). Some scaffolds were soaked in a 25 °C saline solution for 7 days before compression. When compressed at 49 N/s the dry trabecular scaffolds had a compressive stiffness ranging from 2.46±0.55 MPa

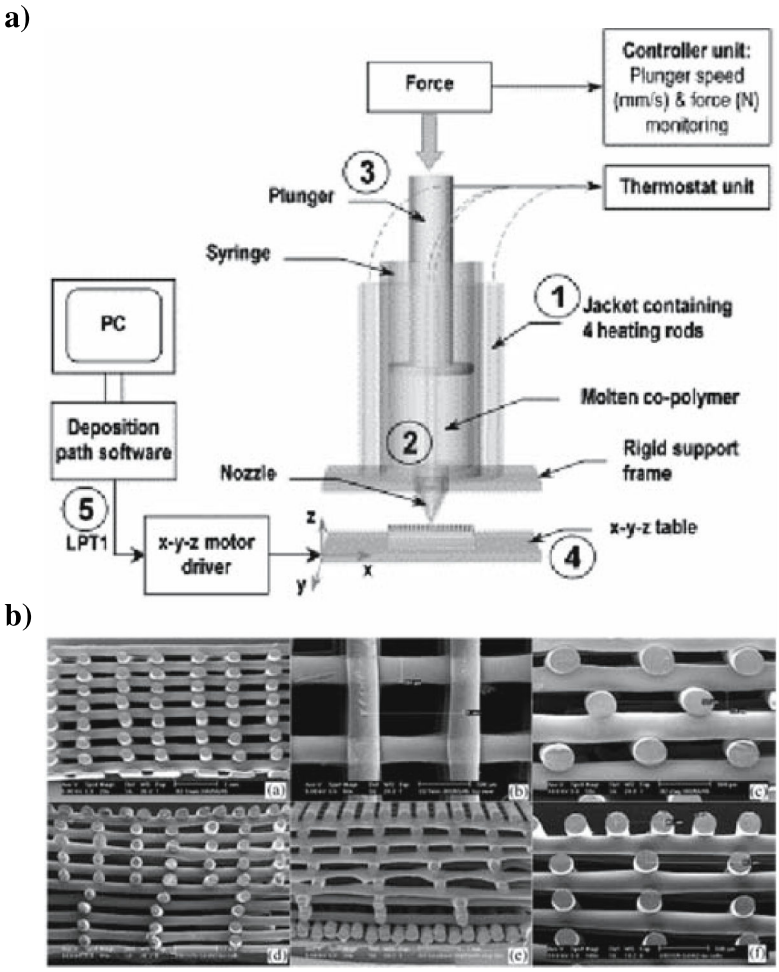

Fig. 8.8 (a) The 3D Fiber Deposition system. (b) SEM sections of 3D deposited scaffolds with varying deposition geometries (Woodfield et al. 2004)

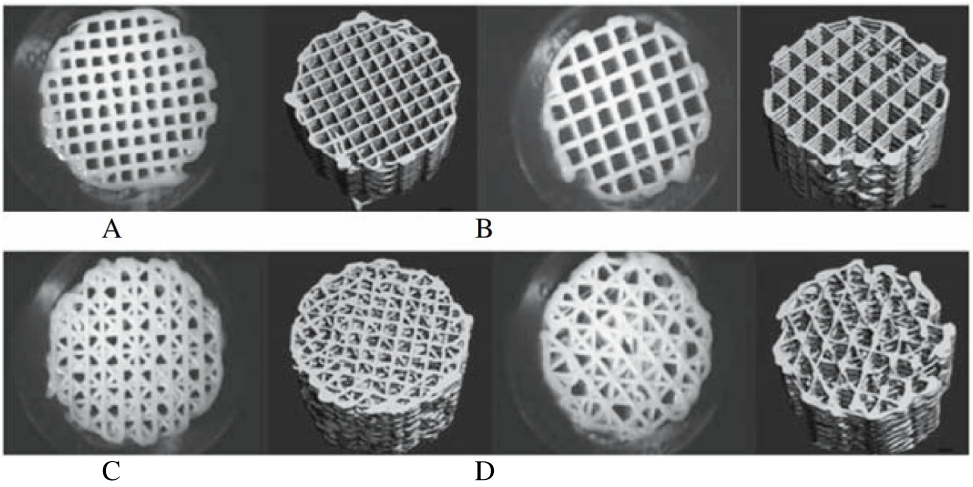

Fig. 8.9 Digital photographs and micro CT 3D segmentations of PBT scaffolds (Tellis et al. 2007)

for the complex interconnected pore structure (case E in Fig. 8.9) to 5.11±1.89 MPa for the simple linear structure (case A in Fig. 8.9). At 294 N/S, the compressive stiffness values roughly doubled. It was also observed that soaking the scaffolds in saline solution had an insignificant effect on stiffness and that compressive stiffness decreased as pore size increased. Compressive trabecular scaffolds matched bone samples in porosity. However, physiologic connectivity density and trabecular separation requires optimisation of scaffold processing.

Drexel University developed a variation of FDM called precision extruding deposition (PED) for fabrication of bone tissue scaffolds. In this process, material in pellet or granule form is fed into a chamber where it is liquefied. Pressure from a rotating screw forces the material down a chamber and out through a nozzle tip. This process was used by Wang et al. (2004) to directly fabricate PCL scaffolds with controlled pore size of 250 μm and designed structural orientations (0°/90°, 0°/120° or combined 0°/120° and 0°/90° patterns). Proliferation studies were performed using cardiomyoblasts, fibroblasts and smooth muscle cells. Similarly, Xiong et al. (2001) proposed the concept of precise extrusion manufacturing (PEM) to fabricate PLLA scaffolds for bone tissue engineering with controlled porous architectures from 200 to 500 μm. The sprayer of this system is equipped with a built-in heating unit to melt the feedstock. Compressed air is used as a piston to push the melted material through the nozzle.

In order to eliminate the elevated temperatures required by the extrusion-based processes, Tsinghua University developed a process called Low-temperature Deposition Manufacturing (LDM) to produce scaffolds at a low temperature environment under 0°C (Xiong et al. 2005). The LDM system comprises a multi-nozzle extrusion process and a thermally induced phase separation process (Fig. 8.10). Scaffolds having a macroporous structure larger than 100 μm in diameter and a microporous structure smaller than 100 μm have been reported. The LDM process was used to produce poly(L-lactide) (PLLA) and TCP composite scaffolds with BMP growth factor. The scaffolds were implanted into rabbit radius and canine radius large-segmental defects. After 12 weeks it was possible to observe that the rabbit radius

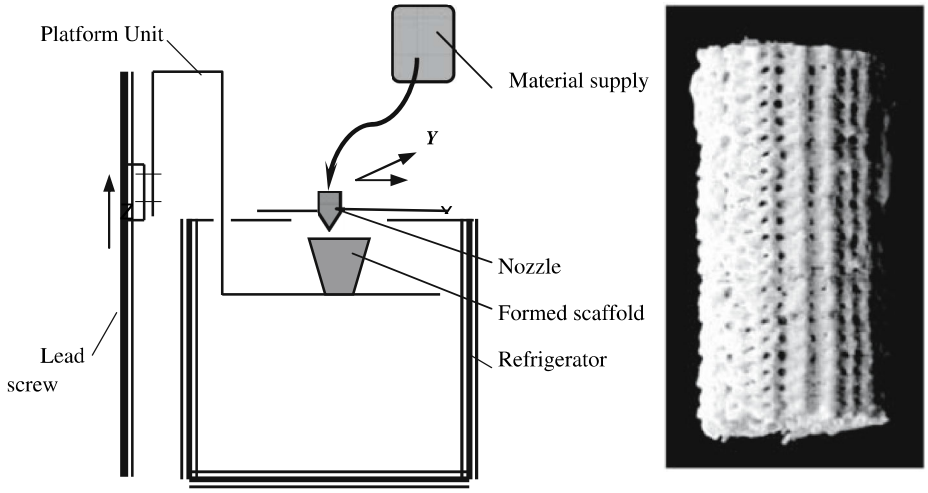

Fig. 8.10 (a) Schematic illustration of the LDM system. (b) Example of a porous PLLA/TCP composite scaffold produced by LDM process (Yan et al. 2003)

defect was successfully repaired and the regenerated bone had properties similar to the healthy bone. For the canine radius it was observed similar results after 24 weeks (Yan et al. 2003a).

Bioplotting (Fig. 8.11) is a technique developed by the Freiburg Materials Research Center and Envisiontec, Germany, that uses a pressure-controlled dispenser to deposit material into a reactive liquid medium of comparable density. This balance of media densities, which allows scaffolds to be created without the need of support structures, is a key characteristic of this process. Buoyancy can be provided to the plotted material, making strands of material remain in the correct position instead of sacking due to gravitational effects. The use of materials such as melts of poly(lactides), poly(lactide-co-glycolide), poly(hydroxybutyrate-co-valeriate), poly(caprolactone), poly(butylenes terephthalate-block-oligoethylene oxide), solutions of agar and gelatine, collagen and reactive biosystems involving

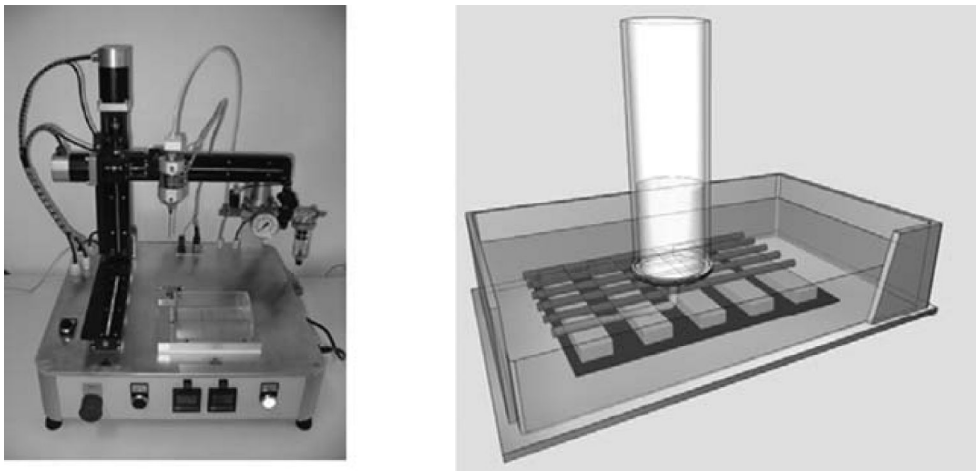

Fig. 8.11 (a) The 3D-Bioplotter system. (b) Process building of the first layer (Carvalho et al. 2005)

fibrin formation and polyelectrolyte complexation have been reported (Pfister et al. 2004). Fig. 8.12 illustrates some examples of scaffold structures made by the 3D-Bioplotter system.

Moroni et al. (2006) reported a novel strategy to create hollow fibers with controlled shell thickness and lumen diameter, organizing them into 3D scaffolds. Hollow fibers (Fig. 8.13), are made by extrusion of a blend of poly(butylmethacrylatemethylmethacrylate) (P(BMA/MMA) and poly(ethylene oxideterephtalate)-co -poly(butylene terephtalate) (PEOT/PBT) using the Bioplotter system. During the flow through the nozzle of the extruder and due to viscosity differences, the polymer with lower viscosity tends to shift towards the walls. The consequent separation of the polymers produces a stratification effect. Hollow fibers are produced by removing the core polymer by selective dissolution. It was also observed that bovine primary articular chondrocytes grow and form ECM not only in the scaffold macropores but also inside the hollow cavities (Fig. 8.14). The use of these hollow matrices for selective drugs release is being investigated.

An alternative process is the pressure assisted microsyringe (PAM) that involves the deposition of polymer dissolved in solvent through a syringe (Vozzi et al. 2003). The thickness of the polymer stream can be varied by changing the syringe pressure, solution viscosity, syringe tip diameter and motor speed. Resolution as low as 10 μm on a 2D structure was achieved.

Robocasting (Fig. 8.15), also known as direct-write assembly, consists on the robotic deposition of highly concentrated colloidal suspensions capable of fully supporting their own weight during assembly due to their viscoelastic properties (Miranda et al. 2006). This technique have been used to β-tricalcium phosphate (β-TCP) scaffolds (Miranda et al. 2006; Saiz et al. 2007).

Ang et al. (2002) developed a rapid prototyping robotic dispersing (RPBOD) system using the same principle as the 3D bio-plotting system, which was used to produce chitosan-HA scaffolds. Solutions of chitosan-HA were extruded into a sodium hydroxide and ethanol medium to induce the precipitation of chitosan. The scaffolds were then hydrated, frozen and freeze-dried.

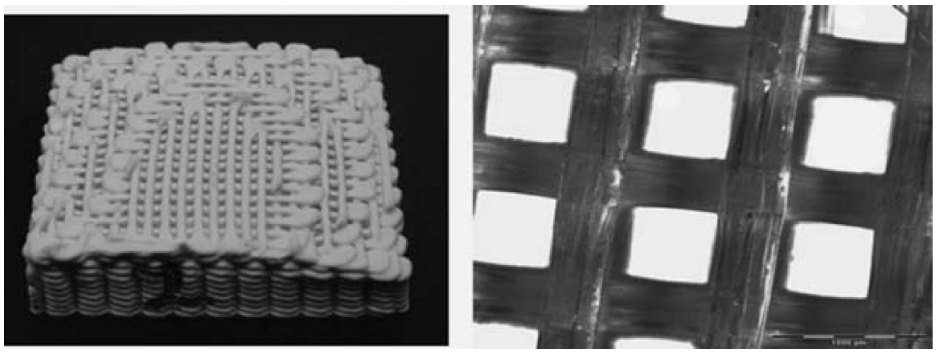

Fig. 8.12 (a) Hydroxyapatite scaffold. (b) PLGA scaffold (Carvalho et al. 2005)

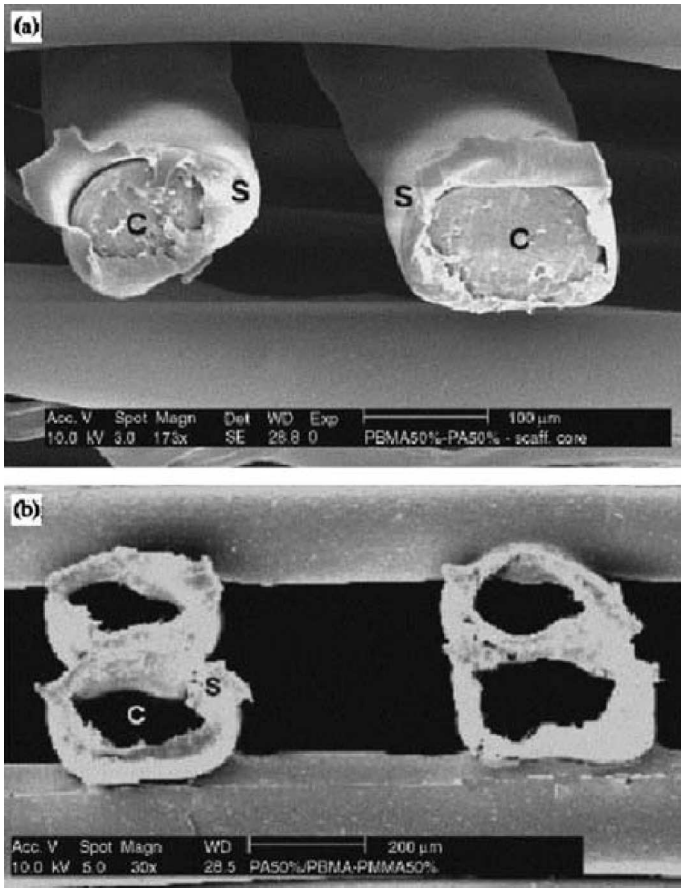

Fig. 8.13 SEM micrographs of a scaffold before (a) and after (b) leaching out the core material (Moroni et al. 2006)

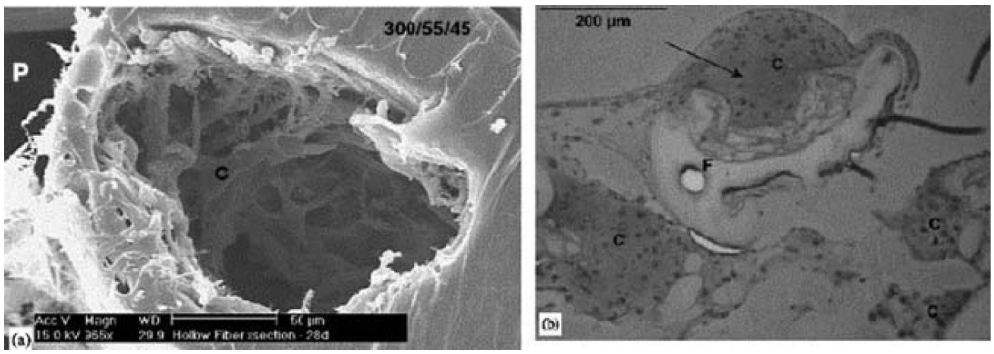

Fig. 8.14 SEM (a) and optical microscope (b) micrographs showing chondrocytes and ECM formation inside and outside the hollow fibers (Moroni et al. 2006). P = pore; F = fiber; C = chondrocytes

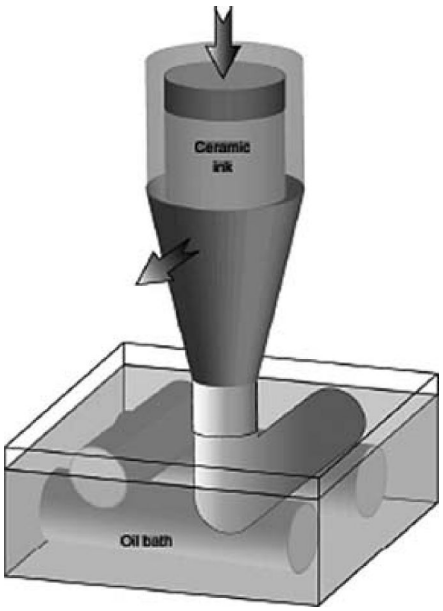

Fig. 8.15 Illustration of the robocasting fabrication process (Miranda et al. 2006)

8.3.4 Three-dimensional Printing

Three-dimensional printing (3DP) was developed at the Massachusetts Institute of Technology (USA) by Sachs et al. (1989). The process deposits a stream of microparticles of a binder material over the surface of a powder bed, joining particles together where the object is to be formed (Fig. 8.16). A piston lowers the powder bed so that a new layer of powder can be spread over the surface of the previous

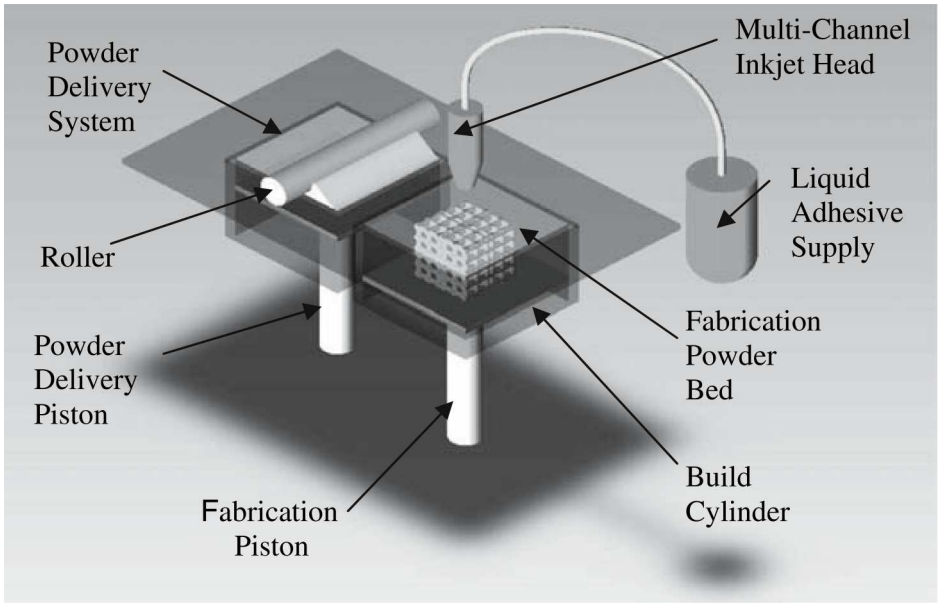

Fig. 8.16 3D Printing process

layer and then selectively joined to it. Therics Incorporated applied the 3DP process to tissue engineering and developed the *TheriForm* process to fabricate drug delivery devices and scaffolds.

Kim et al. (1998) employed 3DP with particulate leaching to create porous scaffolds, using polylactide-coglycolide (PLGA) powder mixed with salt particles and a suitable organic solvent. The salt particles were leached using distilled water. Cylindrical scaffolds measuring 8 mm (diameter) by 7 mm (height) with pore sizes of 45–150 μm and 60% porosity were fabricated. Hepatocytes were successful attached to the scaffolds.

The influence of pore size and porosity on cell adhesion and proliferation were investigated by Zeltinger et al. (2001). Disc shaped poly(L-lactic acid) (L-PLA) scaffolds measuring 10 mm (diameter) by 2 mm (height) were produced through both 3DP and salt and leaching methods. The scaffolds were produced with two different porosities (75 and 90%) and four different pore size distributions (<38, 38–63, 63–106 and 106–150 μm), and tested with cell culture using canine dermal fibroblasts, vascular smooth muscle cells and microvascular epithelial cells.

Lam et al. (2002) developed a blend of starch-based powder containing cornstarch (50%), dextran (30%) and gelatine (20%), bounded by printing distilled water. Cylindrical scaffolds were produced measuring 12.5 mm (diameter) by 12.5 mm (height) and infiltrated with different amounts of a copolymer solution consisting of 75% L-PLA and 25% polycaprolactone in dichloromethane to improve their mechanical properties.

Leukers et al. (2005) produced HA scaffolds with complex internal structures and high resolution. MC3T3-E1 cells were seeded on the scaffolds and cultivated under static and dynamic setups. Dynamic cultivation was performed in perfusion containers. A flow rate of 18 μl/min. Histological evaluation was carried out to characterise the cell ingrowth process. It was observed that the dynamic cultivation method lead to a stronger population compared to the static cultivation method. Static cells culture led to multiple cell layers located on the surface of HA granules. Dynamic cells culture tends to grow in between cavities of the granules. Additionally, it was found that cells proliferated deep into the structure forming close contact to HA granules.

Sachlos et al. (2003) used an indirect approach to produce collagen scaffolds with complex internal morphology and macroscopic shape by using a 3DP sacrificial mould. A dispersion of collagen was cast into the mould and frozen. The mould was then dissolved with ethanol and the collagen scaffold was critical point dried with liquid carbon dioxide. Other research works, like the ones of Taboas et al. (2003), Limpanuphap and Derby (2002) and Park et al. (1998), have also exploited the capabilities of 3DP for tissue engineering.

Ink-jet printing systems have been used to print both aqueous solutions onto supports and cell within a scaffold (Pardo et al. 2003; Saunders et al. 2004). During the droplet formation process the liquid material experiences shear rates close to 10^4 s^{-1} and similar strains occurs during the impact (Saunders et al. 2004). Therefore, cells in suspension are subjected to large stresses and deformation. Nevertheless, ink-jet printing has been reported to be a viable method for cell deposition and patterning (Saunders et al. 2004). Boland et al. (2006), explored a cell and organ printing fabrication strategy to print cells and proteins within 3D hydrogel

structures. Several examples of printed tissues such as contractile cardiac hybrids have been considered. Alginate hydrogels were used as support structures. As indicated in Fig. 8.17 endothelial cell attachment was observed. Filopodia can be seen at the leading edge of the cell and lamellapodia at the trailing edge suggesting cell migration into pores. It was postulated that local variation in the mechanical compliance of alginate structures causes cells to attach to the areas with greatest stiffness or highest stress. Endothelial cells are also known to grow well on surfaces, so it is not surprising to see cell attachment on the inner surfaces of the alginate pores. Nevertheless, the exact mechanism of cell attachment to alginate structures is still unknown and requires further research.

Similar procedures have been used by Mironov et al. (2003) and Yan et al. (2003), which developed the concept of cell printing. This process prints gels, single cells and cell aggregates offering a possible solution for organ printing. An analogous process, called alginate-based rapid prototyping, has been developed at the Polytechnic Institute of Leiria. This process produces alginate solid structures, by extruding a solution of sodium alginate, mixed with a solution of calcium chloride, providing a temporary support for the seeded cells in culture (Bártolo, 2006; Bártolo et al. 2004). Alginate is an anionic copolymer composed of homopolymeric regions of 1,4-linked β-D-mannuronic (M blocks) and α-L-guluronic acid (G blocks), interspersed with regions of alternating structure. Gelation occurs when

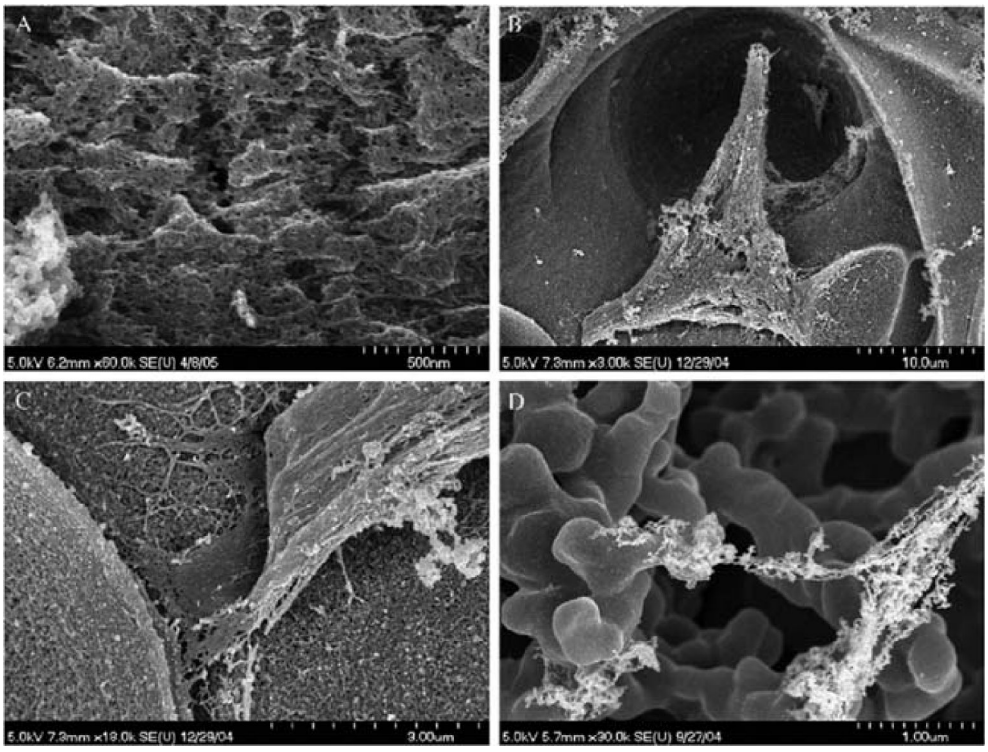

Fig. 8.17 SEM micrographs of endothelial cells attached to alginate structure. (A) Wall with nanosize pores. (B) An endothelial cell attach inside an alginate structure. (C) Filopodia and lamellapodia interacting with the alginate material. (D) Interactions between fibrous secretions and alginate (shellCell-jet printing equipment and some cell-gel mixture printing structures (Boland et al. 2006)

divalent ions take part in the interchain ionic binding between G-blocks in the polymer chain giving rise to a three dimensional network. Such binding zones between the G-blocks are often referred to as "egg boxes". These ions act as cross-linkers that stabilise alginate chains forming a gel structure, which contains cross-linked chains interspersed with more freely movable chains that bind and entrap large quantities of water. The gelification process is characterised by a re-organisation of the gel network accompanied by the expulsion of water. Gels made of M-rich alginate are softer and more fragile, and may also have lower porosity. This is due to the lower binding strength between the polymer chains and to the higher flexibilities of the molecules. The gelification process is highly dependent upon diffusion of gelification ions into the polymer network. Trasmittancy, swelling and viscoelasticity of alginate structures are highly affected by the M/G ratio.

8.4 Conclusions

RP&M technologies have a great potential for tissue engineering. These technologies offer a high degree of freedom for tissue engineering either for the design of scaffolds (pore size, pore geometry, orientation, interconnectivity, etc.) or for its fabrication. Several materials can also be used enabling the production of both soft and hard scaffolds. These characteristics can enhance the fabrication of biomimetic scaffolds and scaffolds for complex biomechanical applications. Future developments will possibly lead to establishing rapid prototyping as a key tool for tissue reconstruction and regeneration. The main advantages and limitations of rapid prototyping scaffolds for tissue engineering are listed in Table 8.4.

Table 8.4 Characteristics of rapid prototyping scaffolds for tissue engineering

Rapid prototyping	Advantages	Limitations
Stereolithoigraphic processes	Relatively easy to achieve small feature	Limited by the development of photo-polymerisable, biocompatible and biodegradable materials; currently limited to reactive and mostly toxic resins
SLS	Relatively higher scaffold strength; solvent free	Powder material trapped in small inner holes can be difficult to remove; high temperatures in the chamber
FDM	No materials trapped in the scaffold; solvent free	High heat effect on raw material; limited geometrical complexity
3DP	Low heat effect on raw powder; easy process; low cost	Materials trapped in small inner holes; low mechanical properties
Bio-plotting	Large variety of materials for both soft and hard tissues	Low geometrical complexity

References

Ang, T.H., Sultana, F.S.A., Hutmacher, D.W., Wong, Y.S., Fuh, J.Y.H., Mo, X.M., Loh, H.T., Burdet, E. and Teoh, S.H., Fabrication of 3D chitosan-hydroxyapatite scaffolds using a robotic dispersing system, *Mater Sci Eng*, C20, 35–42, 2002

Bártolo, P., Mendes, A. and Jardini, A., Bio-prototyping, in Design and Nature II, Edited by M.W. Collins and C.A. Brebbia, WIT Press, Southampton, UK, 535–543, 2004

Bártolo, P.J. and Mitchell, G., Stereo-thermal-lithography, *Rapid Prototyping J*, 9(3), 150–156, 2003

Bártolo, P.J., State of the art of solid freeform fabrication for soft and hard tissue engineering, in Design and nature III: comparing design in nature with science and engineering, 233–243, 2006.

Bertsch, A., Jiguet, S., Bernhards, P. and Renaud, P., Microstereolithography: a review. *Mat Res Soc Symp Proc*, 758: LL.1.1.1–13, 2003.

Boland, T., Tao, X., Damon, B.J., Manley, B. and Kesari, P., Drop-on-demand printing of cells and materials for designer tissue constructs, *Mater Sci Eng*: C 27(3), 372–376, 2007.

Carvalho, C., Landers, R., Mulhaupt, R., Hubner, U. and Schmelzeisen, R., Fabrication of soft and hard biocompatible scaffolds using 3D-Bioplotting, in Virtual Modelling and Rapid Manufacturing – Advanced Research in Virtual and Rapid Prototyping, Edited by P.H. Bártolo et al. Taylor & Francis, London, UK, 2005.

Chu, T.-M.G., Halloran, J.W., Hollister, S.J. and Feinberg, S.E., Hydroxyapatite implants with designed internal architecture, *J Mater Sci: Mater Med*, 12, 471–478, 2001.

Cooke, M.N., Fisher, J.P., Dean, D., Rimnac, C., Mikos, A.G., Use of stereolithography to manufacture critical-sized 3D biodegradable scaffolds for bone ingrowth, *J Biomed Mater Res Part B: Appl Biomater*, 64B, 65–69, 2002

Crump, S.S., Apparatus and method for creating three-dimensional objects, US Pat. 5121329, 1989

Fischer, J.P., Dean, D., Engel, P.S., Mikos, A., Photoinitiated polymerization of biomaterials, *Annu Rev Mater Res*, 31, 171–181, 2001.

Freyman, T.M., Yannas, I.V. and Gibson, L.J., Cellular materials as porous scaffolds for tissue engineering, *Progress in Mate Sci*, 46, 273–282, 2001.

Fuchs, J.R., Nasseri, B.A. and Vacanti, J.P., Tissue engineering: a 21st century solution to surgical reconstruction, *Ann Thorac Surg*, 72, 577–581, 2001.

Gomes, M.E. and Reis, R.L., Biodegradable polymers and composites in biomedical applications: from catgut to tissue engineering. Part 2 Systems for temporary replacement and advanced tissue regeneration, *Int Materials Rev*, 49, 274–285, 2004.

Griffith, M.L. and Halloran, J.W., Freeform fabrication of ceramics via stereolithography, *J Am Ceram Soc*, 79, 2601–2608, 1996.

Ho, M.H., Kuo, P.Y., Hsieh, H.J., Hsien, T.Y., Hou, L.T., Lai, J.Y. and Wang, D.W., Preparation of porous scaffolds by using freeze-extraction and freeze-gelation methods, *Biomaterials*, 25, 129–138, 2004.

Hutmacher, D.W., Schantz, T., Zein, I., Ng, K.W., Teoh, S.H. and Tan, K.C., Mechanical properties and cell cultural response of polycaprolactone scaffolds designed and fabricated via fused deposition modelling, *J Biomed Mater Res*, 55, 203–216, 2001.

Hynes, R.O., Integrins, versatility, modulation, and signalling in cell adhesion, *Cell*, 69, 11–25, 1992.

Kim, S.S., Utsunomiya, H., Koski, J.A., Wu, B.M., Cima, M.J., Sohn, J., Mukai, K., Griffith, L.G. and Vacanti, J.P., Survival and function of hepatocytes o a novel three-dimensional synthetic biodegradable polymer scaffolds with an intrinsic network of channels, *Ann Surg*, 228, 8–13, 1998.

Koh, Y.-H, Jun, I.-K. and Kim, H.-E., Fabrication of poly(ε-caprolactone)/hydroxyapatite scaffold using rapid direct deposition, *Materials Letters*, 60, 1184–1187, 2006.

Kowata, S. and Sun, H.B., Two-photon photopolymerization as a tool for making micro-devices, *Appl Surf Sci* 208/209, 153–158, 2003.

Lam, C.X.F., Mo, X.M., Teoh, S.H. and Hutmacher, D.W., Scaffold development using 3D printing with a starch-based polymer, *Mater Sci Eng*, 20, 49–56, 2002.

Langer, R., Tissue engineering: a new field and its challenges, *Pharm Res*, 14, 840–841, 1997.
Langer, R. and Vacanti, J.P., Tissue engineering, *Science*, 260, 920–926, 1993.
Lee, G. and Barlow, J.W., Selective laser sintering of bioceramic materials for implants, *Proceedings of the '96 SFF Symposium*, Austin, TX, August 12–14, 1996.
Lemercier, G., Mulatier, J.C., Martineau, C., Anémian, R., Andraud, C., Wang, I., Stéphan, O., Amari, N. and Baldeck, P., Two-photon absorption: from optical limiting to 3D microfabrication, *Comptes Rendus Chimie*, 8, 1308–1316, 2005.
Leong, K.F., Cheah, C.M. and Chua, C.K., Solid freeform fabrication of the three-dimensional scaffolds for engineering replacement tissues and organs, *Biomaterials*, 24, 2363–2378, 2003
Leukers, B., Gulkan, H., Irsen, S.H., Milz, S., Tille, C., Schieker, M. and Seitz, H., Hydroxyapatite scaffolds for bone tissue engineering made by 3D printing, *J Mater Sci Mater Med*, 16, 1121–1124, 2005.
Levy, R.A., Chu, T.G.M., Holloran, J.W., Feinberg, S.E. and Hollister, S., CT-generated porous hydroxyapatite orbital floor prosthesis as a prototype bioimplant, *Am J Neuroradiol*, 18, 1522–1525, 1997.
Limpanuphap, S. and Derby, B., Manufacture of biomaterials by a novel printing process, *J Mater Sci Mater Med*, 13, 1163–1166, 2002.
Mahajan, H. P., Evaluation of chitosan gelatine complex scaffolds for articular cartilage tissue engineering, MSc Thesis, Mississipi State University, USA, 2005.
Marler, J.J., Upton, J., Langer, R. and Vacanti, J.P., Transplantation of cells in matrices for tissue regeneration, *Adv Drug Del Rev*, 33, 165–182, 1998.
Matsuda, T. and Mizutani, M., Liquid acrylate-endcapped poly(e-caprolactone-co-trimethylene carbonate). II. Computer-aided stereolithographic microarchitectural surface photoconstructs, *J Biomed Mater Res*, 62, 395–403, 2002.
Miranda, P., Saiz, E., Gryn, K. and Tomsia, A.P., Sintering and robocasting of β-tricalcium phosphate scaffolds for orthopaedic applications, *Acta Biomaterialia*, 2, 457–466, 2006.
Mironov, V., Boland, T., Trusk, T., Forgacs, G. and Markwald, R.R., Organ printing: computer-aided jet-based 3D tissue engineering, *Trends Biotechnol*, 21, 157–161, 2003.
Mooney, D.J., Baldwin, D.F., Suh, N.P., Vacanti, J.P. and Langer, R., Novel approach to fabricate porous sponges of poly(D,L-lactic-co-glycolic acid) without the use of organic solvents, *Biomaterials*, 17, 1417–1422, 1996.
Moroni, L., Schotel, R., Sohier, J., Wijn, J.R. and Blitterswijk, C.A., Polymer hollow fiber three-dimensional matrices with controllable cavity and shell thickness, *Biomaterials*, 27, 5918–5926, 2006.
Nathan, C. and Sporn, M., Cytokines in context, *J Cell Biol*, 113, 981–986, 1991.
O'Brien, F.J., Harley, B.A., Llanas, I.V. and Gibson, L.J., The effect of pore size on cell adhesion in collagen-GAG scaffolds, *Biomaterials*, 26, 433– 441, 2005.
Pardo, L., Wilson, W.C. and Boland, T., Characterization of patterned self-assembled monolayers and protein arrays generated by the ink-jet method, *Langmuir*, 19, 1462–1466, 2003.
Park, A., Wu, B. and Griffith, L.G., Integration of surface modification and 3D fabrication techniques to prepare patterned poly(L-lactide) substrates allowing regionally selective cell adhesion, *J Biomater Sci-Polym E*, 9, 89–110, 1998.
Pfister, A., Landers, R., Laib, A., Hübner, U., Schmelzeisen, R., Mülhaupt, Biofunctional rapid prototyping for tissue-engineering applications: 3D bioplotting versus 3D printing, *Journal of Applied Polymer Science Part A: Polymer Chemistry*, 42, 624–638, 2004.
Popov, V.K., Antonov, E.N., Bagratashvili, B.N., Konovalov, A.N. and Howdle, S.M., Selective laser sintering of 3-D biodegradable scaffolds for tissue engineering, *Mat Res Soc Symp Proc.*, EXS-1, F5.4.1–F.5.4.3, 2004.
Reignier, J. and Huneault, M.A., Preparation of interconnected poly(ε-caprolactone) porous scaffolds by a combination of polymer and salt particulate leaching, *Polymer*, 47, 4703–4717, 2006.
Sachlos, E., Reis, N., Ainsley, C., Derby, B. and Czernuszka, J.T., Novel collagen scaffolds with predefined internal morphology made by solid freeform fabrication, *Biomaterials*, 24, 1487–1497, 2003.
Sachs, E.M., Haggerty, J.S, Cima, M.S. and Williams, P.A., Three-dimensional printing techniques, US Pat. 5204055, 1989.

Saiz, E., Gremillard, L., Menendez, G., Miranda, P., Gryn, K and Tomsia, A.P., Preparation of porous hydroxyapatite scaffolds, Materials Science and Engineering C, 27, 546–550, 2007.

Saunders, R., Derby, B., Gough, J. and Reis, N., Ink-jet printing of human cells, Mat Res Soc Symp Proc, EXS-1, F.6.3.1–F.6.3.3, 2004.

Skalak, R. and Fox, C.F., Tissue engineering, Alan R. Liss, New York, 1988.

Tabata, Y., Recent progress in tissue engineering, *Drug Discov Today*, 6, 483–487, 2001.

Taboas, J.M., Maddox, R.D., Krebsbach, P.H. and Hollister, S.J., Indirect solid free form fabrication of local and global porous biomimetic and composite 3D polymer-ceramic scaffolds, *Biomaterials*, 24, 181–194, 2003.

Tellis, B.C., Szivek, J.A., Bliss, C.L., Margolis, D.S., Vaidyanathan, R.K. and Calvert, P., Trabecular scaffolds created using micro CT guided fused deposition modeling, Materials Science and Engineering C (2007).

Tormen, M., Businaro, L., Altissimo, M., Romanato, F., Cabrini, S., Perennes, F., Proitti, R., Sun, H.B., Kawata, S., Fabrizio, E.D., 3D patterning by means of nanoimprinting, X-ray and two-photon lithography, *Microelectronic Engineering*, 73/74, 535–541 2004.

Vozzi, G., Flaim, C., Ahluwalia, A. and Bhatia, S., Fabrication of PLGA scaffolds using soft lithography and microsyringe deposition, *Biomaterials*, 24, 2533–2540, 2003.

Wang, F., Shor, L., Darling, A., Khalil, S., Güçeri, S. and Lau, A., Precision deposition and characterization of cellular poly-e-caprolactone tissue scaffolds, *Rapid Prototyping J*, 10, 42–49, 2004.

Wei, G., Jin, Q., Giannobile, W.V. and Ma, P.X., The enhancement of osteogenesis by nano-fibrous scaffolds incorporating rhBMP-7 nanospheres, *Biomaterials*, 2087–2096, 2007.

Whang, K., Thomas, C.H., Healy, K.E. and Nuber, G., A novel method to fabricate bioabsorbable scaffolds, *Polymer*, 36, 837–842, 1995.

Williams, J.M., Adewunmi, A., Schek, R.M., Flanagan, C.L., Krebsbach, P.H., Feinberg, S.E., Hollister, S.J. and Das, S., Bone tissue engineering using polycaprolactone scaffolds fabricated via selective laser sintering, *Biomaterials*, 26, 4817–4827, 2005.

Woodfield, T.B.F., Malda, J., de Wijn, J., Péters, F., Riesle, J. and van Blitterswijk, C.A., Design of porous scaffolds for cartilage tissue engineering using a three-dimensional fiber-deposition technique, *Biomaterials*, 25, 4149–4161, 2004.

Xiong, Z., Yan, Y. and Zhang, R. and Sun, L., Fabrication of porous poly(L-lactide acid) scaffolds for bone tissue engineering via precise extrusion, *Scripta Materialia*, 45, 773–779, 2001.

Xiong, Z., Yan, Y., Zhang, R. and Wang, X., Organism manufacturing engineering based on rapid prototyping principles, *Rapid Prototyping J* 11(3), 160–166, 2005.

Yan, Y., Wu, R. and Zhang, R, Biomaterial forming research using RP technology, *Rapid Prototyping J*, 9, 142–149, 2003a.

Yan, Y., Zhang, R. and Lin, F., Research and applications on bio-manufacturing, Proceedings of the 1st International Conference on Advanced Research in Virtual and Rapid Prototyping, Leiria, Portugal, 2003.

Zein, I., Hutmacher, D.W., Tan, K.C. and Teoh, S.H., Fused deposition modeling of novel scaffolds architectures for tissue engineering applications, *Biomaterials*, 23, 1169–1185, 2002.

Zeltinger, J., Sheerwood, J.K., Graham, D.M., Mueller, R. and Griffith, L.G., Effects of pore size and void fraction on cellular adhesion, proliferation, and matrix deposition, Tissue Engineering, 7(5), 557–572, 2001.

Capítulo 3 – O Alginato de Sódio (não-reticulado)

3.1 Introdução

O Capítulo 3 apresenta o trabalho realizado com o alginato de sódio (ou alginato aquoso), ou seja, o alginato diluído em água purificada, uma etapa antes de sua reticulação com cloreto de cálcio. O estudo do alginato aquoso vem ao encontro da necessidade de se conhecer o comportamento deste material antes de sua gelação (reticulação) com cloreto de cálcio, uma vez que, no sistema de biofabricação de *scaffolds* por extrusão (um trabalho que pode ser continuidade do presente), a reticulação do alginato de sódio apenas ocorrerá após sua deposição em um leito com $CaCl_2$. Desta forma, a entrada do sistema de biofabricação é composta por dois recipientes contendo o, primeiro, alginato aquoso e, o outro, cloreto de cálcio.

Os experimentos foram conduzidos com auxílio de um Reômetro Rotacional configurado com uma geometria de pratos, em que duas medidas reológicas diferentes foram realizadas para caracterizar soluções de alginato de sódio. Primeiro, executaram-se testes rotacionais, onde uma tensão controlada é aplicada e o movimento resultante é medido. Em segundo, medidas reológicas oscilatórias foram tomadas a partir da imposição de uma faixa de freqüência ao material. A deformação das amostras é tanto dependente da freqüência quanto da tensão aplicada.

3.2 Artigo Produzido

O Capítulo 3 é apresentado, a seguir, através do artigo intitulado "**Rheological Behavior of Alginate Solutions for Biomanufacturing**". Este artigo foi publicado no periódico internacional "Journal of Applied Polymer Science" (Vol. 113, 3866–3871, 2009).

Rheological Behavior of Alginate Solutions for Biomanufacturing

Rodrigo Alvarenga Rezende,[1,2] Paulo Jorge Bártolo,[1] Ausenda Mendes,[1] Rubens Maciel Filho[2]

[1]*Centre for Rapid and Sustainable Product Development, Mechanical Engineering Department, School of Technology and Management, Polytechnic Institute of Leiria, Leiria, Portugal*
[2]*Laboratory of Optimization, Design and Advanced Control, School of Chemical Engineering, State University of Campinas, Cidade Universitária "Zeferino Vaz", Campinas, São Paulo, CP 6066, Brazil*

Received 22 June 2007; accepted 20 May 2008
DOI 10.1002/app.30170
Published online 27 May 2009 in Wiley InterScience (www.interscience.wiley.com).

ABSTRACT: The rheological behavior of alginate solutions were investigated for the optimal design of a biomanufacturing system to produce alginate structures for tissue engineering. Its rheological properties were determined by a rheometer through rotational and oscillatory tests. Experimental results were used to model the alginate solutions characteristics. The findings suggest that alginate solutions undergo shear-thinning effects with increasing shear rates. It is also possible to observe that its loss modulus is higher than the storage modulus ones being both modulus dependent upon the frequency, which is a typical characteristic of dilute solutions. © 2009 Wiley Periodicals, Inc. J Appl Polym Sci 113: 3866–3871, 2009

Key words: biomaterials; rheology; hydrogels; biopolymers; viscoelastic properties

INTRODUCTION

Tissue engineering represents a novel, emerging interdisciplinary field involving combined efforts of biologists, engineers, material scientists, and mathematicians toward the development of biological substitutes to restore, maintain, or improve tissue functions.[1] It is emerging as a rapidly expanding approach to address the organ shortage problem. In 2003, in United States alone, 87,717 patients were waiting for organs' transplantation.[2] By June 2007, this number has increased to 96,670 as shown in Table I.[3]

In tissue engineering, therapeutic strategies involve cellular implantation, where cells are derived either from an endogenous source in the patient or from a donor are injected into the damaged tissue or combined *in vitro* with a degradable scaffold and then implanted. A scaffold directly implanted into the damaged tissue stimulates the cells promoting local tissue repair.[4]

Scaffolds are support structures used in tissue engineering to provide the three-dimensional growth of cells in an organized way. They are produced from either natural materials (collagen, hydroxyapatite, alginate, etc.) or synthetic polymers (polyglycolic acid, polylactic acid, etc.), which are biocompatible and bioabsorbable, nonimmunogenic, supporting cell growth.[5–7] Scaffolds must also degrade slowly after implantation in the patient, to be replaced by new tissue.[8,9] Biodegradable scaffolds can play an important role as delivery vehicles for the sustained release of tissue growth factors.[10] Ideally, appropriate designed tissue engineering scaffolds promote natural wound healing and regeneration. Recently, a biomanufacturing system, specifically designed for soft tissue repair applications.[6,11] This system is adapted to produce alginate scaffolds by extruding, layer-by-layer, a solution of sodium alginate into a calcium chloride solution (cross-linker agent). The system illustrated in Figure 1, comprises two nozzles, one for the sodium alginate and the other for the calcium chloride deposition not shown in the Figure. In this additive technology, the designed scaffold CAD model is first converted into STL format (a tessellated model that approximates the surfaces representing the solid with a set of triangles), and then sliced into a group of two-dimensional layers, to where the scaffold material is deposited to build the final structure in a layer-by-layer way. The scaffold structure could be controlled through the material properties, process parameters such as pressure, nozzle diameter, distance between the nozzle and the fabrication platform, and the velocity of the nozzle that is controlled through a computer-controlled system.

Correspondence to: P. J. Bártolo (pbartolo@estg.ipleiria.pt).
Contract grant sponsors: The Foundation for Science and Technology (through the projects POCI/SAU-BMA/60287/2004 and POCTI/EME/60650/2004).

TABLE I
The United Network for Organ Sharing Waiting List for Organ Transplant

Type of transplant	No. of patients waiting for transplant
Kidney	72,015
Liver	16,855
Pancreas	1686
Kidney/Pancreas	2337
Heart	2702
Lung	2724
Heart/Lung	119
Intestine	231
All organs	96,670

Alginate scaffolds are usually characterized by smooth surfaces, depending on the cross-linking process, i.e., on the concentration of both alginate and cross-linker as shown in Figure 2. The fabrication of porous alginate scaffolds involves a three-step procedure:[12,13]

- Cross-linking the alginate solution with an appropriate solution.
- Freezing the cross-linked alginate structure.
- Removal of the ice crystals by sublimation.

This article investigates the rheological behavior of alginate solutions, which is particularly important to design an optimized extrusion device and more stable alginate structures. Data collected are important to determine optimal design parameters for the biomanufacturing system, which uses nozzles with different geometries and dimensions and constant cross-sectional area. In the case of circular nozzles, the inner diameter ranges from 1.5 to 0.3 mm with a length of 40 mm. The effect of the type of alginate material, processing parameters, and nozzle characteristics on scaffold structural uniformity and dimensions is not considered.

ALGINATE

Alginate is an anionic copolymer of (1→4)-linked β-D-mannuronate (M) and α-L-guluronate (G) residues (Fig. 3).[14,15] The residues are arranged in a blockwise manner with G blocks and M blocks interspersed with MG alternating blocks.

The industrial manufacture of alginate is based on the extraction of a polymer from brown algae. The seaweed grows in nature mainly in temperate areas, but large amounts are also cultivated in other regions like the Far East, the coast of China or Japan. The seaweed is extracted with a dilute alkaline solution, which solubilizes the alginic acid present. Free alginic acid is obtained treating the resulting viscous material with mineral acids, being then converted to a salt. Sodium alginate is the major form currently used.

Sodium alginate is soluble in water and, when dissolved, forms a viscous solution depending on the concentration and molecular weight of the polymer. Gelation occurs when divalent ions (Ca^{2+}, Ba^{2+}, Fe^{2+}, Sr^{2+}, etc.) or trivalent ions (Al^{3+}, etc.) take part in the interchain ionic binding between G blocks in the polymer chain, giving rise to a three-dimensional network. Such binding zones between the G blocks are often referred to as "egg boxes" (Fig. 4). These ions act as cross-linkers that stabilize alginate chains forming a gel structure, which contains cross-linked chains interspersed with more freely movable chains that bind and entrap large quantities of water. The gelification process is characterized by a reorganization of the gel network accompanied by the expulsion of water.[16]

Gels made of M-rich alginate are softer and more fragile, and may also have lower porosity. This is due to the lower binding strength between the polymer chains and to higher flexibilities of the molecules. The gelification process is highly dependent upon diffusion of gelification ions into the polymer network. Transmittance, swelling, and viscoelasticity

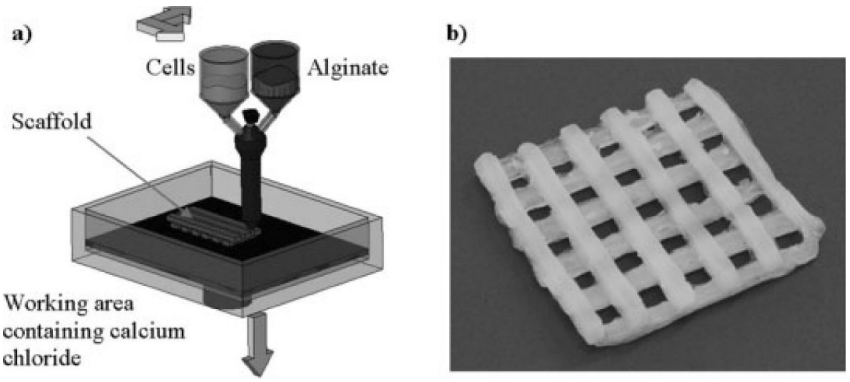

Figure 1 Alginate-based biomanufacturing system (a), and alginate scaffold structure (b).

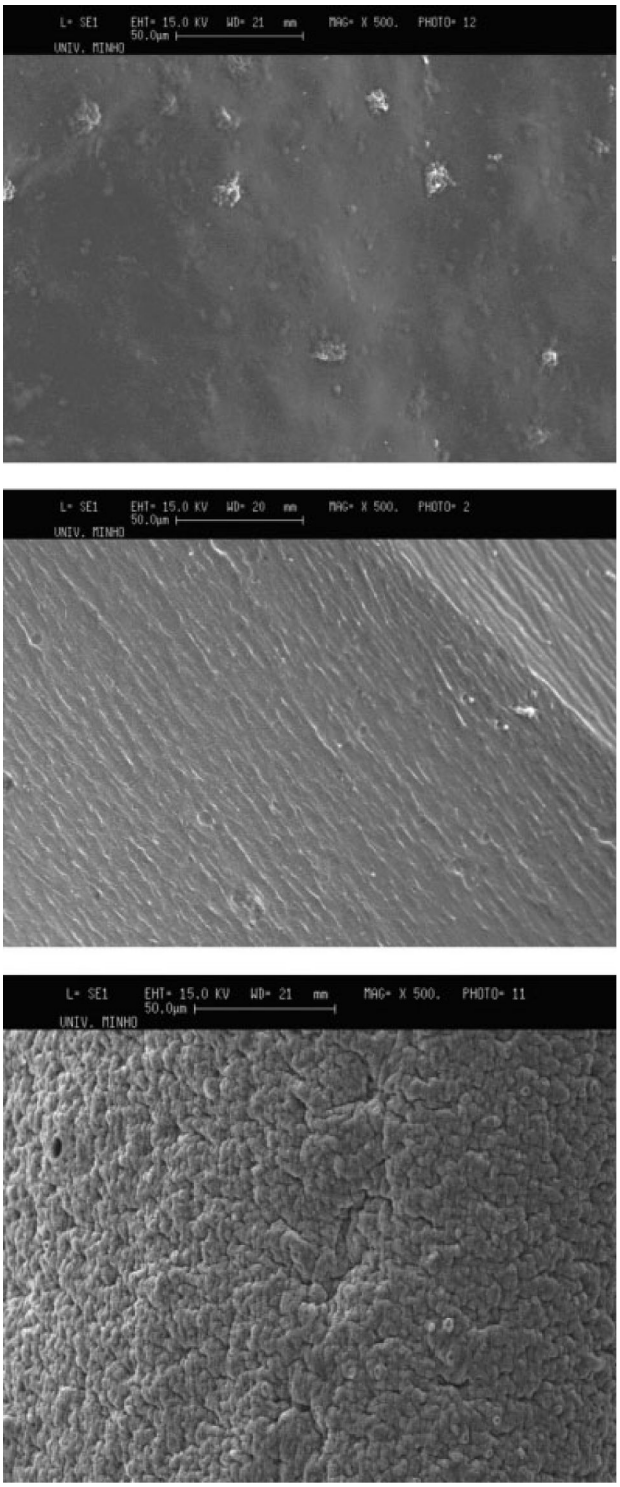

Figure 2 Surface morphology of alginate structures obtained after 48 h of gelation for two different solutions containing different concentrations of alginate and $CaCl_2$: (a) solution containing 3% of alginate mixed with a solution of 1% of $CaCl_2$; (b) solution containing 3% of alginate mixed with a solution of 3% of $CaCl_2$; (c) solution containing 2% of alginate mixed with a solution of of 1% of $CaCl_2$.

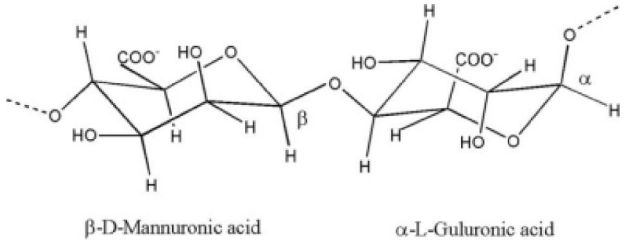

Figure 3 Structure of an alginate showing a linkage between the M and G acids.

of alginate structures are highly affected by the M/G ratio.

Alginic acid and its sodium and calcium salts are nontoxic and biocompatible, being widely used in the medical, pharmaceutical, cosmetic, and food industry.[17] In tissue engineering, alginate gels are currently explored for cell encapsulation and drug delivery.[18,19] For instance, the encapsulation of islets of Langerhans and parathyroid tissue for the treatment of diabetes mellitus and hypoparathyroidism, or the encapsulation of human chondrocytes and mesenchymal stem cells for cartilage repair.[20–23] Alginate materials are also important for wound healing, as they can be converted into a hydrophilic gel by an ion-exchange interaction between calcium in alginate and sodium in the blood and wound fluid.[24]

EXPERIMENTAL

Materials

Sodium alginate was purchased at Panreac (Barcelona, Spain). Calcium chloride was supplied by Carlo Erba (Milano, Italy). All solutions were prepared with pure water, with a conductivity of 0.054 μS/cm. Alginate solutions were prepared by the addition of weighted portions of sodium alginate to measured water volumes. These solutions were agitated by orbital shaking for 3 h at 50°C to ensure good homogeneity, due to their high viscosity. Calcium chloride solution 5% (w/v) was obtained dissolving the salt into water. This solution was diluted to obtain solutions with different concentrations of calcium chloride.

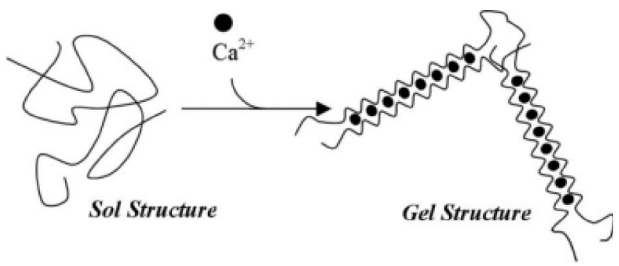

Figure 4 Alginate gelling obtained from reticulation of the chains by calcium ions.

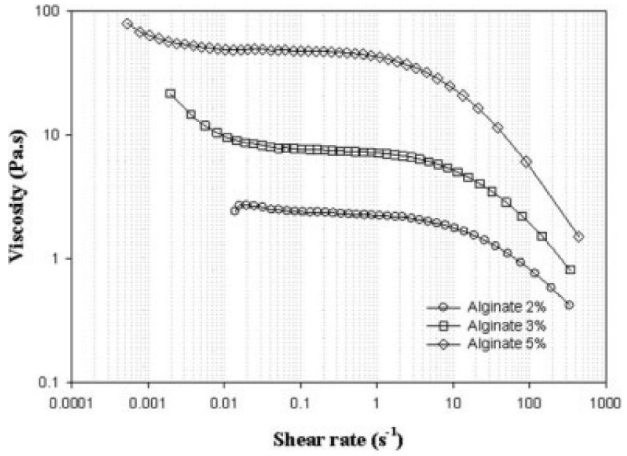

Figure 5 Viscosity variation as a function of shear rate for different alginate solutions.

Rheological tests

The rheological analysis of alginate solutions was carried out using a Reologica StressTech HR rotational rheometer fitted with plate-plate geometry. Two different rheological measurements were made to characterize the alginate solutions. First, rotational tests were considered. It is assumed that the material flows by applying a stress being the response measured alongside time or temperature (not considered in this work). A controlled stress is applied and the resulting movement is measured. The rotational speed depends on sample viscosity, computed by means of stress and shear rate. Second, oscillatory rheological measurements were made over a frequency range from 0.01 to 10 Hz. Sample deformation depends on both frequency and stress. All measurements were carried out at room temperature.

RESULTS AND DISCUSSION

Rotational analysis

Figures 5 shows that viscosity decreases with shear rate indicating a shear-thinning behavior. Increasing the alginate content increases both the viscosity and stress for a specific value of shear rate. The power-law model was used to fit the experimental data. According to this model, the rheological behavior of a material is described by:

$$\tau = k\dot{\gamma}^{n} \tag{1}$$

where τ is the shear stress (Pa), γ the shear rate (s^{-1}), k the consistency index (Pa s^n) and n is the power law index (dimensionless). Three range values can be identified for n:

$n < 1$: shear-thinning system
$n = 1$: Newtonian system
$n > 1$: shear-thickening system.

Table II indicates the values of the power law coefficients for different alginate solutions. A good approximation ($R^2 \approx 0.99$) between the power law and experimental data was obtained. The results confirm that the alginate solution is a shear-thinning system and that the consistency index increases with the alginate content. This observation is particularly important as the nozzles used in the biomanufacturing system can be small in diameter to control macroporosity, reducing the effective flow rate and requiring higher pressures. The shear-thinning behavior of alginate solution facilitates the flow compared with a Newtonian fluid allowing high flow rates for equal deposition pressures. In the case of circular nozzles, the length is 40 mm providing a maximum length-to-diameter ratio (L/D) of 133.3. For solutions containing 3% of alginate the extrusion velocity is 50 mm/s, which allows viscous flows with Reynolds numbers ranging between 0.003 and 0.015, far below the turbulent flow transition boundary. Similar results are observed for the other solutions, with Reynolds numbers ranging from 0.0004 to 0.045. The density of each alginate solution considered in this study varies from 1.11 g/cm^3 and 1.4 g/cm^3.

For a viscous Newtonian fluid, the flow rate is given by the Hagen-Poiseuille equation:[25]

$$Q = \frac{\pi \Delta P}{128\ \eta L} d^4 \tag{2}$$

that establishes a direct proportionality among the flow rate (Q), the pressure differential (ΔP), and nozzle diameter (d), and an inverse proportionality between the flow rate and the viscosity (η), and nozzle length (L). For shear-thinning materials, viscosity decreases with shear rate and the flow rate is given by the following equation:[25]

$$Q = \frac{n(n+1)}{(3n+1)(n+1)} \frac{\pi(\dot{\gamma}_0)^{(n-1)/n}}{(2\eta_0)^{1/n}} \left(\frac{\Delta P}{L}\right)^{1/n} R^{(3n+1)/n} \tag{3}$$

where n is the power-law index, R is the nozzle radius.

TABLE II
Coefficients of the Power Law for Different Alginate Solutions

Alginate content (%)	k (Pa s^n)	n
2	2	0.87
3	6	0.84
5	28	0.84

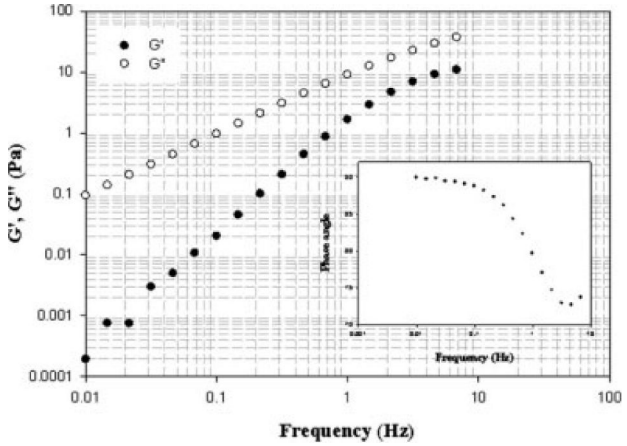

Figure 6 Log-log plot of G'', G' vs. frequency and phase angle vs. frequency for an alginate solution containing 2 wt % of alginate.

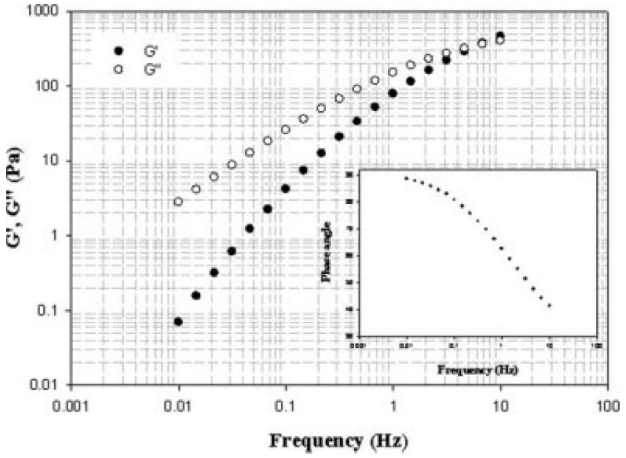

Figure 8 Log-log plot of G'', G' vs. frequency and phase angle vs. frequency for an alginate solution containing 5 wt % of alginate.

Oscillatory analysis

The viscous and elastic responses of viscoelastic systems can be quantified by undertaking dynamic oscillatory measurements. The basis of these measurements is the application of a sinusoidal strain of frequency ω to the system and the measurement of its corresponding stress. For viscoelastic systems, the stress and the strain are out of phase. Oscillatory analysis enables to determine several viscoelastic parameters, such as the complex modulus (G^*), the in-phase elastic component or storage modulus (G') and the out-of-phase viscous component or loss modulus (G'') of the complex modulus and tan δ. The relationships among these parameters are given by the following equations:

$$G^* = \frac{\tau}{\gamma} \tag{4}$$

$$G^* = \sqrt{G'^2 + G''^2} \tag{5}$$

$$G' = G^* \cos\delta \tag{6}$$

$$G'' = G^* \sin\delta \tag{7}$$

Figures 6 to 8 show how the store modulus and loss modulus change as a function of frequency. These modulus increases with frequency as demonstrated by findings. It is also possible to observe that the loss modulus is always higher than the storage one, being the viscous behavior the dominant effect. However, for high alginate content solutions and

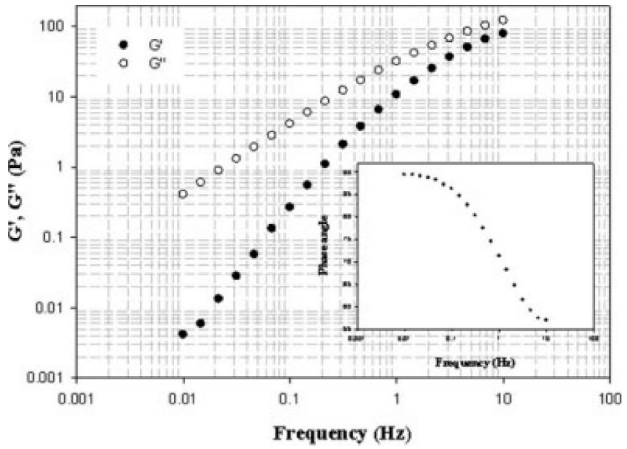

Figure 7 Log-log plot of G'', G' vs. frequency and phase angle vs. frequency for an alginate solution containing 3 wt % of alginate.

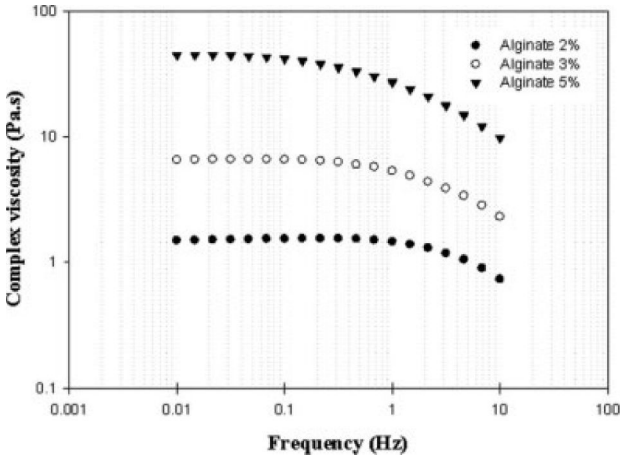

Figure 9 Variation of complex viscosity as a function of frequency for different alginate solutions.

high frequency a shift in this trend can be observed showing a more elastic behavior. Figures also show how the phase angle varies with frequency. At low frequencies (long time scales), the response of alginate solutions is viscous. The phase angle decreases as the frequency increases. For alginate solutions with high alginate content, the system becomes more elastic as the frequency increases.

The complex viscosity variation as a function of frequency is shown in Figure 9. For solutions containing low alginate contents (lower than 5%), the complex viscosity is almost constant. Comparing Figures 9 and 1, it is possible to observe that the Cox-Merz rule hold for these alginates.

CONCLUSIONS

The alginate-based biomanufacturing system is a fabrication technique developed to produce alginate solid structures, by extruding a solution of sodium alginate, mixed with a solution of calcium chloride, providing a temporary support for the seeded cells in culture. The understanding of the rheological behavior of alginate solutions is fundamental either to design optimized extrusion devices or to ensure stable flows. Rotational and oscillatory dynamic tests were carried out to characterize the rheological behavior of different alginate solutions. Experimental results were used to model the alginate solutions characteristics. Stresses and shear rates were correlated using the power-law model. A good correlation was achieved. The results suggest that alginate solutions undergo shear-thinning effects with increasing shear. These findings are particularly important as the shear-thinning effects can be used to maximize flow rates and minimize viscosity.

Results also show that loss modulus is higher than the storage one, being both modulus dependent upon the frequency, which is a typical characteristic of a dilute solution. Increasing the alginate content and frequency enables both modulus to become closer in value.

References

1. Langer, R.; Vacanti, J. P. Science 1993, 260, 920.
2. Mendes, A.; Lagoa, R.; Bártolo, P. J. Proceedings of the 1st International Conference on Advanced Research in Virtual and Rapid Prototyping; Bártolo, P. J., Ed.; Leiria, Portugal, 2003.
3. UNOS website: http://www.unos.org, accessed on July 2007.
4. Bártolo, P. J.; Amorim, H.; Laoui, T. Int J Mater Prod Technol, to appear.
5. Desai, S.; Bártolo, P. J.; Bidanda, B. In Bio-materials & Prototyping Applications in Medicine; Bidanda, B.; Bártolo, P. J., Eds.; Springer: New York, 2007; Chapter 1.
6. Bártolo, P. J. In Design and Nature III: Comparing Design in Nature with Science and Engineering; Brebbia, C. A., Ed.; WIT Press: Southampton, 2006.
7. Gomes, M. E.; Reis, R. L. Int Mater Rev 2004, 49, 274.
8. Lee, J. J.; Lee, S. G.; Park, J. C.; Yang, Y. I.; Kim, J. K. Curr Appl Phys 2007, 7, 37.
9. Sung, H. J.; Meredith, C.; Johnson, C.; Galis, Z. S. Biomaterials 2004, 25, 5735.
10. He, H.; Cao, X.; Lee, L. J. J Control Release 2004, 95, 391.
11. Bártolo, P. J.; Mendes, A.; Jardini, A. In Design and Nature II; Collins, M. W.; Brebbia, C. A., Eds.; WIT Press: Southampton, UK, 2004.
12. Zmora, S.; Glicklis, R.; Cohen, S. Biomaterials 2002, 23, 4087.
13. Shapiro, L.; Cohen, S. Biomaterials 1997, 18, 581.
14. Draget, K. I.; Braek, G. S.; Stokke, B. T. Food Hydrocolloids 2006, 20, 170.
15. Eiselt, P.; Yeh, J.; Latvala, R. K.; Shea, L. D.; Mooney, D. J. Biomaterials 2000, 21, 1921.
16. Serp, D.; Mueller, M.; Stockar, U.; Marison, I. W. Biotechnol Bioeng 2002, 79, 253.
17. Gombotz, W. R.; Wee, S. W. Adv Drug Deliv Rev 1998, 31, 267.
18. Wandrey, C.; Espinosa, D.; Rehor, A.; Hunkeler, D. J. Microencapsulation 2003, 20, 597.
19. Tønnesen, H. H.; Karlsen, J. Drug Dev Ind Pharm 2002, 28, 621.
20. Schneider, S.; Feilen, P. J.; Brunnenmeier, F.; Minnemaan, T.; Zimmermann, H.; Zimmermann, U. Diabetes 2005, 54, 687.
21. Hasse, C.; Klöck, G.; Schlosser, A.; Zimmermann, U.; Rothmund, M. Lancet 1997, 350, 1926.
22. Weber, M.; Steinert, A.; Jork, A.; Dimmler, A.; Thürmer, F.; Schütze, N. Biomaterials 2002, 23, 2003.
23. Chung, T. W.; Yang, J.; Akaike, T.; Cho, K. Y.; Nah, J. W.; Kim, S.; Cho, C. S. Biomaterials 2002, 23, 2827.
24. Ichioka, S.; Harii, K.; Nakahara, M.; Sato, Y. Scand J Plast Reconstr Hand Surg 1998, 32, 311.
25. Crawford, R. J. Plastics Engineering; Butterworth-Heinemann: Oxford, 1998.

3.3 Conclusões

A detecção do comportamento reológico de soluções de alginato de sódio é essencial para o projeto otimizado de equipamentos de extrusão e para se garantir fluxos estáveis. Os experimentos foram realizados com o objetivo de se modelar os perfis das soluções de alginato. Uma boa correlação através da Lei da Potência foi obtida a partir das taxas de tensão e deformação aplicadas, tendo sido determinado um comportamento pseudoplástico sob o aumento dos efeitos de corte. Foi igualmente observado que o módulo de perda é maior que o de ganho, havendo dependência destes com a frequência. Os aumentos do conteúdo de alginato na amostra e da frequência resultam em uma convergência entre os valores dos módulos de ganho e de perda.

Capítulo 4 – O Alginato de Cálcio (reticulado)

4.1 Introdução

Nesta etapa, o material em questão é o alginato, porém, não mais o aquoso (alginato de sódio), e, sim, o alginato de cálcio. O alginato de sódio é reticulado em solução de cloreto de cálcio, originando o alginato de cálcio.

$$\text{Alginato de Sódio}_{aq} + \text{Cloreto de Cálcio}_{aq} \rightarrow \text{Alginato de Cálcio}_{gel}$$

Os experimentos foram realizados com auxílio do DMA, um equipamento orientado à análise mecânica dinâmica, em que dois diferentes testes foram conduzidos: teste de tração (*tension test*) e teste de flexão simples (*single cantilever bending*).

Os ensaios de tração foram realizados com o objetivo de se verificar o comportamento viscoelástico do alginato, observando-se a sua deformação, sob diferentes tensões e diferentes composições de alginato e de cloreto de cálcio na amostra.

O teste de flexão foi destinado a se observar o perfil do módulo elástico do alginato sob diferentes freqüências e também sob a variação de aspectos como as composições de alginato e de cloreto de cálcio e a temperatura.

Parte também integrante deste capítulo é o ajuste de um modelo reológico para representar o comportamento mecânico do alginato de cálcio, a partir das curvas de deformação obtidas dos testes de tração, sendo que os ajustes foram executados com base em três tradicionais modelos viscoelásticos: Kelvin-Voigt, Zener-serie e Burger.

4.2 Artigo Produzido

O Capítulo 4 é desenvolvido e apresentado através do artigo intitulado "**Dynamic Mechanical Analysis and Rheological Model Fitting of Calcium Alginate Strain for Biofabrication**", o qual será brevemente submetido a um periódico internacional.

Dynamic Mechanical Analysis and Rheological Model Fitting of Calcium Alginate Strain for Biofabrication

Rodrigo Alvarenga Rezende[1,2*], Paulo Jorge Bártolo[2], Ausenda Mendes[2], Rubens Maciel Filho[1]

[1] Laboratory of Optimization, Design and Advanced Control, School of Chemical Engineering, University of Campinas, Cidade Universitária ‘‘Zeferino Vaz’’, CP 6066, Campinas, São Paulo, Brazil.

[2] Department of Mechanical Engineering, School of Technology and Management, Polytechnic Institute of Leiria, Portugal.

* Corresponding Author: rezende@feq.unicamp.br

Dynamic Mechanical Analysis and Rheological Model Fitting of Calcium Alginate Strain for Biofabrication

ABSTRACT: Nowadays, many factors have contributed to the creation of alternative solutions to help people with physical problems originated by accidents or by birth. Biofabrication is a novel concept for those reconstructions of organs and damaged tissues in medicine supported by Rapid Prototyping techniques. Biofabrication connects Tissue Engineering and Rapid Prototyping in such way that new solutions never though or never possible before can come true. Many biomaterials have been applied in the searching of those new solutions. One of them, as is presented in this paper, is the alginate, which can be applied as raw-material for scaffolds construction in order to be an important accessory in tissue engineering. The calcium alginate mechanical behavior was studied through Dynamic Mechanical Analysis (DMA) and the results are presented in this paper. The main purpose is to characterize the alginate and to associate it as a biomaterial to be used as scaffolds in tissue engineering being fabricated three-dimensionally using a biomimetic rapid prototyping system.

Key-words: Biofabrication, Alginate, Dynamic Mechanical Analysis, Rheological Model, Rapid Prototyping.

1. Introduction

The world population has been faced many problems in the health issues. One of the important areas that has been required much attention is the transplant. Due to accidents, diseases, aging and by birth problems, many people need to undergo an operation to replace or restore some organ. Many times these people have to expect a long time in a waiting list and also to find a compatible donor in order to proceed to the transplant. As the population has became older in many countries, for instance, United States, Japan, Spain, Italy, Germany, Brazil, researches have been pushed in order to create alternative solutions to solve these problems and therefore either to save lives or at least to restore the quality of life.

Biofabrication can be defined as the production of complex living and non-living biological products, including scaffolds, from raw materials such as living cells, molecules, extracellular matrices, and biomaterials. A scaffold is a temporary supporting structure and according to definition it must be biodegradable. There are synthetic and naturally derived solid scaffolds (Mironov, 2009).

Biofabrication is a new technology that matches Tissue Engineering (TE) and Rapid Prototyping (RP). Tissue Engineering typically involves the assembly of tissue structures by combining cells and biomaterials with the ultimate goal of replacing or restoring physiological functions lost in diseased or damaged organs (Tsang and Bhatia, 2004).

Advanced technologies in Tissue Engineering make use of techniques where the difference is the 3D fabrication of the artifacts. By Rapid Prototyping, physical models can be generated directly from computer-aided design data through an additive process where the parts are constructed layer-by-layer. RP or Solid Freeform Fabrication (SFF) is capable, for instance, to build porous structures in scaffolds for TE with great resolution. Biomaterial is

defined as any substance (other than a drug) or combination of substances either of synthetic or natural origin, which can be used for any period of time, as a whole or as a part of a system which treats, augments, or replaces any tissue, organ, or function of the body (Ratner *et al.*, 1996).

A variety of biodegradable and biocompatible hydrogels, as the alginate, has been used for tissue engineering. The alginate is one of the most popular materials due to its relatively low cost, natural origin and easy handling, besides other physical properties advantages. In this work alginate is purposed to be used as raw-material for scaffolds fabrication.

The scaffold is expected to support cell colonization, migration, growth and differentiation, and to guide the development of the required tissue or to act as a drug delivery device (Hutmacher, 2006) although other possible applications may be explored. The understanding of the rheological behavior of alginate solutions is fundamental either to design optimized extrusion devices or to ensure stable flows (Rezende *et al.*, 2009).

In this sense, the main contribution of this paper is to verify the mechanical behavior of the alginate, especially how the alginate can stretch under different conditions, which means effectively the strain. Strain is the deformation that can be related to stresses (Fung, 1981).

2. The Alginate as Raw-Material for tissue Engineering

The alginate hydrogel is produced by mixing the alginate with a proper cross-linking agent. During the gel formation, cross-links between the alginate chains and the cationic species are formed, changing the elastic behavior of the material controlling the volume change phenomena of gels.

Alginate is a biodegradable and biocompatible natural polymer. Being a linear polysaccharide alginate is derived from brown seaweed and bacteria. Owing to the significantly of higher production cost of alginate from bacterial sources, the primary sources of current commercial alginate materials are various species of brown algae. The major species used for alginate production are Ascophylla, Laminaria and Macroscystus. In early 1970s, alginate was generally recognized as safe (GRAS) to be used in food and pharmaceutical ingredients by the US Food and Drug Administration (FDA).

Alginate is a biopolymer used in issue engineering for wound healing and drug delivery, for instance. Alginates are one of the most versatile biopolymers, with a wide range of pharmaceutical and biomedical applications, such as polymer films, cell encapsulation, wound dressings and surgical sponges (Gombotz and Wee, 1998; Serp *et al.*, 2000; Klöck *et al.*, 1994).

Gelation of an aqueous sodium alginate in calcium chloride solution consists on the linkage of M and G blocks through a bridge by calcium ions in order to stabilize and construct a 3D network.

$$Sodium\_alginate_{aq} + Calcium\_chloride_{aq} \rightarrow Calcium\_alginate\_gel$$

Alginate gels are formed upon formation of ionic bridges between divalent cations (i.e., Ca^{2+}) and various polymer chains of the alginate. The crosslinking density of alginate gels is a function of the monomer units and molecular weight of the polymer. The gelling process is characterized by a re-organization of the gel network accompanied by the expulsion of water (Serp *et al.*, 2002). According to some variables involved in the gelation process such as time of gelation, concentration and type of alginate and calcium chloride, mainly, the formed structure shows different consistency and properties.

Alginate gels degrade slowly in a process in which the mechanical properties of the gels are altered with time (Peppas *et al.*, 2006). It is a co-polymeric natural polysaccharide that contains residues of mannuronic (M) and guluronic (G) acids as can be viewed in Figure 1.

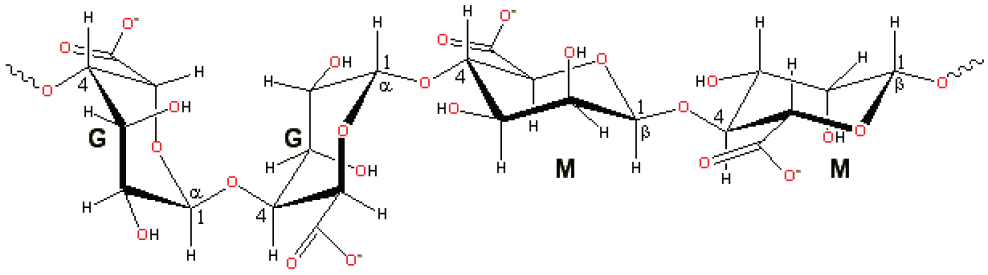

Figure 1. Alginate structure (M and G blocks)

These ions act as cross-linkers that stabilize alginate chains forming a gel structure, which contains cross-linked chains interspersed with more freely movable chains that binds and entraps large quantities of water, what for some medical applications is quite interesting. The G content and its sequential structure significantly affect mechanical properties of gels. The consecutive G residues permit coordinated cavity organization at the molecular level to allow stable ionic binding formation. Therefore, longer G-block length increases binding strength and hence structural integrity and mechanical properties of the alginate gels. In nature, there are many species of alginates containing different proportions of M and G

blocks. In accordance to the M:G ratio, some alginate properties are affected such as viscoelasticity, swelling and transmittance, among others.

Alginate gels have been studied extensively and are useful model systems to elucidate the mechanisms behind the mechanical behavior of reversibly associating polymers (Webber, 2004).

3. Experimental Procedure

In this work sodium alginate was purchased at Panreac (Barcelona, Spain) and calcium chloride was supplied by Carlo Erba (Milano, Italy). All solutions were prepared with pure water, with conductivity of 0.054 S/cm. Alginate solutions of 2%, 3%, 5% and 8% (w/v) were prepared by addition of weighted portions of sodium alginate to measured volumes of water. Due to their high viscosity, these solutions were agitated by orbital shaker (200rpm) for three hours at 20 ºC to ensure good homogeneity. Calcium chloride solutions 2% and 3% (w/v) were obtained dissolving the salt in water. Figure 2 shows how the combination between different alginate and calcium chloride relations affects de product appearance. Small proof-bodies of alginate gelled in calcium chloride were prepared to be carried out into DMA tests. The medium dimensions of them were about 5mm, 3mm and 2mm, corresponding to length, wide and thickness, respectively.

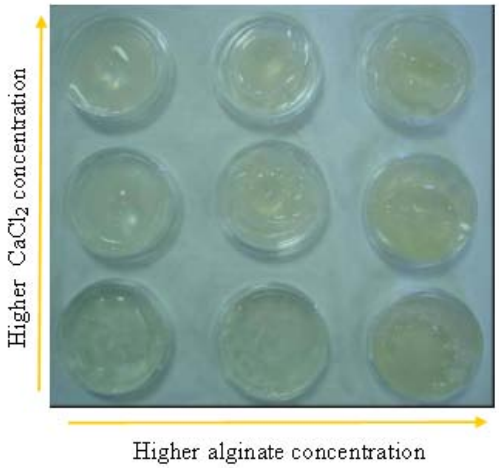

Figure 2. Sodium Alginate appearance for different compositions

Alginate, as a natural biopolymer, becomes an interesting material in this field by owning many advantages such as low toxicity, biocompatibility, carrying of specific protein binding sites and other biochemical signals that may assist in tissue healing or integration as well the minimal cytotoxic effects and reduced hemolysis when in contact with blood (Johnson *et al.*, 1997).

Focusing on alginate as a biocompatible material and intending to employ it in biofabrication, on the scaffolds construction or other kind of artifact, a mechanical study will be presented in the sequence where the Dynamic Mechanical Analyzer was used to check the mechanical behavior of alginate when some conditions as such as frequency, sample composition, load time are modified. Two DMA geometries were exploited: the tension and the single cantilever bending tests.

4. Results

The main purpose is to get the alginate strain experimentally through a Creep Test with Dynamic Mechanical Analysis under tension geometry. Later, a rheological model is proposed and de the experimental data are used to built up a suitable viscoelastic model, to understand how operating conditions affects such property which is important for scaffold manufacture. At last, through the single cantilever bending geometry measurements it was observed the alginate modulus behavior under different frequencies. For the tests, many conditions (scenarios) were created representing each analyzed case.

The mechanical properties of the calcium alginate in this paper were analyzed by using a DMA Tritec 2000 instrument in tension and single cantilever bending modes, as depicted in Figure 3.

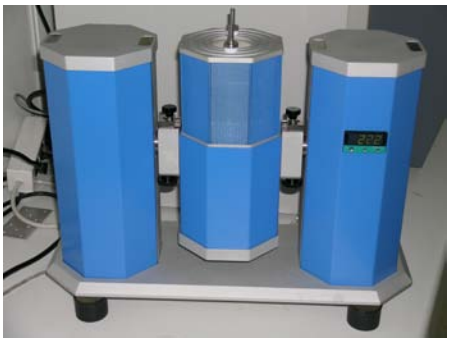

Figure 3. Tritec 2000 Dynamic Mechanical Analyser (DMA). (Triton, 2010).

DMA is also known by other names like Forced Oscillatory Measurements, Dynamic Mechanical Thermal Analysis (DMTA), Dynamic Thermomechanical Analysis and Dynamic Rheology. Menard (1999) states that DMA can be described as “applying an oscillating force to a sample and analyzing the material’s response to that force”.

4.1. Tension Geometry / Creep Test

Creep refers to the general characteristic of viscoelastic materials to undergo increased deformation under a constant stress, until an asymptotic level of strain is reached. Creep test consists of measuring the time dependent strain $\varepsilon(t) = \delta(t)/L_0$ resulting from the application of a steady uniaxial stress σ_0. The tension tests were performed using a body-proof in parallelepiped shape at room temperature equals to 23°C submitted at different tensions values. The loads were constants, during each test. The periods under tensions analyzed were 9, 15 and 250 minutes. The alginate concentrations were varied among the values 2%, 5% and 8% for a same composition of calcium chloride equals to 3%. Figure 4 presents a tension test scheme in DMA. The sample is anchored on one end by a fixed clamp and by the drive shaft on the other. Tension stress is applied by an electric motor.

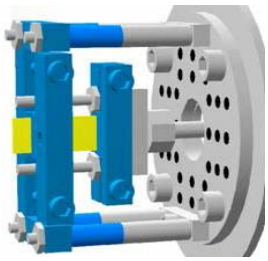

Figure 4 – Tritec 2000 Dynamic Mechanical Analyser (DMA). (Triton, 2010).

The initial conditions for all the scenarios in Tension Test are given in Table 1:

Table 1 – Initial conditions for Scenarios A, B, C and D

Variables / **Scenarios**	**A**	**B**	**C**	**D**
Alginate (%)	2	5	2	8
CaCl2 (%)	3	3	3	3
Load Time (min)	9	9	15	15

4.1.1. The Scenario A

Table 2 depicts the load values and the final tensions and respective strains.

Table 2 – Loads for Scenario A

Alginate 2%

Load (N)	Area (mm^2)	Tension σ (N/mm^2 ou KPa)	δ (%)
0,25	3,86	65	0,95
0,50	3,85	130	1,94
0,75	3,36	225	2,95
1,00	3,42	292	3,88

With respect to the section area underwent to the load, the length was fixed, since it was defined by the gap between the brackets that fasten the body-proof extremities, which corresponded to 10mm. In function of the large difficult in obtaining alginate body-proofs exactly with the same dimensions, it was unavoidable that the width and the thickness varied among the tests. The little volume of the body-proof contained a great percentage of water which did not ease its standardization during the preparation for the tests. Figure 5 presents the strain profiles for scenario A.

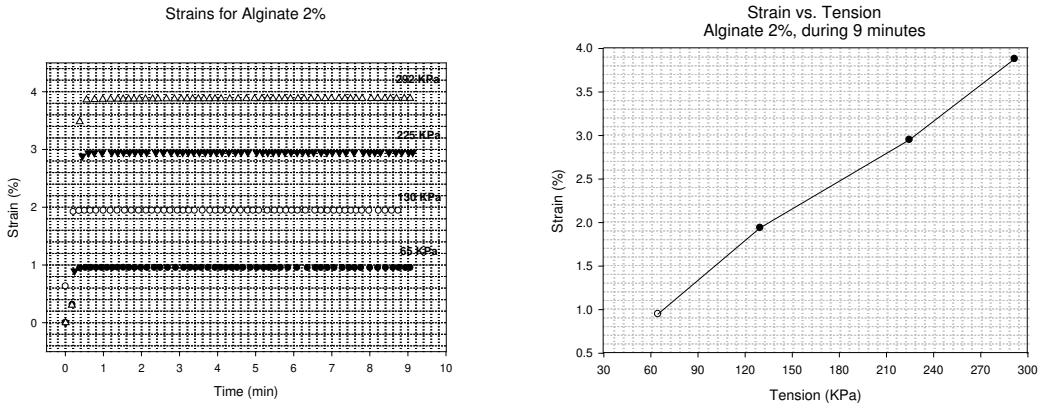

Figure 5 – Scenario A: Strains for Alginate 2% under 9 minutes load.

4.1.2. The Scenario B

Table 3 shows the load values and the final tensions and respective strains.

Table 3 – Loads for Scenario B

Alginate 5%

Load (N)	Area (mm^2)	Tension σ (N/mm^2 ou KPa)	δ (%)
0,25	5,07	49	0,89
0,50	4,79	104	1,88
0,75	5,57	135	2,89
1,00	6,48	154	3,90

In Figure 6 is presented the strain profiles for scenario B.

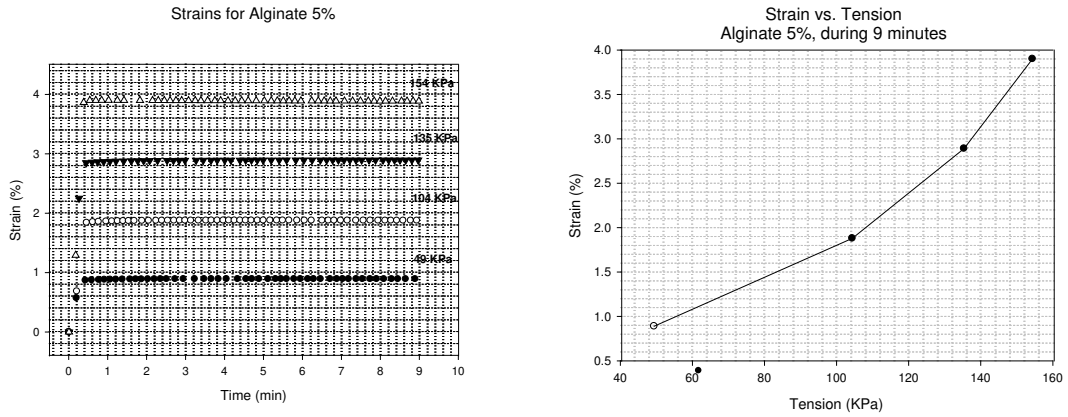

Figure 6 – Scenario B: Strains for Alginate 5% under 9 minutes load.

4.1.3. The Scenario C

Table 4 shows the load values and the final tensions and respective strains.

Table 4 – Loads for Scenario C

Load (N)	Area (mm^2)	Tension σ N/mm^2 ou KPa	δ (%)
0,25	14,88	17	1,01
0,50	11,78	42	2,04
1,00	8,37	119	3,98
1,50	11,25	133	5,78
2,00	12,35	162	7,46
2,50	7,74	323	9,02

Figure 7 presents the strain profiles for scenario C.

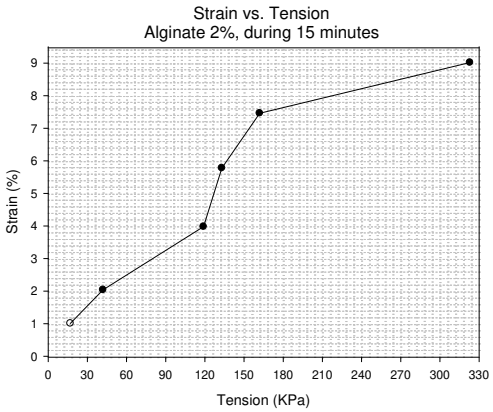

Figure 7 – Scenario C: Strains for Alginate 2% under 15 minutes load.

4.1.4. The Scenario D

In Table 5 are given the load values and the final tensions and respective strains.

Table 5 – Loads for Scenario D

Load (N)	Area (mm^2)	Tension σ N/mm^2 ou KPa	δ (%)
0,25	20,27	12,3	0,91
1,50	8,36	179	5,75
2,00	7,22	277	7,41
2,50	6,98	357	9,03

The strain profiles for scenario D are shown in Figure 8.

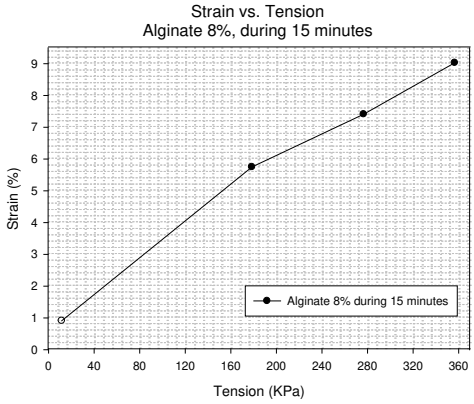

Figure 8 – Scenario D: Strains for Alginate 8% under 15 minutes load.

4.1.5. Comparison between the scenarios

After the experiments are carried out through DMA, it is interesting to compare the body-proofs strain obtained between the scenarios analyzed. All the fitting were approached with a simple Polynomial Quadratic function represented by the equation:

$$f(x) = y_0 + ax + bx^2 \quad (1)$$

where $f(x)$ represents the strain and x the tension.

4.1.5.1. Comparison between Scenarios A and B

Figure 9 shows the relative behaviors between scenarios A and B.

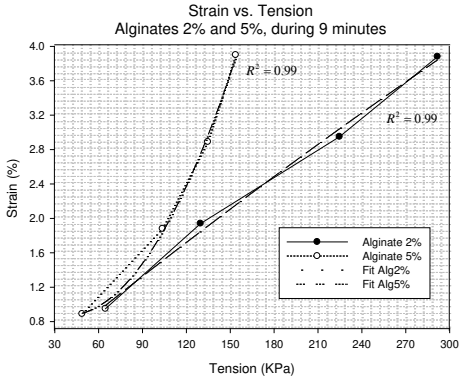

Figure 9 – Comparison of the strains between two different alginates at same period of tension (scenarios A and B).

The alginate 5% suffers higher deformation than alginate 2% under the same tension applied. The tendency after 75KPa is that higher the alginate concentration higher the difference between the respective strains.

4.1.5.2.Comparison between Scenarios A and C

The strain behavior for two different periods of tension for the same alginate composition may be observed in Figure 10.

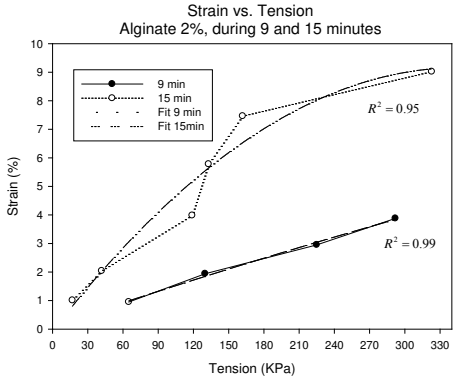

Figure 10 – Comparison of the strains between two different periods of tension for the same alginate (scenarios A and C).

Comparing two different times of tension application, it is noted that the strains present higher values for high times of tension applied.

4.1.5.3.Comparison between Scenarios C and D

Figure 11 illustrates the strain behavior when comparing the scenarios C and D.

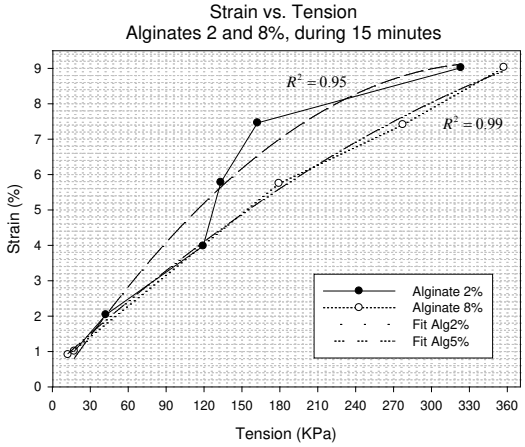

Figure 11 – Comparison of the strains between two different alginates at same period of tension (scenarios C and D).

This comparison is interesting since it can be viewed that, in opposite to the comparison between alginates 2% and 5%, there is a same behavior of alginates 2% and 8% for a range of tension (from the beginning up to 120 KPa), and after that the strains are higher for the low concentration of alginate i.e. 2%, probably due to the necessity of much higher values of tensions to cause some strain in the alginate 8%, which is much more viscous than alginate 2% (and 5%).

4.2. Fitness of the Strain into a Rheological Model

Taking into account that the linear elasticity theory is a generalization of Hooke's Law, some rheological models can be faced as a description of the viscoelastic behavior through the concordance of elastics (springs) and viscous (dashpots) elements.

In Figure 12, the basic elements of a rheological model are shown, to know, the spring and the dashpot. Analogously with the Hooke's Law, the spring owns elastic constant E (Young Modulus), being σ the tension (stress) that actuates over the spring yielding a strain ε, as given by Eq.2:

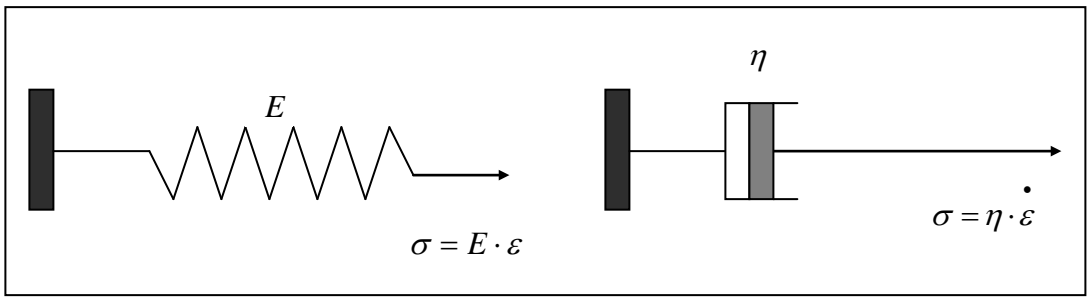

Figure 12 – Basic components of a rheological model - spring (left) and dashpot (right).

$$\sigma = E \cdot \varepsilon \tag{2}$$

In the same way, being η the damp constant of viscous element, the linear relationship between the tension σ applied onto the element and its strain rate $\dot{\varepsilon}$ is given by Eq.3:

$$\sigma = \eta \cdot \dot{\varepsilon} \tag{3}$$

Aiming to achieve a good approach of the experimental strain values with some rheological model, three traditional combinations of springs and dashpots were used: Kelvin-Voigt, Zener-serie and Burger (integration between Maxwell and Voigt models).

4.2.1. Fitting by the Kelvin-Voigt Model

This model consists of a spring of modulus E_1, in parallel with a dashpot of viscosity η_1. If a constant stress σ is applied at time $t = 0$ there can be no instantaneous extension of the spring, as it is retarded by the dashpot. Deformation then occurs at a varying rate, with the stress shared between the two components until, after a time dependent on the dashpot viscosity, the spring approaches a finite maximum extension (Ward and Hadley, 1993). Figure 13 presents the Kelvin-Voigt scheme.

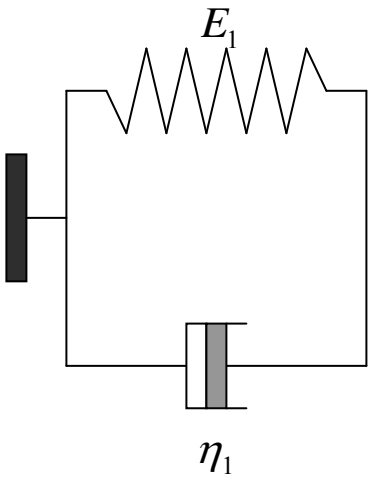

Figure 13 – Kelvin-Voigt model.

The Kelvin-Voigt constitutive equation (Eq.4) for strain is given by:

$$\varepsilon(t) = \delta = \frac{\sigma_0}{E_1} \cdot \left(1 - e^{-\frac{E_1}{\eta_1} \cdot t}\right) \qquad (4)$$

After the experiments and the fitting with the present model, for alginates 2% and 5%, the values obtained are shown in Table 6. These values are used to plot, in Figure 14, the profile of the Young Modulus and the viscous elements for the four tensions applied.

Table 6 – Values gotten from fitting with K-V model.

	Alginate 2%			Alginate 5%		
Load	Tension	E	N	Tension	E	N
0.25	65	6.81	1.77	49	5.52	0.99
0.5	130	6.69	1.67	104	5.55	1.61
0.75	225	7.63	2.21	135	4.65	0.98
1	292	7.52	2.18	154	3.95	0.99

Units: Load (N), Tension (KPa), E (MPa), N (MPa.min).

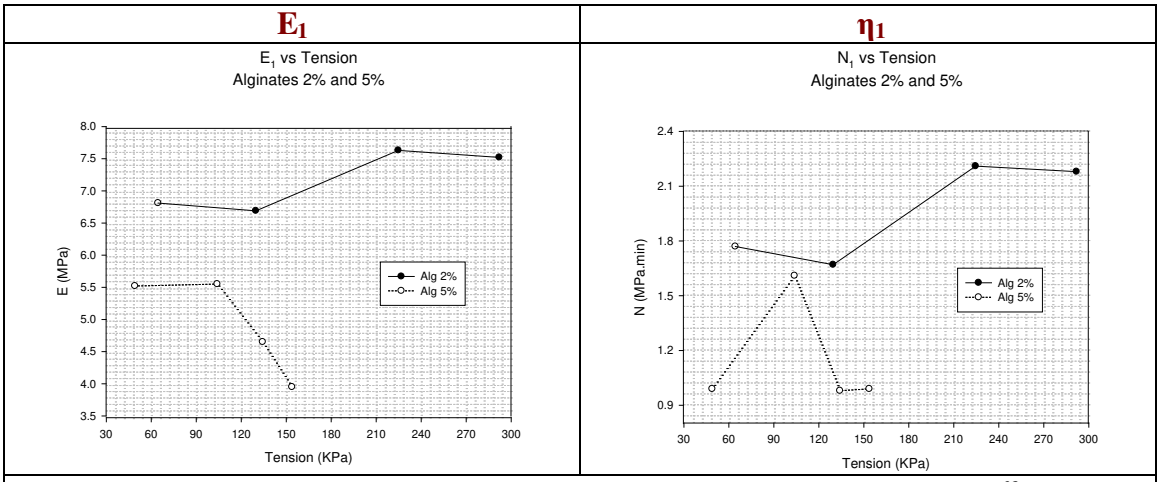

Figure 14 – Profile of Young Modulus (E1) and viscous component (η1) by K-V model.

Table 7 summarizes the variance between the experimental and the K-V model fitting values.

Table 7 – The approaching level (R2) through K-V model.

	R^2 Kelvin-Voigt Model	
Load (N)	Alginate 2%	Alginate 5%
0.25	0.92	0.99
0.5	0.91	0.95
0.75	0.92	0.98
1	0.90	0.96

The worst and the best cases of fitting are illustrated in Figures 15 and 16.

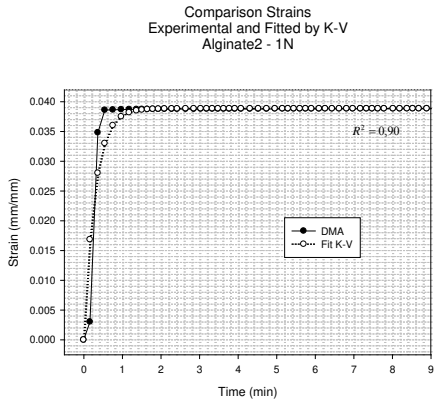

Figure 15 – The worst fitting case by K-V model.

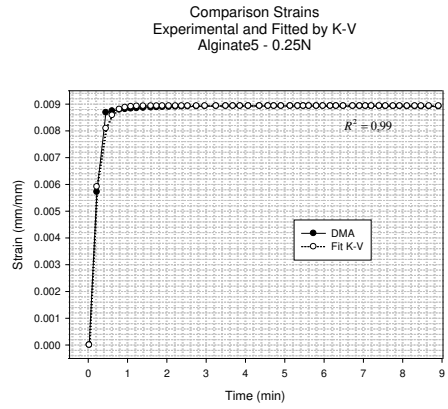

Figure 16 – The best fitting case by K-V model.

4.2.2. Fitting by the Zener-Serie Model

Zener-serie model, in fact a diagram, is a combination of one spring with the Kelvin-Voigt model and is shown in Figure 17.

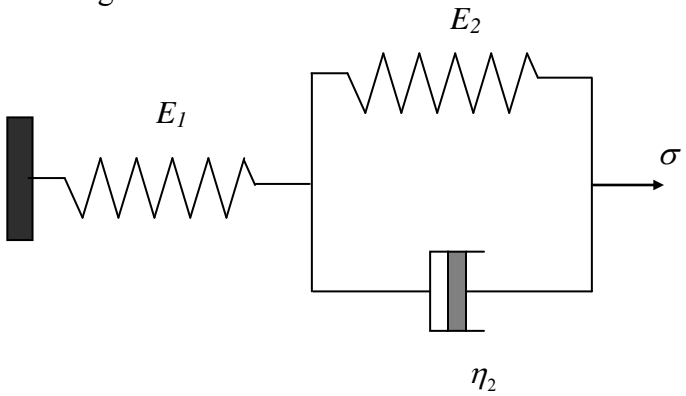

Figure 17 – Zener-serie model.

The Zener-serie constitutive equation (Eq.5) for strain is given by:

$$\varepsilon(t) = \delta = \frac{\sigma_0}{E_1} + \frac{\sigma_0}{E_2} \cdot \left(1 - e^{-\frac{E_2}{\eta_2} \cdot t} \right) \qquad (5)$$

After the experiments and the fitting with the present model, for alginates 2% and 5%, the values obtained are shown in Table 8 and the profile of the Young Modulus and the viscous elements for the four tensions applied are plotted in Figure 18.

Table 8 – Values gotten from fitting with Zener-serie model.

	Alginate 2%				Alginate 5%			
Load	Tension	E_1	N_2	E_2	Tension	E_1	N_2	E_2
0.25	65	11.98	1.58	6.70	49	8.24	0.99	5.56
0.5	130	15.89	1.79	6.51	104	6.90	1.59	5.14
0.75	225	9.04	2.27	6.86	135	5.49	0.56	4.68
1	292	8.64	2.14	7.43	154	5.49	1.16	4.41

Units: Load (N), Tension (KPa), E_1 and E_2 (MPa), N_2 (MPa.min).

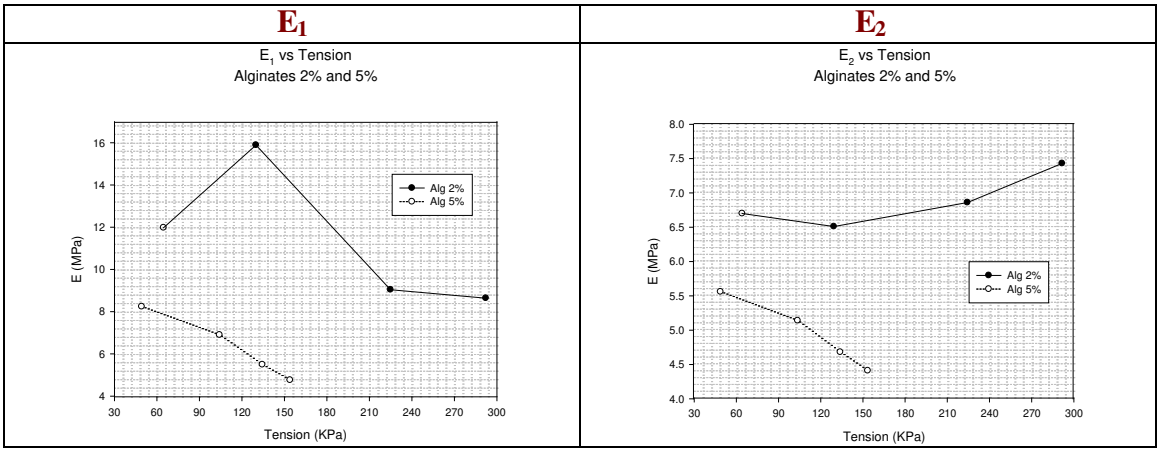

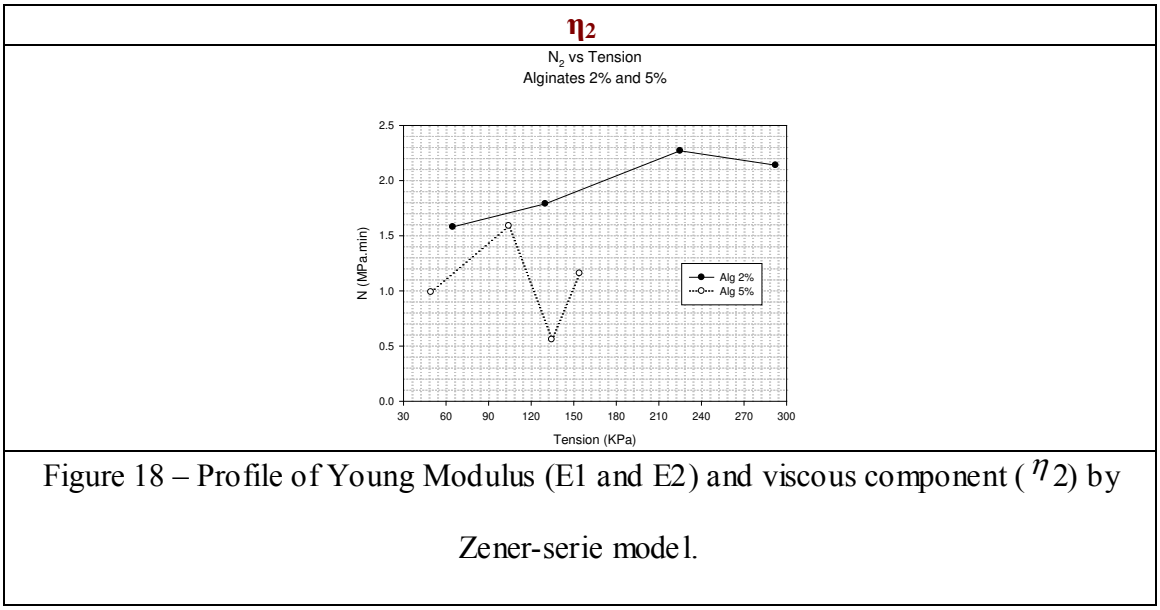

Figure 18 – Profile of Young Modulus (E1 and E2) and viscous component ($\eta 2$) by Zener-serie model.

Table 9 summarizes the variance between the experimental and the Zener-serie fitting model values.

Table 9 – The approaching level (R2) through Zener-serie model.

	R^2 Zener-serie Model	
Load (N)	Alginate 2%	Alginate 5%
0.25	0.89	0.98
0.5	0.88	0.90
0.75	0.86	0.98
1	0.80	0.89

The worst and the best cases of fitting are illustrated in the following Figures 19 and 20.

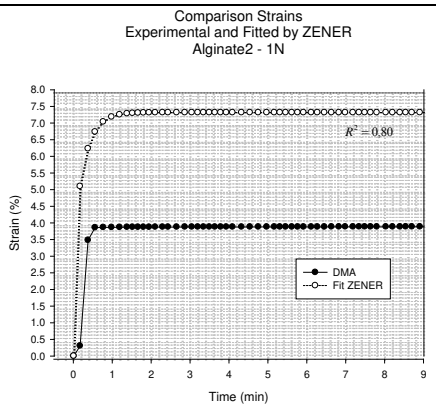

Figure 19 – The worst fitting case by Zener-serie model.

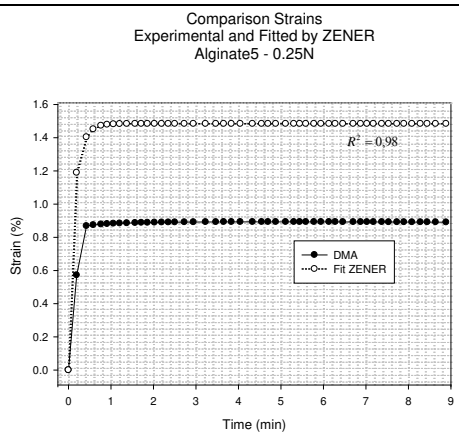

Figure 20 – The best fitting case by Zener-serie model.

4.2.3. Fitting by the Burger Model

Burger's model consists of four mechanical components being a combination of the Maxwell and Kelvin-Voigt models, as shown in Figure 21, where the two spring elements (E_1, E_2) which coincide with the Hookean principle and the two dashpots (η_1, η_2) that follow the Newtonian principle.

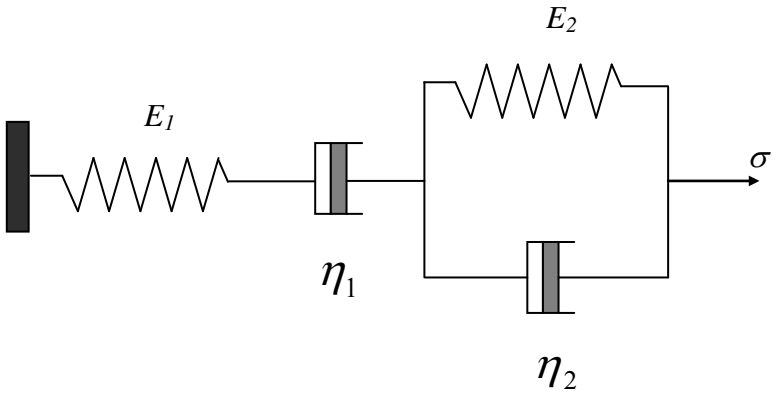

Figure 21 – Burger model.

According to these two principles, Burger's model constitutive equation can be expressed by Equation 6 as follow:

$$\varepsilon(t) = \delta = \frac{\sigma_0}{E_1} + \frac{\sigma_0}{\eta_1} \cdot t + \frac{\sigma_0}{E_2} \cdot \left(1 - e^{-\frac{E_2}{\eta_2} \cdot t} \right) \quad (6)$$

The R^2 Table for Burger and Zener–serie Models shows similar values of fitness between experimental and fitted strain curves (see previous Table 9). So, it can be noted that the extra component of Burger, that is, a dashpot (η_2), causes no much influence in the final fitness reached.

The element values obtained by Burger Model approach are detailed in the Table 10. The values of the other components are very similar and they also indicate a same fitness of these models for sodium alginate.

After the experiments and the fitting with the present model, for alginates 2% and 5%, the values of the Young Modulus and the viscous elements for the four tensions applied calculated are presented in Table 10.

Table 10 – Values calculated from fitting with Burger model.

	Alginate 2%					Alginate 5%				
Load	Tension	E_1	N_1	N_2	E_2	Tension	E_1	N_1	N_2	E_2
0.25	65	11.98	10.78	1.96	6.54	49	8.24	1.62	1.60	5.33
0.5	130	15.89	15.61	1.93	6.44	104	6.90	1.66	1.55	5.17
0.75	225	9.04	12.69	2.11	7.03	135	5.49	3.10	1.33	4.45
1	292	8.64	16.16	2.22	7.40	154	4.76	1.92	1.30	4.32

Units: Load (N), Tension (KPa), E_1 and E_2 (MPa), N_1 (GPa.min) and N_2 (MPa.min).

The profile of the Young Modulus and the viscous elements for the four tensions applied may be seen in Figure 22.

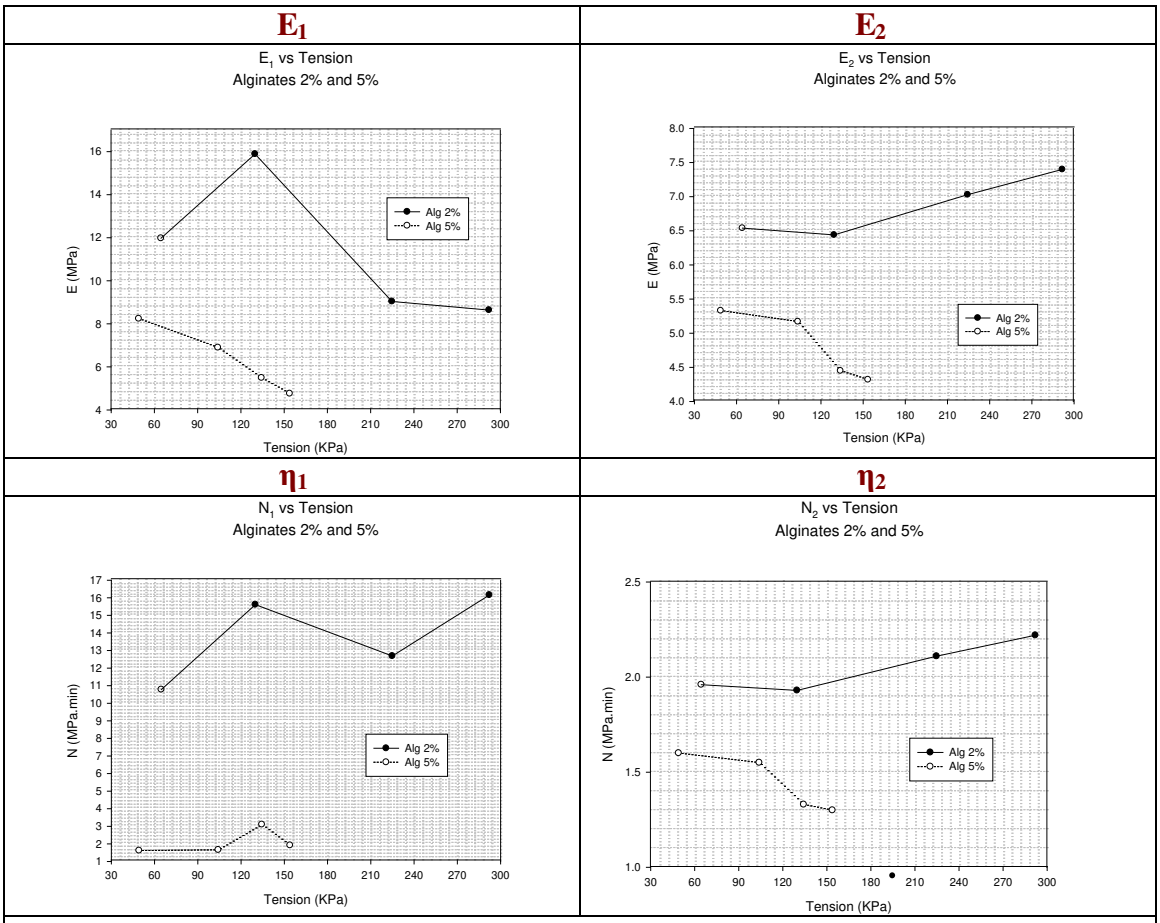

Figure 22 – Profile of Young Modulus (E1 and E2) and viscous component (η1 and η2) by Burger model.

4.2.4. A comparison between the approach gotten from the three analyzed models

In the sequence, two graphs show the final results involving the three models used in this paper for the best and the worst cases. The graphs (Figures 23 and 24) show that, absolutely, the best approaching was achieved by Kelvin-Voigt model.

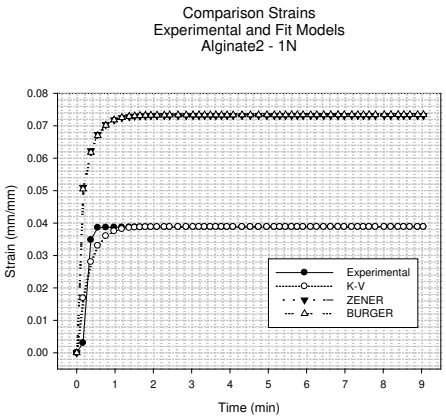

Figure 23 – Experimental and Fit Models strain curves (worst case).

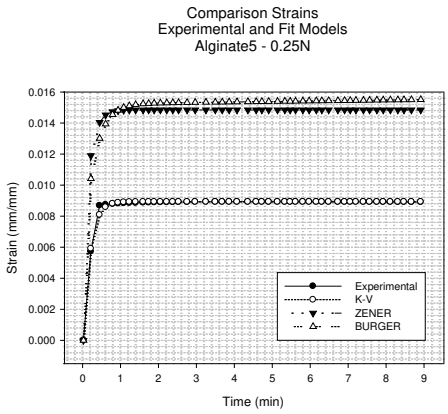

Figure 24 - Experimental and Fit Models strain curves (best case).

4.3. Single Cantilever Bending Test

Single Cantilever Bending mode is excellent procedure for general characterization of most polymeric bar samples. The sample is anchored on one end by a fixed clamp and by the drive shaft on the other. Bending stress is applied by the motor. Figure 25 presents the single cantilever bending test scheme in DMA.

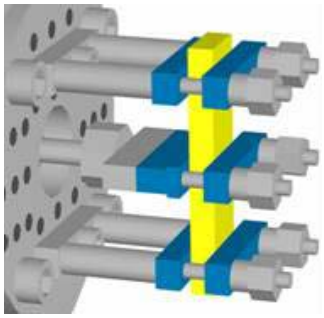

Figure 25 –Single Cantilever Bending test scheme.

These experiments were carried out in order to verify the alginate strain profiles according to some variations through bending. The single cantilever bending tests aimed to know better the alginate behavior (modulus, loss modulus and tan delta) under its own different concentrations, different frequencies, temperature ranges and, also, and the calcium chloride concentration.

4.3.1. Scenario E: Temperature

The initial conditions for this scenario are given in Table 11:

Table 11 – Initial conditions for Scenario E

Alginate (%)	5
$CaCl_2$ (%)	3
f (Hz)	1 / 10
Range of Temperature (ºC)	23-120

Figure 26 presents the modulus, loss modulus and tan delta profiles for scenario E.

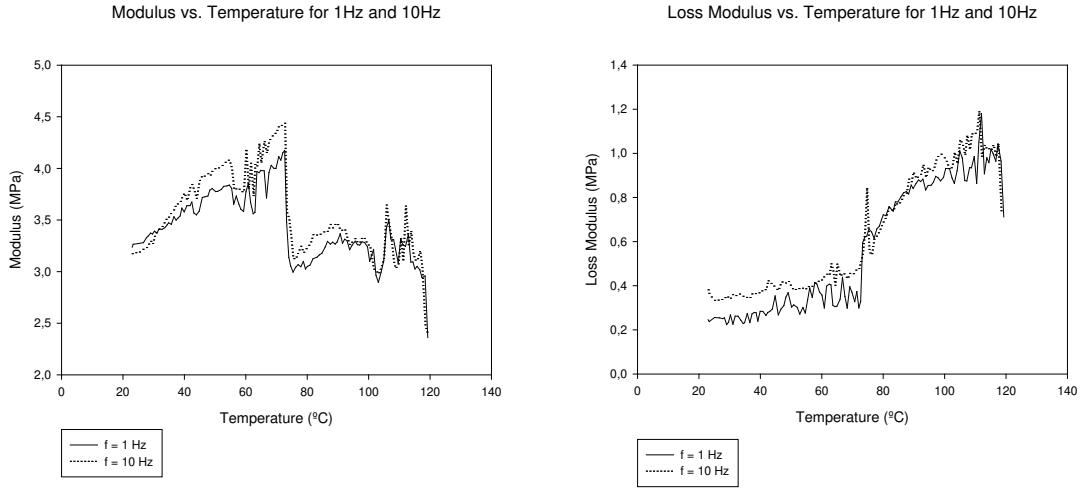

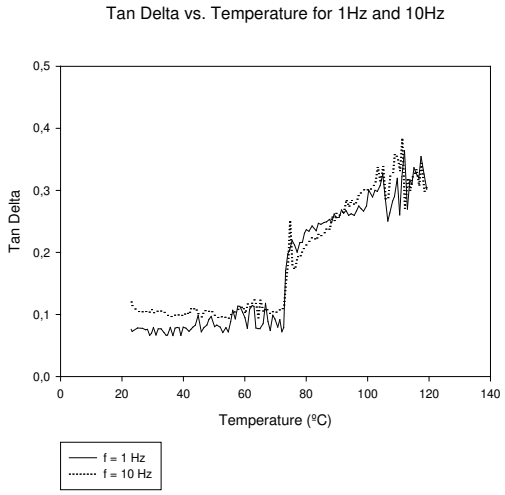

Figure 26 – Scenario E: Mod, Loss Mod and Tan Delta vs. Temperature for 1Hz and 10Hz

4.3.2. Scenario F: Frequency

The initial conditions for this scenario are given in Table 12:

Table 12 – Initial conditions for Scenario F

Alginate (%)	5
$CaCl_2$ (%)	3
f (Hz)	0,316 / 1 / 3,16 / 10 / 31,6
ΔT (ºC)	21-120

The modulus, loss modulus and tan delta profiles for scenario F are depicted in Figure 27.

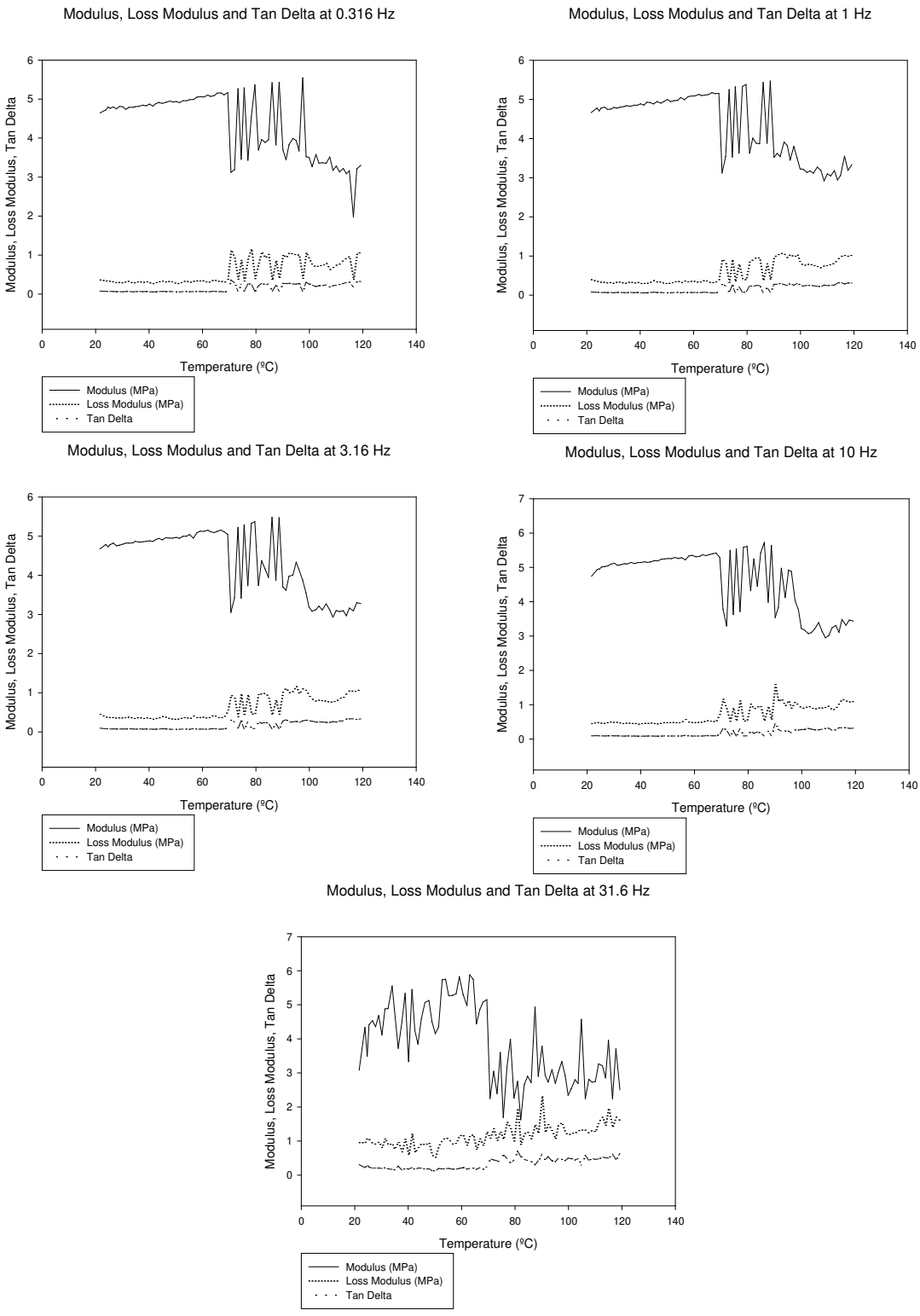

Figure 27 – Scenario F: Mod, Loss Mod and Tan Delta vs. Temperature at 0.316, 1, 3.16, 10, 31.61Hz

4.3.3. Scenario G: Alginate

Comparison between Cases G1 and G2:

The initial conditions for this scenario are given in Table 13:

Table 13 – Initial conditions for Scenario G1 and G2

	G1	G2
Alginate (%)	5	3
$CaCl_2$ (%)	3	3
f (Hz)	1 / 10	1 / 10
ΔT (ºC)	18 -50	17 -50

Figures 28 and 29 present the modulus, loss modulus and tan delta profiles for scenarios G1 and G2, respectively.

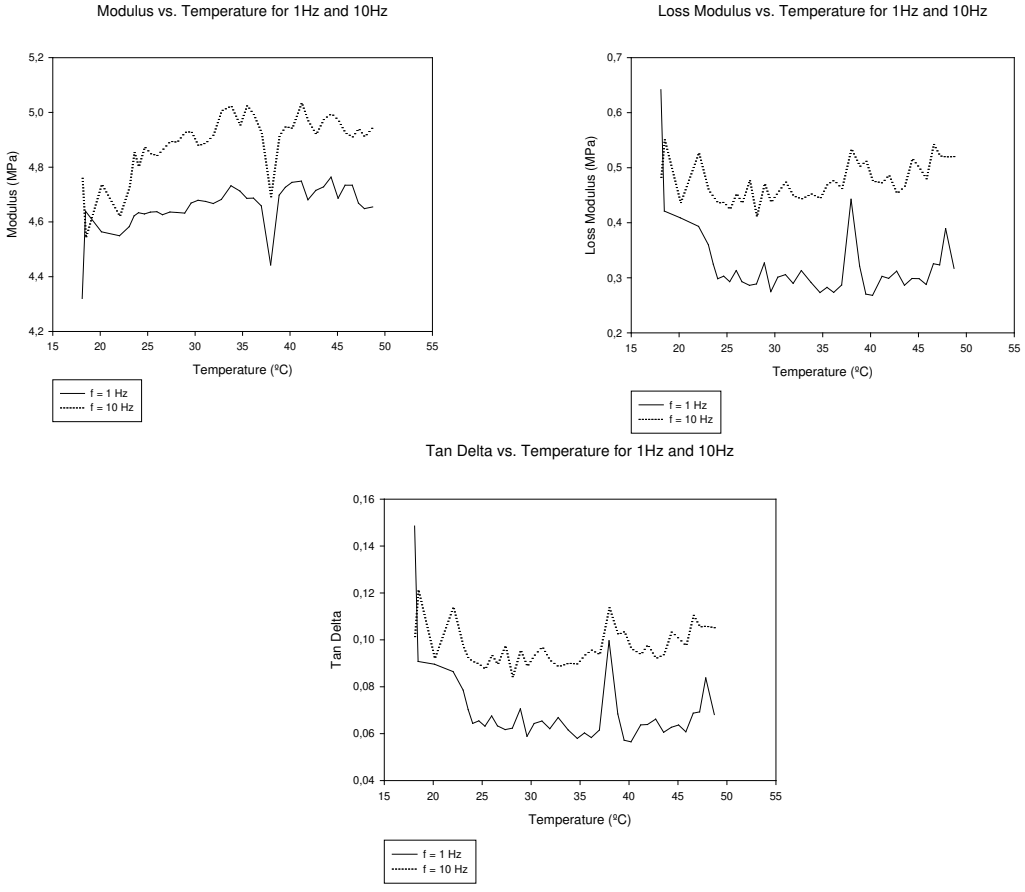

Figure 28 – Scenario G1: Mod, Loss Mod and Tan Delta vs. Temperature at 1 / 10 Hz

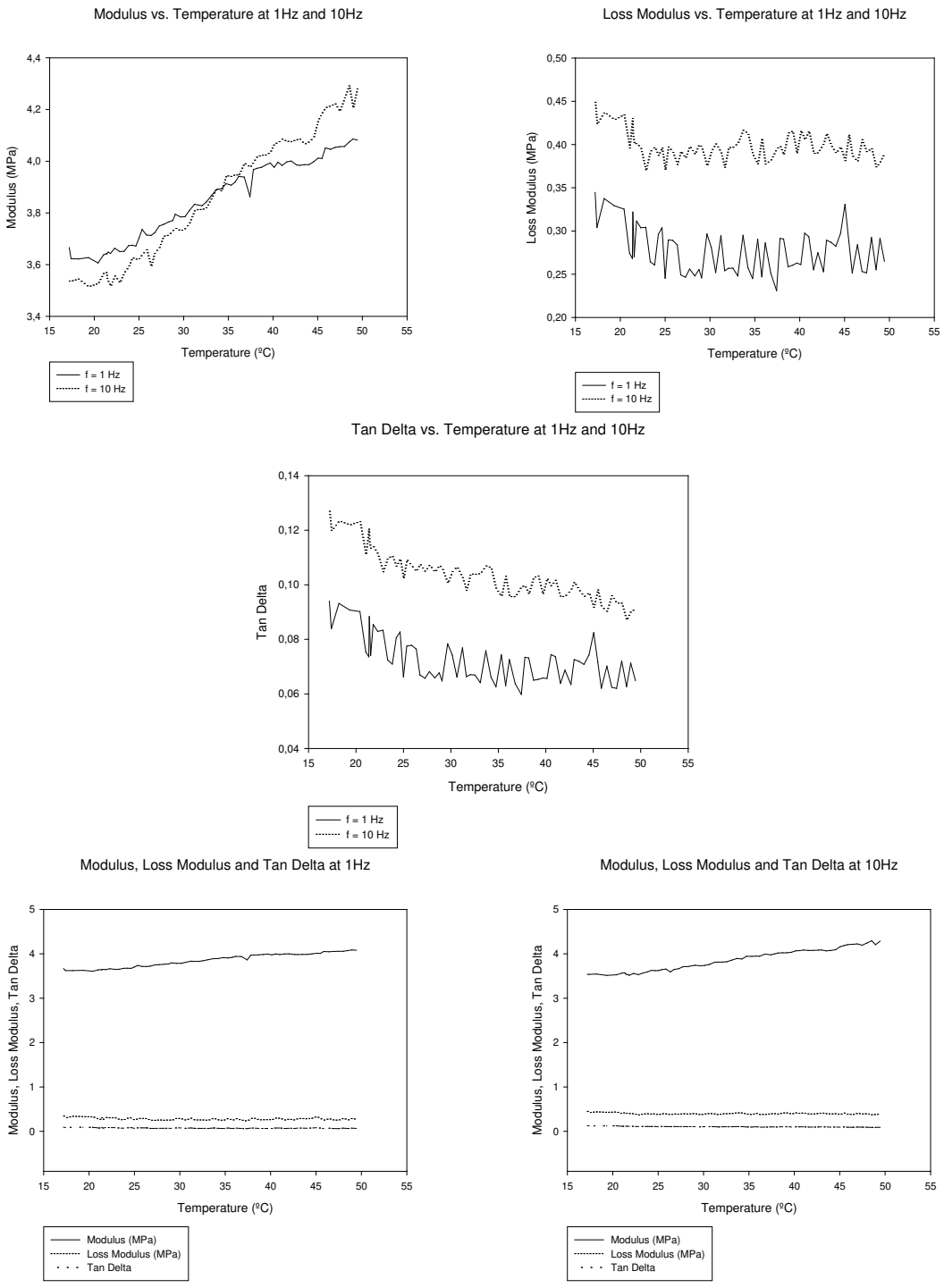

Figure 29 – Scenario G2: Mod, Loss Mod and Tan Delta vs. Temperature at 1 / 10 Hz

4.3.4. Scenario H: CaCl2

Comparison between Cases H1 and H2:

In Table 14 are given the initial conditions for this scenario.

Table 14 – Initial conditions for Scenario H1

	H1	H2
Alginate (%)	5	5
$CaCl_2$ (%)	3	2
f (Hz)	1 / 10	1
ΔT (ºC)	23 -120	22 -150

Figures 30 and 31 present the modulus, loss modulus and tan delta profiles for scenarios H1 and H2.

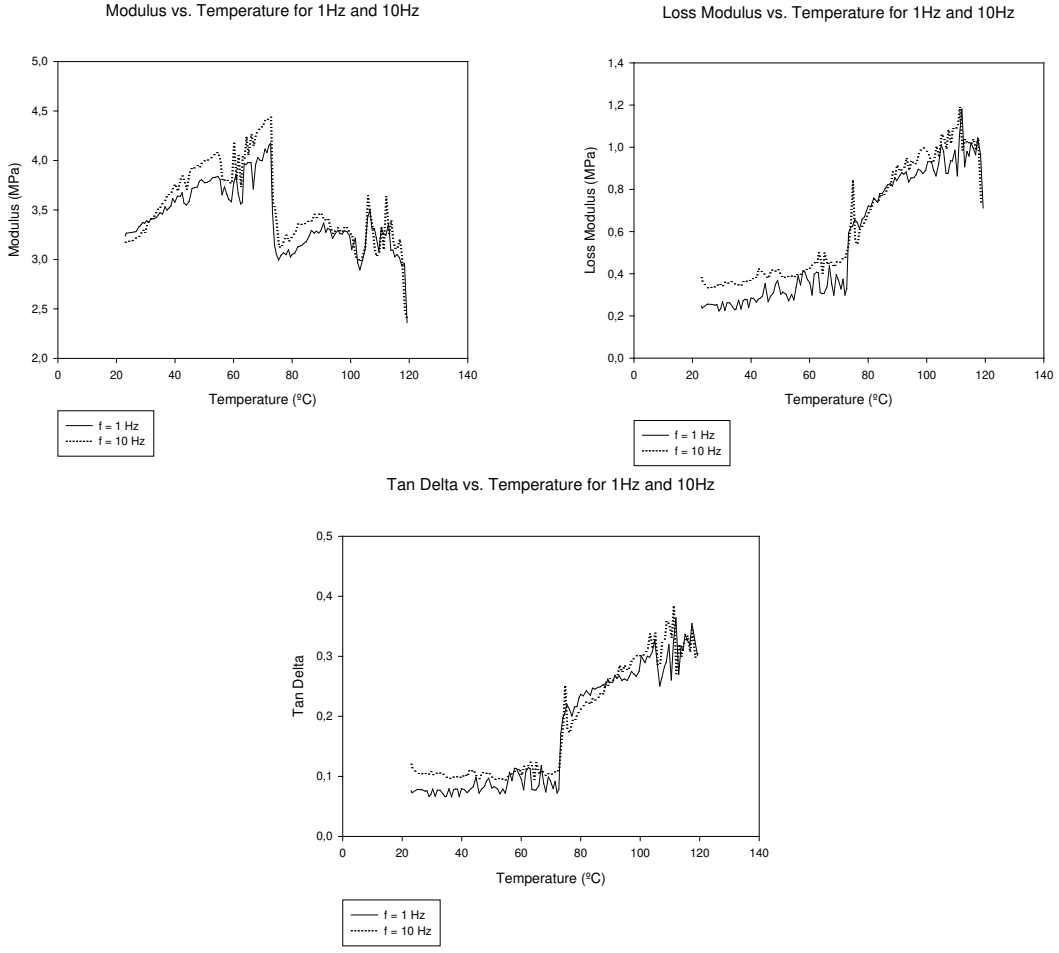

Figure 30 – Scenario H1: Mod, Loss Mod and Tan Delta vs. Temperature at 1 / 10 Hz

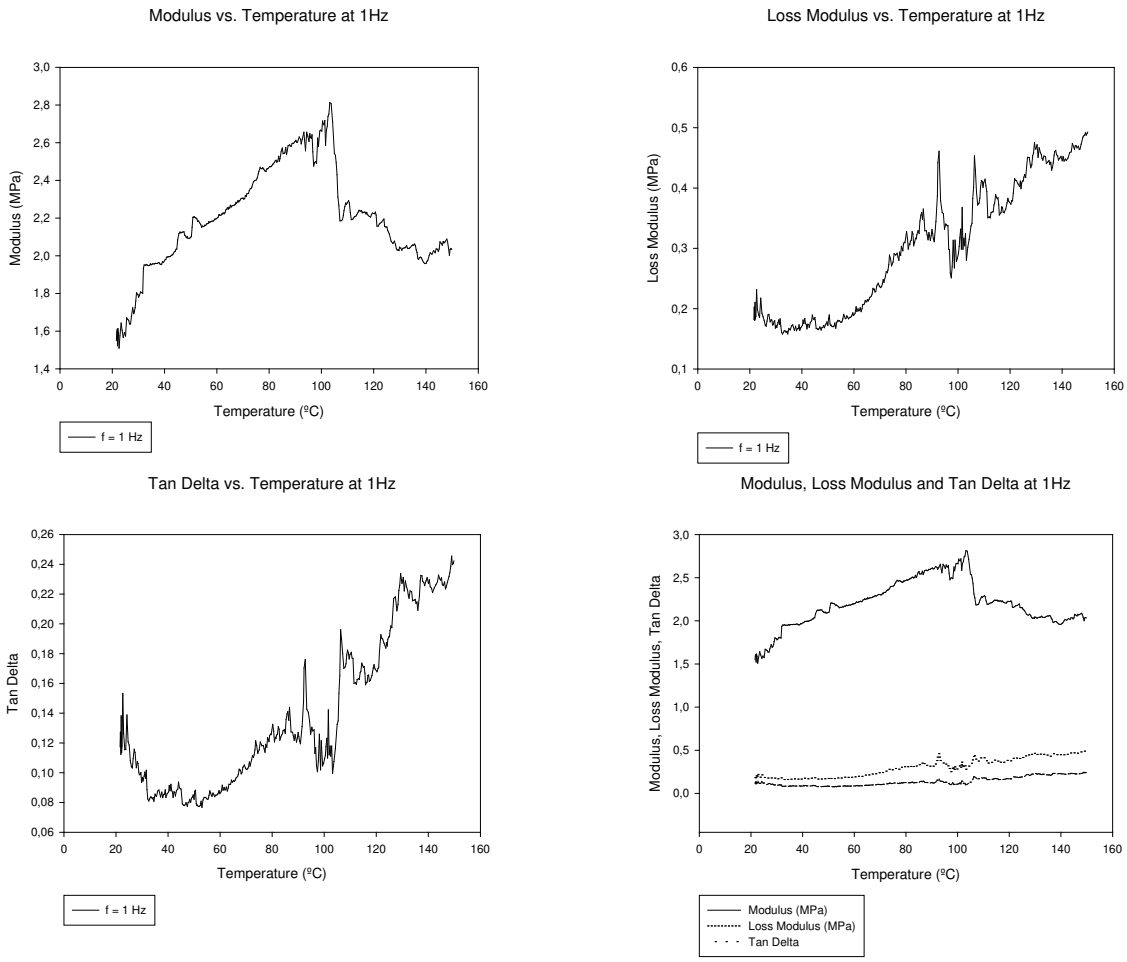

Figure 31 – Scenario H2: Mod, Loss Mod and Tan Delta vs. Temperature at 1 Hz

4.3.5. Scenario I: Fixe Temperature and Variable Frequency

The objective in this section is to check the range of Modulus, Loss Modulus and Tan Delta for a constant temperature and variable frequency.

Comparison between Cases I1 and I2:

The initial conditions for this scenario are given in Table 15:

Table 15 – Initial conditions for Scenario I

	I1	I2
Alginate (%)	5	5
$CaCl_2$ (%)	3	3
f (Hz)	0,1	10
ΔT (ºC)	25	25

Figures 32 and 33 present the distribution of points for modulus, loss modulus and tan delta profiles about scenarios I1 and I2.

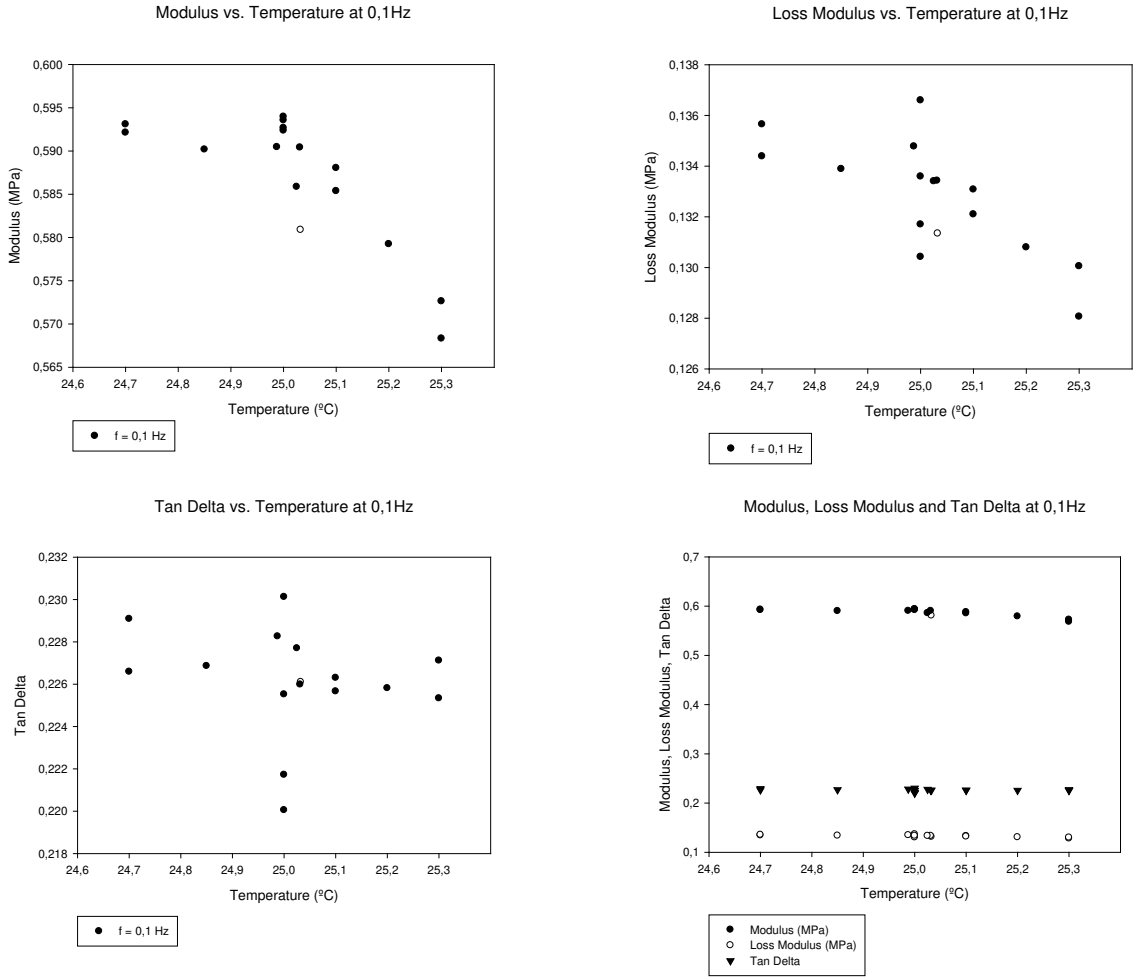

Figure 32 – Scenario I1: Mod, Loss Mod and Tan Delta vs. Temperature at 0,1 Hz

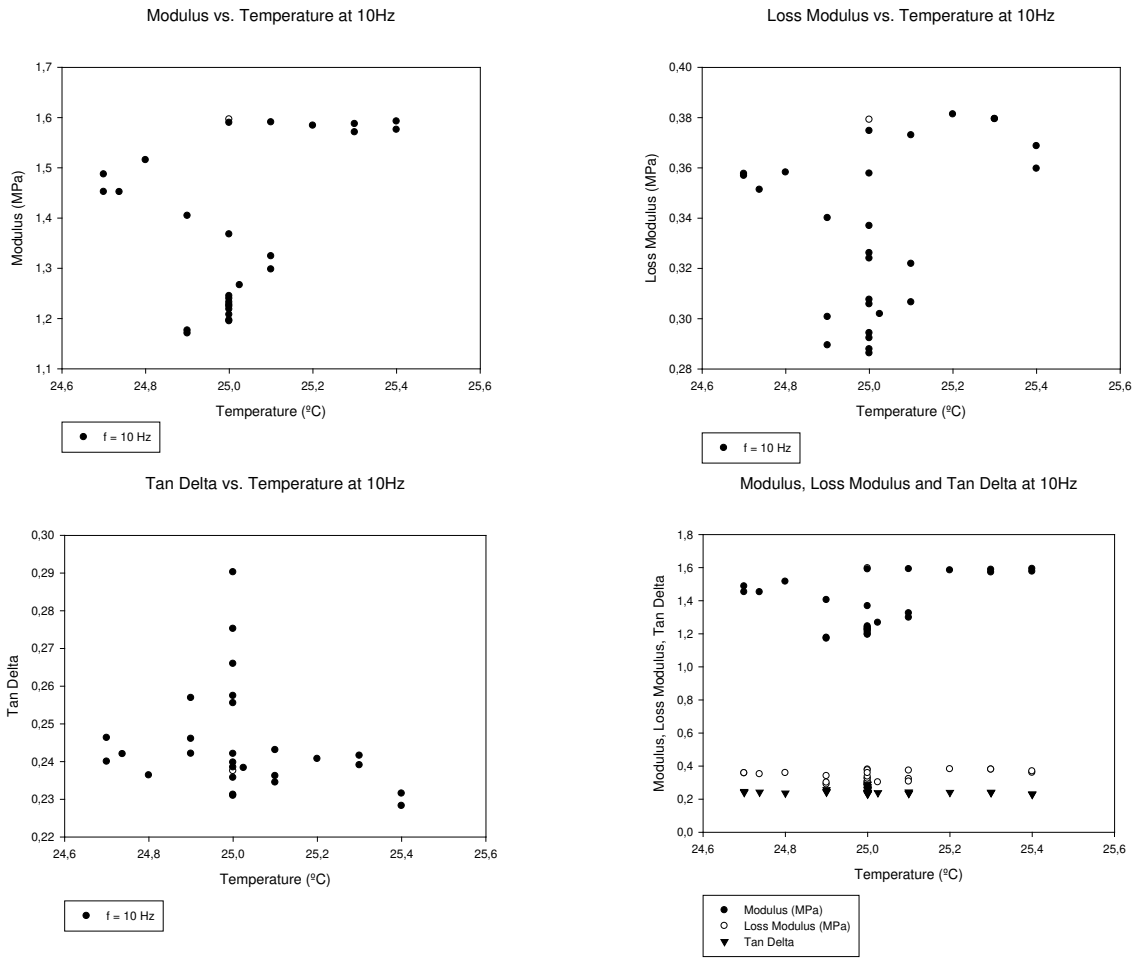

Figure 33 – Scenario I2: Mod, Loss Mod and Tan Delta vs. Temperature at 10 Hz

5. Conclusions

For the biofabrication with the needed requirements as biodegradability and mechanical characteristic aiming at the fabrication of scaffolds in alginate, dynamic mechanical analysis is fundamental to verify the mechanical behavior of calcium alginate for different concentration and submitted to several effort tests. Alginate is a hydrogel and so a very soft material, that contains a large amount of water, which difficult the establishment of the standardization in the body-proof preparation.

The experiments showed the influence of alginate and $CaCl_2$ concentrations, the applied frequency, the tension applied and the time under tension. Very low (2%) and very high (8%) concentrations of alginate presented lower values of strain than an intermediary concentration (5%) which suffered higher deformations. Higher the period of tension submitted to the body-proof, higher the strain. Alginate 5% stretches more than alginate 2% does, so alginate 2% is more rigid. In terms of single cantilever bending tests, normally, higher values of frequency led to higher levels of the Modulus. The temperature increases the modulus until a peak which then starts to decrease after that. Varying the frequency evaluation allow to conclude that higher the frequency higher the disturbance caused and the modulus range reache a minimum about 2MPa. According to the alginate and $CaCl_2$ concentrations, higher concentrations cause higher modulus values. When the temperature is fixed, increasing the frequency, the modulus is sited in a higher range of values.

About the performed fitting through different rheological models, the Kelvin-Voigt model presented a better approach with the experimental results than the other ones. Zener-serie and Burger models practically matched each other which mean that the extra dashpot did not cause siginificant influence.

6. Acknowledgements

The authors would like to thank the support from The National Council for Scientific and Technological Development (CNPq, Brazil), and the Foundation for Science and Technology (FCT, Portugal).

7. References

Fung, Y. C. Biomechanics: Mechanical properties of Living Tissues. Springer-Verlag. New York. 1981.

Gombotz, W. R. and Wee, S. W., 1998, Protein release from alginate matrices, Adv. Drug Deliv. Rev., 31, pp.267-285.

Hutmacher, D. W. Scaffold-based tissue engineering – design and fabrication of matrices using solid freeform fabrication techniques. Advanced Manufacturing Technology for Medical Applications, Ed. by I. Gibson, 163-189, 2006.

Johnson, F.A., Craig, D.Q.M., Mercer, A.D., Characterization of the block structure and molecular weight of sodium alginates, Journal of Pharmacy and Pharmacology, v.49, Issue 7, p. 639-643, 1997.

Klöck, G., Frank, H., Houben, R., Zerkon, T., Horcger, A., Siebers, U., Wöhrle, A., Federlin, K., and Zimmermann, U., Production of purified alginates suitable for use in immunoisolated transplantation, Appl Microbiol Biotechnol, 40, pp.638-643, 1994.

Menard, K. P., Dynamic Mechanical Analysis – A Practical Introduction, CRC Press, 1999.

Mironov, V. Trusk, T. Kasyanov, V. Little, S. Swaja, R. Markwald, R. Biofabrication: a 21st century manufacturing paradigm. Biofabrication. v.1 n.2. 2009.

Peppas, N. A., Hilt, J. Z., Khademhosseini, A., Langer, R. Hydrogels in Biology and Medicine: From Molecular Principles to Bionanotechnology. Advanced Materials, 18, 1345-1360, 2006.

Ratner, B. R., Hoffman, A. S., Schoen, F. J., Lemons, J. E. Introduction to materials in medicine. Biomaterials Science, 1996.

Rezende, R.A., Bártolo, P.J.S., Mendes, A., Maciel Filho, R. Rheological Behavior of Alginate Solutions for Biomanufacturing. Journal of Applied Polymer Science, v.113, 3866-71, 2009.

Serp, D., Cantana, E., Heinzen, C., Stockar, U. and Marison, I. W., Characterization of an encapsulation device for the production of monodisperse alginate beads for cell immobilization, Biotechnology and Bioengineering, 70, pp.41-53, 2000.

Serp, D., M. Mueller, U. Stockar and I.W. Marison, 2002, Low-temperature electron microscopy for the study of polysaccharide ultrastructures in hydrogels. II. Effect of temperature on the structure of Ca2+-alginate beads, Biotechnology and Bioengineering, 79, 253-259.

Triton Technology Ltd: http://www.triton-technology.co.uk/ (accessed April 2010).

Tsang, V. L., Bhatia, S. N. Three-dimensional tissue fabrication. Advanced Drug Delivery Reviews, 56, 1635-1647, 2004.

Ward, I. M. and Hadley, D. W. An Introduction to the Mechanical Properties of Solid Polymers. John Wiley & Sons. 1993.

Webber, Rebecca. Viscoelastic Behavior and Adhesion of Ionic Alginate Hydrogels (2004), Kenneth Shull (Northwestern University): http://flux.aps.org/meetings/YR04/MAR04/baps/abs/S290006.html. (accessed November 2009).

4.3 Conclusões

Após a reticulação do alginato de sódio com cloreto de cálcio originando o alginato de cálcio, ou seja, o fenômeno de formação de pontes iônicas entre os cátions divalentes (Ca^{++}) e as cadeias intrínsecas no polímero, as propriedades físicas do alginato naturalmente sofrem alterações. O material torna-se mais viscoelástico ganhando visivelmente uma maior resistência mecânica.

Visando-se conhecer melhor o comportamento mecânico do alginato reorganizado, em função da deformação causada, sob diferentes condições de concentração do alginato e do cloreto de cálcio, utilizou-se o equipamento DMA, voltado para análises dinâmico mecânicas, para a realização dos ensaios. Foram também analisadas a influência da freqüência e a tensão aplicada.

Para os ensaios de tração, os corpos de prova com concentração intermediária de alginato (5%) apresentaram maior deformação. O maior período de aplicação de tensão ocasiona maior deformação. Alginato 2% apresenta-se mais rígido que alginato 5%. No ensaio de flexão simples, o módulo de ganho apresenta maiores patamares quanto maiores os valores de freqüência. Quanto à variação da temperatura, há um valor de pico para o módulo de ganho que passa, em seguida, a decrescer. Para freqüências maiores, maior a perturbação causada e menor o valor atingido do módulo de ganho.

Para a variação das concentrações de alginato (de sódio – aquele conteúdo que foi preparado para ser reticulado com o cloreto de cálcio) e do próprio cloreto de cálcio, maiores concentrações implicaram em maiores valores do módulo de ganho. Ao se fixar a temperatura e se variar a freqüência em dois valores diferentes, percebe-se um aumento considerável no módulo de ganho, provavelmente de forma logarítmica.

O comportamento viscoelástico do alginato de cálcio foi ajustado por meio de três diferentes modelos reológicos tradicionais, sendo que o Modelo Kelvin-Voigt foi o que melhor se aproximou dos valores experimentais quando dos respectivos valores de correlação (R^2).

Capítulo 5 – Gelação, Inchamento e Preparação de Esponjas

5.1 Introdução

O Capítulo 5 investiga a influência determinante das composições de alginato e de cloreto de cálcio, além do tempo de gelação, sobre o inchaço (*swelling*) e sobre a morfologia de *scaffolds* obtidos pela preparação de esponjas em alginato.

O melhor entendimento tanto das reações cinéticas do processo de gelação (reticulação) dos sistemas baseados em alginato quanto das características reológicas de soluções de alginato é um passo importante para o desenvolvimento de um sistema inteligente que conduza ao projeto, otimização e controle de um novo sistema de prototipagem rápida voltado para o material em questão. Para tanto, é fundamental um domínio maior no que se refere aos aspectos químicos e físicos do processo de gelação.

Para além do processo de gelação propriamente dito, outros fatores comportamentais pertinentes ao alginato devem ser igualmente levados em consideração, tal como o seu inchamento por absorção de fluidos (*swelling*). A fração de inchaço do alginato, que se caracteriza pela capacidade deste material em absorver fluidos, é investigada através das composições de alginato e de cloreto de cálcio na amostra, além do tempo de gelação, sob diferentes condições de preparação e ambiente. O conhecimento do perfil de inchaço do alginato mediante suas variantes é interessante do ponto-de-vista da aplicação do material à engenharia tecidual. Adicionalmente, este capítulo apresenta um estudo acerca das esponjas em alginato (*foaming*) confeccionadas sob diferentes conteúdos de alginato e cloreto de cálcio.

5.2 Artigos Produzidos

O Capítulo 5 é desenvolvido e apresentado em forma de dois artigos. O primeiro deles é intitulado "**Experimental Characterisation of the Alginate Gelation Process for Rapid Prototyping**" e foi publicado nos anais do *ICheaP-8 – The 8th Italian Conference on Chemical and Process Engineering* "Chemical Engineering Transactions" AIDIC Servizi. (v. 11, p. 509-514, 2007). O segundo artigo "**Swelling and Foaming with Calcium Alginate for Biofabrication**", o qual será brevemente submetido a um periódico internacional.

Experimental Characterisation of the Alginate Gelation Process for Rapid Prototyping

R.A. Rezende[1,2], P.J. Bártolo[1], A. Mendes[1] , R. Maciel Filho[2]

[1]Centre for Rapid and Sustainable Product Development and Institute for Polymers and Composites, School of Technology and Management, Leiria Polytechnic Institute
Campus 2, Morro do Lena, Alto do Vieiro, Leiria, Portugal

[2] Laboratory of Optimization, Design and Advanced Control,
School of Chemical Engineering, State University of Campinas
Cidade Universitária "Zeferino Vaz", CP 6066, Campinas, São Paulo, Brazil

Hydrogels have received much attention due to their potential use in a wide variety of biomedical applications, including tissue engineering scaffolds, drug delivery, contact lenses, corneal implants and wound dressing. This research work focuses on a new route to produce three-dimensional scaffolds in alginate hydrogels for medical applications, through the use of a biomimetic rapid prototyping system. This system replicates some natural procedures used by some marine brown algae, namely *Laminaria Hyperborea*, to produce alginate used as a structural component of the algae, in accurate chemical conditions. The biomanufacturing of optimised alginate scaffolds requires the control of the gelation process in order to obtain improved mechanical and biological properties and appropriate surface morphology for cell attachment, proliferation and differentiation. This paper investigates the influence of sodium alginate of both sodium alginate and calcium chloride on the gelation kinetics.

1. Introduction

Tissue engineering is an interdisciplinary field that combines the use of living cells with either natural or synthetic extra-cellular structures (scaffolds) to develop body parts or devices that will enable the restoration, maintenance or enhancement of living tissue and organs. Three-dimensional scaffolds play an important role in promoting and guiding tissue regeneration. Usually, these scaffolds have high porosity (macro-porosity), appropriate surface morphology (micro-porosity), large surface area, suitable pore size and highly connected pore structure. They must also be biocompatible and biodegradable.

Rapid prototyping represents a new group of non-conventional techniques with great potential to produce scaffolds with customised external shape and predefined internal morphology (Leong et al., 2003, p.2363). These processes also allow controlling both pore size and distribution. Ideally, rationally designed tissue engineering scaffolds promote natural wound healing and regeneration. Therefore, we sought to develop a biofabrication system, specifically designed to soft tissue repair applications.

This paper focus on the concept of rapid prototyping to produce alginate scaffolds for medical applications. The effect of the gel composition in terms of both gelation and surface morphology is investigated.

2. Rapid Prototyping for alginate scaffolds

An alginate-based rapid prototyping system has been developed to produce alginate scaffolds by extruding, layer-by-layer, a solution of sodium alginate into a calcium chloride solution (Figure 1). The system comprises two nozzles, one for the sodium alginate and the other for the calcium chloride deposition (Bártolo, 2006, p.56).

a) b)

Figure 1 – Alginate-based rapid prototyping system (a), alginate scaffold structure (b).

3. The chemistry of alginate

Alginate is an anionic copolymer composed (Figure 2) of homopolymeric regions of 1,4-linked β-D-mannuronic (M blocks) and α-L-guluronic acid (G blocks), interspersed with regions of alternating structure. The industrial manufacture of alginate is based on the extraction of a polymer from brown algae. The seaweed grows in nature mainly in temperate areas, but large amounts are also cultivated in other regions like the Far East, the coast of China or Japan. The seaweed is extracted with a dilute alkaline solution which solubilises the alginic acid present. Free alginic acid is obtained treating the resulting viscous material with mineral acids, being then converted to a salt. Sodium alginate is the major form currently used.

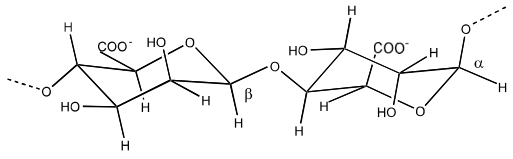

β-D-Mannuronic acid α-L-Guluronic acid

Figure 2 - Structure of an alginate showing a linkage between the M and G acids.

Gelation occurs when divalent ions (Ca^{2+}, Ba^{2+}, Fe^{2+}, Sr^{2+}, etc.) or trivalent ions (Al^{3+}, etc.) take part in the interchain ionic binding between G-blocks in the polymer chain giving rise to a three dimensional network. Such binding zones between the G-blocks are often referred to as "egg boxes". These ions act as cross-linkers that stabilise alginate chains forming a gel structure, which contains cross-linked chains interspersed with more freely movable chains that bind and entrap large quantities of water. The gelification process is characterised by a re-organisation of the gel network accompanied by the expulsion of water (Serp et al., 2002, p. 253).
Gels made of M-rich alginate are softer and more fragile, and may also have lower porosity. This is due to the lower binding strength between the polymer chains and to the higher flexibilities of the molecules. The gelification process is highly dependent upon diffusion of gelification ions into the polymer network. Trasmittancy, swelling and viscoelasticity of alginate structures are highly affected by the M/G ratio.
Alginic acid and its sodium and calcium salts are non-toxic and biocompatible, being widely used in the medical, pharmaceutical, cosmetic and food industry (Gombotz and Wee, 1998, p.267). In tissue engineering, alginate has been used as a delivery vehicle or supporting matrix.

4. Material

Sodium alginate was purchased at Panreac (Barcelona, Spain). Calcium chloride was supplied by Carlo Erba (Milano, Italy). All solutions were prepared with pure water, with conductivity of 0.054 μS/cm. Alginate solutions were prepared by addition of weighted portions of sodium alginate to measured volumes of water. Due to their high viscosity, these solutions were agitated by orbital shaking for three hours at 50 ºC to ensure good homogeneity. Calcium chloride solution 5% (w/v) was obtained dissolving the salt in water. This solution was diluted to obtain solutions containing different concentrations of calcium chloride.

5. Results

To evaluate the kinetics of the gelation process solutions, containing different concentrations of both alginate and calcium chloride ($CaCl_2$), were prepared and mixed at room temperature. The effect of the alginate concentration is shown in Figure 3, which describes the weight loss as a function of gelation time for solutions containing 1% and 2% (w/v) mixed with a solution of 5% (w/v) $CaCl_2$. Figure 4 shows the variation of weight loss as a function of gelation time for a solution containing 2% (w/v) of alginate mixed with solutions containing different concentrations of $CaCl_2$. The experimental data were fitted using a sigmoidal equation. To correlate the experimental data and the values obtained from the sigmoidal equation, a numerical routine using the Marquardt-Levenber multivariable non-linear regression method was employed. A good correlation was achieved by controlling the number of steps, the increment and a small tolerance parameter, corresponding to the difference of values at the step n+1 and values at the step n, which is used for convergence purposes.

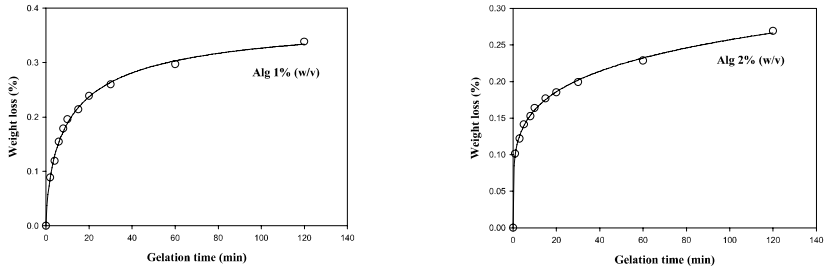

Figure 3 - Weight loss vs gelation time for two solutions containing different concentrations of alginate mixed with a solution of of 5%(w/v) of $CaCl_2$.

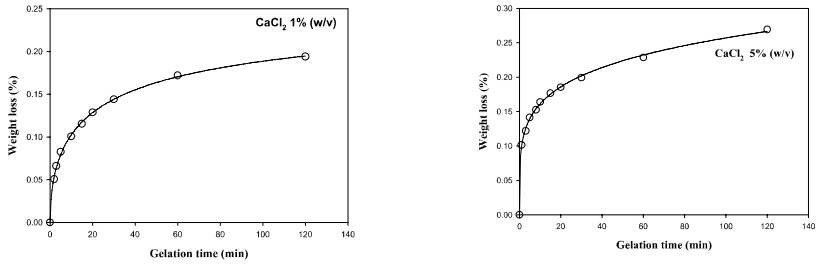

Figure 4 - Weight loss versus gelation time for a solution containing 2% (w/v) of alginate mixed with solution containing different concentrations $CaCl_2$.

It can be observed that the weight loss increases with time and is more significant for samples produced by solutions containing low contents of alginate and high contents of calcium chloride. This is due to two main reasons:

- the amount of water present in the initial alginate solution, which is higher in more dilute solutions;
- the kinetics of the gelation process, which is higher whenever solutions containing higher concentrations of $CaCl_2$ are used.

The calcium divalent ions act as cross-linkers that stabilise alginate chains forming a gel structure. Therefore, increasing the concentration $CaCl_2$ present in the solution increases the cross-linking of polymeric chains and the expulsion of water (Mendes et al., 2003, p.419). The effect of the gel composition can be observed in Figures 5 and 6.
The concentration of both sodium alginate and $CaCl_2$ determines not only the kinetics of the gelation process, but also the internal (not shown in this paper) and surface morphology of alginate gels as indicated in Figure 7. This Figure indicates that gels obtained from solutions containing higher sodium alginate and low $CaCl_2$ contents have smooth surfaces.

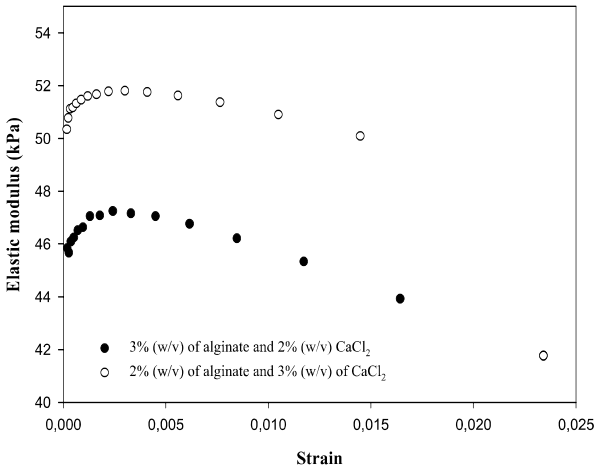

Figure 5 – Elastic modulus versus strain for two different alginate gels.

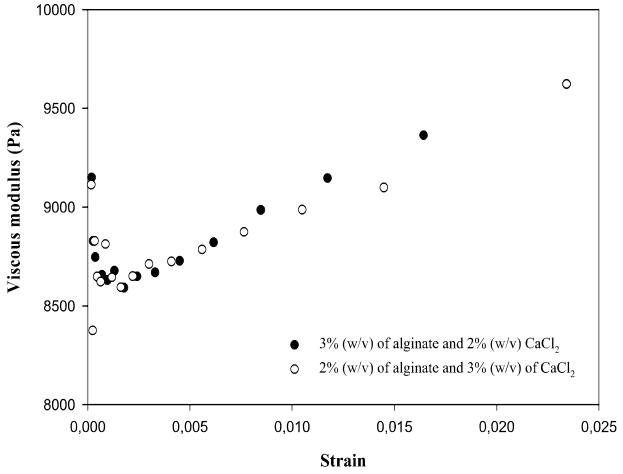

Figure 6 – Viscous modulus versus strain for two different alginate gels.

6. Conclusion

Alginate is a biodegradable and biocompatible biopolymer that can be used in tissue engineering as a scaffold that promotes wound healing. This paper presents a new rapid prototyping approach to produce three-dimensional alginate scaffolds for tissue engineering. This kinetics of the gelation process to obtain such scaffolds is discussed. It was found that the gelation mechanism is strongly dependent on both the alginate and calcium chloride concentrations. Additionally, the concentration of both sodium alginate and calcium chloride determine the mechanical behaviour of alginate gels and its surface morphology.

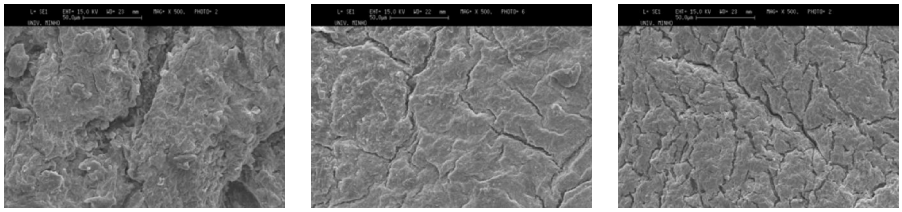

a) b) c)

Figure 7 – SEM for gels containing 2% alginate and 1% $CaCl_2$ (a), 3% alginate and 1% $CaCl_2$ (b) and 2% alginate and 2% $CaCl_2$ (c).

7. Ackowledgements

The Portuguese Foundation for Science and Technology has been sponsoring this research through the projects POCI/SAU-BMA/60287/2004 and POCTI/EME/60650/2004.

8. References

Bártolo, P. J. S., 2006, State of the art of solid freeform fabrication for soft and hard tissue engineering. Design and Nature III: Comparing Design in Nature with Science and Engineering, 87, p.56.

Gombotz, W. R. and Wee, S. W., 1998, Protein release from alginate matrices, Adv. Drug Deliv. Rev., 31, pp.267-285.

Mendes, A., R. Lagoa, and P. Bártolo, 2003, Rapid Prototyping System for Tissue Engineering, Proceedings of Advanced Research in Virtual and Rapid Prototyping, Edited by P.J. Bártolo, G. Mitchell, A. Mateus, F. Batista, J. Vasco, M. Correia, N. André, P. Lima, P. Novo, P. Custódio, P. Martinho, School of Technology and Management, Polytechnic Institute of Leiria, Portugal.

Leong, K. F., C. M. Cheah, C-K. Chua, 2003, Solid freeform fabrication of three-dimensional scaffolds for engineering replacement tissues and organs. Biomaterials, 24, 2363-2378.

Serp, D., M. Mueller, U. Stockar and I.W. Marison, 2002, Low-temperature electron microscopy for the study of polysaccharide ultrastructures in hydrogels. II. Effect of temperature on the structure of Ca^{2+}-alginate beads, Biotechnology and Bioengineering, 79, 253-259.

Swelling and Foaming with Calcium Alginate for Biofabrication

Rodrigo A. Rezende[1,2*], Paulo J. Bártolo[2], Ausenda Mendes[2], Rubens Maciel Filho[1]

[1] Laboratory of Optimization, Design and Advanced Control, School of Chemical Engineering, University of Campinas, Cidade Universitária ‘‘Zeferino Vaz’’, CP 6066, Campinas, São Paulo, Brazil.

[2] Department of Mechanical Engineering, School of Technology and Management, Polytechnic Institute of Leiria, Portugal.

[*] Corresponding Author: rezende@feq.unicamp.br

ABSTRACT

This paper investigates the influence of sodium alginate and the calcium chloride compositions as well as the gelation time on the swelling and morphology of foam alginate scaffolds. Alginates are linear unbranched polysaccharides containing beta-(1-4) linked D-mannuronic acid and alpha-(1-4) linked L-guluronic acid. The alginate hydrogels are produced by mixing the alginate with a proper crosslinking agent. During the gel formation, crosslinks between alginate chains and cationic species are formed, changing the elastic behaviour of the material controlling the volume change phenomena of gels. This overall research study focuses on a new route to produce three-dimensional patterns (or scaffolds) in alginate hydrogels for tissue engineering applications. This process involves a generation of foams from a network calcium alginate polymer by lyophilisation. Different structures were produced using different alginate compositions. It was observed that the alginate composition determines both the rheological characteristics of the solution and the morphological characteristics of the scaffolds further the quantity of liquid, especially water, that a structure in alginate can absorb which is defined as swelling. Hydrogels are crosslinked, polymer-based networks that are very hydrophilic, causing them to be highly swollen with water. Then, it becomes essential to know straightly better how the structures in calcium alginate swell as well as the morphology of foams obtained.

1. INTRODUCTION

By leveraging novel cell culture and the design of bio-resorbable polymers, tissue engineering strategies have recently emerged as one of the most advanced therapeutic strategy for regenerative medicine. Tissue engineering encompasses the use of cells and artificial constructs. It is based upon scaffold guided tissue regeneration and involves the seeding of porous, biodegradable scaffolds with donor cells, which differentiate and mimic naturally occurring tissues. These tissue engineered constructs are then implanted into the patient to replace diseased or damaged tissues.

Investigations have shown that alginate scaffolds can sustain the growth of various cell types. Chondrocytes maintained a round morphology and expressed type II collagen within alginate hydrogels. Other forms of alginate, such as a sponge, were found to support the adhesion of fibroblasts. Hepatocytes, the functional cell type in liver, were also found to proliferate within alginate scaffolds. Additionally, hepatocytes seeded within three-dimensional porous alginate secreted albumin, indicating proper cell function. Other cells demonstrating function within alginate hydrogels include cardiomyocytes, rat marrow cells and Schwann cells. (Yoon and Fisher, 2009).

Scaffolds must also degrade slowly after implantation in the patient, to be replaced by new tissue (Lee et al, 2007; Sung et al, 2004; Glicklis et al. 2000; Leor et al., 2000; Shapiro, 1997; Jen et al, 1996). Biodegradable scaffolds can play an important role as delivery vehicles for the sustained release of tissue growth factors (He et al, 2004). Ideally, appropriate designed tissue engineering scaffolds promote natural wound healing and regeneration. (Bártolo, 2004) and Bártolo et al (2004, 2006) developed a biomanufacturing system specifically designed for soft tissue repair applications. This system is adapted to produce alginate scaffolds by extruding, layer-by-layer, a solution of sodium alginate into a calcium chloride solution (crosslinker agent) (Rezende et al., 2009). The system illustrated in Figure 1, comprises two nozzles, one for the sodium alginate and the other for the calcium chloride deposition, not shown in Figure 1.

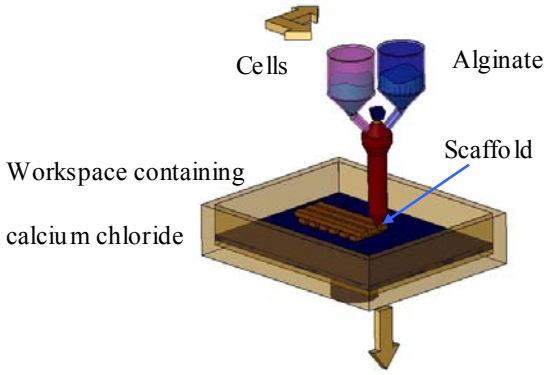

Figure 1. Alginate-based biofabrication system purpose.

While two-dimensional patterning of hydrogels continues to be widely investigated and has proven useful for numerous and elegant in vitro studies, the most promising and versatile methods for constructing mimics of native tissue are those techniques which enable the creation of true three-dimensional constructs (Miller and West, 2008).

Alginate scaffolds are usually characterized by smooth surfaces, depending on the crosslinking process, i.e., on the concentration of both alginate and crosslinker. The fabrication of porous alginate scaffolds involves a three step procedure (Zmora et al., 2002):

- Crosslinking the alginate solution with an appropriate solution
- Freezing the crosslinked alginate structure
- Removal of ice crystals by sublimation

2. HYDROGELS

Hydrogels are an exciting class of materials for applications in tissue engineering, regenerative medicine and drug delivery due to their excellent biocompatibility, hydrophilicity and the ease with

which their mechanical properties can be tuned to match those of soft tissues (Miller and West, 2008).

Various hydrogels, both synthetic and naturally derived, have recently been used as synthetic extracellular matrices (ECMs) for cell immobilization, cell transplantation and tissue engineering. Synthetic ECMs replace many functions of the native ECM, organizing cells into a three-dimensional architecture, providing mechanical integrity to the new tissue, and providing a hydrated space for the diffusion of nutrients and metabolites to and from the cell [5-7] (Rowley, 1999).

Hydrogels are crosslinked (Figure 2), polymer-based networks that are very hydrophilic, causing them to be highly swollen by water. Hydrogels can be formed by physically or covalently crosslinking a liquid prepolymer solution into a solid hydrogel. A great variety of material compositions can be used to make hydrogels, including agarose, alginate, hyaluronic acid, chitosan, polyhydroxyethylmethacrylate (pHEMA), dextran, polyvinyl alcohol, acrylamide derivatives, polyethylene glycol (PEG), etc.

Hydrogels were used in many applications, including contact lenses, implant coatings, tissue coatings and wound dressings, cell transplantation, microfluidic valves, actuators, and sensors. An important application domain is the production of drug delivery systems. In this case, drug molecules are loaded in the dried hydrogel and later slowly released, due to the slow diffusion of water through the glassy matrix of the dried hydrogel.

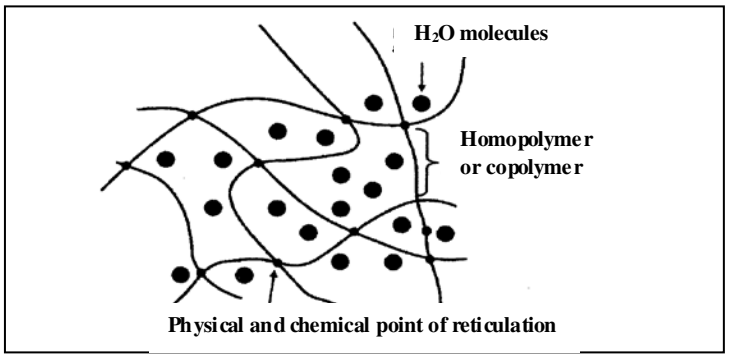

Figure 2. Hydrogel structure.

Lately, it was created a new sort of biomaterial for artificial skin foam-like mixing hydrogels. The foam was physically and metabolically stabilized by introducing reticulations. Films of hydrogels, as chitosan, have been tested in the recovering of burn people showing the great advantage of its future unnecessary remotion (Mei, 2006).

Alginate has a long history of applications in wound management. It is reported that early sailors used seaweeds to treat wounds, burns and eczema, and during the World Wars, because of shortage of cotton, dried sea moss dressings were sent to field hospitals to treat wounded soldiers. During WorldWar II, Blaine investigated tissue reactions to alginate fibers and reported the use of alginate fibers for hemostasis and as a bone wax substitute (Qin, Y., 2008).

Due to their hydrophilic nature, seeding mammalian cells onto the scaffold is simple and rapid (Glicklis et al., 2000).

In despite of its advantages features, alginate itself may not be an ideal material because it degrades via a process involving loss of divalent ions into the surrounding medium and subsequent dissolution. This process is generally uncontrolled and unpredictable. Therefore, covalent cross-linking with various types of molecules has been attempted to control precisely the mechanical and swelling properties of alginate gels. (Srichana, 2009).

Ultimately, the vascularization of hydrogels through three-dimensional rapid prototyping and three-dimensional biochemical patterning at subcellular resolution enables the investigation of small tissue mimics and continue progress towards true synthetic tissues and organs for human transplantation (Miller and West, 2008).

2.1. BIOPOLYMERS OF CALCIUM-ALGINATE HYDROGELS

Alginate is a natural linear polysaccharide that contains 1,4-linked β-D-mannuronic (M) and α-L-guluronic (G) acid residues (Figure 3), arranged in a non-regular and block-wise fashion along the chain.

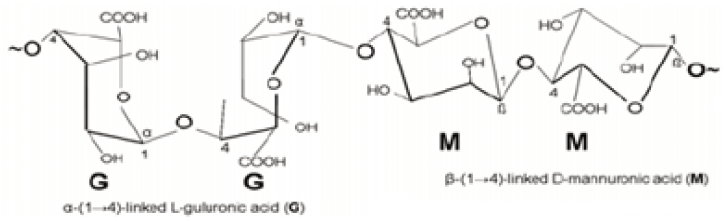

Figure 3. Typical GGMM block of alginate.

Carboxylic groups have the possibility to form salts such as sodium alginates, being the monovalents sodium ions bonded ionically to the carboxylic groups, as shown in the Figure 4.

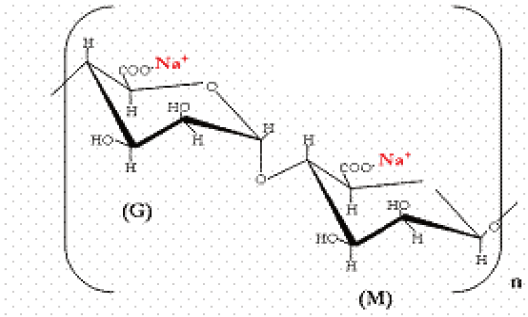

Figure 4. The sodium alginate.

The sodium alginate is water soluble and, after the dissolution forms a viscous solution that depends on both the concentration and the molecular weight of the biopolymer. In the presence of divalentes calcium ions, these ions exchange with sodium ions into the G blocks, and switch adjacent chains crosslinking the alginate, linking sodium alginate ionically (Figure 5).

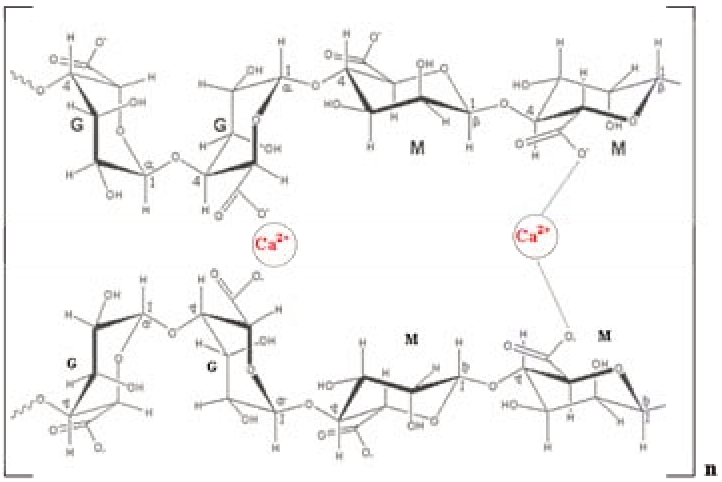

Figure 5. The crosslinked biopolymer.

Gelation of an aqueous sodium alginate in calcium chloride solution consists on the linkage of M and G blocks through a bridge by calcium ions in order to stabilize and construct a 3D network.

$$Sodium\_alginate_{aq} + Calcium\_chloride_{aq} \rightarrow Calcium\_alginate\_gel$$

Alginate is readily degraded by naturally occurring enzymes, including alginate lysases. These enzymes primarily degrade alginate at the β(1-4) linkage site (Yoon and Fisher, 2009).

3. SWELLING

Porous bulks of alginate were prepared from Sodium Alginate purchased at Panreac (Barcelona, Spain). Calcium chloride was supplied by Carlo Erba (Milano, Italy).

All solutions were prepared with pure water, with a conductivity of 0.054 μS/cm. Alginate solutions were prepared by the addition of weighted portions of sodium alginate to measure volumes of

water. These solutions were agitated by orbital shaking for three hours at 50 ºC to ensure good homogeneity due to their high viscosity.

Variations in the alginate and calcium compositions were taken such as alginate 1%, 2%, 3% and 5% and calcium 1% and 2%. The gelation time corresponds to the period in which happened the interaction between the sodium alginate and the calcium chloride solutions when the gel formed is taken off from the recipient (Petri dishes) and washed with deionized water to break the gelation.

3.1. SWELLING WITH NYTROGEN

The objective in this section is to verify the effect of the variations of sodium alginate and calcium chloride concentrations on the swelling of calcium alginate bulks being frozen by liquid nitrogen bath. This procedure leads to dry the liquid component inside the sample, allowing knowing better the absorbed volume from the alginate structure. Swelling is seen as the capability of a material has to absorb liquid substances.

The swelling ratio (SR) is expressed, by Equation 1, as the ratio:

$$SR\ (\%) = \frac{W_h - W_f}{W_f} \times 100 \quad (1)$$

where W_h is weight of the hydrated bulk and W_f is the weight of frozen bulk.

The samples were weighed immediately after the gelation process to obtain the W_h and reweighed after spend 8 hours in the nitrogen container to obtain W_f.

3.1.1. CALCIUM CHLORIDE 1% CONCENTRATION

Calcium Chloride 1% is relative to the dissolution of 10 g of $CaCl_2$ in 1l of pure water.

The calcium alginate samples with $CaCl_2$ 1% were prepared with 1 ml of sodium alginate crosslinked by 2 ml calcium chloride. Three samples of each combination were experimented and the final result for each combination is an average of them.

The Table 1 points up the up-and-down of swelling ratio behavior in function of alginate and gelation time for $CaCl_2$ 1%. Basically, there is a similarity in all the cases, excepting the first variation of gelation time from 10 minutes to 3 hours.

Table 1. Up-and-down variation of swelling in function of time ($CaCl_2$ 1%).

$CaCl_2$ 1%	Alg 1%	Alg 2%	Alg 3%	Alg 5%
10 min	-	-	-	-
3 h	↑	↑	↓	↓
4 h	↑	↑	↑	↑
12 h	↓	↓	↓	↓
48 h	↓	↓	↓	↓
72 h	↑	↑	↑	↑

The Figure 6 illustrates the variance of gelation time for a calcium alginate gel crosslinked with $CaCl_2$ 1%.

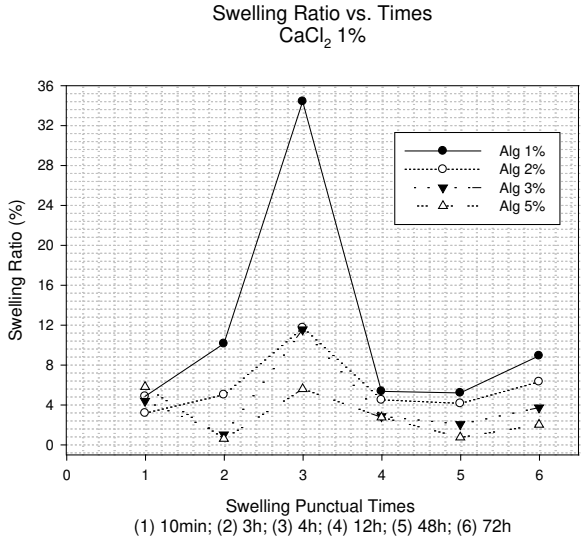

Figure 6. Swelling ratio versus gelation time – $CaCl_2$ 1%.

There are two peaks in the swelling ratio, a maximum at 4 hours of gelation and other at the higher gelation time, that is, 72 hours.

Table 2 which details the up-and-down variations in function of alginate composition only diverges for 10 minutes gelation.

Table 2. Up-and-down variation of swelling in function of alginate composition ($CaCl_2$ 1%).

	Gelation Times					
$CaCl_2$ 1%	10 min	3 h	4 h	12 h	48 h	72 h
Alg 1%	-	-	-	-	-	-
Alg 2%	↓	↓	↓	↓	↓	↓
Alg 3%	↑	↓	↓	↓	↓	↓
Alg 5%	↑	↓	↓	↓	↓	↓

The following graph (Figure 7) shows a trend in which the swelling ratio decreases as the sodium alginate increases (except to 10 minutes gelation), due to the larger presence of alginate chains in the bulk seizing space and at the same time less space for water to be taken in by a same volume.

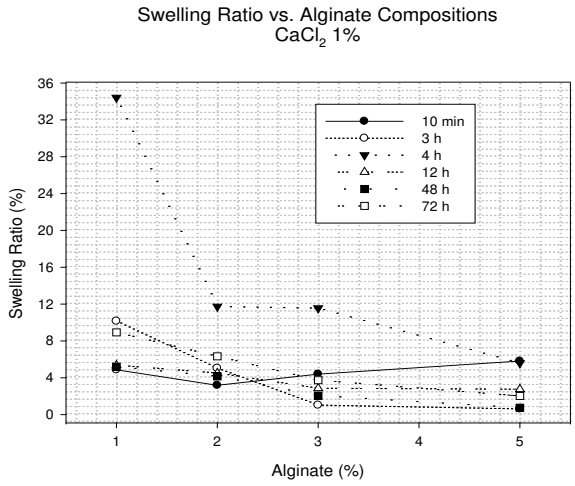

Figure 7. Swelling Ratio versus Calcium Alginate ($CaCl_2$ 1%).

Regarding the gelation times, the swelling ratio pictures its higher level for 4 minutes at alginate 1% reaching a reasonable level at alginate 5%. There is no a logical profile in terms of gelation time influence. Higher the alginate portion, the swelling ratio values seem to converge to each other.

3.1.2. CALCIUM CHLORIDE 2% CONCENTRATION

Calcium Chloride 2% implicates the dissolution of 20 g of $CaCl_2$ in 1l of pure water. Figure 8 presents how the Swelling Ratio behaviors at Time Gelation changing. The higher the gelation time the lower the Swelling Ratio is. Differently from $CaCl_2$ 1%, it is clear to see that the increase of the gelation time leads to a decrease in the Swelling ratio for $CaCl_2$ 2%.

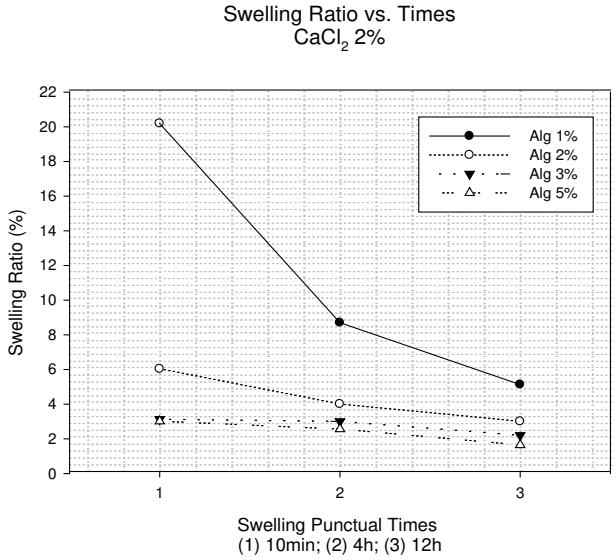

Figure 8. Swelling ratio versus gelation time – $CaCl_2$ 2%.

Figure 9 depicts the decrease of the Swelling ratio against the increase of the calcium alginate.

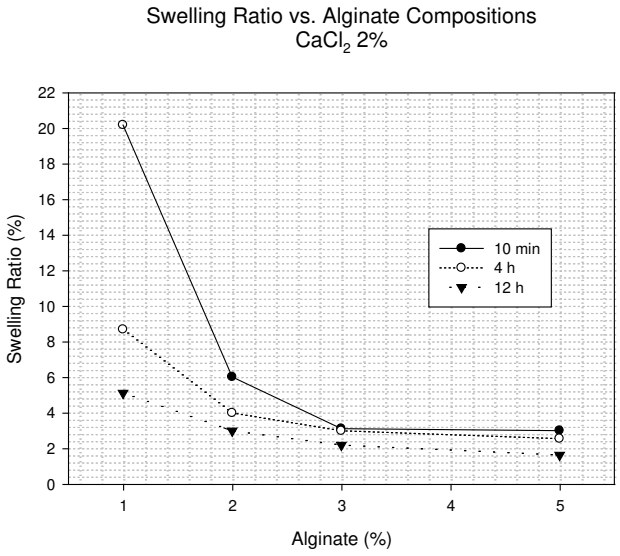

Figure 9. Swelling ratio versus gelation time – $CaCl_2$ 2%.

3.1.3. REWEIGHTING FOR $CACL_2$ 2%

The measurements carried out to $CaCl_2$ 2% samples were kept and weighted again 1 hour later (dried-1h) after the samples have been removed from nitrogen room. In case of 12 hours gelation time samples, there was an extra measurement, 1 hour later (dried-2h). Figure 10 pictures the obtained values of mass (g) for the samples and Figures 11, 12 and 13 with calculated normalized masses bring a better understood of how the samples lose their masses dependent on alginate concentration.

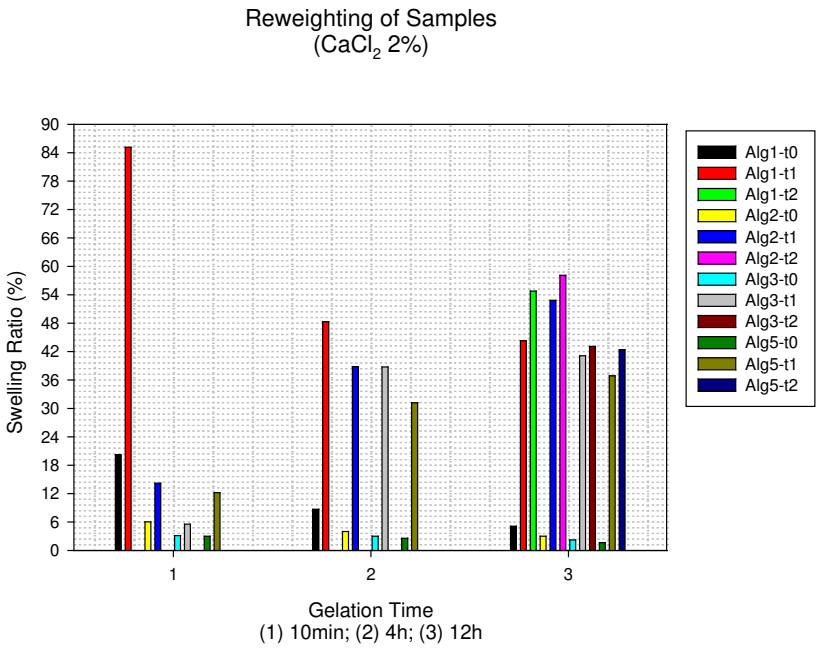

Figure 10. Remeasurements of samples masses for $CaCl_2$ 2% (t0=dried-0h; t1=dried-1h; t2=dried-2h).

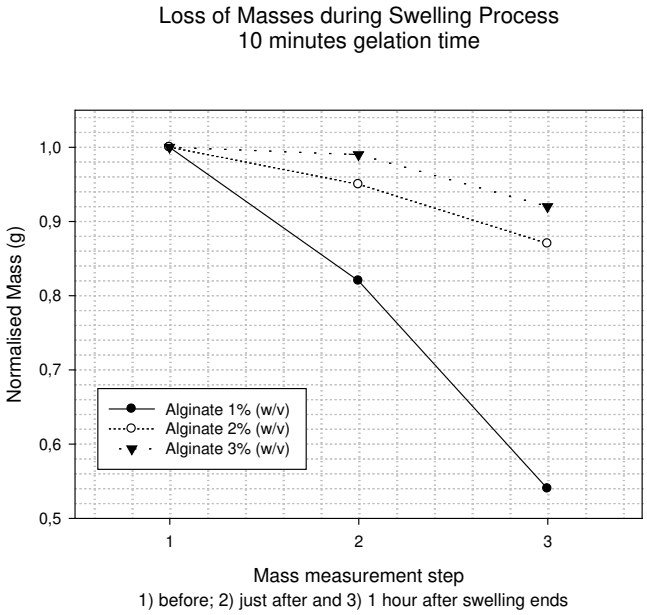

Figure 11. Normalized masses for 10 minutes gelation.

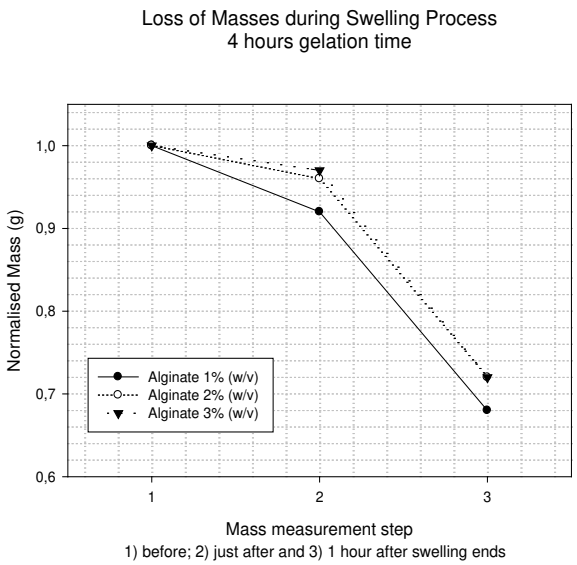

Figure 12. Normalized masses for 4 hours gelation.

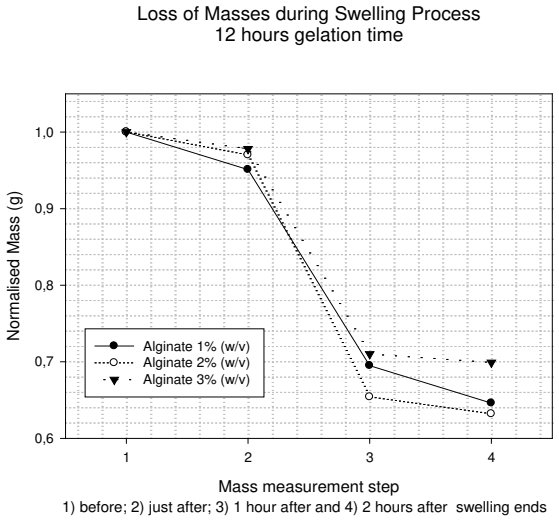

Figure 13. Normalized masses for 12 hours gelation.

It can be noted that after 1 hour gelation, the weight of masses starts to stabilize, that is, they do not show a great decrease and therefore there is no much more lost of mass.

The whole set of swelling ratio values obtained in terms of the combinations between sodium alginate and calcium chloride proportions was calculated based on the mass of each hydrated sample. Table 3 describes all the SR(%) found after drying and freezing every specimen of calcium alginate.

Table 3. All the measured masses for $CaCl_2$ 2%.

	Alg 1%			**Alg 2%**		
Ts	$SR\%_{dried\text{-}0h}$	$SR\%_{dried\text{-}1h}$	$SR\%_{dried\text{-}2h}$	$SR\%_{dried\text{-}0h}$	$SR\%_{dried\text{-}1h}$	$SR\%_{dried\text{-}2h}$
10 min	*20.19*	*85.15*	-	*6.04*	*14.22*	-
4 h	*8.70*	*48.29*	-	*4.01*	*38.82*	-
12 h	*5.13*	*44.26*	*54.77*	*3.01*	*52.83*	*58.12*
	Alg 3%			**Alg 5%**		
Ts	$SR\%_{dried\text{-}0h}$	$SR\%_{dried\text{-}1h}$	$SR\%_{dried\text{-}2h}$	$SR\%_{dried\text{-}0h}$	$SR\%_{dried\text{-}1h}$	$SR\%_{dried\text{-}2h}$
10 min	*3.13*	*5.56*	-	*3.02*	*12.20*	-
4 h	*3.01*	*38.75*	-	*2.57*	*31.18*	-
12 h	*2.21*	*41.11*	*43.10*	*1.65*	*36.87*	*42.35*

3.2. SWELLING– MASS LOSS AT ROOM TEMPERATURE

Some different samples with variation of alginate/$CaCl_2$ composition were prepared in order to be verified how their respective masses behavior at room temperature. Those masses were measured four times in 10 days of gelation according to the presented in Figure 14 and in Figures 15 and 16 whose curve fitness was conducted by a general polynomial quadratic equation, as given by Equation 2, where LM and t mean the loss mass and the time, respectively.

$$LM(t) = LM_0 + at + bt^2 \tag{2}$$

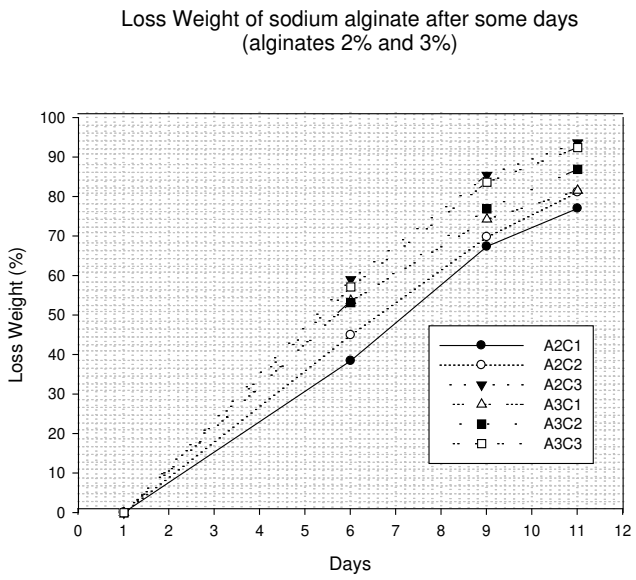

Figure 14. Loss Weight of all the samples (calcium alginate 2% and 3%).

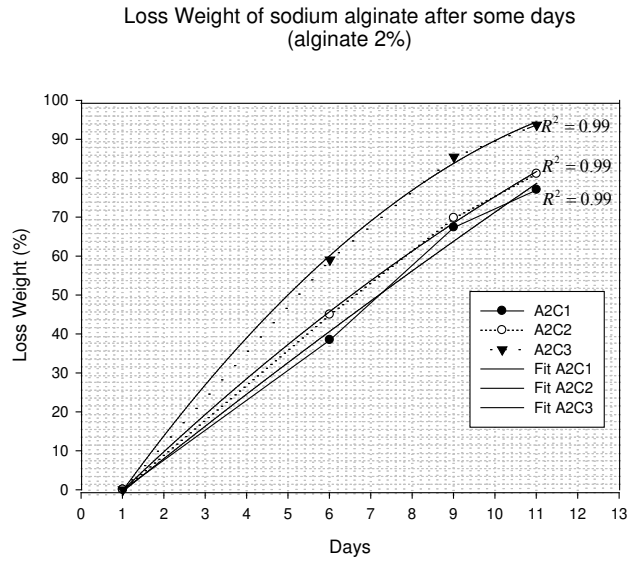

Figure 15. Loss Weight and Fitness of samples kept at ambient moisture for calcium alginate 2%.

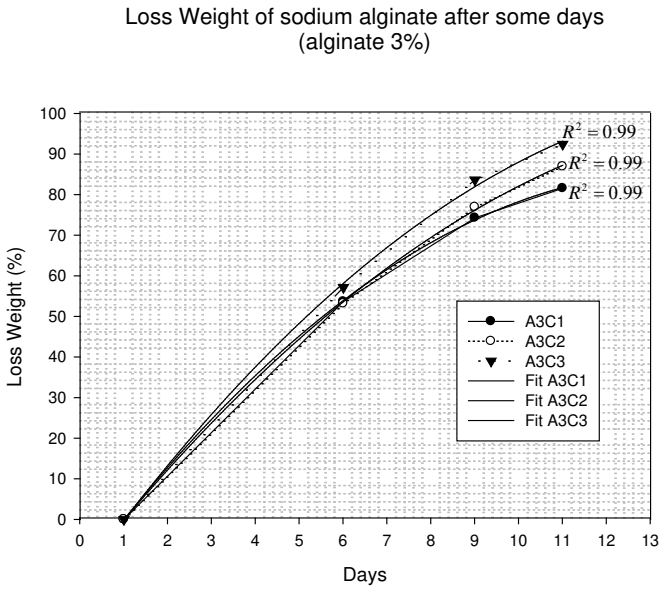

Figure 16. Loss Weight and Fitness of samples kept at ambient moisture for calcium alginate 3%.

4. FOAMING

Skin substitutes or wound healings for burn areas made with biodegradable materials have been developed. Lately, a new sort of biomaterial for artificial skin, like foam, was developed combining collagen with gel (Mei, 2006).

Foams were produced through freeze-drying method. Freeze-drying, also known as lyophilization, is a dehydration process typically used to preserve a perishable material or make the material more convenient for transport. Freeze-drying works by freezing the material and then reducing the surrounding pressure and adding enough heat to allow the frozen water in the material to sublime directly from the solid phase to the gas phase.

4.1. MATERIAL AND FOAMING METHOD

Different samples of calcium alginate were prepared with alginates 2%, 3% and 5% and $CaCl_2$ 1%, 2% and 3% in the ratio of 1:2 (alginate:$CaCl_2$). Two gelation times were conducted, 7 and 25 hours,

and the samples reticulation was interrupted with deionized water. The samples were then weighed and put in a vacuum camera with -1 Bar pressure, during 6 hours vacuum.

The method for porous structure preparation is a four-step process, which consist of:

a) Preparation of sodium alginate stock solutions at concentrations of 2%, and 5% (w/v);

b) Crosslinking of the alginate by adding different concentrations of divalent-crosslinked calcium chloride solutions: 1% and 3% (w/v);

c) Freezing the cross linked alginate in a cool environment, the liquid nitrogen;

d) Lyophilization to produce a sponge-like scaffold. These scaffolds are sterilized using an ethylene oxide gas apparatus and kept at room temperature until being used.

4.2. RESULTS

The samples were interrupted and measured 10 days later than their fabrication, that is, when sodium alginate and calcium chloride were mixed. Table 4 presents the values of the mass of each stock for before and for after 6 hours under vacuum environment.

Table 4. All the values of the measured masses during vacuum.

	Mass (g)		
Sample	Before vacuum	After vacuum	Swelling Ratio (%)
A5C1	3.20	0.36	88.75
A5C2	2.39	0.34	85.77
A5C3	3.15	0.54	82.86
A2C3	2.20	0.12	94.54
A3C3	2.47	0.22	91.09

Figures 17 and 18 illustrate the effect of vacuum to remove water from the sample. A2, A3, A5 and C1, C2 and C3 are Sodium Alginates and Calcium Chloride, respectively, and their concentrations.

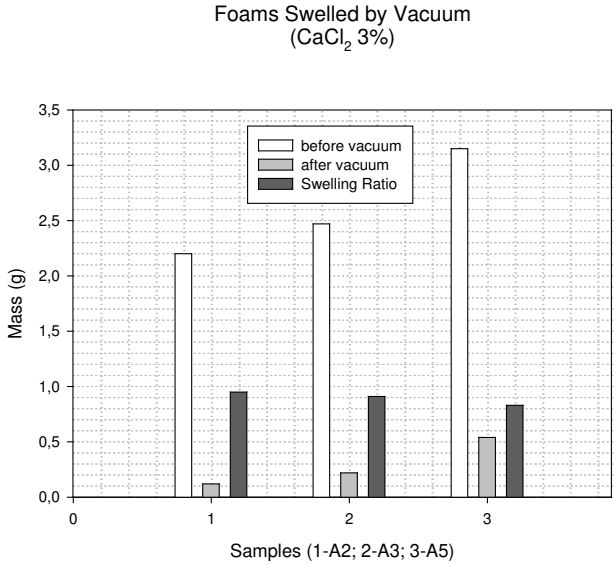

Figure 17. Foams weight after vacuum ($CaCl_2$ 3%).

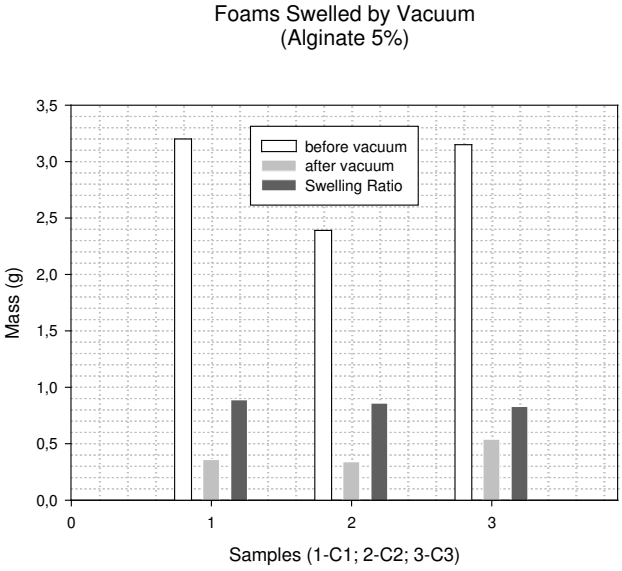

Figure 18. Foams weight after vacuum (Alginate 5%).

4.3. MORPHOLOGY OF THE FOAMS

The surfaces of the dried alginate scaffolds were analyzed by Scanning Electron Microscopy (SEM), using a Leica Cambridge s -360 in the tension 15 Kv. The magnifications used were 50× and 500×. In this case, samples were coated with a thin layer of gold to avoid the forming of charges at the surface of the polymer, made by the electronic bombardment. Figure 11 shows the surface micrographs of alginate foam scaffolds obtained by crosslinking solutions of sodium alginate 2% and 5% with calcium chloride 1% (m/v) and 3% during the gelation time of 7 hours and 25 hours. From these images, it is possible to observe that the boundaries of the foaming cells increase by increasing the gelation time. Figures 19, 20 and 21 depict scanning electron micrographs of alginate scaffolds after 7 and 25 hours of gelation, for different alginate and calcium chloride concentrations.

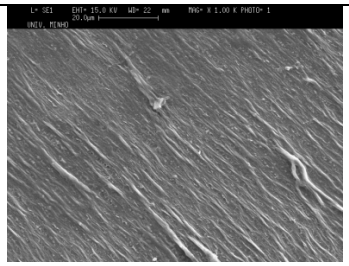	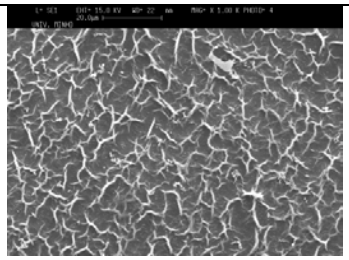
Alginate 2% Calcium 1% – 25 hours.	Alginate 5% Calcium 1% – 7 hours.
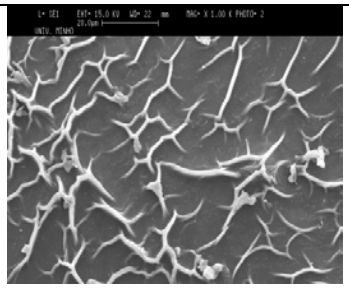	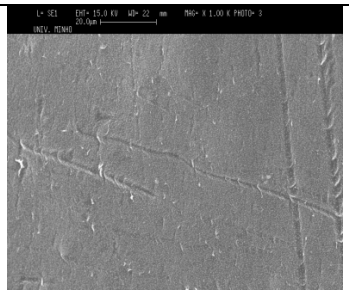
Alginate 5% Calcium 1% – 25 hours.	Alginate 5% Calcium 3 % – 25 hours.

Figure 19. A surface image of a porous structure of alginate scaffold (1000x and 20 μm scale).

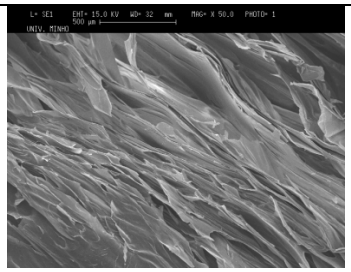	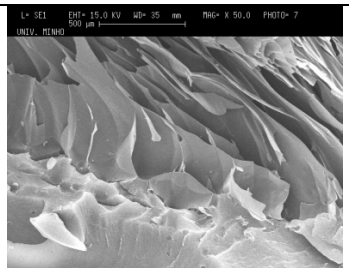
Alginate 2% Calcium 1% – 25 hours 15 kV	Alginate 5% Calcium 1% – 7hours15 kV
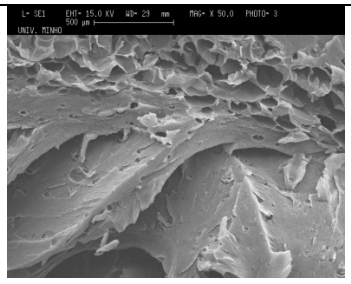	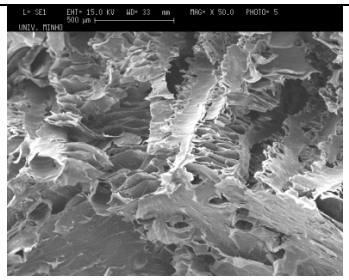
Alginate 5% Calcium 1% – 25 hours15 kV	Alginate 5% Calcium 3 % – 25 hours 15 kV

Figure 20. Low-magnification image of the internal section (50x and 500 μm scale).

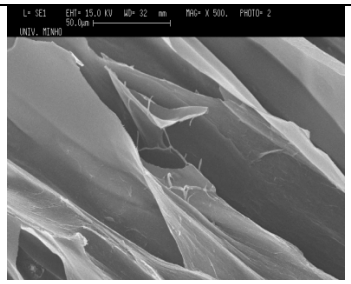	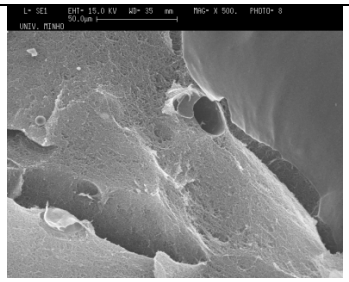
Alginate 2% Calcium 1% – 25 hours	Alginate 5% Calcium 1% – 7hours15 kV
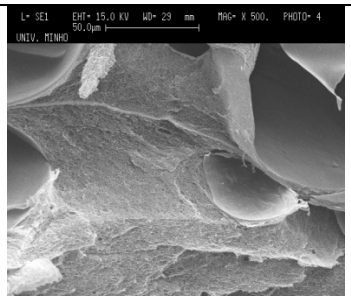	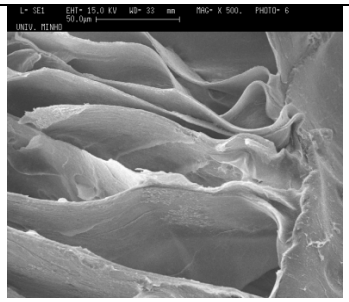
Alginate 5% Calcium 1% – 25 hours15 kV	Alginate 5% Calcium 3 % – 25 hours 15 kV

Figure 21. Great magnification image of the internal section (500× and 50 μm scale).

The concentration of both sodium alginate and $CaCl_2$ determines not only the kinetics of the gelation process, but also the internal and surface morphology of alginate gels (Rezende et al., 2007). Appropriate porosity macro- and microstructure of the pores and shape, highly interconnected pores structure and large surface area to allow high seeded cells and to promote neovascularisation. Large number of pores may be able to enhance vascularisation, while smaller diameter of pore is preferable to provide large surface per volume ratio (Bártolo et al., 2008).

The grooves saw in the internal sections hint there is the possibility of making use of these materials to seed cells, for instance, since these cells can adhere appropriately. Of course, the porous region requires much attention which means that a more rigorous study should be carried out crossing the range of variables involved in this process in order to reach a better control of the porosity.

5. CONCLUSIONS

This paper describes the preparation and analysis of alginate swelling and also the handling of foams in alginate that can be possibly used as artifacts in biofabrication as wound healing, as scaffolds for cell growth and transplantation.

About the swelling results, the higher the alginate percentage in the sample, the less the water retention. For 4 hours gelation time there is a peak in the swelling ratio for $CaCl_2$ 1%, maybe, showing that this is the time that the reticulation reaches its maximum. Greater values of swelling ratio happen for shorter gelation times. At room temperature, in ten days, calcium alginate samples lost mass in a range from 70% to 90%. When drying the alginate samples by vacuum, the swelling ratio obtained was so high from 80% on.

Alginate foam scaffolds were produced by crosslinking alginate and calcium chloride followed by freezing and lyophilization. Different cell-like structures were produced depending on the concentration of both alginate and calcium chloride. Larger pores were obtained with high alginate

concentrations. In the future cell proliferation and differentiation studies will be conducted in order to understand the biological behavior of these scaffolds.

Alginate is opportunely a convenient material for transplantation since it is biocompatible and hydrophilic, which is confirmed with the swelling data. The morphology images by SEM showed that are dependence between the sodium alginate and the calcium chloride in the composition, further the gelation time. That more porous alginate structures are closer to be used as scaffolds since the cells can be well seeded into them and grow up and the vascularization can occur as desired.

6. ACKNOWLEDGEMENTS

The authors would like to thank the support from The National Council for Scientific and Technological Development (CNPq, Brazil), and the Foundation for Science and Technology (FCT, Portugal).

REFERENCES

Bártolo, P.J., Mendes, A. and Jardini, A.- Bio-manufacturing in Design and Nature: Comparing design in nature with science and engineering, Edited by C.A. Brebbia, L. Sucharov and P. Pascolo, WIT Press, Southampton, UK, 2004

Bártolo, P.J., State of the art of solid freeform fabrication for soft and hard tissue engineering, in Design and nature III: comparing design in nature with science and engineering, 2006.

Bártolo, P.J., Almeida, H. A., Rezende, R. A., Laoui, T., Bidanda, B. Advanced processes to fabricate scaffolds for tissue engineering. Virtual Prototyping & Bio-manufacturing in Medical Applications, Edited by B. Bidanda and P.J. Bartolo, Springer Science+Business Media, New York, Chap. 8, pp. 149-170, 2008.

Glicklis R, Shapiro L, Agbaria R, Merchuk JC, Cohen S. Hepatocyte behavior within three-dimensional porous alginate scaffolds. Biotechnol Bioeng. 67:344–53, 2000.

He, H., Cao, X., Lee, L.J.- Design of a novel hydrogel-based intelligent system for controlled drug release, Journal of Controlled Release, 95, 391-402, 2004

Jen, A.C., Wake, M.C. and Mikos, A.G- Review: Hydrogels for Cell Immobilization, Biotechnology and Bioengineering, vol.50, 357-364, 1996.

Lee, J.J., Lee, S.G., Park, J.C., Yang, Y.I. and Kim, J.K.- Investigation ob biodegradabale PLGA scaffold with various pore size structure for skin tissue engineering, Current Applied Physics, 7S1, 37-40, 2007

Leor, J., Aboulafia-Etzion, S., Dar, A., Shapiro, L., Barbash, I. M., Battler, A., Granot, Y., Cohen, S. Bioengineered cardiac grafts: a new approach to repair the infarcted myocardium. Circulation;102;III-56-III-61, 2000.

Mei, L. H. I. Polímeros biodegradáveis. Biomateriais, Fundamentos e Aplicações. Edited by Oréfice, R. L., Pereira, M. M., Mansur, H. S. Ed. Cultura Médica. 175-184, 2006.

Miller, J. S. and West, J. L. Rapid prototyping of hydrogels to guide tissue formation. In: Bio-Materials and Prototyping Applications in Medicine. Edited by Bártolo, P. J. S. and Bidanda, B. Springer, 2008.

Qin, Y. The gel swelling properties of alginate fibers and their applications in wound management. Polym. Adv. Technol., 19: 6–14, 2008.

Rezende, R.A., Bártolo, P.J., Mendes, A. and Maciel Filho, R. - Experimental characterisation of the alginate gelification process for rapid prototyping, Chemical Engineering Transactions, Aidic. 2007.

Rezende, R.A., Bártolo, P.J.S., Mendes, A., Maciel Filho, R. Rheological behavior of alginate solutions for biomanufacturing. Journal of Applied Polymer Science, v.113, 3866-71, 2009.

Rowley, J. A., Madlambayan, G., Mooney, D. J. Alginate hydrogels as synthetic extracellular matrix materials. Biomaterials, 20, 45-53, 1999.

Shapiro L, Cohen S.- Novel alginate sponges for cell culture and transplantation. Biomaterials 18:583–590, 1997.

Srichana, T. and Domb, A.J. Polymeric biomaterials. In: Biomedical Materials. Edited by Narayan, R. Springer, 2009.

Sung, H.J., Meredith, C., Johnson, C. and Galis, Z.S., The effect of scaffold degradation rate on three-dimensional cell growth and angiogenesis, Biomaterials, 25, 5735-5742, 2004.

Yoon, D. M., Fisher, J. P. Natural and synthetic polymeric scaffolds. In: Biomedical Materials. Edited by Narayan, R. Springer, 2009.

Zmora S, Glicklis R, Cohen S. Tailoring the pore architecture in 3-D alginate scaffolds by controlling the freezing regime during fabrication. Biomaterials, 23, 4087-4094, 2002.

5.3 Conclusões

O alginato pode ser aplicado na engenharia tecidual na forma de esponjas como forma de curativo para ferimentos e queimaduras e como *scaffolds* para crescimento e transplante de células. Daí, também, o interesse em se mensurar a taxa de inchaço do alginato.

A partir dos experimentos, observou-se que a maior concentração de alginato na solução leva a uma menor retenção de água do material. Um pico da taxa de inchamento ocorreu para uma solução reticulada com cloreto de cálcio 1% com tempo de gelação de 4 horas. As concentrações mais baixas de alginato implicam em maiores taxas de inchamento. Medindo-se a massa de diferentes amostras de alginato de cálcio expostas à temperatura ambiente por 10 dias, verificou-se que a ocorrência de uma perda significativa de massa da ordem de 70% a 90% da massa inicial, faixa esta dependente das composições de alginato e cloreto de cálcio na amostra. Quando se força a perda de água por vácuo, a taxa de inchamento mínima supera 80%.

As esponjas de alginato foram produzidas a partir das seguintes etapas: reticulação do alginato, congelamento (*freezing*) e liofilização. Diferentes estruturas foram produzidas de acordo com a variação de alginato de sódio e cloreto de cálcio na amostra. Por meio de microscopia eletrônica de varredura (MEV), verificou-se que as estruturas mais porosas foram obtidas quando da maior concentração de alginato na amostra.

O alginato por ser um material biocompatível e hidrofílico, o que pôde ser comprovado com os resultados de inchamento, apresenta-se como uma matéria-prima importante na ciência da engenharia dos tecidos. A morfologia revelada pelas imagens de MEV mostrou haver a dependência direta entre a proporção alginato de sódio versus cloreto de cálcio na amostra, além do próprio tempo de gelação. As estruturas mais porosas são fortes candidatas a serem utilizadas como *scaffolds* uma vez que as células poderiam ser bem implantadas e crescer, e a vascularização ocorrer como o desejado. No futuro, o estudo sobre a proliferação de células e de sua diferenciação possibilitará o conhecimento do comportamento biológico destes *scaffolds*.

Capítulo 6 – Ansys: Escoamento do Alginato

6.1 Introdução

O Capítulo 6 apresenta uma aplicação do software Ansys, baseado no Método dos Elementos Finitos, como uma ferramenta de apoio à caracterização do alginato que vem sendo discutida neste trabalho. O ANSYS é uma ferramenta computacional para análise, por elementos finitos, de problemas de engenharia. É um *software* comercial de simulação para tratamentos e análises em diversas áreas de engenharia, tais como análises termodinâmicas (transferência de calor, análises de resfriamento, gradientes de temperatura, respostas térmicas) e análises de estruturas (vibração, análises de *stress*, elasticidade) (Rezende, 2006).

As simulações têm um interesse voltado ao comportamento do fluxo de alginato. Foi projetada uma parede lisa, tendo sido gerado um conjunto geometria/malha tridimensional sem maiores complexidades, em que o alginato de sódio (não-reticulado) é depositado. Para duas diferentes composições de alginato consideradas, pode-se observar o escoamento deste material, medindo-se sua velocidade e sua fração de volume ao longo do tempo. Os dados de entrada destas simulações foram importados dos dados experimentais, obtidos pelo reômetro de pratos, apresentados no Capítulo 3.

6.2 Artigo Produzido

O Capítulo 6 é desenvolvido e apresentado através do artigo intitulado "**CAPE of the Physical Behaviour of Structures in Alginate for Biofabrication**", publicado nos anais do 19th International Congress of Chemical and Process Engineering (como resumo estendido v. 3, pp.1173-74, 2010 – e como artigo completo na mídia do congresso).

CAPE of the Physical Behaviour of Structures in Alginate for Biofabrication

R. A. Rezende[1*], A. R. R. Bineli[1], A. G. Quiroga[1], R. Maciel Filho[1]

[1] Laboratory of Optimization, Design and Advanced Control, School of Chemical Engineering, University of Campinas, Cidade Universitária ‘‘Zeferino Vaz’’, CP 6066, Campinas, São Paulo, Brazil.

[*]e-mail: rezende@feq.unicamp.br

Abstract

The world population has been facing many problems in the health issues. One of the important areas that have been required attention is the transplant. Due to accidents, diseases, aging and birth problems, many people need to undergo a surgery to replace or restore some organ. Many times these people have to expect a long time in a waiting list and also to find a compatible donor in order to effect the transplant.

Biofabrication essentially refers to the approaches used to manufacture complex 3D tissues and organs by printing and 3D fabrication technologies to overcome the limitations of conventional Tissue Engineering methods. Biofabrication, which connects Tissue Engineering (TE) and Rapid Prototyping (RP), can be defined as the production of complex living and non-living biological products from raw materials such as living cells, molecules, extracellular matrices and biomaterials.

Tissue Engineering is a multidisciplinary field that combines the principles of biology, engineering and medicine to create biological substitutes for lost or defective native tissues. Rapid Prototyping (or Solid Free Form, SFF) technology enables Tissue Engineering to have full control over the design, fabrication and modeling of the scaffold being constructed, providing a systematic learning channel for investigating cell-matrix interactions.

The technology transfer of Rapid Prototyping into Tissue Engineering may be the key to produce scaffolds (and medical artifacts in general) with customized external shape and predefined and reproducible internal morphology, which not only can control pore size, porosity and pore distribution, but can also make structures to increase the mass transport of oxygen and nutrients throughout the scaffold.

A scaffold is a temporary supporting structure and according to definition it must be biodegradable. The function of a degradable scaffold is to act as a temporary support matrix for transplanted or host cells so as to restore, maintain, or improve tissue. A variety of

biodegradable and biocompatible hydrogels have already been used for Tissue Engineering. Among them alginate is one of the most popular material due to its relatively low cost, natural origin and easy handling. In the case of scaffolds, it is appreciated that computer control of complex internal features of scaffolds, such as pore size, porosity, pore distribution and an artificial vascular system, offered by SFF technologies is a great advantage to the TE.

The design of a polymeric scaffold plays a significant role in proper cell growth. Therefore, several important properties must be considered: fabrication, structure, biocompatibility, biodegradability, and mechanical strength. In this sense, beyond the physical characterization of biomaterials, as alginate, with equipments as dynamic mechanical analysis and rheometers, computer tools have been helping to validate and foresee the behaviour of structures with more details and resources. Ansys packet has also been used in our lab. Analyses as flow and shear strain rates of alginate and also strength of alginated-structures can be studied computationally cooperating with the Biofabrication development.

Key-words: Alginate, Biofabrication, Ansys, Biomaterials, Tissue Engineering.

1. Introduction

Biofabrication can be defined as the production of complex living and non-living biological products from raw materials such as living cells, molecules, extracellular matrices, and biomaterials. Biofabrication uses cells or biologics as the basic building blocks in which biological models, systems, devices and products are manufactured. (Sun, 2009). Biofabrication joins the Tissue Engineering and the Rapid Prototyping technologies.

The intrinsic purpose of Biofabrication is to construct complex 3D tissues and organs beyond present Tissue Engineering technology. Biofabrication essentially refer to the approaches used to manufacture complex 3D tissues and organs by printing and 3D fabrication technologies to overcome the limitations of conventional Tissue Engineering methods.

Following statistics from The United Network for Organ Sharing (UNOS) report that, in 2003, in USA alone, 87 717 patients were waiting for organs' transplantation (Mendes *et al*, 2003). On June 2007 this number had increased to 96 670 and on May 2010 this number had reached 106 thousand people, as illustrated in Figure 1. The disparity between the need and availability of donor tissues has motivated the Tissue Engineering approach, aimed at creating cell-based substitutes of native tissues.

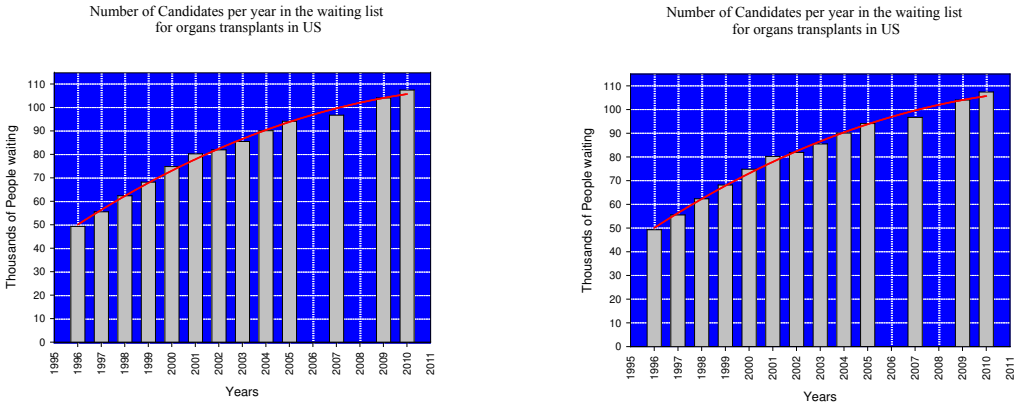

Figure 1. Statistics from United Network for Organ Sharing (UNOS, 2010)

According to Skalak and Fox (1988), Tissue Engineering (Figure 2) can be described as "the application of the principles and methods of engineering and life sciences toward the fundamental understanding of structure-function relationships in normal and pathological mammalian tissues and the development of biological substitutes to restore, maintain, or improve function". This new research field emerged to address the organ shortage problem that represents a world problem. According to Chu (2003), Tissue Engineering is defined by the ability to regenerate tissue through the help of artificial materials and devices.

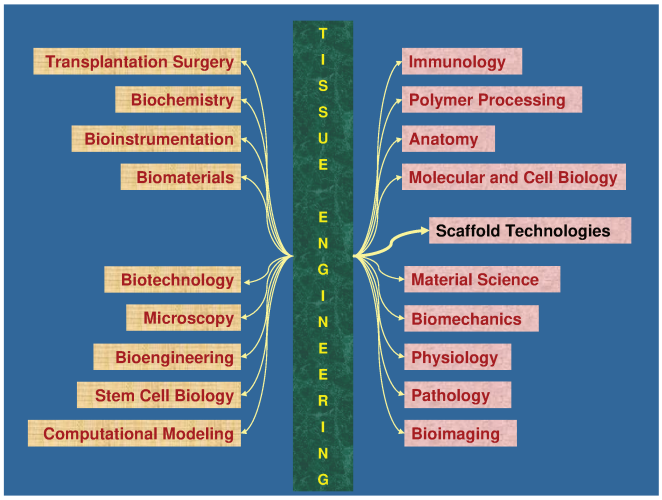

Figure 2. Tissue Engineering as a multidisciplinary approach.

Tissue Engineering approach permits experimental manipulations at three levels to achieve optimal construct: the cells, the polymer scaffolds and the construction method (Jennifer *et al.*, 1998). The most common concept underlying Tissue Engineering is to the combination of a scaffold/matrix, living cells and/or biologically active molecules to form a 'Tissue Engineering construct' (TEC) to promote the repair and regeneration of tissues.

TE approaches are complex and include architecture, structural mechanics, surface properties, degradation products and composition of biological components and the changes of these factors with time in vitro and/or in vivo (Hutmacher *et al.*, 2004; Reece and Patrick, 1998). A scaffold is a temporary supporting structure and according to definition it must be biodegradable. There are synthetic and naturally derived solid scaffolds (Mironov, 2009).

In order to become possible the recovering of an wound organ, a new tissue, obviously, with a set of new cells, must grows at the affected local respecting to the same properties, with ability to work similarly as the original cells, presenting good capacity of regeneration and of performing their vital functions.

Rapid Prototyping is a recent technology based on the advanced development of computer and manufacturing that offers new solutions, much better quality, and the ability to produce complex products rapidly directly from a computer model. Rapid Prototyping is a wide technology comprehending interactions between physical, chemistry, engineering, mathematical, computing science and other ones. Rapid Prototyping technology (RP) emerged as a step forward in the product cycle, reducing lead times for new products as well as improving design manufacturing and tooling costs (Jacobs, 1995; Burns, 1993). Through Rapid Prototyping, a model is built up by adhering successive thin cross section of the object to be built until the model is complete.

The most likely direction of development in using RP on TE scaffold will lead to the development of a specialized machine for TE manufacture. Once the application is narrowed to scaffold fabrication, the material and microstructure capabilities become much more important than the part size capacity and building speed, which, however, are major concerns for industry-oriented systems (Yang *et al.*, 2002).

The solution of real engineering problems through numerical process simulation with a relatively detailed representation is now a reality in academic and industrial plants. A growing in exponential scale of modern computers especially in terms of high calculation speed, memory availability and graphical facilities is enabling increasingly complex problems to be solved through numerical techniques. Another factor that also contributed to this trend is related to the project cost, which makes it possible that hours of testing laboratories at high costs are replaced by simulations on computers, reducing the costs and left the testing laboratory only for the refinements of the project (Versteeg and Malalasekera, 1995; Maliska, 2004).

2. Biomaterials

Over the years, various definitions of the term biomaterials have been proposed. For example, a biomaterial can be simply defined as a synthetic material used to replace part of a living system or to function in intimate contact with living tissue (Park and Bronzino, 2003). Other definitions have included "materials of synthetic as well as of natural origin in contact with tissue, blood, and biological fluids, and intended for use for prosthetic, diagnostic, therapeutic, and storage applications without adversely affecting the living organism and its components" (Bruck, 1980) and "any substance (other than drugs) or combination of substances, synthetic or natural in origin, which can be used for any period of time, as a whole or as a part of a system which treats, augments, or replaces any tissue, organ, or function of the body" (Williams, 1987).

The success of biomaterials in the body depends on factors such as the material properties, design, and biocompatibility of the material used, as well as other factors not under the control of the engineer, including the technique used by the surgeon, the health and condition of the patient, and the activities of the patient (Park and Bronzino, 2003). In addition, a biocompatible material has been defined as a material that does not induce an acute or chrome inflammatory response and does not prevent a proper differentiation of implant-surrounding tissues (Williams, 1987).

2.1. Natural Biopolymers

Natural biopolymers are one of the most applicable materials in Biofabrication. Natural polymers offer the advantage of being very similar, often identical, to macromolecular substances which the biological environment is prepared to recognize and to deal with metabolically. The problems of toxicity, and stimulation of a chronic inflammatory reaction, which are frequently provoked by many synthetic polymers, may thereby be suppressed (Yannas, 1996). Following Table 1 describes the main advantages and limitations of Natural Biopolymers.

Table 1. Advantages and limitations of Natural Biopolymers

Main advantages
• Similarity to materials familiar to the body • Low toxicity • Biocompatibility • Carrying of specific protein binding sites and other biochemical signals that may assist in tissue healing or integration
Limitations
• Problems of immunogenicity • Tendency to denature or decompose at temperatures below their melting points

Biodegradable polymers must be fabricated into stable textile structures before they can be used as the scaffold for Tissue Engineering or regeneration. The stability of the scaffold structure is important during Tissue Engineering and regeneration in order to maintain its proper size, shape, or form upon the shear force imposed by the circulating culture media in a bioreactor, the contractile force imposed by the growing cells on the scaffold surface, and other forces like the compression from surrounding tissues (Chu, 2003).

A variety of biodegradable and biocompatible hydrogels have already been used for Tissue Engineering. Among them alginate is one of the most popular material due to its relatively low cost, natural origin and easy handling. Alginate gels are currently being also explored for cell encapsulation and drug delivery (Wandrey *et al.*, 2003).

2.2. Hydrogels: Alginate

Hydrogel provides the field for cell growth and microenvironments for the cells and hydrogel is expected to be very effective in controlling cell behaviour in 3D products, by providing biofunctional materials together with or independently of cells in 3D space (Nakamura *et al.*, 2010). The roles of hydrogel in Biofabrication are summarized in Figure 3.

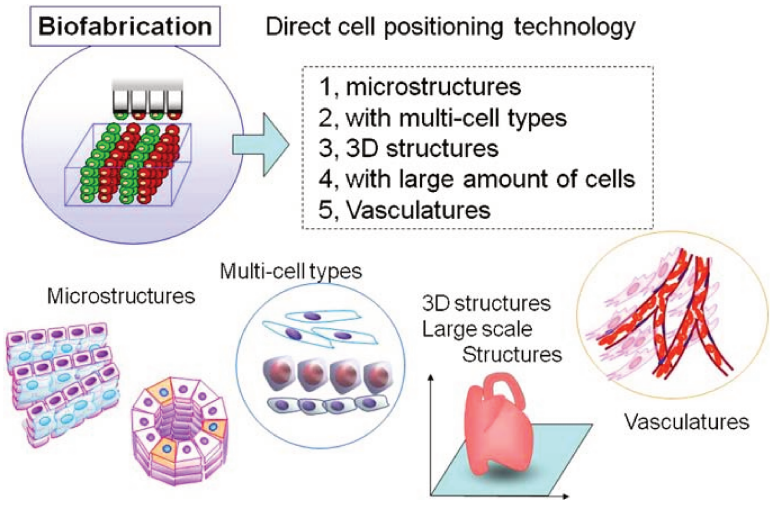

Figure 3. Requirements for Biofabrication technologies to successfully manufacture biological tissues and organs (Nakamura *et al., 2010*).

Alginate is a biodegradable and biocompatible natural polymer. It can be extracted from certain seaweeds or produced by some bacteria. Owing to the significantly higher production cost of alginate from bacterial sources, the primary sources of current commercial alginate materials are various species of brown algae (Figure 4). The major species used for alginate production are Ascophylla, Laminaria and Macroscystus. In early 1970s, alginate was recognized as safe (GRAS) to be used in food and pharmaceutical ingredients by the US Food and Drug Administration (FDA).

Figure 4. Marine brown algae.

Alginate is an anionic copolymer composed of homopolymeric regions of 1,4-linked β-D-mannuronic (M blocks) and α-L-guluronic acid (G blocks), as seen in Figure 5, interspersed with regions of alternating structure. Gelation occurs when divalent ions (Ca^{2+}, Ba^{2+}, Fe^{2+}, Sr^{2+}, etc.) or trivalent ions (Al^{3+}, etc.) take part in the interchain ionic binding between G-blocks in the polymer chain giving rise to a three dimensional network.

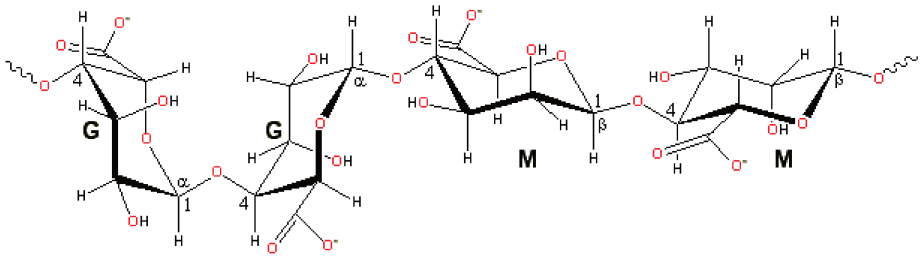

Figure 5. Possible alginate structure.

Alginate can be ionically cross-linked with a non-toxic divalent cation solution, like calcium chloride. The calcium ions (Ca2+) bind the G-blocks in the polymer chain giving rise to a three-dimensional network. Such binding zones between the G-blocks are often referred to as "egg boxes". These ions act as cross-linkers that stabilize alginate chains forming a gel structure, which contains cross-linked chains interspersed with more freely movable chains that binds and entraps large quantities of water. The gelling process is characterized by a re-organisation of the gel network accompanied by the expulsion of water (Serp *et al.*, 2002). The G content and its sequential structure significantly affect mechanical properties of gels. The consecutive G residues permit co-ordinated cavity organization at the molecular level to allow stable ionic binding formation. Therefore, longer G-block length increases binding strength and hence structural integrity and mechanical properties of the alginate gels.

Nakamura *et al.* (2010) states that alginate has good mechanical properties for keeping 3D structures, as well as biocompatibility. Alginate hydrogel supports the 3D morphological architecture of the product and the position of the living cells in the 3D structures.

Alginate has been widely used for drug delivery. Tablets and capsules are the most frequently used oral dosage forms. Sodium alginate has been used as a tablet binding agent, while alginic acid is used as a tablet disintegrant in compressed tablets designed for immediate drug release. Alginate has also been used as a coating to achieve sustained release since the alginate layer can serve as a barrier to reduced the diffusion rate of the drug compounds.

Immunoisolation is another important area in which various alginates have been the primary materials of interest. Immunoisolation is the enclosure of allogeneic (from the same species but not the recipient) or xenogeneic (from species different from the recipient) cells or tissues in a semipermeable membrane or matrix in order to protect them from immune rejection. The application can be in the form of either implants or extracorporeal devices. The materials should allow nutrients and metabolic wastes to diffuse through so that the encapsulated cells or tissues remain living and functional. They should also allow the therapeutic molecules produced by the encapsulated cells or tissues to diffuse out to function as biohybrid artificial organs.

Although there are many types of variations of the encapsulation process, the basic process is to extrude a cell containing sodium or potassium alginate solution dropwise into a solution that contains divalent or multivalent ions.

In addition to the controlled release and microencapsulation of cells, alginate has been used in a wide range of other biomedical applications, such as gene therapy, oral vaccination and wound dressing. The main advantages of Alginate are the minimal cytotoxic effects and reduced hemolysis when in contact with blood (Johnson *et al.*, 1997).

2.3. Rheological Characterization of Sodium Alginate

The alginate viscosity decreases with shear rate indicating a shear-thinning behaviour, as shown in Figure 6. Increasing the alginate content increases both the viscosity and stress for a specific value of shear rate.

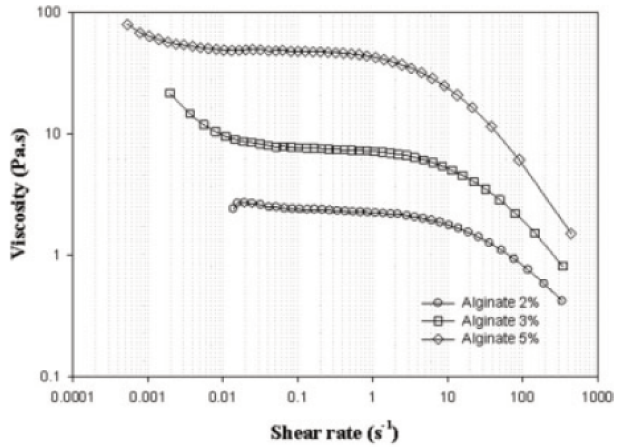

Figure 6. Viscosity variation as a function of shear rate for different alginate solutions.

The Power-Law model was used to fit the experimental data (Rezende, *et al.*, 2009). According to this model, the rheological behaviour of a material is described by the Eq. 1:

$$\tau = k \cdot \dot{\gamma}^n \qquad (1)$$

where s is the shear stress (Pa), c the shear rate (s^{-1}), k the consistency index ($Pa.s^n$) and n is the Power-Law index (dimensionless).

n < 1: shear-thinning system.
n = 1: Newtonian system.
n > 1: shear-thickening system.

Table 2 shows the values of the power law coefficients for two different alginate solutions.

Table 2. Coefficients of the Power Law for the 2% and 5% Alginate Solutions

Alginate content (%)	Consistency Index (k) ($Pa.s^n$)	Power-Law index (n)
2	2	0.87
5	28	0.84

3. Results and Discussion

As Biofabrication aims to develop alternatives to replace and reconstruct damaged organs and tissues, the alginate has been studied as raw-material for scaffolds and to grow new tissues inside them. In this sense, beyond the studies about mechanical and chemical properties of alginates, there are new perspectives, for example, about the implementation of seeded alginated-scaffolds inside bioreactors in order to simulate a live and real environment. Also, alginate with live cells could be deposited into a bioreactor containing a $CaCl_2$ solution which would reticulate the alginate with cells protecting this material being possible to create an appropriate environment to grow a new tissue.

As this idea would immerse sodium alginate into a calcium chloride solution, it would be much relevant to know better how the flowage of the alginate behaviours since their viscosities are different according to the composition which could change the expected conditions. Some analyses about alginate flow were performed through Ansys software. A comparison between two different compositions of alginate – 2% and 5% – was done where the flows were analyzed over spatial profiles representing the bulk at certain instants.

3.1. Use of Computational Fluid Dynamics (CFD)

In order to produce a computer simulation involving flow it is required an analysis of data and parameters involved in the process. The quality of these data in terms of adequacy and accuracy will determine the attribute of the final results. Because of this, users of CFD software should be very familiar with the problems which they wish to simulate (Shaw, 1992), especially concerning details that may affect flow distribution locally.

3.2. Mathematical Modeling

The differential equations which are solved express a principle of conservation and are known as continuity (2), momentum (3-4) and energy equations (5-6). To discretize the governing equations the software ANSYS CFX® makes use of an element-based finite

volume method, which firstly involves discretizing the spatial domain using a mesh. The mesh is used to construct finite volumes, which are used to conserve relevant quantities such as mass, momentum, and energy. A control volume is constructed around each mesh node and these equations are integrated over each control volume (ANSYS CFX® Guide, 2006).

The instantaneous equations (Eqs. 2 to 6) of mass, momentum and energy conservation can be written as follows:

The Continuity Equation:

$$\frac{\partial \rho}{\partial t} + \nabla \cdot (\rho U) = 0 \qquad (2)$$

The Momentum Equation:

$$\frac{\partial (\rho U)}{\partial t} + \nabla \cdot (\rho U \otimes U) = -\nabla p + \nabla \cdot \tau + S_M \qquad (3)$$

where the stress tensor, τ, is related to the strain rate by:

$$\tau = \mu \left(\nabla U + (\nabla U)^T - \frac{2}{3} \delta \nabla \cdot U \right) \qquad (4)$$

The Total Energy Equation:

$$\frac{\partial (\rho h_{tot})}{\partial t} - \frac{\partial p}{\partial t} + \nabla \cdot (\rho U h_{tot}) = \nabla \cdot (\lambda \nabla T) + \nabla \cdot (U \cdot \tau) + U \cdot S_M + S_E \qquad (5)$$

where h_{tot} is the total entalphy, related to the static entalphy $h(T,p)$ by:

$$h_{tot} = h + \frac{1}{2} U^2 \qquad (6)$$

The term $\nabla \cdot (U \cdot \tau)$ represents the work due to viscous stresses and is called the viscous work term. The term $U \cdot S_M$ represents the work due to external momentum sources and is currently neglected.

3.3. Boundary Conditions

The boundary conditions are used to create input required by the Solver. Table 3 exhibits the pre-conditions for the performed simulations.

Table 3. The Boundary Conditions assumed as input in Ansys.

Properties	*Materials*		
	Air	**Alginate**	
Reference Pressure (atm)	**1 (dry)**	**1 (liquid (water))**	
Reference Temperature (°C)	**25 °C**	**36 °C**	
Equation of State			
Density [kg m^{-3}]	**1.185**	**1.200**	
Molar Mass [kg $kmol^{-1}$]	**28.96**	**18.02**	
Specific Heat Capacity			
Specific Heat Capacity [J kg^{-1} K^{-1}]	**1004.4**	**4181.7**	
Specific Heat Type	**Constant Pressure**		
Thermal Conductivity			
Thermal Conductivity [W m^{-1} K^{-1}]	**0.0261**	**0.6069**	
Non Newtonian Viscosity Model			
		Alg. 2%	**Alg. 5%**
Maximum Shear Strain Rate [s^{-1}]	**-**	**1000**	
Minimum Shear Strain Rate [s^{-1}]	**-**	**0.0001**	
Option	**-**	**Ostwald de Waele (Power Law Model)**	
Power Law Index	**-**	**0.87**	**0.84**
Time Constant [s]	**-**	**1**	
Viscosity Consistency [Pa.s]	**-**	**2**	**28**

Dynamic Viscosity			
		Alg. 2%	**Alg. 5%**
Dynamic Viscosity Range [kg m-1 s-1]	**$1.831 \cdot 10^{-5}$**	**1.01 - 2.30**	**14.5 – 74.6**
Option	**value**	**non newtonian model**	

3.4. Simulation

The objective of this process is to produce a mesh to serve as input to the physical preprocessor. Before a mesh can be produced, a closed geometric solid is required. The geometry and mesh can be created in CFX-Mesh or any of the other geometry/mesh creation tools (Bineli *et al.*, 2010).

The simulation performed in this paper has as goal to check the flowage of alginate in a smooth surface where no attrition was regarded. It was thought of a simple geometry which no great details, where an alginate solution could be injected and flowed but possible to extract this behaviour through the computational fluid dynamics (*CFD).* The mesh can be viewed in Figure 7.

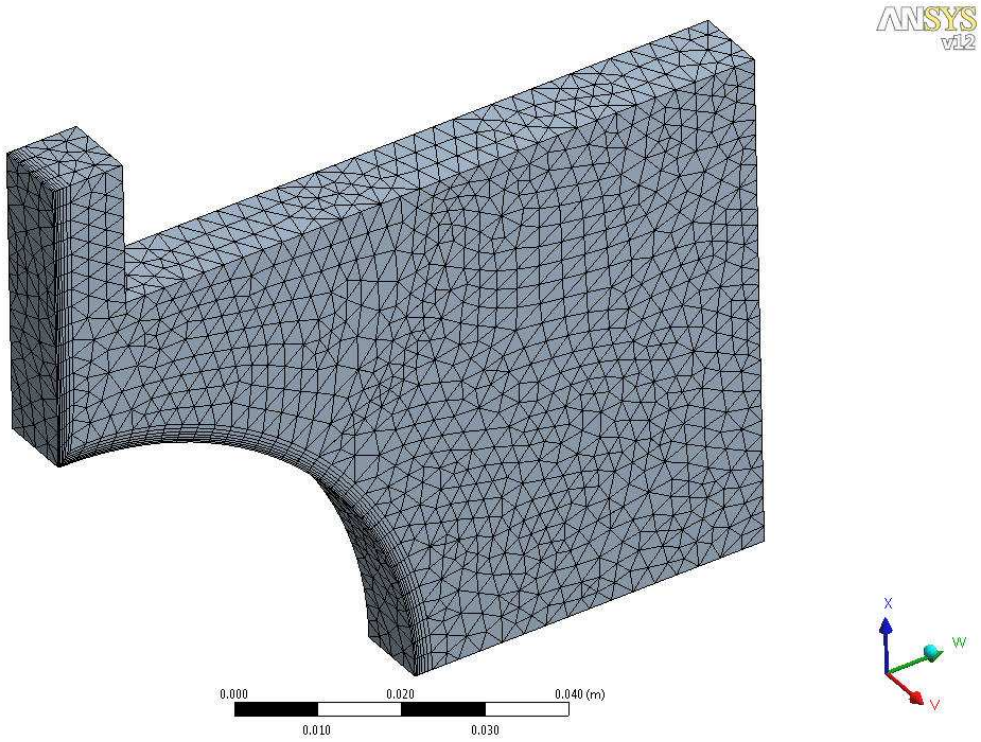

Figure 7. The mesh of the used geometry

Table 4 describes the dimension of the mesh with its particular number of elements.

Table 4. Number of elements in the mesh.

Mesh Statistic	
Total Number of Nodes	7464
Total Number of Elements	29964
Total Number of Tetrahedrons	27318
Total Number of Prisms	2646
Total Number of Faces	4808

3.4.1. Volume Fraction

As the purpose is to apply the alginate as a raw-material for biofabricating artifacts (scaffolds, for instance) for the Tissue Engineering, it is suitable to analyze the flowage of alginate, since in the fabrication process it will pass through a syringe and should flow onto

a $CaCl_2$ bed to be reticulated. The volume fraction analysis can present the velocity an alginate solution can be drained and deposited.

The volume fraction is measured according to the content of alginate that has been inserted in the bulk. Obviously, in the beginning (t=0s), there is no volume fraction. This property was taken during 20 seconds and reached a peak of almost $2.1 \cdot 10^{-6}$ m^3 and $5.2 \cdot 10^{-6}$ m^3 for alginate 2% and 5%, respectively, as can be observed in the Figure 8.

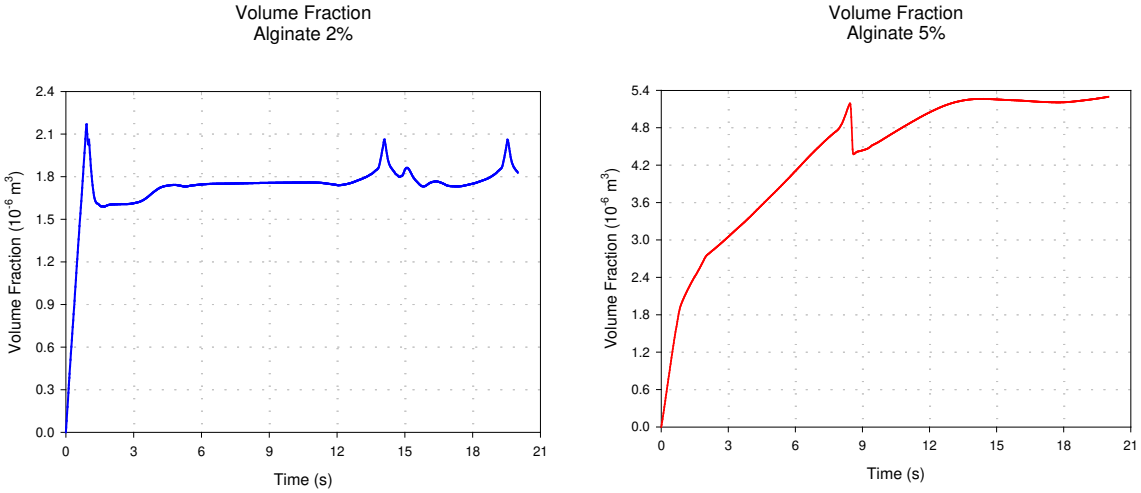

Figure 8. Volume Fraction for alginates 2% (left) and 5% (right).

3.4.2. Shear Strain Rate

A non-Newtonian fluid is a fluid for which the shear stress in not linearly proportional to the shear-strain rate. For such fluids, the apparent viscosity is the ratio of shear stress to shear-strain rate for a given shear-strain rate (ANSYS CFX® Guide, 2006). The shear strain rate in the whole volume can be conferred in the following sketch (Figures 9, 10, 11 and 12), where each one is a photograph of the shear strain rate status at, respectively, 5s, 10s, 15s and 20s of the two alginate kinds flowing.

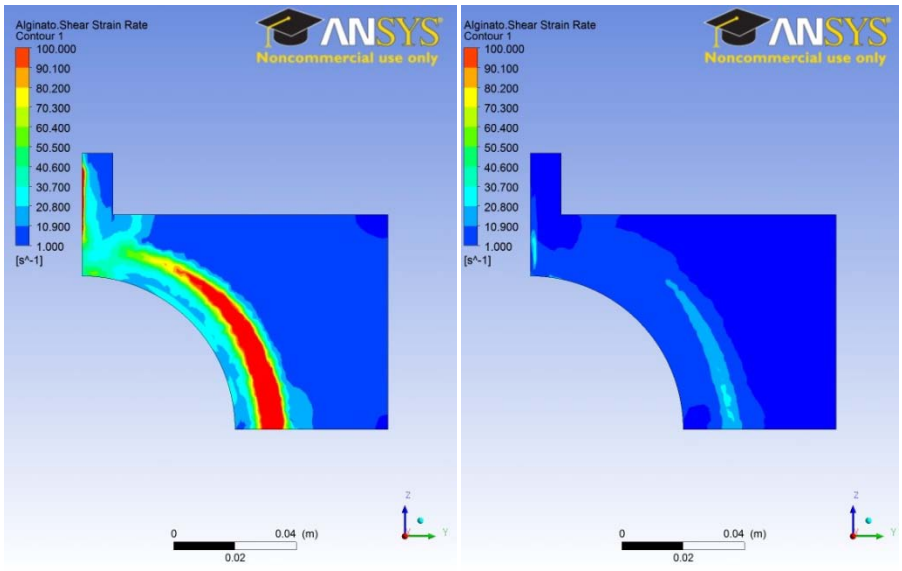

Figure 9. Shear Strain Rate for alginates 2% (left) and 5% (right) at 5s flowing.

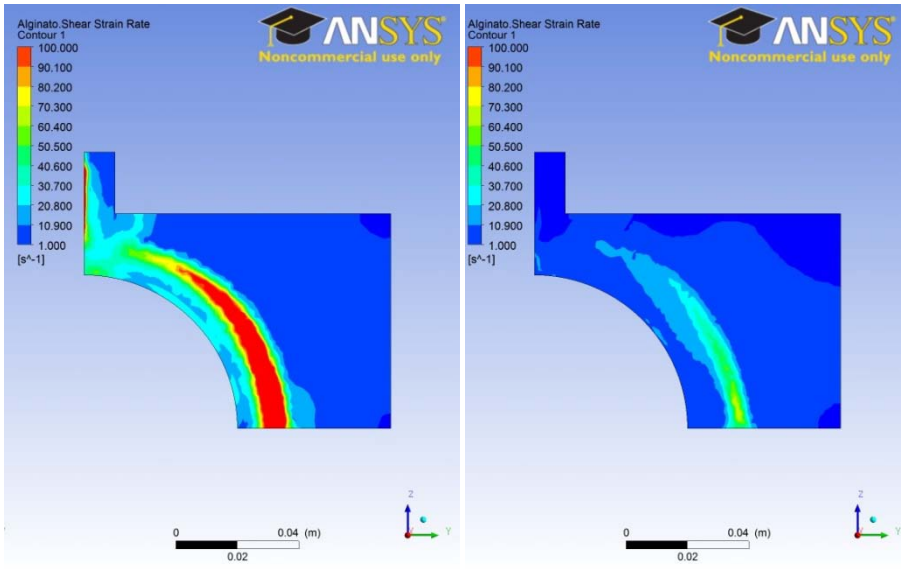

Figure 10. Shear Strain Rate for alginates 2% (left) and 5% (right) at 10s flowing.

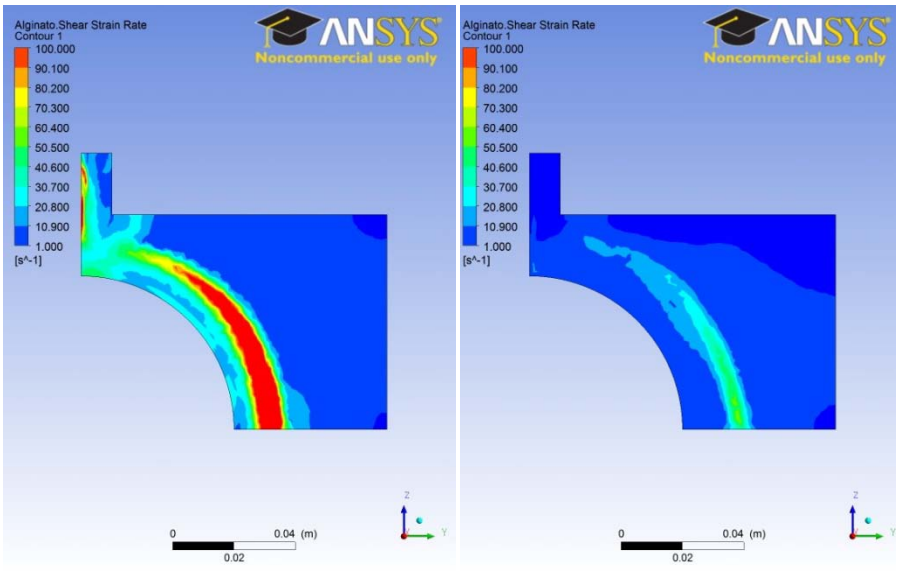

Figure 11. Shear Strain Rate for alginates 2% (left) and 5% (right) at 15s flowing.

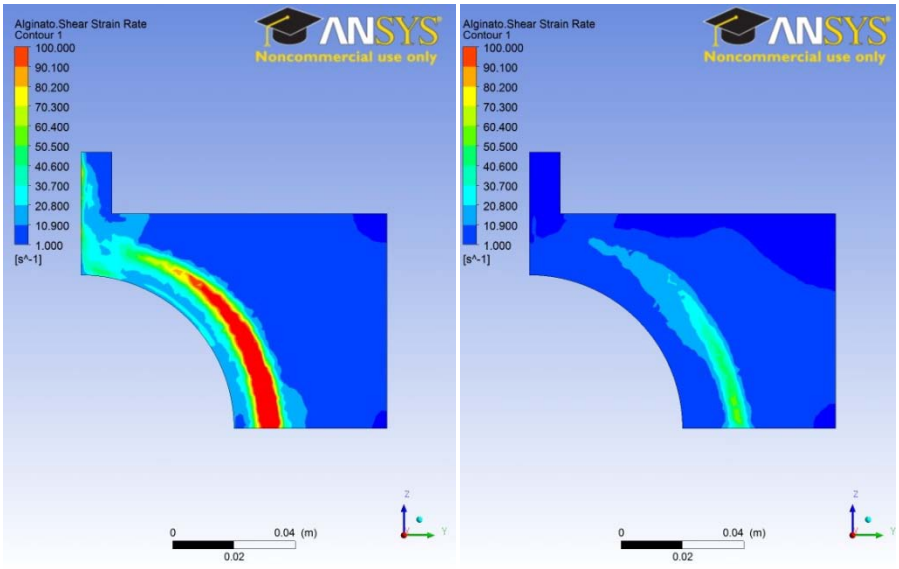

Figure 12. Shear Strain Rate for alginates 2% (left) and 5% (right) at 20s flowing.

So higher the viscosity, much more time is spent to flow completely the volume of alginate and, therefore, there is a larger gathering of material in the bulk.

Figure 13 shows the average of the shear strain rate in the entire volume during the 20 seconds for alginates 2% and 5%, respectively. In the beginning, there were two so high peaks, especially for alginate 5%, reaching 4200 s^{-1} because the higher viscosity of this

content. Inside the graph in Figure 13-right was inserted a zoom in of the shear rate in the range 0 to 15 s^{-1}.

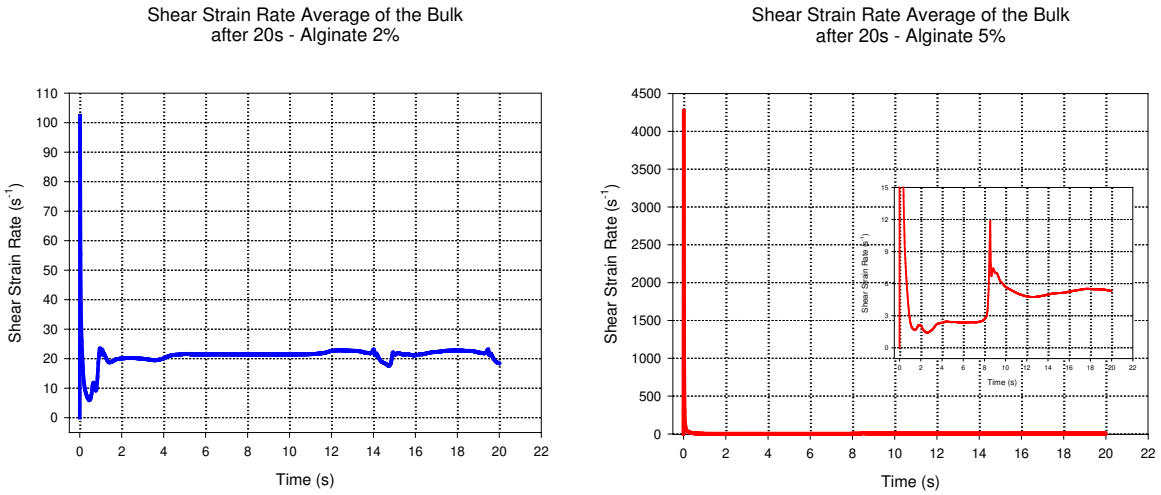

Figure 13. Shear Strain Rate for alginates 2% (left) and 5% (right).

3.4.3. Superficial Velocity

In CFX language, from Ansys packet, the vector variable Fluid.Superficial Velocity is defined as the Fluid.Volume Fraction multiplied by Fluid.Velocity. This is sometimes also referred to as the fluid volume flux. The components of this vector variable are available as scalar variables (e.g. Fluid.Superficial Velocity X).

Superficial velocity is the velocity at which the flow would travel if the porosity of the domain were 100%. It is less than the true velocity.

The Superficial Velocity in a monophasic flow is equal to its mean velocity, while in multiphase flows it is defined as the ratio of the velocity and the volume fraction of the considered phase in a multiphase system.

Superficial Velocity is simply defined as the following ratio (Eq. 7):

$$\boldsymbol{Superficial\ Velocity} = \frac{\boldsymbol{Volumetric\ flow\ rate}}{\boldsymbol{Cross\ section\ area}} \qquad (7)$$

Figures 14 to 17 present the superficial velocities obtained for the scenario analyzed. At 5s of flowage, the maximum superficial velocities for alginates 2% and 5% are about 0.082 and 0.028 m/s, respectively.

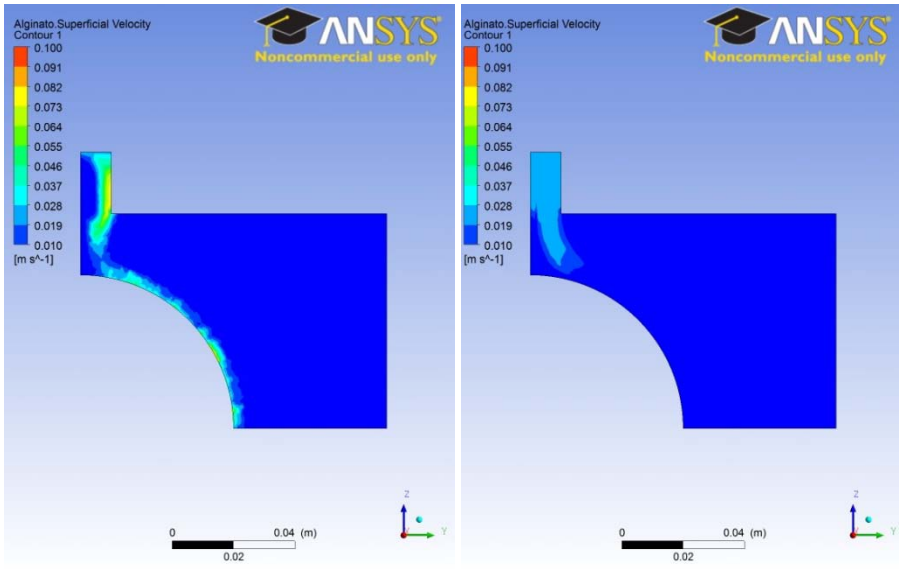

Figure 14. Superficial Velocity for alginates 2% (left) and 5% (right) at 5s flowing.

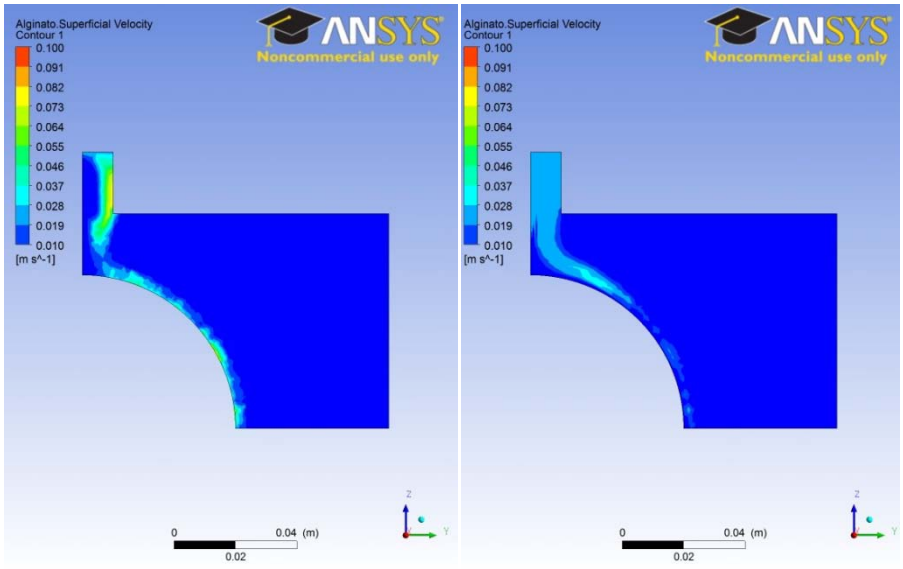

Figure 15. Superficial Velocity for alginates 2% (left) and 5% (right) at 10s flowing.

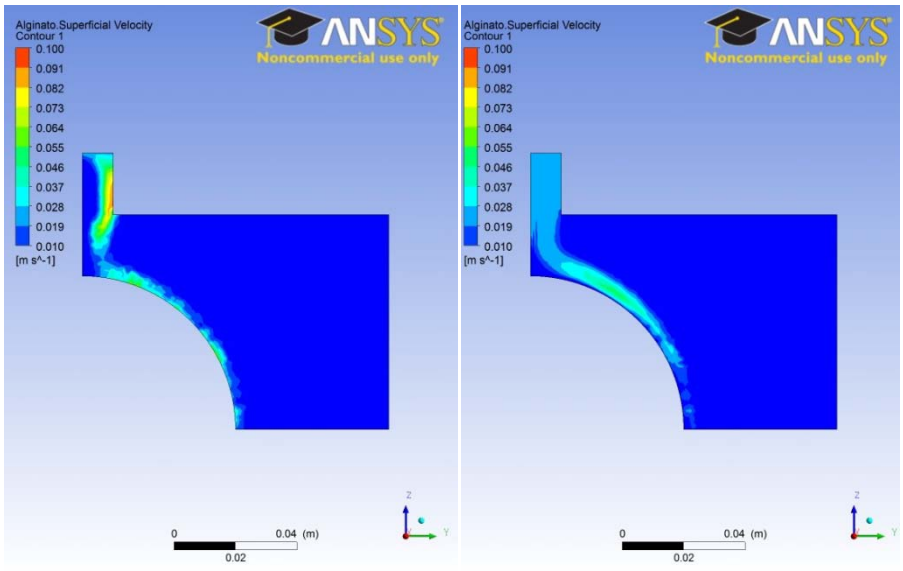

Figure 16. Superficial Velocity for alginates 2% (left) and 5% (right) at 15s flowing.

At the end that is after 20s of flowage, the maximum superficial velocities for alginates 2% and 5% are about 0.1 and 0.037 m/s, respectively. This shows the higher viscosity of alginate 5% and its difficult to spread itself.

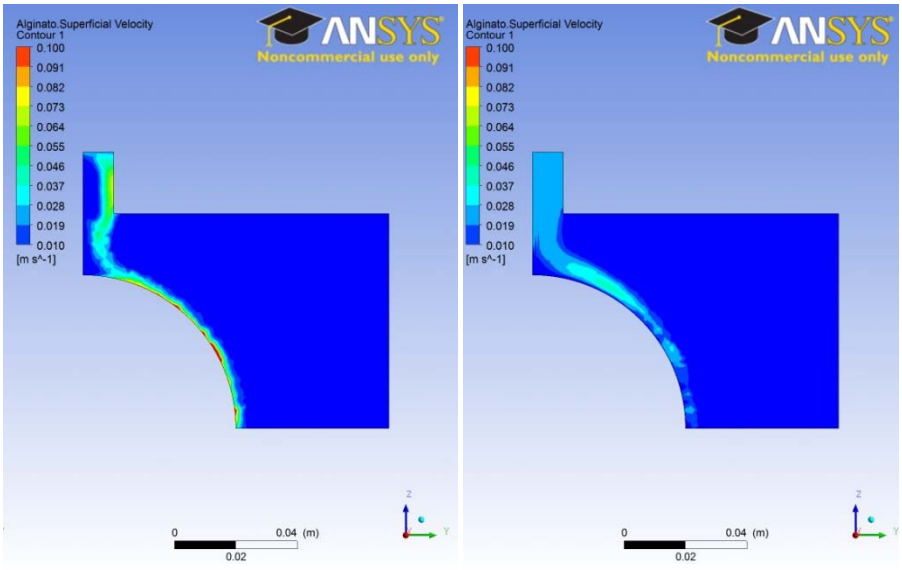

Figure 17. Superficial Velocity for alginates 2% (left) and 5% (right) at 20s flowing.

4. Conclusions

Biofabrication, by means of Rapid Prototyping and Tissue Engineering association, has become an important field in the science. The possibility to regenerate tissues and to allow people to have back a life closer to the normal motivates the fast growth of this technology. The way the artifacts are produced is a very important element to achieve great results. Alginate has high potential of applicability due to present good mechanical properties for keeping 3D structures and also biocompatibility further relatively low cost and easy handling.

Computational and mathematical modelings (CAPE) have been contributed to the prediction of the biomaterials and biomedical artifacts behaviour and the accuracy of the final bioproducts. The software Ansys, based on Finite Element Methods, was employed in this paper. Analysis about the flowage of alginate in a simple structure was done. Since it is foreseen to mix calcium alginate (pure alginate) with calcium chloride through extrusion, it is fundamental to understand how the alginate flows in different concentrations, that is, its superficial velocity and volume fraction, for instance. The input for Ansys was based on rheological data, like viscosity and some parameters, obtained from a prior study of calcium alginate through a plate rheometer.

5. Acknowledgements

The authors would like to express the gratefulness for the financial support of CNPQ (National Counsel of Technological and Scientific Development) through National Institute of Biofabrication (Biofabris).

REFERENCES

Ansys CFX, 2006, “Users Guide”.

Bineli, A. R. R., Barbosa, M. I. R., Jardini, A. L., Maciel Filho, R. Simulation to Analyze Two Models of Agitation System in Quench Process. 20th European Symposium on Computer Aided Process Engineering – Escape20. S. Pierucci and G. Buzzi Ferraris (Editors). 2010.

Bruck, S.D. Properties of Biomaterials in the Physiological Environment (Boca Raton, FL: CRC Press). 1980.

Burns, M., Automated Fabrication: Improving Productivity in Manufacturing, Prentice Hall, New Jersey, 1993.

Chu, C-C. Biodegradable Polymeric Biomaterials: An Updated Overview. In: Biomaterials Principles and Applications. Edited by Park, J. and Bronzino, J. 2003.

Hutmacher, D. W., Sittinger, M., Risbud M. V. Scaffold-based tissue engineering: rationale for computer-aided design and solid free-form fabrication systems. Trends in Biotechnology, 22 (7), 354-362, 2004.

Jacobs, P.F., Stereolithography and Other RP&M Techno logies: From Rapid Prototyping to Rapid Tooling, SME, Dearborn, 1995.

Jennifer, J. M. *et al.* Transplantation of cells in matrices for tissue regeneration. Adv. Drug Deliv. Rev., 33, 165-162, 1998.

Johnson, F. A., Craig, D. Q. M., Mercer, A. D., Characterization of the block structure and molecular weight of sodium alginates, Journal of Pharm Pharmacol, 49, pp.639-643, 1997.

Maliska, C.R., Transferência de Calor e Mecânica dos Fluidos Computacional, 2nd ed. LTC editora, 452. 2004.

Mendes, A., Lagoa, R., Bártolo, P. J., Rapid Prototyping system for tissue engineering. Proceedings of the International Conference on Advanced Research in Virtual and Physical Prototyping, pp.419-426, 2003.

Mironov, V. Trusk, T. Kasyanov, V. Little, S. Swaja, R. Markwald, R. Biofabrication: a 21st century manufacturing paradigm. Biofabrication. v.1 n.2. 2009.

Nakamura, M., Iwanaga, S., Henmi, C., Arai, K., Nishiyama, Y. Biomatrices and biomaterials for future developments of bioprinting and biofabrication. Biofabrication. n.2. pp.1-6. 2010.

Park, J. Bronzino, J. Preface. In: Biomaterials Principles and Applications. Edited by Park, J. and Bronzino, J. 2003.

Reece, G. P., Patrick, C. W., Jr. Tissue engineered construct design principles. Frontiers in Tissue Engineering, 166-196, 1998.

Rezende, R.A., Bártolo, P.J.S., Mendes, A., Maciel Filho, R. Rheological behavior of alginate solutions for biomanufacturing. Journal of Applied Polymer Science, v.113, 3866-71, 2009.

Serp, D., Mueller, M., Stockar, U. and marison, I. W., Low-temperature electron microscopy for the study of polysaccharide ultrastructures in hydrogels. II. Effect of temperature on the structure of Ca2+-alginate beads, Biotechnology and Bioengineering, 79, pp.253-259, 2002.

Shaw, C.T. Using Computational Fluid Dynamics, Prentice Hall, 325. 1992.

Skalak, R. and Fox, C. F., Tissue engineering, Alan R. Liss, 1988.

Sun, W. Welcome to Biofabrication. Biofabrication. v.1, n.1, 2009.

UNOS, U. S. Scientific Registry for Organ Transplantation and the Organ Procurement and Transplant Network. UNOS http://www.unos.org/. Accessed on May, 2010.

Versteeg, H.K., Malalasekera, W. An introduction to Computational Fluid Dynamics (The Finite Volume Method). Prentice Hall, 257. 1995.

Wandrey, C., Espinosa, D., Rehor, A. and Hunkeler, D. J. Microencapsulation, 20, 597-611, 2003.

Williams, D.F. Definition in Biomaterials. In: Progress in Biomedical Engineering (Amsterdam: Elsevier), p. 67. 1987.

Yang, S., Leong, K-F., Zhaohui, D., Chua, C-K. The Design of Scaffolds for Use in Tissue Engineering. Part II. Rapid Prototyping Techniques. Tissue Engineering, 8 (1), 1-11, 2002.

Yannas, L.V. Natural Materials - Classes of Materials Used in Medicine. In: Biomaterials Science: An Introduction to Materials in Medicine. pp. 84-94. Edited by Ratner, B., Hoffman, A., Schoen, F., Lemons, J. Academic Press. 1996.

6.3 Conclusões

A computação e a modelagem matemática têm sido ferramentas fundamentais para o desenvolvimento de novas técnicas e artefatos voltados para a biofabricação. O auxílio do computador tem sido extremamente importante para a predição de comportamentos de biomateriais e métodos de fabricação, além da precisão exigida do bioproduto final. Vários softwares baseados no método dos elementos finitos vêm sendo empregados na biofabricação. Neste trabalho, foi utilizado o software Ansys.

O objetivo foi a exploração do Ansys para a análise do perfil de escoamento do alginato de sódio (não-reticulado). Uma estrutura simples tridimensional foi construída. A idéia de se realizar a análise de escoamento está voltada à possibilidade da aplicação futura do alginato para fabricação de artefatos para a engenharia tecidual, mais especificamente, à forma com que o alginato será depositado em um leito de cloreto de cálcio (ou outro íon divalente reticulador), ou seja, através de válvulas de extrusão. Para este fim, o dimensionamento da válvula é diretamente ligado ao perfil de escoamento do alginato de sódio, por exemplo, com que velocidade este material escoa de acordo com a variação da composição do alginato.

Como entrada do modelo no Ansys, foram utilizados resultados obtidos dos experimentos do Capítulo 3, através do reômetro de pratos, tais como aqueles referentes à viscosidade do alginato.

O alginato de menor concentração (2%) escoa com maior rapidez devido à sua menor viscosidade. Para o alginato 5%, após o pico de escoamento próximo a 9 seg, ocorre uma não-linearidade motivada por sua própria viscosidade, já que ocorre uma espécie de desprendimento de parte do volume com o restante escoando posteriormente e atingindo novamente um valor próximo ao pico de fração de volume em 5,1 (μm^3).

Capítulo 7 – Algoritmos Genéticos: Otimização de Estruturas em Alginato

7.1 Introdução

Neste capítulo é apresentado um estudo sobre a aplicação da técnica dos algoritmos genéticos na biofabricação na busca dos melhores pares "composição de alginato, porosidade inicial", quando da fabricação de estruturas em alginato.

Um *scaffold* a ser empregado na engenharia tecidual precisa possuir características dinâmicas e adaptativas. O trabalho de predição do comportamento mecânico destas estruturas ao longo do tempo ganha muito espaço, uma vez que se torna possível projetar circunstâncias reais mais próximas às ideais no ato de fabricação dos bioartefatos.

Um *scaffold*, por exemplo, deve garantir resistência mecânica suficiente para garantir a sua funcionalidade, enquanto o novo tecido está em pleno crescimento, mas que não é ainda capaz de assumir todo o papel do próprio *scaffold*, ou seja, ainda é mecanicamente imaturo para servir de completo suporte ao novo tecido. Como o *scaffold* deve degradar-se ao longo do tempo e, consequentemente, ocorre uma deficiência mecânica e a decadência do módulo elástico, os algoritmos genéticos podem atuar no sentido de selecionar qual a condição mais apropriada do material (alginato) em preparação, para que se tenha, no caso aqui presente, o melhor módulo elástico em determinado momento.

Através de um modelo matemático simples obtido a partir de dados experimentais descreve-se o comportamento físico de estruturas em alginato, mais especificamente, a degradação. Desta forma, integrando-se este modelo aos algoritmos genéticos, podem-se encontrar os melhores valores para o par "composição de alginato, porosidade inicial".

7.2 Conceitos Fundamentais dos AGs

Os algoritmos evolutivos (EA) são métodos de procura adaptativos utilizados na solução de problemas de otimização. Inspiram-se nos princípios e modelos da evolução e seleção natural (Neo-Darwinismo), utilizando mecanismos, apoiados em princípios biológicos, que mantêm uma população em constante evolução. Os EAs baseiam-se nas diferentes teorias que, ao longo da história, avançaram para explicar a origem da vida e a evolução das espécies (MADEIRA, 2004). Dentre os EA, inserem-se os algoritmos genéticos.

Os algoritmos genéticos são métodos de busca e otimização inspirados na teoria de Darwin de sobrevivência do indivíduo mais adaptado (Rezende, 2007). Baseada nos princípios da evolução populacional, esta técnica está também alinhada ao conceito de biomimetismo, que estuda os modelos da natureza e imita-os ou obtém inspiração a partir dos seus designs e processos para resolver os problemas humanos (Benyus, J., 1997).

No início do século XIX, o biólogo zoologista francês Jean Baptiste de Lamarck apresentou a sua teoria da evolução, exposta no trabalho teórico *Philosofie Zoologique*. Para Lamarck, as características adquiridas por um organismo ao longo da vida podiam ser transmitidas aos seus descendentes através da hereditariedade, também denominada lei do uso e do desuso (MADEIRA, 2004).

Em 1858, Darwin apresentou a teoria da evolução através da seleção natural em sua obra “The origin of the species”. Em 1900, surgiu o princípio básico de Genética Populacional, no qual a variabilidade entre indivíduos em uma população de organismos que se reproduzem sexualmente é produzida pela mutação e pela recombinação genética. Nos anos 1930 e 1940, esse princípio foi desenvolvido por biólogos e matemáticos. Nos anos 1950 e 1960, foram desenvolvidas simulações computacionais de sistemas genéticos. Em 1975, Holland publicou o livro Adaptation in Natural and Artificial Systems (Holland, 1975), uma importante referência sobre algoritmos genéticos em que estes algoritmos são considerados tanto como uma

abstração na evolução biológica, como um enquadramento teórico para a sua adaptação ao meio ambiente; e nos anos 1980, Goldberg (1989) conseguiu o primeiro sucesso em aplicação industrial dos algoritmos genéticos.

Na natureza, os animais competem entre si por recursos como comida, água e refúgio. Aqueles que não obtêm êxito na competição tendem a ter um número reduzido de descendentes, portanto, há menor probabilidade de seus genes serem propagados ao longo de sucessivas gerações. A combinação entre os genes dos indivíduos que perduram na espécie pode produzir um novo indivíduo mais adaptado às características de seu meio ambiente.

Os algoritmos genéticos utilizam uma analogia ao fenômeno de evolução da natureza. Nesses algoritmos, cada indivíduo representa uma possível solução para um dado problema. A cada indivíduo é atribuído uma função de avaliação dependendo da resposta dada ao problema por este indivíduo. Aos mais adaptados, é dada a oportunidade de se reproduzir mediante cruzamentos com outros indivíduos da população, produzindo descendentes com características de ambas as partes. Se um Algoritmo Genético for desenvolvido corretamente, a população (conjunto de possíveis soluções) evoluirá a uma solução ótima ou suas cercanias para o problema proposto.

Existem alguns operadores genéticos que contribuem para a evolução, como a seleção/reprodução, o cruzamento (crossover) e a mutação. Dentre os componentes de um Algoritmo Genético, podem ser citados o espaço de busca (Figura 7.1), onde são consideradas todas as possibilidades de solução de um dado problema, e a função de avaliação, uma maneira de avaliar os membros do espaço de busca.

Os AGs, em relação a métodos clássicos de otimização (por exemplo, SQP), têm como vantagem o fato de não requererem manipulação da estrutura matemática da função objetivo e/ou restrições e não requererem estimativa inicial (Rezende, 2007; Deb, 2000; Leboreiro e Acevedo, 2004; Costa, 2006). Tais características têm aumentado a aplicação dos AGs em vários problemas de otimização.

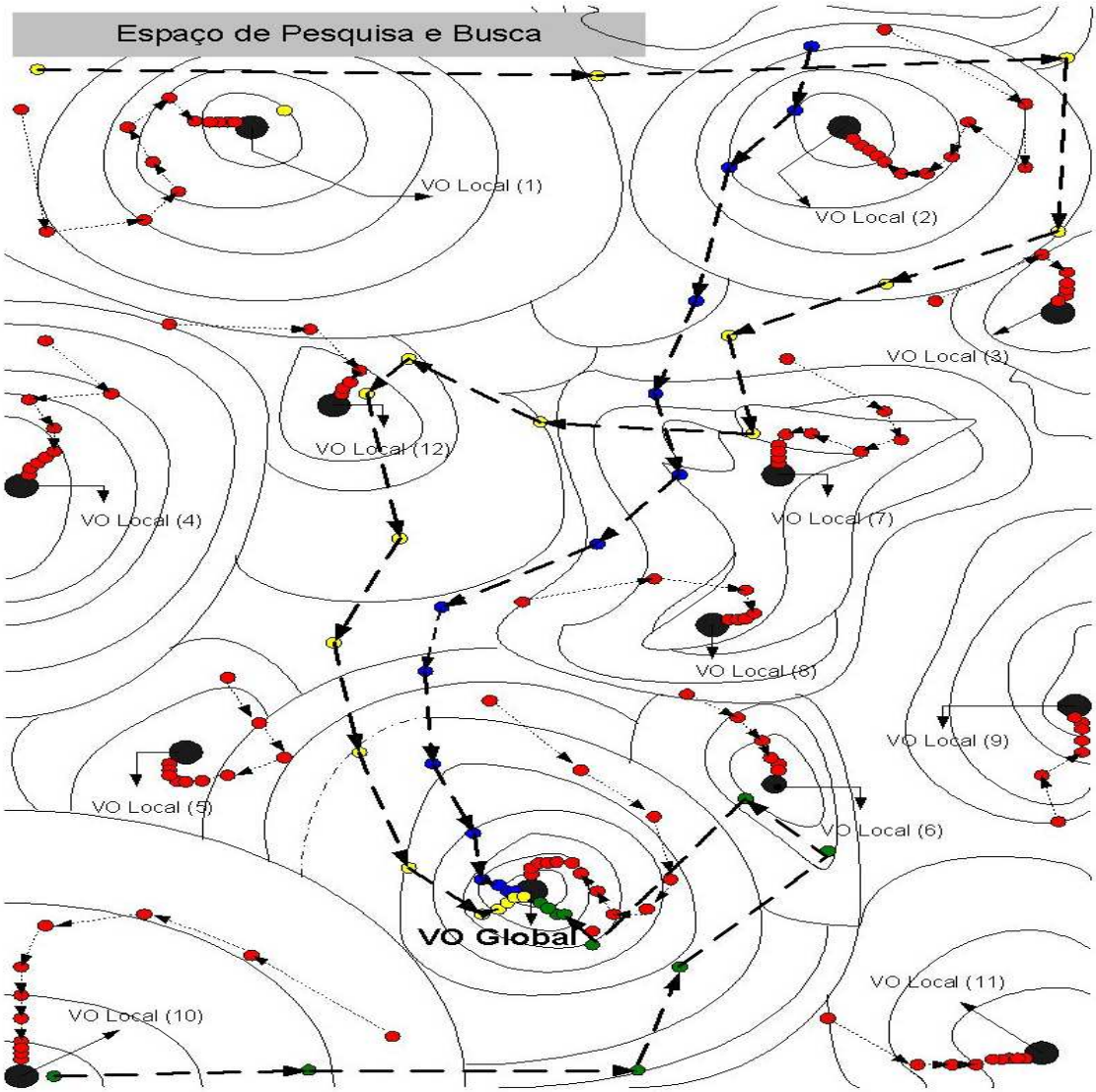

Figura 7. 1 Espaço de busca – AGs x Métodos Convencionais (Victorino, 2005).

Basicamente, o código de um AG começa com uma população de cromossomos, que são um conjunto de soluções para o problema de otimização. Cada solução é avaliada por uma função de avaliação que associa um valor a cada uma destas soluções, a fim de determinar a melhor delas. Neste ponto, são aplicados os operadores genéticos, responsáveis por promover a evolução das soluções. Este procedimento é repetido ao longo de iterações (ou gerações) até que um critério de terminação seja satisfeito.

Os operadores genéticos classificam-se em três tipos: seleção, cruzamento e mutação. O operador de seleção escolhe as melhores soluções na população. A seleção por torneio, em que os indivíduos são escolhidos aleatoriamente para participar de um torneio que seleciona os indivíduos mais adaptados de acordo com o valor do fitness (Deb, 1999), e a roleta probabilística (*roulette wheel*), em que para cada indivíduo da população é associado um espaço na roleta, o qual é proporcional ao fitness do indivíduo, são dois operadores de seleção bastante comuns. O operador de cruzamento consiste na troca de algumas partes dos cromossomos pais objetivando a troca de informações entre as soluções "pais" para gerar as soluções "descendentes". Quando apenas um ponto de cruzamento é escolhido no cromossomo para trocar informação genética, este é o chamado cruzamento em um ponto; quando a escolha do ponto de cruzamento é múltipla e aleatória, este é o chamado cruzamento uniforme. O operador de mutação faz trocas aleatórias nos genes de alguns cromossomos, contribuindo para aumentar a diversidade da população.

Os critérios de parada de um AG podem ser encontrados com certa variedade na literatura. Para citar dois deles, o trabalho de Dudek (2004) usa um AG que termina quando o número máximo de gerações é atingido. No trabalho de Leboreiro e Acevedo (2004), o operador de mutação é usado como direcionador para definir quando a busca deve ser parada, dado um critério de convergência.

A maior parte dos problemas de otimização envolve algum tipo de restrição que deve ser satisfeita pela solução ótima. Os AGs empregam, na maior parte das suas aplicações de problemas de otimização com restrição, o método da função penalidade. A necessidade de um parâmetro de penalidade é fazer a violação da restrição da mesma ordem de magnitude do valor da função objetivo. No método proposto por Deb (2000), parâmetros de penalidade não são necessários, pois as soluções nunca são comparadas em termos de ambos, valores da função objetivo e informação de violação de restrição. Este método é baseado na habilidade dos AGs de comparação de soluções aos pares usando o operador de seleção por torneio, durante o qual os seguintes critérios são sempre enfatizados: (i) quando duas soluções viáveis são comparadas aquela com melhor valor da função objetivo é escolhida, (ii) quando uma solução viável e uma

inviável são comparadas, a solução viável é escolhida, (iii) quando duas soluções inviáveis são comparadas, aquela com menor violação da restrição é escolhida. O fluxograma a seguir (Figura 7.2) ilustra o AG empregado neste trabalho no âmbito da biofabricação.

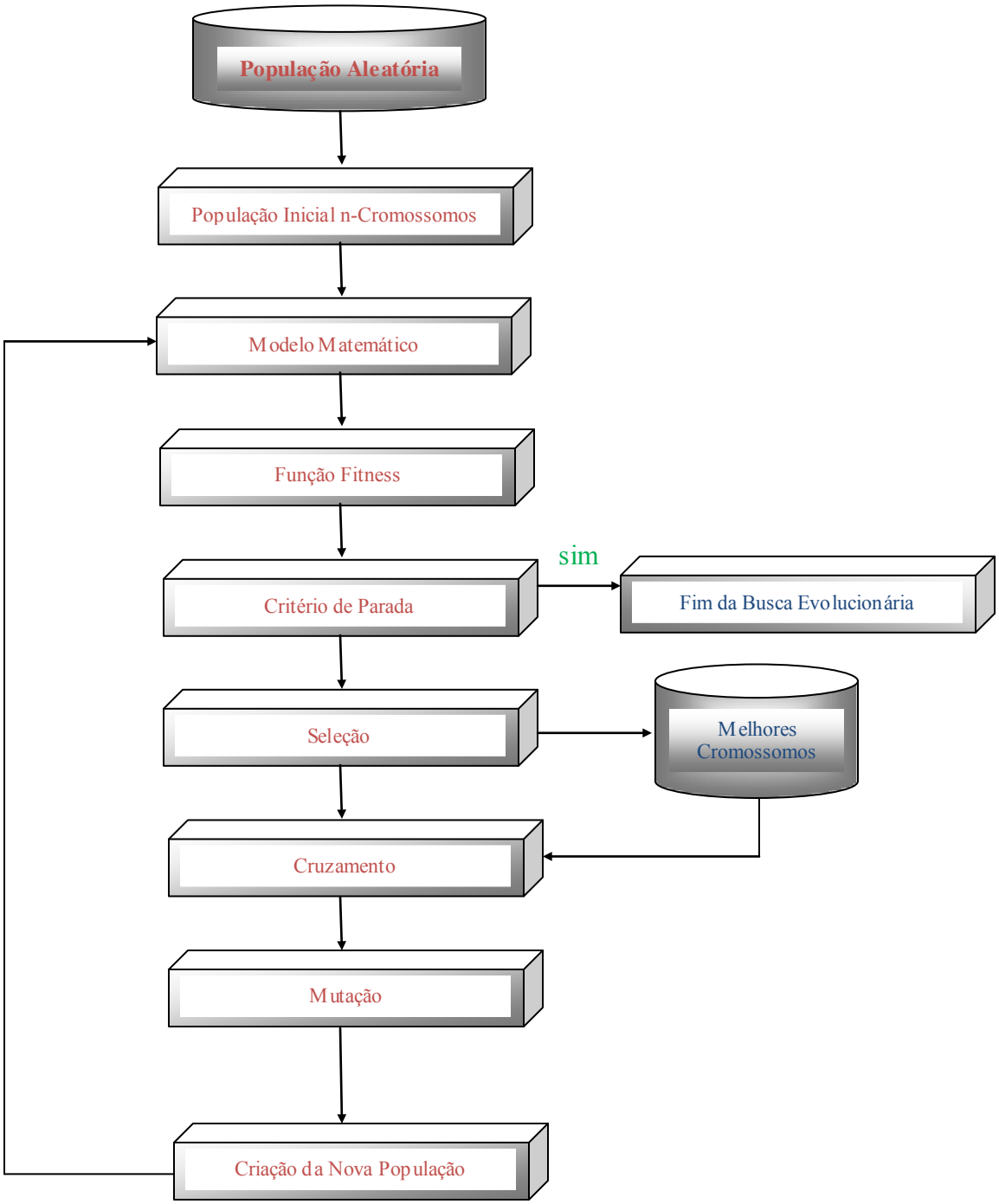

Figura 7. 2 Fluxograma do algoritmo genético.

7.3 Artigo Produzido

O Capítulo 7 é desenvolvido e apresentado em forma do artigo intitulado "**Adopting Genetic Algorithms for Optimizing *Scaffolds* in Alginate for Biofabrication**" e foi publicado no AIDIC (Associação Italiana de Engenharia Química) Conference Series (v. 9, 243-252, 2009).

AIDIC Conference Series, Vol. 9, 2009
Editor Sauro Pierucci
DOI: 10.3303/ACOS0909028

ISBN 978-88-95608-10-5 ISSN 2036-5969

Adopting Genetic Algorithms for Optimizing Scaffolds in Alginate for Biofabrication

Rezende, R.A.[a*], Rezende, M.C.A.F.[a], Maciel Filho, R.[a], Bártolo, P.J.S.[b], Mendes, A.[b]

[a] School of Chemical Engineering, University of Campinas (Unicamp), Campinas-SP, Brazil.
[b] Centre for Rapid and Sustainable Product Development, Polytechnic Institute of Leiria, Portugal.

Alternative ways of restoring and replacing tissues have been researched and implemented successfully against the increase of the rate of transplants due to damaged or affected tissues or organs by accidents or diseases and also by the aging of the population in many countries. Biofabrication by means of Rapid Prototyping techniques can help in the fashioning and final production of scaffolds devoted to support and stimulate the growth of new tissues. For soft tissues, a biomaterial known as Alginate has been studied and used as raw-material for scaffolds fabrication. A Scaffold should own very dynamical and adaptive characteristics. In this sense, it is fundamental to know better the mechanical and chemical properties since the scaffold must guarantee good strength and stiffness at the same time the material degrades gradually. The present and future of biomedical materials development requires this degree of control prediction in the design, synthesis, and function of next-generation materials. A prediction job is possible and it has already been used so that the scaffold state can be forecasted before its fabrication and, as a good alternative, to know how and how much alginate should be used. A single mathematical model experimentally obtained describes an interesting physical behaviour, that is, in the case of this work, the degradation of alginated-scaffolds. Evolutionary algorithms, like Genetic Algorithms (GAs), represent a class of stochastic optimization procedures based on natural systems according to Darwin's observations, and the modern synthetic theory of evolution. In the present work, the objective of GAs is to find out the best values of alginate amount and initial porosity for scaffold fabrication that maximize the elastic modulus. In summary, the paper presents an optimization process scheme using Genetic Algorithms to maximize the elastic modulus and therefore to aid the design of scaffolds in alginate. The optimization is very welcome to Tissue Engineering and Biofabrication.

1. INTRODUCTION

Biofabrication can be defined as the production of complex living and non-living biological products from raw materials such as living cells, molecules, extracellular matrices, and biomaterials. A scaffold, as an extracellular matrix, is a temporary supporting structure. There are synthetic and naturally derived solid scaffolds (Mironov, 2009). Biofabrication uses cells or biologics as the basic building blocks in which biological models, systems, devices and products are manufactured (Sun, 2009). Biofabrication links the Tissue Engineering and the Rapid Prototyping technologies. According to Skalak and Fox (1988), Tissue Engineering can be described as the application of the principles and methods of engineering and life sciences toward the fundamental understanding of structure-function relationships in normal and pathological mammalian tissues and the development of biological substitutes to restore, maintain, or improve function. Rapid Prototyping helps in the fashioning and final production of scaffolds devoted to support and stimulate the growth of new tissues. For soft tissues, a biomaterial known as Alginate has been studied and used as raw-material for scaffolds fabrication (Fundueanu *et al.*, 1999). A scaffold must own very dynamical and adaptive characteristics in order to be implanted and to take its main roles which are to carry the stem live cells inside it, to back the growth of these cells and besides this to biodegradate appropriately since the minimum material

Please cite this article as: Rezende R., Rezende M.C., Maciel Filho R., Bartolo P.J.S. and Mendes A., (2009), Adopting genetic algorithms for optimizing scaffolds in alginate for biofabrication, AIDIC Conference Series, 09, 243-252
DOI: 10.3303/ACOS0909028

should remain after the tissue is reconstructed (Rezende *et al.*, 2009). It is fundamental to be aware of the mechanical and chemical properties since the scaffold must guarantee good strength and stiffness at the same time the material degrades gradually. In this way, the optimization process comes, supported by Genetic Algorithms, to maximize the elastic modulus and therefore to aid the design of scaffolds in alginate.
To know how the mechanical behaviour of the scaffold will be, some time later, is the keyword. And the understanding about the match between biodegradation and Young Modulus is mandatory.
The present and future of biomedical materials development requires this degree of control prediction in the design, synthesis, and function of next-generation materials (Hutmacher, 2006). A prediction job is possible and it has already been used so that the scaffold state can be forecasted before its fabrication and, as a good alternative, to know how and how much alginate should be used. Other future analyses can be around the best geometry to be adopted during Rapid Prototyping technique actuation.

2. SCAFFOLDS

The function of a degradable scaffold is to act as a temporary support matrix for transplanted or host cells so as to restore, maintain, or improve tissue. A scaffold, as shown in Figure 1, may be created from various types of materials, including polymers. Polymeric scaffolds may be used to support a variety of cells for numerous tissues within the body. The design of a polymeric scaffold plays a significant role in proper cell growth. Therefore, several important properties must be considered: fabrication, structure, biocompatibility, biodegradability, and mechanical strength, as illustrated in Figure 2. Scaffolds guide cells to grow, synthesize extracellular matrix and other biological molecules and facilitate the formation of functional tissues and organs (Ma, 2004; Zhang and Ma, 2000).
The scaffold is expected to support cell colonization, migration, growth and differentiation, and to guide the development of the required tissue or to act as a drug delivery device (Hutmacher, 2006).

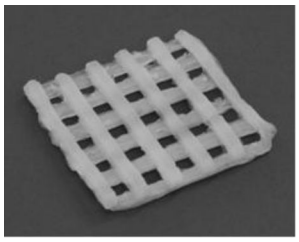

Figure 1: Example of a handcraft scaffold.

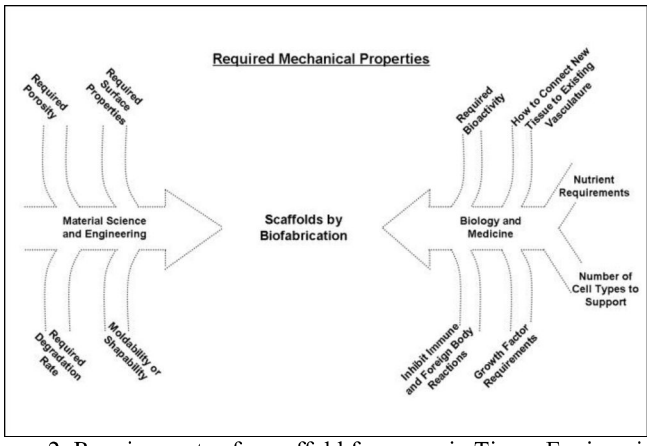

Figure 2: Requirements of a scaffold for usage in Tissue Engineering.

3. ALGINATES

Alginate is an anionic copolymer composed (Figure 3) of homopolymeric regions of 1,4-linked β-D-mannuronic (M blocks) and α-L-guluronic acid (G blocks), interspersed with regions of alternating structure. The industrial manufacture of alginate is based on the extraction of a polymer from brown algae. Gelation occurs when divalent ions (Ca2+, Ba2+, Fe2+, Sr2+, etc.) or trivalent ions (Al3+, etc.) take part in the interchain ionic binding between G-blocks in the polymer chain giving rise to a three dimensional network. Such binding zones between the G-blocks are often referred to as "egg boxes". These ions act as cross-linkers that stabilise alginate chains forming a gel structure, which contains cross-linked chains interspersed with more freely movable chains that bind and entrap large quantities of water.

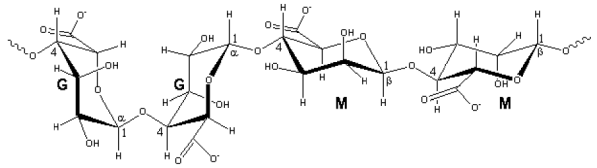

Figure 3: Structure of alginate.

3.1 Alginate Shrinkage

A match between the alginate shrinkage in terms of time was obtained experimentally for three different proportions of alginate: 1%, 2% e 5%, and got through the mixture of solutions with 1g, 2g and 5g of alginate, respectively, in 100 ml of water with a $CaCl_2$ 0,3 Molar solution (Rezende *et al.*, 2007). All solutions were prepared with pure water, with conductivity of 0.054 μS/cm. Alginate solutions were prepared by addition of weighted portions of sodium alginate to measured volumes of water. Due to their high viscosity, these solutions were agitated by orbital shaking for three hours at 50 ºC to ensure good homogeneity. Calcium chloride solution 5% (w/v) was obtained dissolving the salt in water. This solution was diluted to obtain solutions containing different concentrations of calcium chloride. Sodium alginate was purchased at Panreac (Barcelona, Spain). Calcium chloride was supplied by Carlo Erba (Milano, Italy).
The mechanical properties vary along time due to degradation and porosity changes. The degradation of alginate structures was determined through the analysis of the shrinkage variation along time as shown in Figure 4 (Rezende *et al.*, 2008).

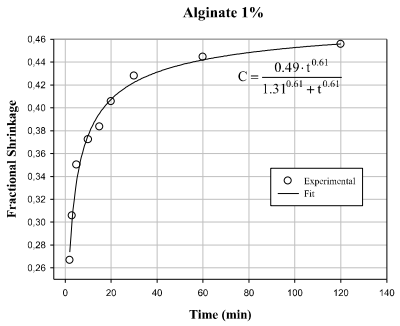

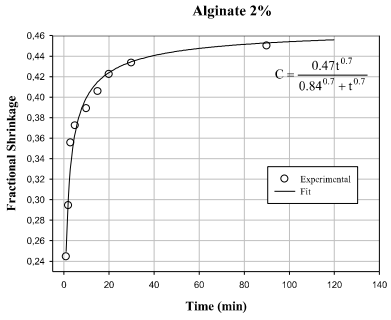

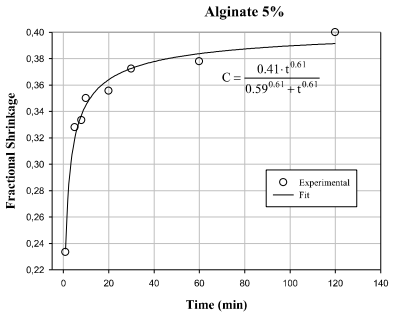

Figure 4: Fractional Shrinkage in terms of alginate concentration.

4. THE GENETIC ALGORITHMS (GAs)

Evolutionary algorithms, like Genetic Algorithms (GAs), represent a class of stochastic optimization procedures based on natural systems according to Darwin's observations, and the modern synthetic theory of evolution. The Genetic Algorithms approach starts with a random population of chromosomes that are a set of solutions for the optimization problem. Traditionally, solutions are represented in binary as strings of algorisms 0 and 1, but a real encoding is also possible. In each generation, the fitness of every individual in the population is evaluated, multiple individuals are stochastically selected from the current population (based on their fitness), and modified (recombined and possibly randomly mutated) to form a new population. The new population is then used in the next generation. Usually, the algorithm terminates when either a maximum number of generations has been reached, or a satisfactory fitness level has been found for the population.

5. MODELLING DOR THE OPTIMIZATION

The optimization problem is to determine optimal features for the fabrication of optimized alginate scaffolds for Tissue Engineering. The optimization goal aims at finding optimal values of alginate composition and initial porosity in order to fabricate scaffolds with, at a pre-determined time, a maximal mechanical behaviour (elastic modulus).

The optimization problem is given by (Rezende *et al.*, 2007):

$$\underset{[\alpha,\phi_0]}{\text{Maximize}} \quad E(\phi_0, \alpha, t)$$

$$\text{Subject to:} \quad 1\% \le \alpha \le 8\%, \quad 30\% \le \phi_0 \le 80\% \qquad \textbf{(1)}$$

where E is the elastic modulus (shear effects are not considered), α is the alginate composition and ϕ_0 is the initial porosity.

It is important to emphasize that after certain period of time, the natural biomaterial degradation reduces the mechanical properties of the scaffold, that is, reduces the Young Modulus. In this sense, the objective is to determine which are the optimum values of the pair [alginate composition (%alg), initial porosity (ϕ_0)] for the fabrication of a scaffold that, after some long time, assure the objective function optimization given by the maximization of the Young Modulus. According to the values of this pair at scaffold fabrication, different values of Young Modulus can be achieved.

The shrinkage process can be modeled through a three parameters sigmoidal model given by:

$$C(\alpha,t)=\frac{\varsigma(\alpha)\cdot t^{\vartheta(\alpha)}}{\lambda^{\vartheta(\alpha)}+t^{\vartheta(\alpha)}} \quad \textbf{(2)}$$

where t is the time and $\varsigma,\vartheta,\lambda$ are variables that depend on the alginate composition (α). Porosity at each time is also a function of alginate composition and shrinkage:

$$\phi(\phi_0,\alpha,t)=\phi_0+\zeta(\phi_0,\alpha)\cdot C(\phi_0,\alpha,t)+\psi(\phi_0,\alpha)\cdot C^2(\phi_0,\alpha,t) \quad \textbf{(3)}$$

where ζ,ψ are constants depending on alginate composition and C is the shrinkage.
The Young Modulus E is given by an expression that reports straightly the initial Young Modulus and the final porosity of the scaffold and indirectly the pair [alginate composition, initial porosity]. The dependence between the elastic modulus and porosity for different alginate compositions is given by the following equation:

$$E(\phi_0,\alpha,t)=E_0(\phi_0,\alpha)+k_1(\phi_0,\alpha)\cdot\phi(\phi_0,\alpha,t)+k_2(\phi_0,\alpha)\cdot\phi(\phi_0,\alpha,t)^2+k_3(\phi_0,\alpha)\cdot\phi(\phi_0,\alpha,t)^3 \quad \textbf{(4)}$$

with E_0 being the initial elastic modulus, k_1,k_2,k_3 constants dependent on both the alginate composition and the initial porosity and ϕ the final porosity of the scaffold.
A single constrained optimization problem, which maximises the elastic modulus, constraints considers four cases of constraints at shrinkage and final porosity: 1) no constraint, 2) shrinkage higher than 25%, 3) final porosity higher than 80% and 4) Shrinkage < 35% and Final Porosity > 75%.
To solve the constrained problem, a constraint handling method based on the penalty function approach was used, not requiring any penalty parameter (Deb, 2000). In this case, the expression of the fitness function for a minimisation problem, where infeasible solutions are compared based only on their constraint violation, is given by Deb (2000):

$$F(\mathbf{x})=\begin{cases} f(\mathbf{x}) & \text{if } g_j(\mathbf{x})\geq 0 \quad \forall j=1,2,...,nc \\ f_{\max}+\sum_{j=1}^{m}\langle g_j(\mathbf{x})\rangle & \text{otherwise} \end{cases} \quad \textbf{(5)}$$

where $f_{\max}$ is the objective function value of the worst feasible solution in the population.
The GAs used in this research work, to solve the formulation indicated above in section 3, are a Fortran binary code (Carroll, 2008). The employed genetic operators are the tournament selection, the uniform crossover, the creep and the jump mutation. Niching and elitism are also employed. The input parameters, chosen by a trial and error method, are indicated in Table 1.

Table 1: The GAs input parameters.

GAs input parameters	Value
Population size per generation	50
Maximum number of generations	30
Crossover probability	0.60
Jump mutation probability	0.077
Creep mutation probability	0.077
Initial random number seed for the GAs run	-1000

6. ANALYSIS OF THE SCAFFOLD OPTIMIZATION USING GAs

The analyses were shared in four cases including the first one with no constraint and the remaining cases constrained.

6.1 Constraint Considerations

Four different cases with respective conditions were evaluated. The single objective constrained optimization problem which maximises the elastic modulus considers one case with no constraint and three cases of constraints at shrinkage and final porosity (Table 2).

Table 2: The Four Cases Analyzed.

Cases	Conditions
1	No constraint
2	Shrinkage > 25%
3	Final Porosity > 80%
4	Shrinkage < 35% and Final Porosity > 75%

6.2 Results

This section presents the results of the scaffolds optimization using Genetic Algorithms for the constrained and unconstrained problem.

a) No constraint

Results obtained for this case are shown in Table 3:

Table 3: Optimization results for the constrained problem (no constraint)

Optimization Variables	Initial Alginate composition (%)	8,00
	Initial Porosity (%)	30,00
Objective Function	Elastic modulus (KPa)	23,38
Constraint	Shrinkage (%)	16,24
Output Variable	Final Porosity (%)	59,17

Figure 5 shows the evolution of the objective function along all the generations. Profiles of the objective function, shrinkage and final porosity are illustrated in Figure 6. As can be seen through these figures, for the Young Modulus with no constraint the alginate composition trends to values close to the superior edge, while that for initial porosity the tendency is close to inferior limit.

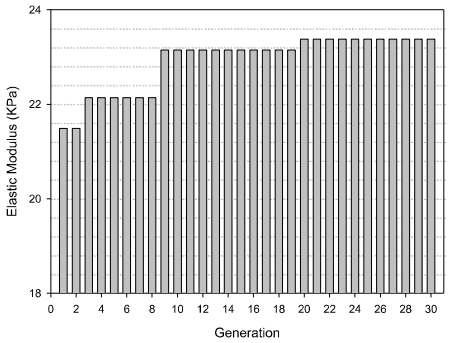

Figure 5: Young Modulus through generations (No Constraint).

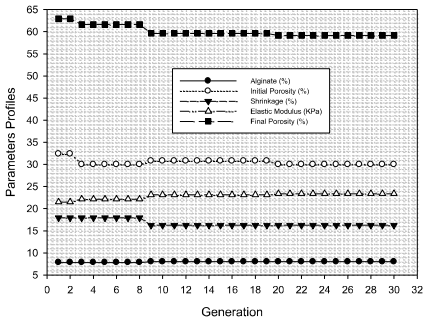

Figure 6: Profiles after all the generations (No Constraint).

b) Constraint 1: Shrinkage higher than 25%

Results obtained for this case are shown in Table 4:

Table 4: Optimization results for the constrained problem (shrinkage > 25%)

Optimization Variables	Initial Alginate composition (%)	7.06
	Initial Porosity (%)	30.00
Objective Function	Elastic modulus (KPa)	17.52
Constraint	Shrinkage (%)	25.22
Output Variable	Final Porosity (%)	70.97

Figure 7 shows the evolution of the objective function along all the 30 generations. In Figure 8, the profiles of the objective function, shrinkage and final porosity are also presented.

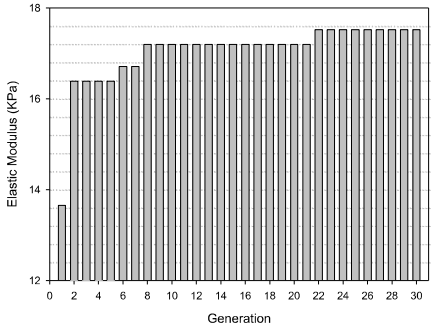

Figure 7: Young Modulus through generations (Shrinkage>25%).

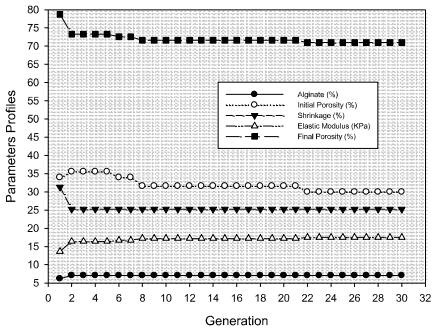

Figure 8: Profiles after all the generations (Shrinkage>25%).

In order to the Young Modulus have a maximum value without violation of the constraint (shrinkage > 25%), alginate composition should be close to 7.06% and the initial porosity close to 30%.

c) Constraint 2: Final porosity higher than 80%

Results obtained for this case are shown in Table 5:

Table 5: Optimization results for the constrained problem (final porosity > 80%).

Optimization Variables	Initial Alginate composition (%)	5.79
	Initial Porosity (%)	32.38
Objective Function	Elastic modulus (KPa)	12.99
Output Variable	Final Porosity (%)	80.01
Constraint	Shrinkage (%)	33.29

Figure 9 presents how the objective function progresses along the generations. Profiles of the objective function, shrinkage and final porosity are shown in Figure 10.

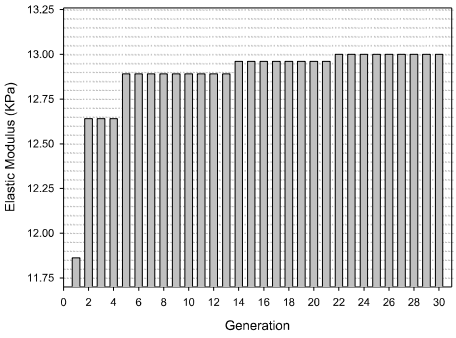

Figure 9: Young Modulus through generations (Final Porosity>80%).

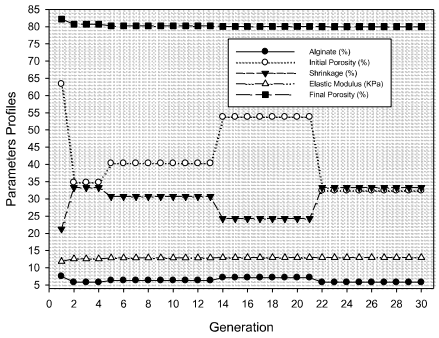

Figure 10: Profiles after all the generations (Final Porosity>80%).

The alginate composition should be close to 5.79% and the initial porosity close to 32.38%, in order that the Young Modulus reach a maximum value without violation of the constraint (shrinkage > 25%).

d) Constraint 3: Shrinkage < 35% and Final Porosity > 75%

Results obtained for this case are shown in Table 6:

Table 6: Optimization results for the constrained problem (Shrinkage < 35% and Final Porosity > 75%).

Optimization Variables	Initial Alginate composition (%)	7,45
	Initial Porosity (%)	47,46
Objective Function	Elastic modulus (KPa)	15,51
Output Variable	Final Porosity (%)	21,78
Constraint	Shrinkage (%)	75,03

Figure 11 reports the evolution of the objective function along the generations and Figure 12 illustrates the profiles of the objective function, shrinkage and final porosity.

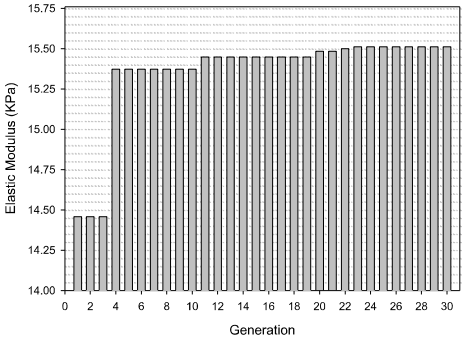

Figure 11: Young Modulus through generations (Shrinkage < 35% and Final Porosity > 75%).

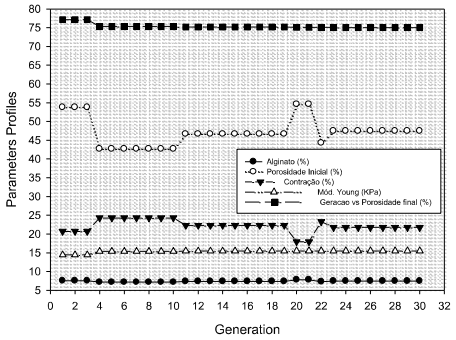

Figure 12: Profiles after all the generations (Shrinkage < 35% and Final Porosity > 75%).

For the maximal fitness (Young Modulus) without violation of the constraint (shrinkage > 25%), alginate composition should be close to 7.45% and the initial porosity close to 47.46%.

6.3 Visual summary of the results

As a summary of the best values obtained after the Gas run, Figure 13 illustrates in a 3D chart of the Objective Function (Young Modulus) and the Optimization Variables.

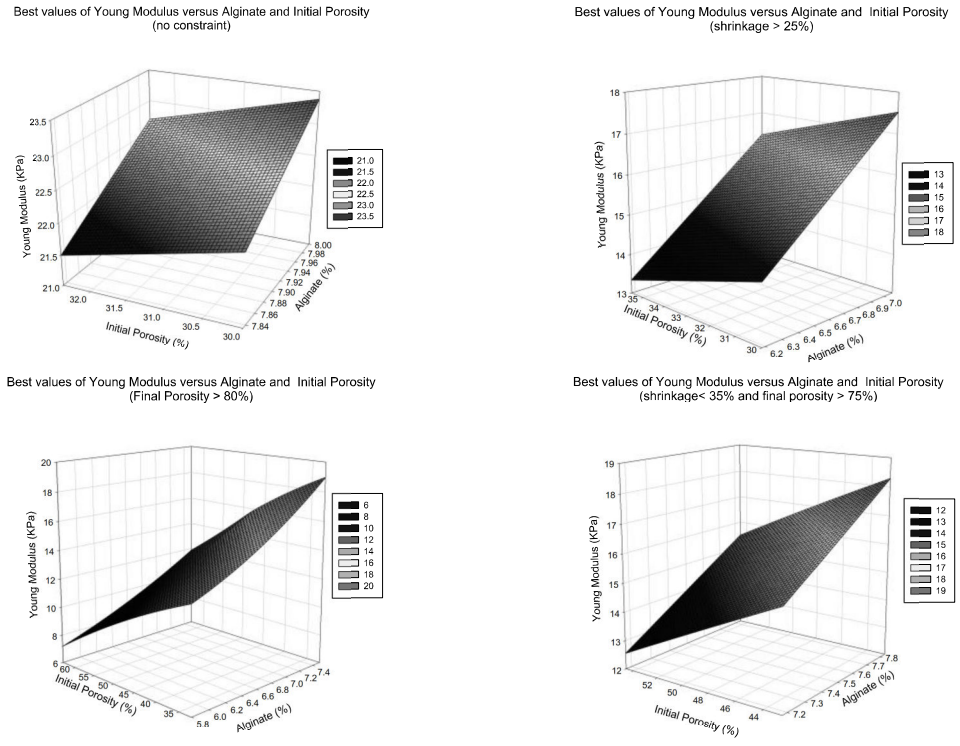

Figure 13: A 3D graph of the best values for the Objective Function versus the Optimization Variables.

7. CONCLUSIONS

This research uses Genetic Algorithms to optimize the mechanical behaviour of alginate scaffolds for Tissue Engineering. The mathematical model was experimentally obtained and the values for both alginate composition and initial porosity of the scaffold were evaluated under different constraints being found that best values of the pair which maximizes the Young Modulus with no violation. The constrained maximization of the elastic modulus was determined through the optimization code. The next work is to extend this tool to perform topological optimization regarding other expressive effects like topology, for instance, integrating them with a broader simulation code.

8. ACKNOWLEDGEMENTS

The authors would like to thank CNPq (National Council for Scientific and Technological Development/Brazil) and BIOFABRIS (National Institute in Biofabrication/Brazil).

9. REFERENCES

Carroll, D. (2008), Carroll's Fortran Genetic Algorithm Driver. In http://cuaerospace.com/carroll/ga.html accessed in November 16th.

Deb, K. (2000). An Efficient Constraint Handling Method for Genetic Algorithms. *Computer Methods in Applied Mechanics Engineering*, 186, 311-338.

Fundueanu, G., Nastruzzi, C., Carpov, A., Desbrieres, J. and Rnaudo, M. (1999). Physico-Chemical Characterization of Ca-Alginate Microparticles Produced with Different Methods. *Biomaterials*, 20, 1427-1435.

Hutmacher, D. W. (2006). Scaffold-Based Tissue Engineering: Design and Fabrication of Matrices Using Solid Freeform Fabrication Techniques. *Adv. Manufact. Tech. for Medical Applications*, Ed. by I. Gibson, 163-189.

Mironov, V. Trusk, T. Kasyanov, V. Little, S. Swaja, R. Markwald, R. (2009). Biofabrication: a 21st Century Manufacturing Paradigm. *Biofabrication*. v.1 n.2.

Rezende, R. A., Bártolo, P.J., Mendes, A., Maciel Filho R. (2007). Experimental Characterisation of the Alginate Gelification Process for Rapid Prototyping, *Chemical Engineering Transactions*. ICheaP-8.

Rezende, R. A., Rezende, M. C. A. F., Maciel Filho, R., Bártolo, P.J.S., Mendes, A. (2009). Genetic Algorithms for Optimising Alginated-Scaffolds for Tissue Engineering. *Chemical Engineering Transactions*. ICheaP-9.

Rezende, M.C.A.F., Rezende, R.A., Mendes, A. ; Bártolo, P.J., Costa, A.C., Maciel Filho, R. (2008). Evolutionary Optimization for Soft Tissue Engineering. *Advanced Research in Virtual and Rapid Manufacturing*. London, UK: Taylor & Francis, 81-85.

Skalak, R. and Fox, C. F. (1988). *Tissue engineering*, Alan R. Liss. Inc., New York.

Sun, W. (2009). Welcome to Biofabrication. Editorial. *Biofabrication*. v.1. n.1.

7.4 Conclusões

O modelo matemático empregado neste trabalho foi experimentalmente obtido e os valores do par "composição de alginato, porosidade inicial" foram avaliados sob diferentes restrições, sendo encontrados os melhores valores para o par que maximizam o Módulo de Young sem violação.

Foram analisadas quatro condições diferentes: sem restrição (1 caso), com restrição única (2 casos) e com restrição dupla ou múltipla (1 caso). No caso sem restrição, observou-se a busca das variáveis de otimização para os limites máximo da composição de alginato e mínimo da porosidade inicial. Isto de fato faz sentido já que, sem considerar restrições, a melhor estrutura será aquela composta pelo menor valor de porosidade final (e isto está diretamente ligado com o menor valor de porosidade inicial, ou seja, 30%) e a maior concentração de alginato (8%) que, por possuir maior viscosidade, segundo apresentado no Capítulo 4, possui menor deformação e maior rigidez.

Nos demais casos, com uma restrição, percebe-se que o algoritmo genético fixa uma das variáveis de otimização em um extremo ou próximo dele, e busca a outra variável numa faixa mais intermediária; e com duas restrições, os dois valores fogem mais às extremidades, o que demonstra o trabalho de busca e evolução do algoritmo genético. Obviamente, o caso sem restrição é aquele que apresenta melhor valor do módulo elástico. No entanto, o mais relevante é perceber que os algoritmos genéticos fazem a busca pelos melhores resultados das variáveis de otimização de acordo com as condições iniciais impostas ao problema.

Os algoritmos genéticos são um aliado muito benvindo à biofabricação, uma vez que, de acordo com a sua estratégia de funcionamento, o início da execução ocorre com a escolha de uma população randômica de cromossomos, sem haver a necessidade de se estimar valores iniciais.

Capítulo 8 – Conclusões e Propostas para Trabalhos Futuros

8.1 Conclusões

Mesmo sendo uma área relativamente nova, embora haja registros de desenvolvimentos já de algumas décadas, mais especificamente no que tange a engenharia tecidual, a biofabricação, contando com o auxílio da computação, vem crescendo a passos largos e conseguindo gerar inovação constante na busca por soluções que possam resgatar a saúde de milhões de pacientes ou, pelo menos, trazer um pouco mais de conforto e garantir a dignidade de acidentados e doentes.

A biofabricação é baseada em um triângulo composto pelos materiais biodegradáveis, técnicas de fabricação e as células (*stem cells*) de forma geral. Este trabalho apresentou uma interação entre os materiais e ferramentas computacionais.

O alginato, um polímero bastante utilizado industrialmente, principalmente como base de cosméticos e de alimentos, embora seja um material bastante sensível à temperatura e que exige delicado manuseio em sua preparação, ganha importância na aplicação à engenharia tecidual por ser natural e possuir propriedades físicas e mecânicas condizentes com aplicações desta área.

Este hidrogel mostrou-se fortemente dependente das concentrações de alginato de sódio e cloreto de cálcio, quando do processo de gelação (reticulação), impactando o comportamento mecânico e de morfologia de superfície de estruturas em alginato.

O comportamento reológico do alginato puro foi aferido a partir de reômetro de prato, sendo que as observações sobre as propriedades mecânicas do material são essências para que se possa dimensionar e projetar dispositivos, como extrusoras, capazes de fabricar artefatos, como os *scaffolds*. Taxas de tensão e de corte apresentaram boa

correlação com os modelos da lei da potência e de Herschel-Bulkely. Contudo, para o modelo de Herschel-Bulkely, valores negativos foram obtidos para a tensão aparente produzida. Estes resultados sugerem que as soluções de alginato são categorizadas como pseudoplásticos, e podem ser usados para maximizar taxas de fluxo e minimizar a viscosidade.

Foi estudado também o comportamento mecânico do alginato reticulado com auxílio do Analisador Dinâmico Mecânico (DMA). O alginato é um hidrogel e um material muito mole, e que contém grande quantidade de água, o que dificultou a padronização na preparação dos corpos de prova para os ensaios realizados no DMA. Igualmente ao alginato não-reticulado, observou-se grande influência da relação de concentração entre o alginato puro e o cloreto de cálcio, além de fatores como a frequência e tensão.

Realizou-se um ajuste dos dados experimentais obtidos pelo DMA com três modelos reológicos mais tradicionais. O modelo Kelvin-Voigt foi aquele que apresentou melhor aproximação.

No âmbito do comportamento químico do alginato, o processo de gelação, a capacidade de inchamento e a produção de esponjas foram também considerados e analisados. Mais uma vez, há relação direta com as composições de alginato de sódio e o cloreto de cálcio na composição das amostras, em que a taxa de inchamento é menor para quantidades maiores de alginato. À temperatura ambiente, após 10 dias, apresentaram perda de massa na faixa de 70% a 90%. Quando as amostras foram secas por vácuo, a taxa de inchamento mínima foi de 80%.

Esponjas em alginato foram produzidas por liofilização após terem sido congeladas com nitrogênio líquido. Esponjas mais porosas foram obtidas com maiores concentrações de alginato. A porosidade observada nas imagens por microscopia eletrônica de varredura mostra que esponjas em alginato podem apresentar boa capacidade de aderir células implantadas e favorecê-las em seu crescimento, em especial, aquelas estruturas com poros maiores.

O auxílio por computador e as ferramentas computacionais disponíveis e em desenvolvimento contínuo têm contemplado um avanço significativo da biofabricação. Neste trabalho, o software Ansys, baseado em elementos finitos, e os algoritmos genéticos, uma técnica de otimização, foram empregados e obtiveram um bom retorno em termos de resultados.

A predição de fenômenos físicos por meio de simulações no Ansys, no caso deste trabalho, propicia uma oportunidade visual e numérica de se flagrar o comportamento do material sob diferentes situações, além da possibilidade rápida de se variar condições e se determinar os efeitos de diferentes variáveis.

Os algoritmos genéticos, por sua vez, foram importantes no processo de fabricação na função da predição de propriedades mecânicas de estruturas em alginato. Há muito ainda a ser explorado com os AGs na biofabricação, contudo os resultados e a própria aplicação dos AGs foram importantes no sentido de demonstrarem também a versatilidade desta técnica e que a biofabricação está aberta a inovações.

Por fim, este trabalho permite verificar que o alginato pode ser de fato um material bastante promissor para a biofabricação, assim como as ferramentas computacionais apresentadas (e outras que possam ser incorporadas) são bem recebidas e podem beneficiar imensamente a criação se soluções inéditas nesta área da ciência.

8.2 Trabalhos Futuros

Após a conclusão deste trabalho, é possível enumerar algumas etapas que poderiam sistematicamente enriquecer o que já foi desenvolvido até o momento. Há várias sugestões para a continuidade desta vertente da biofabricação, incluindo caracterização de material e aplicações computacionais. São elas:

- Estudo da citotoxicidade do alginato;

- Determinação das propriedades térmicas do alginato através do DSC;

- Padronização da fabricação dos corpos de prova para ensaios mecânicos;

- Desenvolvimento de um método de caracterização química em função do efeito de luz natural nas condições físicas do alginato;

- Análise do comportamento do alginato em termos fisiológicos quando em interação com células vivas;

- Simulações através do Ansys:

    - Esforços mecânicos em estruturas de alginato;

    - Fenômeno de extrusão do alginato;

- Avançar na otimização de outras propriedades do alginato (topologia, degradação do alginato, por exemplo) com algoritmos genéticos;

    - Validar os resultados obtidos com valores experimentais;

- Estruturação via processos de manufatura aditiva utilizando plataformas experimentais de deposição;

- Controle da gelação da camada no leito de $CaCl_2$.

Referências Bibliográficas

Ang, T.H., Sultana, F.S.A., Hutmacher, D.W., Wong, Y.S., Fuh, J.Y.H., Mo, X.M., Loh, H.T., Burdet, E. and Teoh, S.H., Fabrication of 3D chitosan-hydroxyapatite scaffolds using a robotic dispersing system, Mater Sci Eng, C20, 35–42, 2002

Ansys CFX, 2006, "Users Guide".

Azonano, 2006. (http://www.azonano.com/Details.asp?ArticleID=1703 . (Acessed in May, 2010).

Barbanti, S. H., Zavaglia, C. A. C., Duek, E. A. R. Polímeros Bioreabsorvíveis na Engenharia tecidual. Polímeros: Ciência e Tecnologia, vol.15, n.1, p. 13-21, 2005.

Bártolo, P., Mendes, A. and Jardini, A., Bio-prototyping, in Design and Nature II, Edited by M.W. Collins and C.A. Brebbia, WIT Press, Southampton, UK, 535–543, 2004.

Bártolo, P. J.; Amorim, H.; Laoui, T. Rapid prototyping and manufacturing for tissue engineering scaffolds. Int J Mater Prod Technol, v.36, n.1, pp.1-9, 2009.

Bártolo, P.J. and Mitchell, G., Stereo-thermal-lithography, Rapid Prototyping J, 9(3), 150–156, 2003.

Bártolo, P.J., State of the art of solid freeform fabrication for soft and hard tissue engineering, in Design and nature III: comparing design in nature with science and engineering, 233–243, 2006.

Bártolo, P. J. In Design and Nature III: Comparing Design in Nature with Science and Engineering; Brebbia, C. A., Ed.; WIT Press: Southampton, 2006.

Bártolo, P.J., Almeida, H. A., Rezende, R. A., Laoui, T., Bidanda, B. Advanced processes to fabricate scaffolds for tissue engineering. Virtual Prototyping & Bio-manufacturing in Medical Applications, Edited by B. Bidanda and P.J. Bartolo, Springer Science+Business Media, New York, Chap. 8, pp. 149-170, 2008.

Benyus, J. (1997), Biomimicry: Innovation Inspired by Nature, Quill Publishers (site: http://pessoa.fct.unl.pt/mas16674/Biodesigner/index_ficheiros/Page3076.htm) (acessado em 12 de outubro de 2010).

Bertsch, A., Jiguet, S., Bernhards, P. and Renaud, P., Microstereolithography: a review. Mat Res Soc Symp Proc, 758: LL.1.1.1–13, 2003.

Bineli, A. R. R., Barbosa, M. I. R., Jardini, A. L., Maciel Filho, R. Simulation to Analyze Two Models of Agitation System in Quench Process. 20th European Symposium on Computer Aided Process Engineering – Escape20. S. Pierucci and G. Buzzi Ferraris (Editors), 2010.

Boland, T., Tao, X., Damon, B.J., Manley, B. and Kesari, P., Drop-on-demand printing of cells and materials for designer tissue constructs, Mater Sci Eng: C 27(3), 372–376, 2007.

Burns, M., Automated Fabrication: Improving Productivity in Manufacturing, Prentice Hall, New Jersey, 1993.

Callegari, B. Análise da Interface Formada entre o Poli (Fluoreto de Vinilideno), Piezoelétrico e Não Piezoelétrico e o Tecido Muscular e Ósseo de Ratos: Dissertação (mestrado) – Faculdade de Ciências Médicas, Universidade Estadual de Campinas-SP, 2004.

Carroll, D. Carroll's Fortran Genetic Algorithm Driver. In http://cuaerospace.com/carroll/ga.html (acessado em 16 de Novembro de 2008).

Carvalho, C., Landers, R., Mulhaupt, R., Hubner, U. and Schmelzeisen, R., Fabrication of soft and hard biocompatible scaffolds using 3D-Bioplotting, in Virtual Modelling and Rapid Manufacturing – Advanced Research in Virtual and Rapid Prototyping, Edited by P.H. Bártolo *et al.* Taylor & Francis, London, UK, 2005.

Chu, T.-M.G., Halloran, J.W., Hollister, S.J. and Feinberg, S.E., Hydroxyapatite implants with designed internal architecture, J Mater Sci: Mater Med, 12, 471–478, 2001.

Chu, C-C. Biodegradable Polymeric Biomaterials: An Updated Overview. In: Biomaterials Principles and Applications. Edited by Park, J. and Bronzino, J., 2003.

Chung, T. W.; Yang, J.; Akaike, T.; Cho, K. Y.; Nah, J. W.; Kim, S.; Cho, C. S. Biomaterials, 23, 2827, 2002.

Cohen, S., Bano, M. C., Cima, L. G., *et al.* Design of synthetic polymeric structures for cell transplantation and tissue engineering. Clin. Mater. 13, 3, 1993.

Cooke, M.N., Fisher, J.P., Dean, D., Rimnac, C., Mikos, A.G., Use of stereolithography to manufacture critical-sized 3D biodegradable scaffolds for bone ingrowth, J Biomed Mater Res Part B: Appl Biomater, 64B, 65–69, 2002.

Costa, C.B.B. Modelagem detalhada e otimização de processos de cristalização. Campinas, SP: Universidade Estadual de Campinas, 2006, Tese (Doutorado).

Crawford, R. J. Plastics Engineering; Butterworth-Heinemann: Oxford, 1998.

Crump, S.S., Apparatus and method for creating three-dimensional objects, US Pat. 5121329, 1989.

Deb, K. An introduction to genetic algorithms. Sadhana-Academy Proceedings in Engineering Sciences, 24, 293-315 Part 4-5, 1999.

Deb, K. An Efficient Constraint Handling Method for Genetic Algorithms. Computer Methods in Applied Mechanics Engineering, 186, 311-338, 2000.

Desai, S.; Bártolo, P. J.; Bidanda, B. In Bio-materials & Prototyping Applications in Medicine; Bidanda, B.; Bártolo, P. J., Eds.; Springer: New York, Chapter 1, 2007.

Draget, K. I.; Braek, G. S.; Stokke, B. T. Food Hydrocolloids, 20, 170, 2006.

Dudek, G. Unit commitment by genetic algorithm with specialized search operators. Electric Power Systems Research, 72, 299-308, 2004.

Eiselt, P.; Yeh, J.; Latvala, R. K.; Shea, L. D.; Mooney, D. J. Biomaterials, 21, 1921, 2000.

Fischer, J.P., Dean, D., Engel, P.S., Mikos, A., Photoinitiated polymerization of biomaterials, Annual Rev Mater Res, 31, 171–181, 2001.

FMC Biopolymer – http://www.fmcbiopolymer.com (acessado em Novembro de 2010).

Freyman, T.M., Yannas, I.V. and Gibson, L.J., Cellular materials as porous scaffolds for tissue engineering, Progress in Mate Sci, 46, 273–282, 2001.

Fuchs, J.R., Nasseri, B.A. and Vacanti, J.P., Tissue engineering: a 21st century solution to surgical reconstruction, Ann Thorac Surg, 72, 577–581, 2001.

Fundueanu, G., Nastruzzi, C., Carpov, A., Desbrieres, J. and Rnaudo, M. Physico-Chemical Characterization of Ca-Alginate Microparticles Produced with Different Methods. Biomaterials, 20, 1427-1435, 1999.

Fung, Y. C. Biomechanics: Mechanical properties of Living Tissues. Springer-Verlag. New York. 1981.

Glicklis R, Shapiro L, Agbaria R, Merchuk JC, Cohen S. Hepatocyte behavior within three-dimensional porous alginate scaffolds. Biotechnol Bioeng. 67:344–53, 2000.

Goldberg, D.E. Genetic Algorithms in Search, Optimization, and Machine Learning Addison-Wesley Publishing Company, INC, 1989.

Gombotz, W. R. and Wee, S. W., Protein release from alginate matrices, Adv. Drug Deliv. Rev., 31, pp.267-285, 1998.

Gomes, M.E. and Reis, R.L., Biodegradable polymers and composites in biomedical applications: from catgut to tissue engineering. Part 2 Systems for temporary replacement and advanced tissue regeneration, Int Materials Rev, 49, 274–285, 2004.

Griffith, M.L. and Halloran, J.W., Freeform fabrication of ceramics via stereolithography, J Am Ceram Soc, 79, 2601–2608, 1996.

Hasse, C.; Klöck, G.; Schlosser, A.; Zimmermann, U.; Rothmund, M. Lancet, 50, 1926, 1997.

He, H., Cao, X., Lee, L.J.- Design of a novel hydrogel-based intelligent system for controlled drug release, Journal of Controlled Release, 95, 391-402, 2004.

Hench, L.L., Erthridge, E.C. Biomaterials — An Interfacial Approach, Vol. 4, A. Noordergraaf, Ed. New York: Academic Press, 1982.

Ho, M.H., Kuo, P.Y., Hsieh, H.J., Hsien, T.Y., Hou, L.T., Lai, J.Y. and Wang, D.W., Preparation of porous scaffolds by using freeze-extraction and freeze-gelation methods, Biomaterials, 25, 129–138, 2004.

Holland, J.H. Adaptation in Natural and Artificial Systems, University of Michigan Press, 1975.

Hutmacher, D.W., Schantz, T., Zein, I., Ng, K.W., Teoh, S.H. and Tan, K.C., Mechanical properties and cell cultural response of polycaprolactone scaffolds designed and fabricated via fused deposition modelling, J Biomed Mater Res, 55, 203–216, 2001.

Hutmacher, D. W., Sittinger, M., Risbud M. V. Scaffold-based tissue engineering: rationale for computer-aided design and solid free-form fabrication systems. Trends in Biotechnology, 22 (7), 354-362, 2004.

Hutmacher, D. W. Scaffold-based tissue engineering – design and fabrication of matrices using solid freeform fabrication techniques. Advanced Manufacturing Technology for Medical Applications, Ed. by I. Gibson, 163-189, 2006.

Hynes, R.O., Integrins, versatility, modulation, and signalling in cell adhesion, Cell, 69, 11–25, 1992.

Ichioka, S.; Harii, K.; Nakahara, M.; Sato, Y. Scand J Plast Reconstr Hand Surg, 32, 311, 1998.

Jacobs, P.F., Stereolithography and Other RP&M Technologies: From Rapid Prototyping to Rapid Tooling, SME, Dearborn, 1995.

Jen, A.C., Wake, M.C. and Mikos, A.G- Review: Hydrogels for Cell Immobilization, Biotechnology and Bioengineering, vol.50, 357-364, 1996.

Jennifer, J. M. *et al.* Transplantation of cells in matrices for tissue regeneration. Adv. Drug Deliv. Rev., 33, 165-162, 1998.

Johnson, F.A., Craig, D.Q.M., Mercer, A.D., Characterization of the block structure and molecular weight of sodium alginates, Journal of Pharmacy and Pharmacology, v.49, Issue 7, p. 639-643, 1997.

Miguel Junior, A. 2006. http://www.medicinageriatrica.com.br/2006/12/13/como-sera-a-populacao-mundial-em-2025/ (acessado em 13 de outubro de 2010)

Kester, J.J.; Fennema, O.R. Edible films and coatings: a review. Food Technology, v.40, n.12, p.47-59, 1986.

Kim, S.S., Utsunomiya, H., Koski, J.A.,Wu, B.M., Cima, M.J., Sohn, J., Mukai, K., Griffith, L.G. and Vacanti, J.P., Survival and function of hepatocytes o a novel three-dimensional synthetic biodegradable polymer scaffolds with an intrinsic network of channels, Ann Surg, 228, 8–13, 1998.

Klöck, G., Frank, H., Houben, R., Zerkon, T., Horcger, A., Siebers, U., Wöhrle, A., Federlin, K., and Zimmermann, U., Production of purified alginates suitable for use in immunoisolated transplantation, Appl Microbiol Biotechnol, 40, pp.638-643, 1994.

Koh, Y.-H, Jun, I.-K. and Kim, H.-E., Fabrication of poly(ε-caprolactone)/hydroxyapatite scaffold using rapid direct deposition, Materials Letters, 60, 1184–1187, 2006.

Kowata, S. and Sun, H.B., Two-photon photopolymerization as a tool for making micro-devices, Appl Surf Sci 208/209, 153–158, 2003.

Lam, C.X.F.,Mo, X.M., Teoh, S.H. and Hutmacher, D.W., Scaffold development using 3D printing with a starch-based polymer, Mater Sci Eng, 20, 49–56, 2002.

Langer, R., Tissue engineering: a new field and its challenges, Pharm Res, 14, 840–841, 1997.

Langer, R. and Vacanti, J.P., Tissue engineering, Science, 260, 920–926, 1993.

Leboreiro, J., Acevedo, J. Processes synthesis and design of distillation sequences using modular simulations: a genetic algorithm framework, Comps. and Chem. Eng., v. 28, p. 1223-1236, 2004.

Lee, G. and Barlow, J.W., Selective laser sintering of bioceramic materials for implants, Proceedings of the '96 SFF Symposium, Austin, TX, August 12–14, 1996.

Lee, K.Y., Mooney, D.J. Hydrogels for Tissue Engineering, Chemical Reviews, Vol. 101 No. 7, 2001.

Lee, J.J., Lee, S.G., Park, J.C., Yang, Y.I. and Kim, J.K.- Investigation ob biodegradabale PLGA scaffold with various pore size structure for skin tissue engineering, Current Applied Physics, 7, 37-40, 2007.

Lemercier, G., Mulatier, J.C., Martineau, C., Anémian, R., Andraud, C., Wang, I., Stéphan, O., Amari, N. and Baldeck, P., Two-photon absorption: from optical limiting to 3D microfabrication, Comptes Rendus Chimie, 8, 1308–1316, 2005.

Leor, J., Aboulafia-Etzion, S., Dar, A., Shapiro, L., Barbash, I. M., Battler, A., Granot, Y., Cohen, S. Bioengineered cardiac grafts: a new approach to repair the infarcted myocardium. Circulation;102;III-56-III-61, 2000.

Leukers, B., Gulkan, H., Irsen, S.H., Milz, S., Tille, C., Schieker, M. and Seitz, H., Hydroxyapatite scaffolds for bone tissue engineering made by 3D printing, J Mater Sci Mater Med, 16, 1121–1124, 2005.

Levy, R.A., Chu, T.G.M., Holloran, J.W., Feinberg, S.E. and Hollister, S., CT-generated porous hydroxyapatite orbital floor prosthesis as a prototype bioimplant, Am J Neuroradiol, 18, 1522–1525, 1997.

Limpanuphap, S. and Derby, B., Manufacture of biomaterials by a novel printing process, J Mater Sci Mater Med, 13, 1163–1166, 2002.

Madeira, J.F.A. Optimização Multi-Objectivo da Topologia de Estruturas com Algoritmos Genéticos: Tese (doutorado) – Instituto Superior Técnico, Universidade Técnica de Lisboa, 2004.

Mahajan, H. P., Evaluation of chitosan gelatine complex scaffolds for articular cartilage tissue engineering, MSc Thesis, Mississipi State University, USA, 2005.

Maliska, C.R., Transferência de Calor e Mecânica dos Fluidos Computacional, 2nd ed. LTC editora, 452, 2004.

Malmonge, S.M. Hidrogel sintético para reparo de defeitos da cartilagem articular. Campinas, 1997. (Tese - Doutorado – Universidade Estadual de Campinas).

Marler, J.J., Upton, J., Langer, R. and Vacanti, J.P., Transplantation of cells in matrices for tissue regeneration, Adv Drug Del Rev, 33, 165–182, 1998.

Matsuda, T. and Mizutani, M., Liquid acrylate-endcapped poly(e-caprolactone-co-trimethylene carbonate). II. Computer-aided stereolithographic microarchitectural surface photoconstructs, J Biomed Mater Res, 62, 395–403, 2002.

Mei, L. H. I. Polímeros biodegradáveis. Biomateriais, Fundamentos e Aplicações. Edited by Oréfice, R. L., Pereira, M. M., Mansur, H. S. Ed. Cultura Médica. 175-184, 2006.

Menard, K. P., Dynamic Mechanical Analysis – A Practical Introduction, CRC Press, 1999.

Mendes, A., Lagoa, R., Bártolo, P. J., Rapid Prototyping system for tissue engineering. Proceedings of the 1st International Conference on Advanced Research in Virtual and Physical Prototyping, pp.419-426, 2003.

Miller, J. S. and West, J. L. Rapid prototyping of hydrogels to guide tissue formation. In: Bio-Materials and Prototyping Applications in Medicine. Edited by Bártolo, P. J. S. and Bidanda, B. Springer, 2008.

Ministério da Saúde do Brasil. Lista de Espera, Transplantes, 2010. http://portal.saude.gov.br/portal/saude/area.cfm?id_area=1004 . (acessado em 16 de novembro de 2010).

Miranda, P., Saiz, E., Gryn, K. and Tomsia, A.P., Sintering and robocasting of β-tricalcium phosphate scaffolds for orthopaedic applications, Acta Biomaterialia, 2, 457–466, 2006.

Mironov, V., Boland, T., Trusk, T., Forgacs, G. and Markwald, R.R., Organ printing: computeraided jet-based 3D tissue engineering, Trends Biotechnol, 21, 157–161, 2003.

Mironov, V. Trusk, T. Kasyanov, V. Little, S. Swaja, R. Markwald, R. Biofabrication: a 21st century manufacturing paradigm. Biofabrication. v.1 n.2. 2009.

Moroni, L., Schotel, R., Sohier, J., Wijn, J.R. and Blitterswijk, C.A., Polymer hollow fiber three-dimensional matrices with controllable cavity and shell thickness, Biomaterials, 27, 5918–5926, 2006.

Nakamura, M., Iwanaga, S., Henmi, C., Arai, K., Nishiyama, Y. Biomatrices and biomaterials for future developments of bioprinting and biofabrication. Biofabrication. n.2. pp.1-6, 2010.

Nathan, C. and Sporn, M., Cytokines in context, J Cell Biol, 113, 981–986, 1991.

NIH. National Institutes of Health Consensus Development Conference Statement. Clinical Applications of Biomaterials, 1982. http://consensus.nih.gov/1982/1982Biomaterials034html.htm. (acessado em 16 de novembro de 2010).

O'Brien, F.J., Harley, B.A., Llanas, I.V. and Gibson, L.J., The effect of pore size on cell adhesion in collagen-GAG scaffolds, Biomaterials, 26, 433– 441, 2005.

Oréfice, R.L., Pereira, M.M., Mansur, H.S. Biomateriais: Fundamentos e Aplicações. 1. ed. Rio de Janeiro: Cultura Médica, v. 1. 538 p., 2006.

Pardo, L., Wilson, W.C. and Boland, T., Characterization of patterned self-assembled monolayers and protein arrays generated by the ink-jet method, Langmuir, 19, 1462–1466, 2003.

Park, A., Wu, B. and Griffith, L.G., Integration of surface modification and 3D fabrication techniques to prepare patterned poly(L-lactide) substrates allowing regionally selective cell adhesion, J Biomater Sci-Polym E, 9, 89–110, 1998.

Park, J. Bronzino, J. Preface. In: Biomaterials Principles and Applications. Edited by Park, J. and Bronzino, J., 2003.

Peppas, N. A., Hilt, J. Z., Khademhosseini, A., Langer, R. Hydrogels in Biology and Medicine: From Molecular Principles to Bionanotechnology. Advanced Materials, 18, 1345-1360, 2006.

Pfister, A., Landers, R., Laib, A., Hübner, U., Schmelzeisen, R., Mülhaupt, Biofunctional rapid prototyping for tissue-engineering applications: 3D bioplotting versus 3D printing, Journal of Applied Polymer Science Part A: Polymer Chemistry, 42, 624–638, 2004.

Popov, V.K., Antonov, E.N., Bagratashvili, B.N., Konovalov, A.N. and Howdle, S.M., Selective laser sintering of 3-D biodegradable scaffolds for tissue engineering, Mat Res Soc Symp Proc., EXS-1, F5.4.1–F.5.4.3, 2004.

Qin, Y. The gel swelling properties of alginate fibers and their applications in wound management. Polym. Adv. Technol., 19: 6–14, 2008.

Ratner, B. R., Hoffman, A. S., Schoen, F. J., Lemons, J. E. Introduction to materials in medicine. Biomaterials Science, 1996.

Reece, G. P., Patrick, C. W., Jr. Tissue engineered construct design principles. Frontiers in Tissue Engineering, 166-196, 1998.

Reignier, J. and Huneault, M.A., Preparation of interconnected poly(ε-caprolactone) porous scaffolds by a combination of polymer and salt particulate leaching, Polymer, 47, 4703–4717, 2006.

Rezende, R.A., Análises de Parâmetros Físicos e Operacionais no Fenômeno da Cura Localizada do Processo Termolitográfico da Prototipagem Rápida: Dissertação (mestrado) – Faculdade de Engenharia Química, Universidade Estadual de Campinas-SP, 2006.

Rezende, R.A., Bártolo, P.J., Mendes, A. and Maciel Filho, R. - Experimental characterisation of the alginate gelification process for rapid prototyping, Chemical Engineering Transactions, Aidic. 2007.

Rezende, M.C.A.F. Modelagem e Otimização de Processos para Implementação em Tempo Real: Tese (doutorado) – Faculdade de Engenharia Química, Universidade Estadual de Campinas-SP, 2007.

Rezende, M.C.A.F., Rezende, R.A., Mendes, A. ; Bártolo, P.J., Costa, A.C., Maciel Filho, R. Evolutionary Optimization for Soft Tissue Engineering. Advanced Research in Virtual and Rapid Manufacturing. London, UK: Taylor & Francis, 81-85, 2008.

Rezende, R.A., Bártolo, P.J.S., Mendes, A., Maciel Filho, R. Rheological behavior of alginate solutions for biomanufacturing. Journal of Applied Polymer Science, v.113, 3866-71, 2009-a.

Rezende, R. A., Rezende, M. C. A. F., Maciel Filho, R., Bártolo, P.J.S., Mendes, A. Optimization of Scaffolds in Alginate for Biofabrication by Genetic Algorithms. Computer Aided Chemical Engineering, Volume 27, Pages 1935-1940, 2009-b.

Rosiak, J. M., Yoshii, F. Hydrogels and their medical applications. Nuclear Instruments in Physics Research B, 151, 56-64, 1999.

Rowley, J. A., Madlambayan, G., Mooney, D. J. Alginate hydrogels as synthetic extracellular matrix materials. Biomaterials, 20, 45-53, 1999.

Sachlos, E., Reis, N., Ainsley, C., Derby, B. and Czernuszka, J.T., Novel collagen scaffolds with predefined internal morphology made by solid freeform fabrication, Biomaterials, 24, 1487–1497, 2003.

Sachs, E.M.,Haggerty, J.S, Cima,M.S. andWilliams, P.A., Three-dimensional printing techniques, US Pat. 5204055, 1989.

Saiz, E., Gremillard, L., Menendez, G., Miranda, P., Gryn, K and Tomsia, A.P., Preparation of porous hydroxyapatite scaffolds, Materials Science and Engineering C, 27, 546–550, 2007.

Saunders, R., Derby, B., Gough, J. and Reis, N., Ink-jet printing of human cells,Mat Res Soc Symp Proc, EXS-1, F.6.3.1–F.6.3.3, 2004.

Schneider, S.; Feilen, P. J.; Brunnenmeier, F.; Minnemaan, T.; Zimmermann, H.; Zimmermann, U. Diabetes, 54, 687, 2005.

Serp, D., Cantana, E., Heinzen, C., Stockar, U. and Marison, I. W., Characterization of an encapsulation device for the production of monodisperse alginate beads for cell immobilization, Biotechnology and Bioengineering, 70, pp.41-53, 2000.

Serp, D., M. Mueller, U. Stockar and I.W. Marison. Low-temperature electron microscopy for the study of polysaccharide ultrastructures in hydrogels. II. Effect of temperature on the structure of Ca2+-alginate beads, Biotechnology and Bioengineering, 79, 253-259, 2002.

Shapiro L, Cohen S.- Novel alginate sponges for cell culture and transplantation. Biomaterials 18 :583 –590, 1997.

Shaw, C.T. Using Computational Fluid Dynamics, Prentice Hall, 325, 1992.

Shi, D. Introduction to Biomaterials. Edited by Shi, World Scientific, 2006.

Silva, M. A. Desenvolvimento e Caracterização de Filmes Compostos de Alginato e Quitosana Contendo Natamicina como Agente Antimicótico: Tese (doutorado) – Faculdade de Engenharia Química, Universidade Estadual de Campinas-SP, 2009.

Skalak, R. and Fox, C.F., Tissue engineering, Alan R. Liss, New York, 1988.

Smidsrød, O. Molecular basis for some physical properties of alginates in the gel state. Faraday Discussions Chemical Society, v.57, p.263-274, 1974.

Srichana, T. and Domb, A.J. Polymeric biomaterials. In: Biomedical Materials. Edited by Narayan, R. Springer, 2009.

Sun, W. Welcome to Biofabrication. Biofabrication. v.1, n.1, 2009.

Sung, H.J., Meredith, C., Johnson, C. and Galis, Z.S., The effect of scaffold degradation rate on three-dimensional cell growth and angiogenesis, Biomaterials, 25, 5735-5742, 2004.

Tabata, Y., Recent progress in tissue engineering, Drug Discov Today, 6, 483–487, 2001.

Taboas, J.M., Maddox, R.D., Krebsbach, P.H. and Hollister, S.J., Indirect solid free form fabrication of local and global porous biomimetic and composite 3D polymer-ceramic scaffolds, Biomaterials, 24, 181–194, 2003.

Tellis, B.C., Szivek, J.A., Bliss, C.L.,Margolis, D.S., Vaidyanathan, R.K. and Calvert, P., Trabecular scaffolds created using micro CT guided fused deposition modeling, Materials Science and Engineering C (2007).

Tønnesen, H. H.; Karlsen, J. Drug Dev Ind Pharm, 28, 621, 2002.

Tormen, M., Businaro, L., Altissimo, M., Romanato, F., Cabrini, S., Perennes, F., Proitti, R., Sun, H.B., Kawata, S., Fabrizio, E.D., 3D patterning by means of nanoimprinting, X-ray and twophoton lithography, Microelectronic Engineering, 73/74, 535–541 2004.

Triton Technology Ltd: http://www.triton-technology.co.uk/ (acessado em Abril de 2010).

Tsang, V. L., Bhatia, S. N. Three-dimensional tissue fabrication. Advanced Drug Delivery Reviews, 56, 1635-1647, 2004.

UNOS, U. S. Scientific Registry for Organ Transplantation and the Organ Procurement and Transplant Network. UNOS http://www.unos.org/. (acessado em Maio de 2010).

Vacanti, J. and Vacanti, C. The challenge of tissue engineering. In: Lanza R. P., Langer, R., Chick, W. L., eds. Principles of Tissue Engineering. Austin, TX: Academic Press, pp.1-6, 1997.

Versteeg, H.K., Malalasekera, W. An introduction to Computational Fluid Dynamics (The Finite Volume Method). Prentice Hall, 257. 1995.

Victorino, I.R.S. Otimização de um Processo Industrial de Produção de Álcool Cíclico

Utilizando Algoritmos Genéticos. Campinas, SP: Universidade Estadual de Campinas, Tese (Doutorado). 2005.

Vozzi, G., Flaim, C., Ahluwalia, A. and Bhatia, S., Fabrication of PLGA scaffolds using soft lithography and microsyringe deposition, Biomaterials, 24, 2533–2540, 2003.

Wandrey, C.; Espinosa, D.; Rehor, A.; Hunkeler, D. J. Microencapsulation, 20, 597, 2003.

Wang, F., Shor, L., Darling, A., Khalil, S., Güçeri, S. and Lau, A., Precision deposition and characterization of cellular poly-e-caprolactone tissue scaffolds, Rapid Prototyping J, 10, 42–49, 2004.

Ward, I. M. and Hadley, D. W. An Introduction to the Mechanical Properties of Solid Polymers. John Wiley & Sons. 1993.

Webber, Rebecca. Viscoelastic Behavior and Adhesion of Ionic Alginate Hydrogels (2004), Kenneth Shull (Northwestern University): http://flux.aps.org/meetings/YR04/MAR04/baps/abs/S290006.html. (acessado em Novembro de 2009).

Weber, M.; Steinert, A.; Jork, A.; Dimmler, A.; Thürmer, F.; Schütze, N. Biomaterials, 23, 2003, 2002.

Wei, G., Jin, Q., Giannobile,W.V. and Ma, P.X., The enhancement of osteogenesis by nano-fibrous scaffolds incorporating rhBMP-7 nanospheres, Biomaterials, 2087–2096, 2007.

Whang, K., Thomas, C.H., Healy, K.E. and Nuber, G., A novel method to fabricate bioabsorbable scaffolds, Polymer, 36, 837–842, 1995.

Williams, D.F. Definition in Biomaterials. In: Progress in Biomedical Engineering (Amsterdam: Elsevier), p. 67, 1987.

Williams, J.M., Adewunmi, A., Schek, R.M., Flanagan, C.L., Krebsbach, P.H., Feinberg, S.E., Hollister, S.J. and Das, S., Bone tissue engineering using polycaprolactone scaffolds fabricated via selective laser sintering, Biomaterials, 26, 4817–4827, 2005.

Woodfield, T.B.F., Malda, J., de Wijn, J., Péters, F., Riesle, J. and van Blitterswijk, C.A., Design of porous scaffolds for cartilage tissue engineering using a three-dimensional fiber-deposition technique, Biomaterials, 25, 4149–4161, 2004.

Xiong, Z., Yan, Y. and Zhang, R. and Sun, L., Fabrication of porous poly(L-lactide acid) scaffolds for bone tissue engineering via precise extrusion, Scripta Materialia, 45, 773–779, 2001.

Xiong, Z., Yan, Y., Zhang, R. and Wang, X., Organism manufacturing engineering based on rapid prototyping principles, Rapid Prototyping J 11(3), 160–166, 2005.

Yan, Y., Wu, R. and Zhang, R, Biomaterial forming research using RP technology, Rapid Prototyping J, 9, 142–149, 2003a.

Yan, Y., Zhang, R. and Lin, F., Research and applications on bio-manufacturing, Proceedings of the 1st International Conference on Advanced Research in Virtual and Rapid Prototyping, Leiria, Portugal, 2003.

Yang, S., Leong, K-F., Zhaohui, D., Chua, C-K. The Design of Scaffolds for Use in Tissue Engineering. Part I. Rapid Prototyping Techniques. Tissue Engineering, 7 (6), 679-689, 2001.

Yang, S., Leong, K-F., Zhaohui, D., Chua, C-K. The Design of Scaffolds for Use in Tissue Engineering. Part II. Rapid Prototyping Techniques. Tissue Engineering, 8 (1), 1-11, 2002.

Yannas, L.V. Natural Materials - Classes of Materials Used in Medicine. In: Biomaterials Science: An Introduction to Materials in Medicine. pp. 84-94. Edited by Ratner, B., Hoffman, A., Schoen, F., Lemons, J. Academic Press, 1996.

Yeong, W-Y., Chua, C-K., Leong, K-F., Chandrasekaran, M. Rapid prototyping in tissue engineering: challenges and potential. Trends in Biotechnology, 22 (4), December 2004.

Yoon, D. M., Fisher, J. P. Natural and synthetic polymeric scaffolds. In: Biomedical Materials. Edited by Narayan, R. Springer, 2009.

Zein, I., Hutmacher, D.W., Tan, K.C. and Teoh, S.H., Fused deposition modeling of novel scaffolds architectures for tissue engineering applications, Biomaterials, 23, 1169–1185, 2002.

Zeltinger, J., Sheerwood, J.K., Graham, D.M., Mueller, R. and Griffith, L.G., Effects of pore size and void fraction on cellular adhesion, proliferation, and matrix deposition, Tissue Engineering, 7(5), 557–572, 2001.

Zmora S, Glicklis R, Cohen S. Tailoring the pore architecture in 3-D alginate scaffolds by controlling the freezing regime during fabrication. Biomaterials, 23, 4087-4094, 2002.